It is the glory of God to conceal a thing: but the honour of kings is to search out a matter.

Proverbs 25: 2

University of Alberta

Design, Development and Mechanistic Study of Ruthenium-Based Catalysts for the Hydrogenation of Imides and Amides

by

Jeremy Michael John

A thesis submitted to the Faculty of Graduate Studies and Research
in partial fulfillment of the requirements for the degree of

Doctor of Philosophy

Department of Chemistry

Spring 2014
Edmonton, Alberta

Dedication

I dedicate this thesis to my mother, Brenda Chin Leung Fatt–John. You are a source of encouragement and inspiration to me throughout my life. Your honesty, integrity and work ethic are unparalleled. Thank you for the opportunity to accomplish all that I have, the ability to strive harder, to find and realize my potential, and for the myriad of ways throughout my life, that you have supported me. You have taught me to be all that I am.

Abstract

Prior mechanistic studies demonstrate that *trans*-[RuH_2((*R*)-BINAP)((*R*,*R*)-dpen)] is a remarkably active carbonyl reducing agent at low-temperatures in THF-d_8. This dissertation describes the monohydrogenation of cyclic *meso*-imides using this catalyst and related complexes under mild conditions. Bicyclic *meso*-imides were chemo-, diastereo- and enantio-selectively desymmetrized to form chiral hydroxy lactams (90-99% conversion, 88-97% *ee*, dr >93:7, C=O/C=C selectivity >99%) with up to five stereogenic centers in one hydrogenation under the reported reaction conditions (0.1-1 mol% Ru, 0.9-9.9 mol% KO*t*-Bu under 50 atm H_2 at 0-22 °C in 3-57 h). Compounds of academic and commercial interest were also synthesized from these hydroxy lactams.

A detailed low-temperature investigation into the desymmetrization-hydrogenation reaction led to the discovery of a previously unobserved active pathway for carbonyl hydrogenation. Reaction intermediates resulting from the unexpected deprotonation and di-deprotonation respectively of the parent dihydrides *i.e. trans*-M[RuH_2((*R*,*R*)-$HN^-CH(Ph)CH(Ph)NH_2$)((*R*)-BINAP)], where *M* = K^+ or Li^+, and *trans*-M_2[RuH_2((*R*,*R*)-$HN^-CH(Ph)CH(Ph)N^-H$)((*R*)-BINAP)] where *M* = Li^+, were synthesized and characterized. The mono-deprotonated dihydrides were found to have unprecedented activity towards the hydrogenation of imide and amide carbonyls at low temperatures in THF-d_8. The origins of the enantioselection for this reaction were also proposed using simple well-defined models based on current literature and the outcomes of this investigation.

The hydrogenation of amides using *trans*-[RuH_2((*R*)-BINAP)((*R*,*R*)-dpen)] and its variants is also described herein. In contrast to the high activity of *trans*-[RuH_2((*R*)-BINAP)((*R*,*R*)-dpen)] towards ketones, imides (*in the presence of base*), and esters, the

catalyst exhibited low to moderate activity towards amides. This difference in activity was attributed to thermal instability of the catalyst at high temperatures. By tethering the phosphine and amine units together, a robust pre-catalyst, [Ru(η^3-C_3H_5)($Ph_2P(CH_2)_2NH_2)_2$]BF_4 was prepared, which, when combined with NaOMe (Ru:NaOMe:Amide = 1:500:10,000), catalyzes the hydrogenation of amides with a TON up to 7120. The analogous base-free system comprising [Ru(η^3-C_3H_5)($Ph_2P(CH_2)_2NH_2)_2$]BF_4 and $NaBH_4$ was also shown to be an efficient catalyst system for this reaction under reported conditions (0.1 mol% Ru, 0.2 mol% $NaBH_4$ under 50 atm H_2 at 100 °C in 24 h) in contrast to *trans*-[RuH(η^1-BH_4)((*R*)-BINAP)((*R*,*R*)-dpen)].

Acknowledgements

I would like to express my sincerest gratitude to the people who have helped me through the completion of this dissertation. Foremost, is my advisor, Prof. Steven Bergens, whose commentaries, engagement, enthusiasm, knowledge, motivation and patience were critical to my understanding of the assigned projects. In addition to the mentorship of my advisor, I consider it an honor to have Prof. Jillian Buriak, Prof. Dennis Hall, Prof. Eric Rivard, Prof. Arno De Klerk and Prof. Laurel Schafer as knowledgeable participants on my defense committee.

I am indebted to my colleagues, past and present, who have supported me practically and emotionally throughout the entire process: Dr. Robin Hamilton, Dr. Satoshi Takebayashi, Dr. Matthew Markiewicz, Michael Hass, Andrew Sullivan, Dr. Sonja Francis, Dr. Elizabeth Corkum, Suneth Kalapugama, Rasu Loorthuraja, Austin Penner, Sarah Sutherland and Evan Antoniuk. Working with each of you was truly a blessing. You are responsible for broadening the value of this research.

I would also like to acknowledge the individuals whose advice, expertise and services have contributed to the completion of my degree: Administrative Assistants Bonnie Gover and Lynne Lechelt; Wayne Moffat of the Analytical and Instrumentation Laboratory; Andrew Yeung, Bernie Hippel, Matthew Kingston, Ryan Lewis, Marcel Munroe and Margaret Sisley of Chemical Stores and Receiving; Allan Chilton of Electronics Repair; Jason Dibbs of Glassblowing; Anita Weiler and Darryl McGee of Graduate Student Services; Mark Miskolzie and Nupur Dabral of the Nuclear Magnetic Resonance Laboratory; Dr. Angie Morales-Izquierdo of the Mass Spectrometry Laboratory; Shelley Garrett and Tyler Peterson of Information Technology; Dirk Kelm and Paul Crothers of Machine Fabrication; The support staff of the general office: Laura

Pham, Corrine Chorney and Joe Fiorillo, and Undergraduate Lab Coordinators: Dr. Norman Gee and Dr. Jason Cooke. Thank you for supporting me in your own unique way.

I am beyond grateful for the support and love of my mother, Brenda, my father, Cyril, my brothers, Joel and Jared, and my friends. Finally, I would like to thank my Lord and Savior, Jesus Christ, for helping me complete this endeavor.

Table of Contents

List of Tables

Chapter 2

Chapter 3

Chapter 4

List of Figures

Chapter 1

Chapter 2

Chapter 3

Chapter 4

List of Schemes

Chapter 1

Chapter 2

Chapter 3

Chapter 4

List of Equations

Chapter 1

Chapter 3

Chapter 4

List of Abbreviations and Symbols

[18]-crown-6 – 1,4,7,10,13,16-hexaoxacyclooctadecane

1° – primary

2° – secondary

3° – tertiary

Ac – acetyl

acac – acetylacetonate

appH – 2-amino-2-(2-pyridyl)propane

B/C – base to catalyst ratio

BINAL–H – 2,2'-dihydroxy-1,1′-binaphtyllithiumaluminum hydride

BINAP – 2,2'-bis(diphenylphosphino)-1,1'-binaphthyl

bis(diphenylphosphino)butane

Bn – benzyl

Boc – *tert*-butyloxycarbonyl

Br – broad

Bu – butyl

CAGR – compound annual growth rate

Cbz – carboxybenzyl

COD – 1,5-cyclooctadiene

Cp* – 1,2,3,4,5- pentamethylcyclopentadienyl

d – doublet

dr – diastereoisomeric ratio

daipen – 1,1-bis(4-methoxyphenyl)-3-methyl-1,2-butanediamine

dba – dibenzylideneacetone

DBU – 1,8-diazabicyclo[5.4.0]undec-7-ene

dd – doublet of doublet

ddd – doublet of doublet of doublet

DFT – density functional theory

DIBAL-H – diisobutylaluminium hydride

diop – (–)-2,3-*O*-isopropylidene-2,3-dihydroxy-1,4-

DIP – 4,7-diphenyl-1,10-phenanthroline

DIPAMP – 1,2-bis[(2-methoxyphenyl)(phenylphosphino)]ethane

DME – dimethyl ether

dmp – 2,9-dimethylphenanthroline

dpen – 1,2-diphenylethylenedamine

dppb – 1,4-bis(diphenylphosphino)butane

dppe – 1,2-bis(diphenylphosphino)ethane

dt – doublet of triplet

ee – enantiomeric excess

ESI MS – electrospray ionization mass spectroscopy

Et – ethyl

eu – unit of entropy

FDA – Food and Drug Association

FTIR – Fourier transform infrared

gCOSY – gradient correlation spectroscopy

GDP – gross domestic product

gHMBC – gradient heteronuclear multiple bond coherence

gHSQC – gradient heteronuclear multiple quantum coherence

HCNN – 6-(4'-methylphenyl)-2-pyridylmethylamine

HOMO – highest occupied molecular orbital

HPLC – high pressure liquid chromatography

HSAG – high surface area graphite

K_a – acid dissociation constant

KIE – kinetic isotope effect

LUMO – lowest unoccupied molecular orbital

m – multiplet

mp – melting point

m/z – mass to charge ratio

Me – methyl

MS – molecular sieves

MSA – methanesulfonic acid

na – not applicable

nd – not determined

NMR – nuclear magnetic resonance

oaTOF – orthogonal acceleration time of flight

ORTEP – Oak Ridge Thermal Ellipsoid Plot

Ph – phenyl

Phe – phenylalanine

i-Pr – *iso*-propyl

q – quartet

s – singlet

S/C – substrate to catalyst ratio

sex – sextuplet

t – triplet or time

t-Bu – *tert*-butyl

THF – tetrahydrofuran

TLC – thin layer chromatography

tmen – tetramethylethylenediamine

TOF – turnover frequency

TolBINAP – 2,2'-bis(di-*p*-tolylphosphino)-1,1'-binaphthyl

TON – turnover number

TOSCY – total correlation spectroscopy

$TriPhos^{Ph}$ – 1,1,1-tris(diphenylphosphinomethyl)ethane

TROESY – transverse rotating frame overhauser enhancement spectroscopy

Ts – tosyl

TS – transition state

tt – triplet of triplet

USD – United States dollar

XylBINAP – 2,2'-bis[di(3,5-xylyl)phosphino]-1,1'-binaphthyl

$\Delta G^{\circ\ddagger}$ – standard Gibbs free energy of activation

$\Delta H^{\circ\ddagger}$ – standard enthalpy of activation

$\Delta S^{\circ\ddagger}$ – standard entropy of activation

Chapter 1

Introduction

Catalysis plays an important role in everyday life.[1] It is an essential technology utilized by many industries to maintain present-day standards of living and quality of life through the variety of products and energy related activities derived from its application.[2,3] By definition, catalysis is a process by which a substance, called a catalyst, accelerates the rate of a chemical reaction by lowering the activation energy of that reaction without itself being consumed during the reaction.[2] Catalysis is one of the principal drivers of the modern economy contributing greater than 35% of global gross domestic product (GDP).[4] Economically, the use of catalysis can significantly reduce waste streams, simplify synthetic procedures and reduced both cycle times and volume requirements, especially in chemical manufacturing. This in turn enables businesses to keep the costs to lower than the 0.1% of the sales revenue generated from the high-value products that they create.[4] Catalysis also allows businesses to reap the benefits associated with employing environmentally responsible manufacturing practices through utilizing one of the 12 principles of green chemistry.[5] In light of these advantages, it is projected that this materials industry will grow from $19.2 billion (USD) in 2012 to $24.1 billion (USD) by the end 2018 at a compound annual growth rate (CAGR) of 3.90%.[6]

The National Research Council, the working arm of the United States National Academies, highlighted catalysis as a field that deserves high priority.[7] Indeed, the significance of this field to both academia and industry has been recognized with the awarding of three Nobel prizes in chemistry in the first decade of this century: asymmetric hydrogenation and oxidation (2001; Knowles,

Noyori and Sharpless), metathesis (2005; Chauvin, Grubbs and Schrock), and cross coupling reactions (2010; Heck, Negishi and Suzuki).

Despite intense academic study only a few classes of catalytic reactions are applied in industry.[8] Among these are palladium-cross coupling reactions and hydrogenations. The former plays a pivotal role in the pharmaceutical industry. However, few large-scale applications exist for the production of agrochemicals, flavors and fragrances and monomers for polymers. For example, the Heck, Suzuki and Negishi cross-coupling reactions are used in the synthesis of prosulfuron (a herbicide), boscalid (a fungicide) and adapalene (a topical retinoid) by Syngenta, BASF and Galderma, respectively, Scheme 1-1–1-3.[9]

Scheme 1-1 *Synthesis of prosulfuron by Syngenta.*

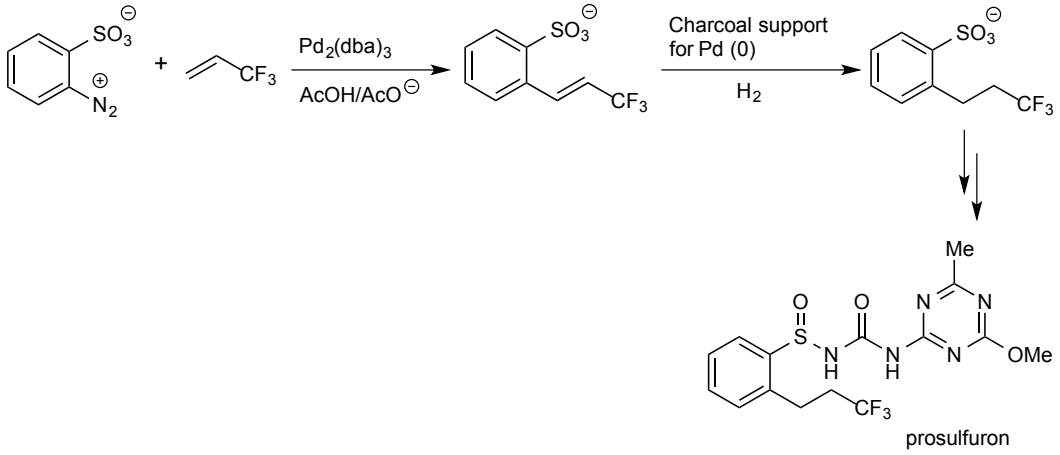

Scheme 1-2 *Synthesis of boscalid by BASF.*

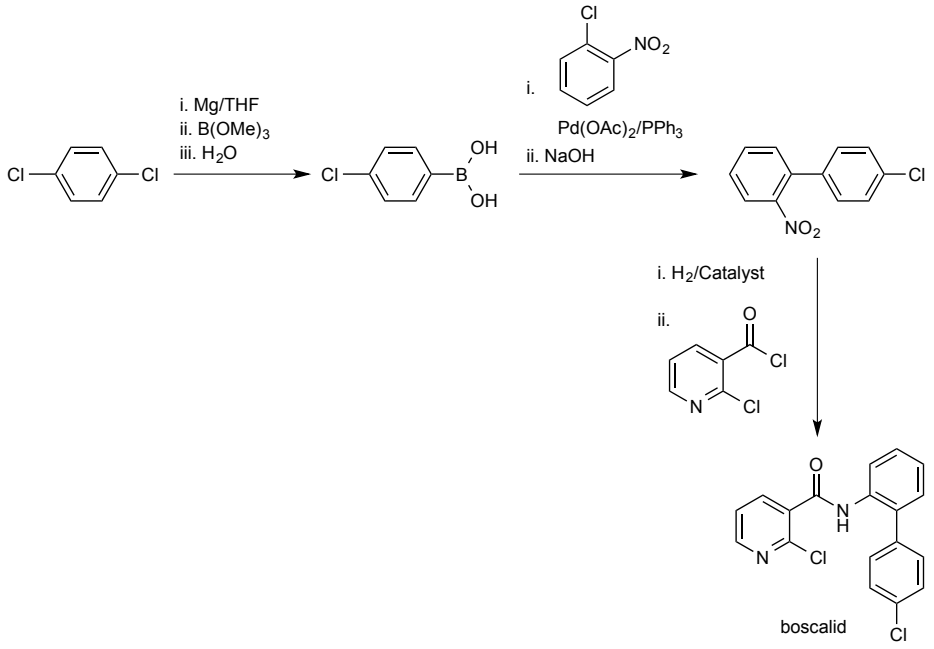

Scheme 1-3 *Synthesis of adapalene by Galderma.*

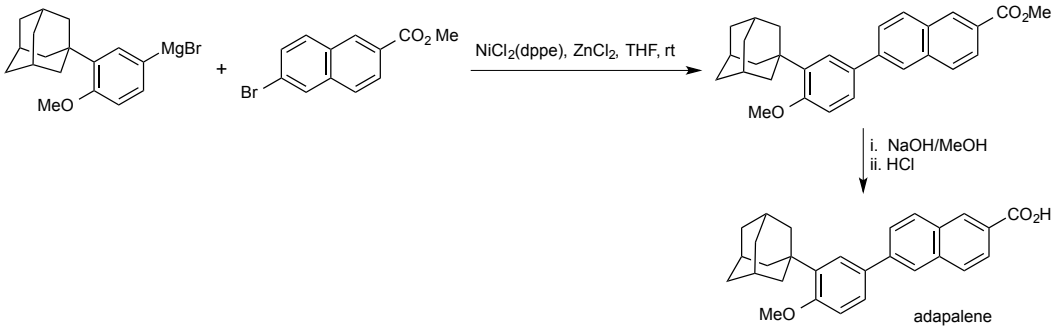

On the other hand, the selective catalytic hydrogenation of organic functional groups is arguably one of the most useful, versatile and acceptable methodologies available. In many respects, it can be considered a mature field in that:[10]

- a diverse number of ligands, catalyst precursors and molecular catalysts are commercially available in screening and/or technical quantities for academic research and industrial manufacturing,
- the catalysts, substrate scope, and inherent limitations (activity, functional group tolerance, productivity and selectivity) of this technology are well documented in the literature, and
- it is routinely considered as an efficient tool in the laboratory and industrial-scale synthesis of target molecules. Moreover, 10–20% of industrial chemical reactions are hydrogenations.

In addition to the above, there are several reasons why hydrogenation has been fully embraced by industry. From an operational perspective, hydrogen is a cheap, benign and atom-efficient reducing agent when compared to traditional methods that employ stoichiometric amounts of metal hydride reagents, such as $LiAlH_4$, $NaBH_4$, and their derivatives.[11] The technology requires limited operator retraining and minimal capital investment. Furthermore, dramatic improvements in the efficiency of chiral catalysts have been realized *i.e.* high turnover numbers (TONs) and turnover frequencies (TOFs) using low catalyst loading.[10] Some of these characteristics have been exemplified in the L-dopa process developed by Monsanto in the early 1970s.[12,13] The process was successfully applied to produce *L*-3,4-dihydroxyphenylalanine, a drug used for the relief of Parkinson's disease on *ca*. ton scale for many years. The key step in this transformation was the enantioselective hydrogenation of an enamide intermediate using a $[Rh((R,R)\text{-DIPAMP})(COD)]BF_4$ catalyst ((*R*,*R*)-DIPAMP: (*R*,*R*)-1,2-Bis[(2-methoxyphenyl)(phenylphosphino)]ethane, COD: 1, 5-cyclooctadiene) under *ca*. 10 atm H_2 at 25 °C in an $EtOH/H_2O$ mixture. The catalyst performance was

superior, even by today's standards, with an enantiomeric excess (*ee*) of 95%, TONs of 20,000 and TOFs of 1000 h^{-1}, Scheme 1-4.

Scheme 1-4 *Synthesis of L-dopa by Monsanto.*

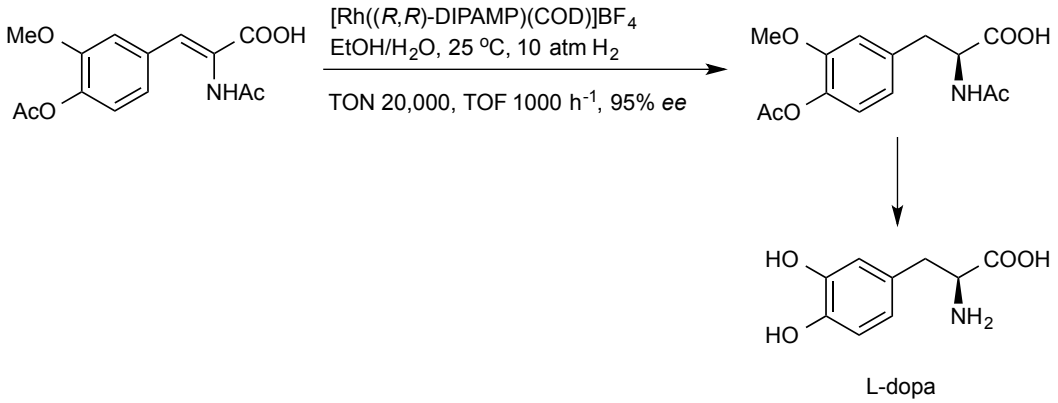

L-dopa

L-dopa is still produced at ton scale using the original process developed by Monsanto as well as by biotechnological methods. For example, Ajinomoto has reported a one-pot three-component synthesis of L-dopa using tyrosine phenol lyase (strain: *Erwinia herbicola*), Scheme 1-5. A key feature of this technology is the extremely high volumetric productivity of 110 g/L of the desired process. Annual capacity of this process is 250 tons.[14]

Scheme 1-5 *Production of L-dopa using tyrosine phenol lyase.*

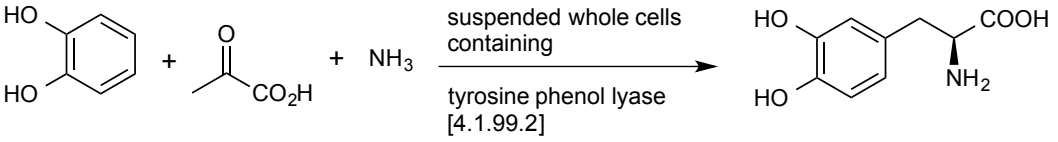

L-dopa

Further, hydrogenation has been embraced by industry because of new marketing guidelines concerning the commercialization of single enantiomer

drugs introduced by the United States Food and Drug Association (FDA). The idea behind this regulation was a shared view that the use of single enantiomer drugs would have substantially less adverse side effects and toxicity than racemates.[15] An example of this, is the case of levalbuterol, the (*R*)-(–)-isomer of the anti-asthma drug albuterol. The (*R*)-isomer was an effective treatment for asthma, whereas the (*S*)-isomer caused symptoms such as increased pulse rate, tremors and decreases in blood glucose and potassium levels. Industry has also found creative ways to use this FDA regulation to their advantage. For example, AstraZeneca initially marketed the antiulcer drug omeprazole (Prilosec) as a racemate. The company was able to extend the life of the drug by re-patenting the active (*S*)-isomer, esomeprazole (Nexium), saving a valuable revenue stream. It is noteworthy, that in some cases, it may not be beneficial to market single enantiomer drugs. For example, marketing racemic mixtures of rosiglitazone (Avandia) and fluoxetine (Prozac) is possible because the enantiomers of these drugs interconvert, and have synergistic pharmacological activities *in vivo*, respectively, Figure 1-1.

Figure 1-1 *Structure of albuterol, omeprazole, fluoxetine and rosiglitazone.*

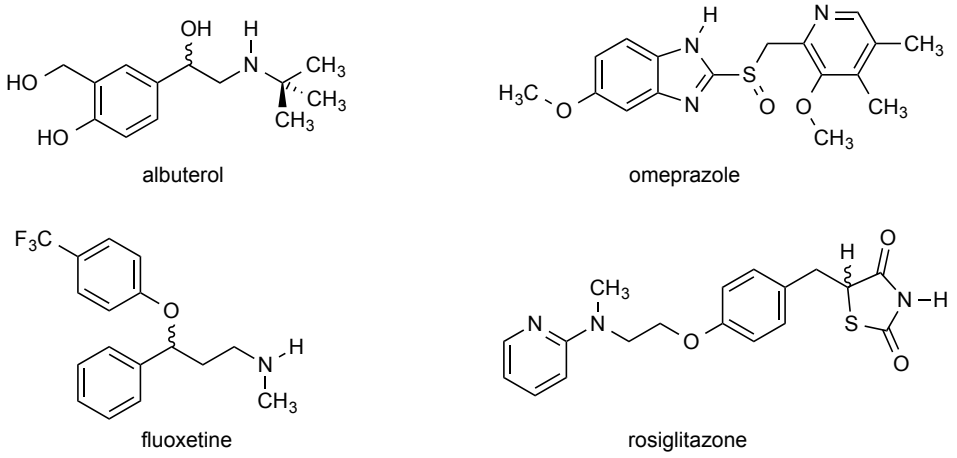

As can be seen from the examples shown above, transition metal catalyzed reactions have made a significant contribution to industry. In particular, a variety of stoichiometric and catalytic methods have now been reported using the Group 8 transition metal, ruthenium.[16] Indeed, it was only until the discovery of RuO_2 and $RuCl_2(PPh_3)_3$ (Scheme 1-6) as selective hydrogenation catalysts, that the impetus to develop Ru-based transition metal complexes as catalysts had been provided. A number of homogeneous Ru-containing systems are now known to reduce C=C, C=O and C=N functionalities with the level of sophistication required by both academia and industry.[17]

Scheme 1-6 *Hydrogenation of hept-1-ene or hex-1-yne by $RuCl_2(P(C_6H_5)_3)_3$.*

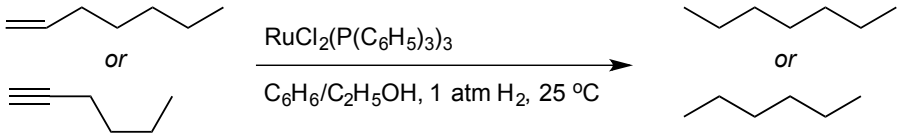

Since the discovery of metal hydride reducing agents by Brown and Schlesinger in the 1940s, a number of well-established procedures applying stoichiometric amounts of $NaBH_4$, $LiAlH_4$ and their derivatives have been reported for the chemo-, diastereo- and enantio-selective reduction of ketones.[18] In particular, $NaBH_4$, selectrides (hindered trialkylborohydrides) and chiral stoichiometric reducing agents such as BINAL-H, DIP chloride, alpine borane, and the Corey-Bakshi-Shibata (CBS) method, utilizing diborane or catecholborane and a chiral oxazaborolidine catalyst, have been shown to effect these transformations in high yields, Scheme 1-7–1-10.[19]

Scheme 1-7 *Enantioselective reduction of butyrophenone using (S)-BINAL-H.*

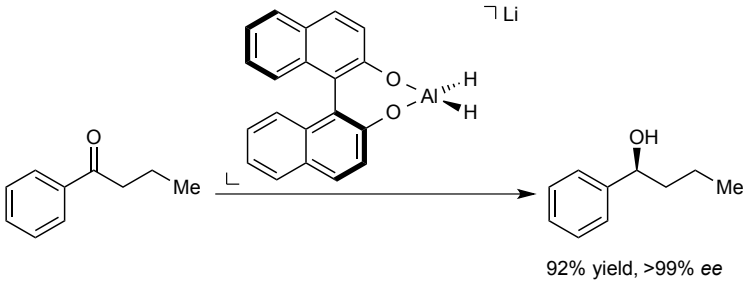

Scheme 1-8 *Enantioselective reduction of 3-chloropropiophenone using (–)-DIP chloride.*

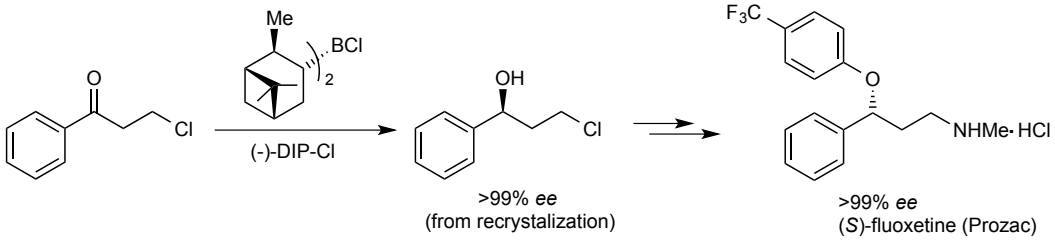

Scheme 1-9 *Enantioselective reduction of 2-methyl-4-hexyn-3-one using alpine borane.*

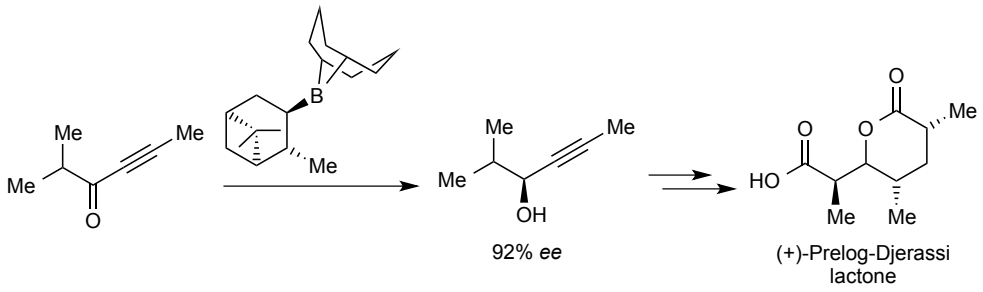

Scheme 1-10 *Enantioselective reduction of 2-(2,2-dimethoxyethyl)-2-cyclopentenone using the CBS method.*

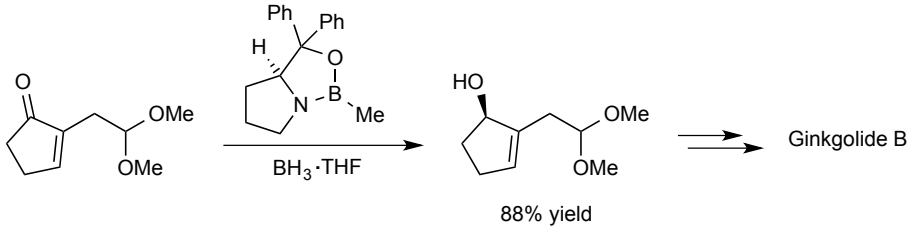

Prior to 1995, the enantioselective hydrogenation of simple unactivated ketones proved to be quite challenging. This stimulated the search for more sustainable strategies to access chiral alcohols that are essential to industry. A major breakthrough occurred when Noyori and coworkers discovered that $RuCl_2$(diphosphine)(diamine) complexes and base could catalyze the hydrogenation of prochiral ketones in high yields, TONs (>1,000,000), TOFs (>100 s) and *ee* in 2-PrOH.[20-26] For example, only 2.2 mg of *trans*-[$RuCl_2$((*R*)-TolBINAP)((*R*,*R*)-dpen)] (TolBINAP: 2,2′-Bis(di-*p*-tolylphosphino)-1,1′-binaphthyl, dpen: (1*R*,2*R*)-(+)-1,2-diphenylethylenedamine) and 5.6 g KO*t*-Bu is needed to quantitatively produce 611 g of 1-phenylethanol in 80% *ee* from 601 g acetophenone under 45 atm H_2 at 30 °C for 48 h in 2-PrOH, Eq. 1-1.

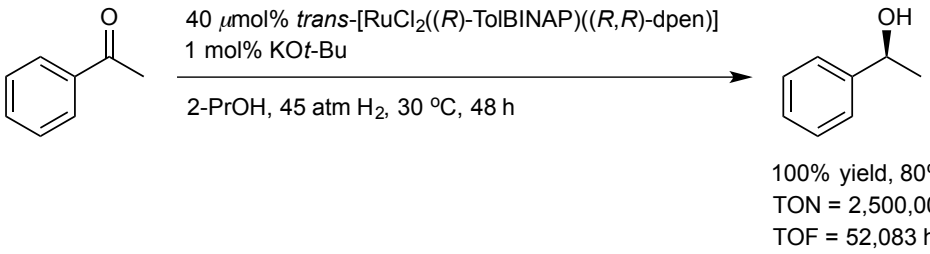

1-1

Furthermore, a wide variety of alkyl arylketones, fluoroketones, diarylketones, heteroaromatic ketones, dialkylketones and unsaturated ketones can be hydrogenated to give the corresponding secondary alcohols with excellent chemo-, diastereo- and enantio-selectivities using the appropriate chiral diphosphine/diamine Ru-complexes. Among the many described catalyst systems, the combination of *trans*-[$RuCl_2$((*R*)-XylBINAP)((*R*,*R*)-daipen)] (XylBINAP: 2,2′-bis[di(3,5-xylyl)phosphino]-1,1′-binaphthyl, daipen: 1,1-bis(4-methoxyphenyl)-3-methyl-1,2-butanediamine)) and KO*t*-Bu (as base) has been

shown to exhibit remarkable selectivity >99% *ee*, with substrate to catalyst (S/C) ratios up to 100,000 under 1-10 atm H_2. Notably, it has been found that the steric and electronic influence of substituents on enantioselectivities are small while, increasing the steric bulk of the alkyl group and aromatic ring substituents in substrates tends to increase the degree of enantioselection.

The next major breakthrough occurred when Noyori and coworkers discovered ruthenium hydrido tetrahydrido complexes *e.g. trans*-[RuH(η^1-BH_4)(diphosphine)(diamine)], facilitates the hydrogenation of base sensitive substrates.[27] For example, (*R*)-glycidyl 3-acetylphenyl ether is quantitatively hydrogenated in the presence of *trans*-[RuH(η^1-BH_4)((*S*)-XylBINAP)((*S*,*S*)-dpen)] using 8 atm H_2 in 99% *ee*, leaving the base-labile epoxide ring intact. Remarkably, simply substituting the metal and/or phosphine and/or diamine ligands in this system has led to new bifunctional catalysts that can hydrogenate a wide range of ketones with high chemo- and enantio-selectivities, TONs and TOFs.[28-33]

Mechanism – Noyori asymmetric hydrogenation

Scheme 1-11 *Proposed mechanism for the hydrogenation of ketones using RuX_2(diphosphine) under acidic conditions.*

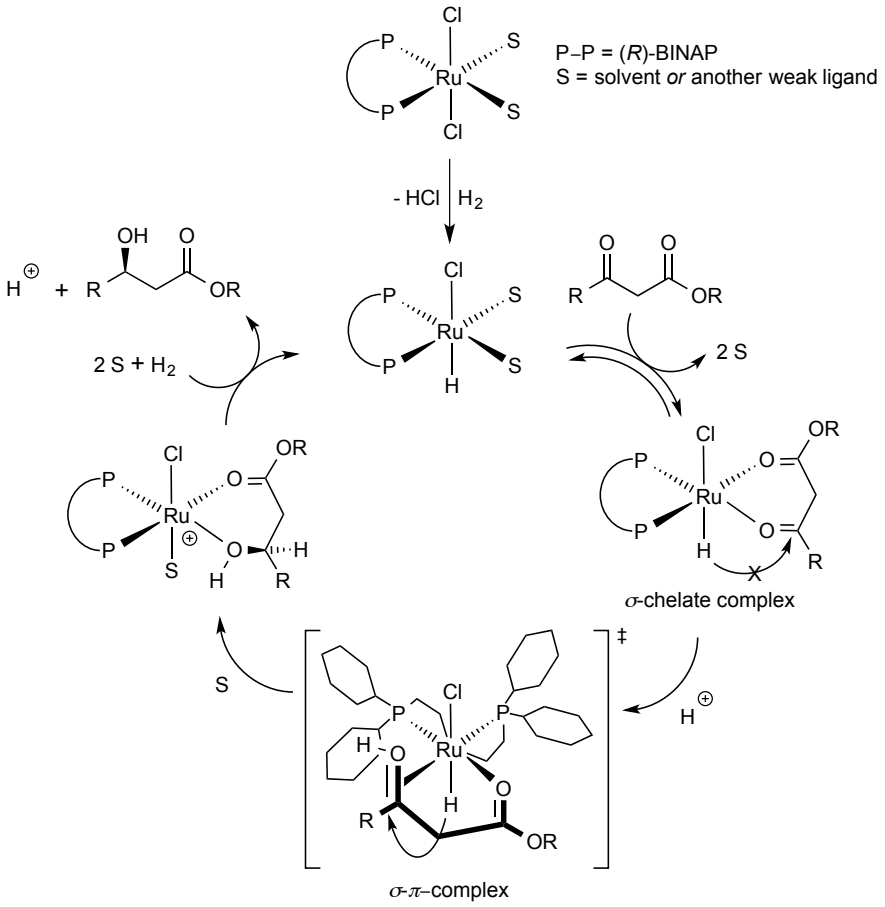

Scheme 1-11 illustrates the proposed catalytic cycle for the chemo- and enantio-selective hydrogenation of *β*-keto esters using Noyori's first generation catalysts under acidic conditions.[34] The mechanism was proposed to proceed via coordination of the ketone to form a *σ*-chelate complex whose geometry is unfavorable for M-H transfer. Ligand rearrangement to an η^2-*π*-ligand with protonation at the carbonyl oxygen (to render the carbonyl carbon more electrophilic) facilitates hydride migration to the carbonyl carbon.[35] Replacement

of the hydroxy ester with solvent molecules followed by catalyst regeneration completes the catalytic cycle. These constraints were used to explain the high reactivity and selectivity of these systems towards functionalized ketones versus weakly coordinating, non-functionalized ketones. It was also used to explain the poor C=O/C=C selectivity exhibited by these systems.

Daley and Bergens reported a mechanistic investigation into the enantioselective hydrogenation of ketones using the first generation catalyst model, $[RuH((R)\text{-BINAP})(CH_3CN)_n(sol)_{3-n}]BF_4$ (**1**) (sol = THF or CH_3OH) and dialkyl 3,3-dimethyoxaloactate ketones (alkyl = Me, *i*Pr_2 and *t*-Bu) as substates.[36] They described the first complete identification of diastereomeric Ru-alkoxides as the only observable intermediates (without prior coordination of the ketone as an η^2-π-ligand *cis* to the hydride) on mixing solutions of catalyst model and dialkyl 3,3-dimethyloxaloacetates starting at temperatures as low as –30 °C using NMR spectroscopy. These results illustrated that there is little impediment for ketone-hydride insertion for an analogous system in the absence of acid. Moreover, they concluded that the turnover-limiting step for the stoichiometric and catalytic reduction of dialkyl 3,3-dimethyloxaloacetates (under 50 atm H_2 at 50 °C) was the hydrogenolysis of the Ru-alkoxide to liberate free alcohol and regenerate the active catalyst. Consequently, they proposed that the possible role of acid (*e.g.* HBF_4·OEt) in these systems is to increase the rate of reaction by facilitating the protonolysis of the Ru–O bond.

Scheme 1-12 *General mechanism for the hydrogenation of ketones using trans-[$RuCl_2$((R)-BINAP)((R,R)-dpen)] and base.*

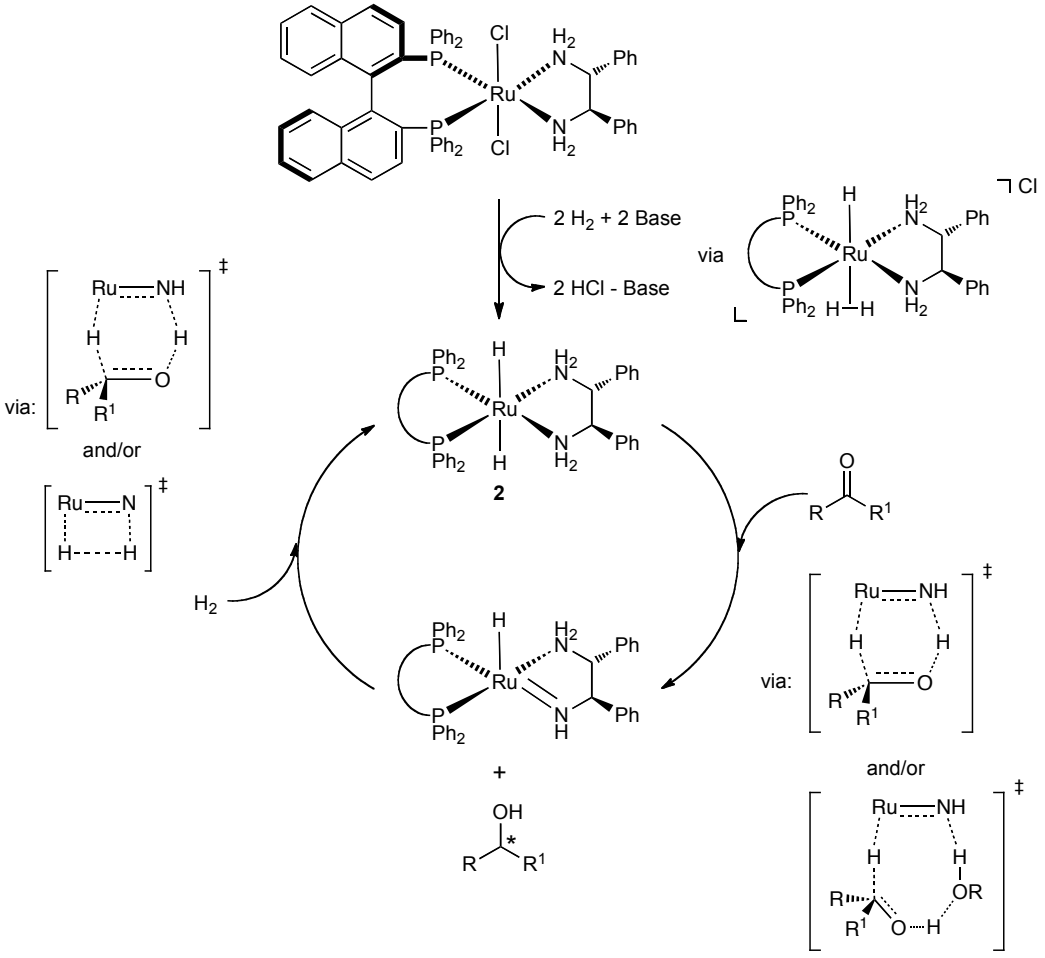

In contrast, saturated 18-electron complexes such as *trans*-Ru[((*R*)-BINAP)[(*R*,*R*)-dpen)], **2**, (Scheme 1-12), which are substantially more active due to the mutual *trans* disposition of the hydride ligands do not require ketone coordination prior to reduction.[37-47] Rather, a non-classical, outer sphere ligand assisted bifunctional mechanism is assumed to operate.[42] This process was first proposed to proceed by the concerted addition of a nucleophilic hydride on ruthenium and a protic hydrogen on nitrogen, to the carbon and oxygen of the carbonyl group assisted by an activating C=O---H–N hydrogen bond to form the

product alcohol and Ru-amide, (Ru=N). Moreover, it was suggested that the pericyclic nature of this transition state minimizes conformational freedom of the ketone, thereby maximizing net asymmetric induction and accounting for the high C=O versus C=C selectivity of the reaction. The resulting five-coordinate Ru-amide can then react with H_2 (or via a sacrificial hydrogen donor *e.g.* formate, $[HCOO][NHEt_3]$ or 2-PrOH in transfer hydrogenation)[32,48-50] to regenerate the active catalyst.

Scheme 1-13 *Pathways for the formation of the model complexes,* ***3*** *and* ***4****.*

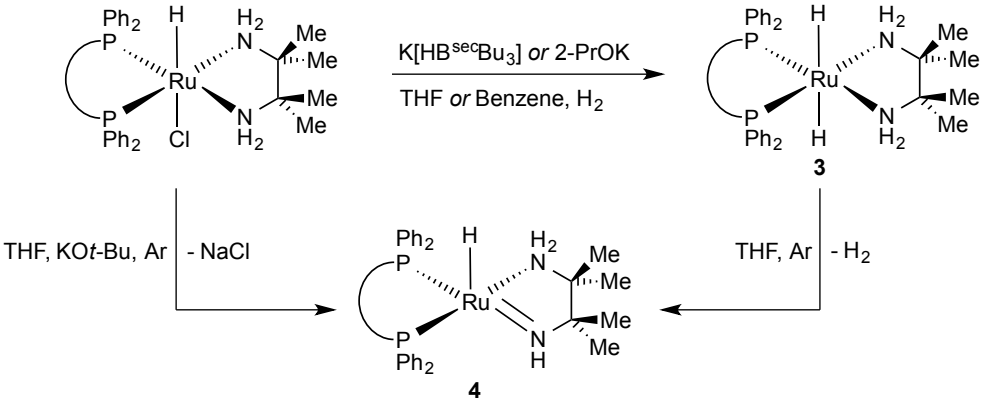

This early mechanism was supported in part by stoichiometric reactions and calculations put forward by Morris and coworkers.[37,39] Specifically, they synthesized the model catalyst, *trans*-$[Ru(H)_2((R)\text{-BINAP})(tmen)$, **3** (tmen: $H_2N(CMe_2)_2NH_2$), that contained the *cis*-Ru-H-NH motif that is proposed to be of fundamental importance to the mechanism of the bifunctional addition, Scheme 1-13.

Morris and coworkers reported that the model catalyst **3** reacts with 1 equiv. of acetophenone on mixing at room temperature in the absence of base and H_2 to form 1-phenylethanol and the corresponding Ru-amide, **4**, in C_6D_6. This

was predicted by the original mechanism for the bifunctional addition, Eq. 1-2. This reactivity was supported by the immediate color change of the dihydride solution upon the addition of acetophenone, as well as the subsequent appearance of the ^{1}H NMR resonances for **4**. Moreover, they reported that **4** could activate H_2 at temperatures as low as –60 °C (no rate data given) to regenerate the active catalyst, **3**. They proposed that the products of this addition were in equilibrium (K_{eq} not given) with an alcohol-amide adduct, **5**, Scheme. 1-14. Compound **5** was not characterized but was proposed based on broadened Ru-amide ^{1}H NMR resonances, as well as support from DFT calculations between the model amide, $RuH(HN(CMe_2)_2NH_2)(PH_3)_2$ and acetone.

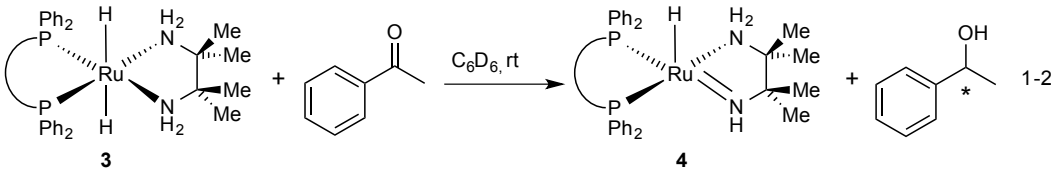

Scheme 1-14 *Proposed pathway for the formation of* ***5.***

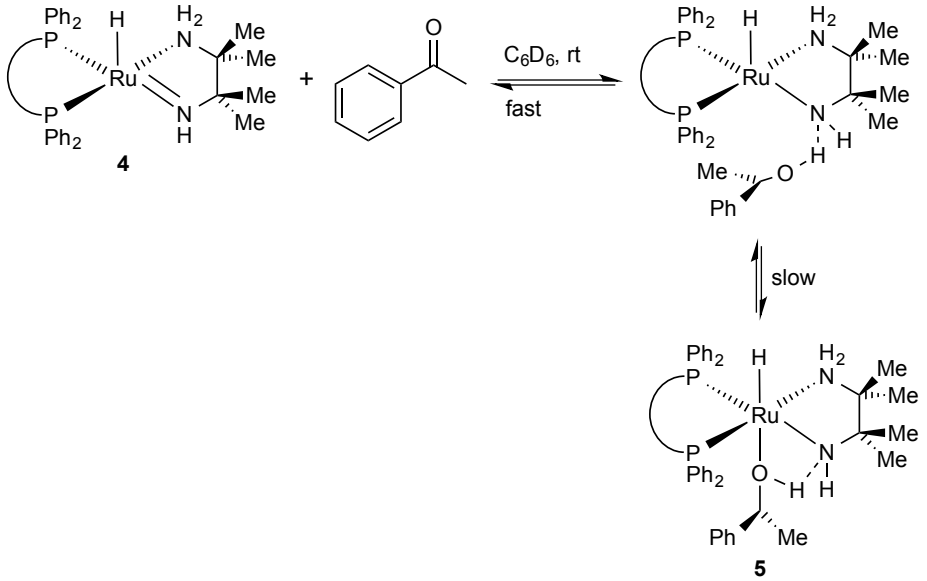

Interestingly, the addition of 20 equiv. of acetophenone to $RuH(HN(CMe_2)_2NH_2)(PPh_3)_2$, **6**, also results in a similar broadening and lower field shift of the hydride NMR resonance. Consistent with the previous discussion, they attributed these results to the fast rate of exchange between the alcohol adduct, $RuH(HN(CMe_2)_2NH_2)(HOCH(Me)(Ph))(PPh_3)_2$, **7**, and the Ru-amide, **6**, and the free alcohol. The identity of **7** was not unambiguously assigned, but was proposed to be bound to ruthenium by either the oxygen atom, **7a**, or via a C–H agostic interaction with the metal center, **7b**, Scheme 1-15.

Scheme 1-15 *Proposed structures for the alcohol-amide adduct,* ***7****.*

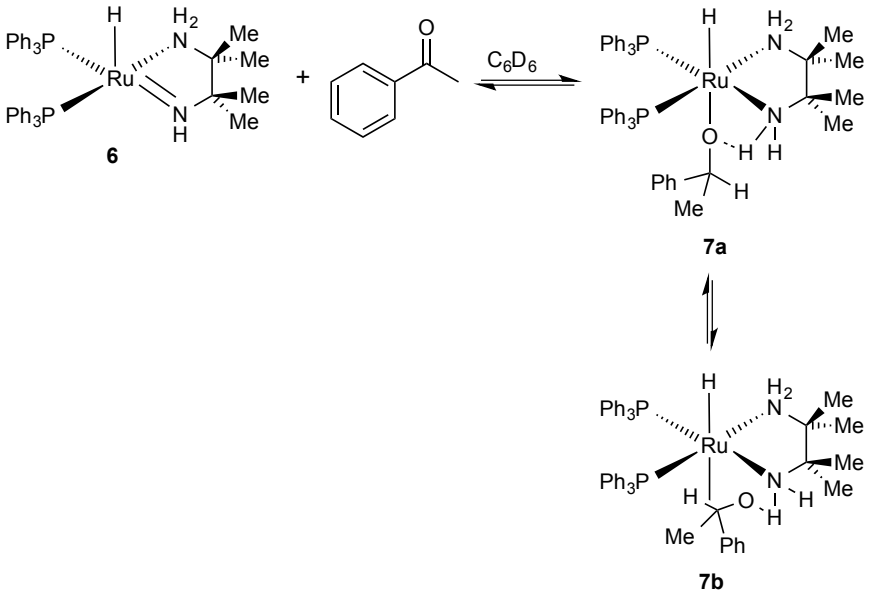

The alcohol adducts were proposed to be in a slow equilibrium (K_{eq} not given) with the Ru-alkoxide species. Notably the Ru-amide, **6**, containing the PPh_3 ligands were studied and not **4**, which contains the (*R*)-BINAP ligand, Eq. 1-3. Only the hydride and phosphorous resonances were used to characterize the alkoxide, **8**.

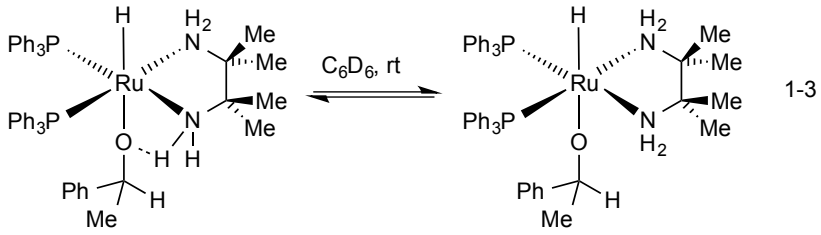

Morris and coworkers also observed that **4** (as well as **6**) will react with excess acetophenone to form an oxygen bound Ru-enolate, **10**. It was suggested that these species were formed from the facile deprotonation of the aliphatic C-H of an undetected ketone-amide adduct, **9**, Scheme 1-16. Notably, complex **10** was identified by two signals for the inequivalent hydrogens in the CH_2 group in the ^{1}H NMR as well as the independent carbon resonances in the $^{13}C\{^{1}H\}$ NMR.

Scheme 1-16 *Proposed pathway for the formation of* ***10****.*

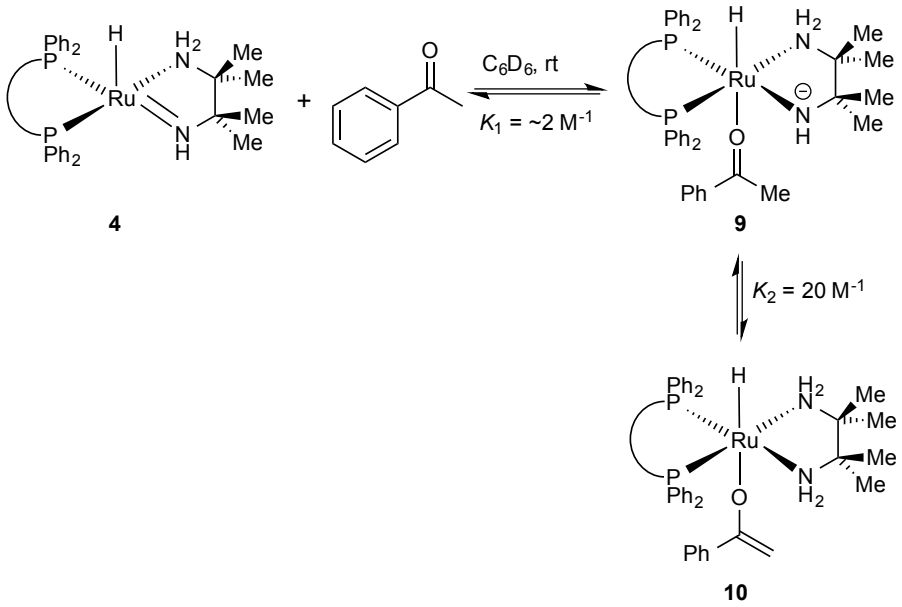

Morris and coworkers also proposed that diastereomeric Ru-alkoxides *i.e.* (*R*)- and (*S*)- *trans*-[RuH(OCH(Me)(Ph)((*R*)-BINAP)(tmen)], could be prepared

from the addition of (*S*)-1-phenylethanol (90% *ee*) to solutions of the model dihydride, **3**, at room temperature in C_6D_6 (based on the broadening of the ^1H NMR resonances of **3**). Specifically, the authors suggested that the alcohol protonates the dihydride to form **11**, which is subsequently transformed into an η^2-H_2 compound that is ion-paired with 1-phenylethoxide, **12**. Displacement of the weakly-coordinated η^2-H_2 ligand by 1-phenylethoxide gives the diastereomeric alkoxides, **13**, Scheme 1-17. The authors also suggested that the equilibrium shifts towards **13** if more alcohol is added, while the addition of a strong base regenerates the dihydride, **3**. Based on these proposals, as well as computational studies, they recommended a mechanism consistent to that shown in Scheme 1-12.

Scheme 1-17 *Proposed pathway for the formation of the diastereomeric alkoxides.*

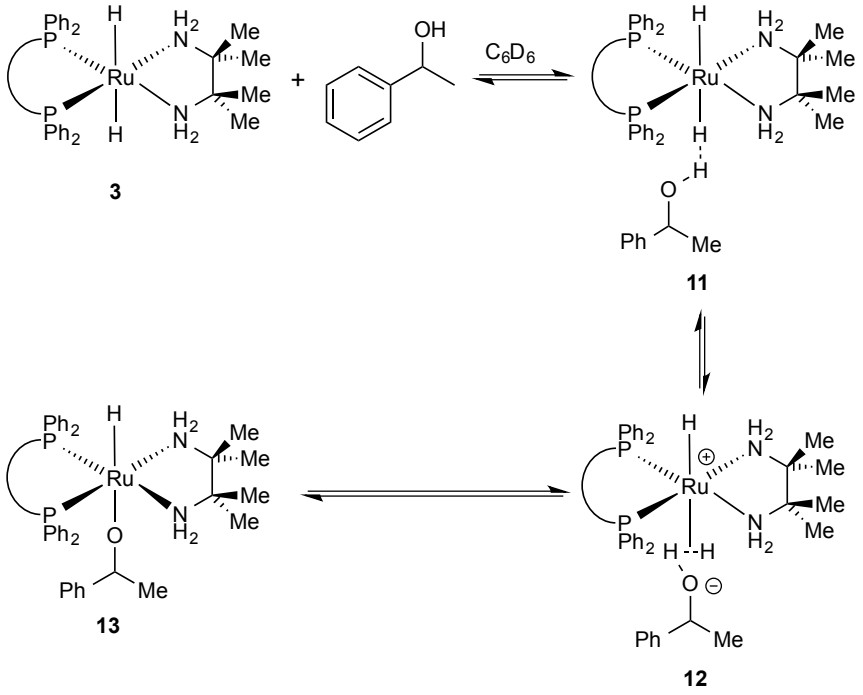

Modified dihydrogen splitting transition states have also been proposed to account for Lewis acid co-catalysts being essential to the high activity of Noyori-type catalysts.[38,41] In addition, alcohols such as 2-propanol and ethanol were suggested to be the best solvents for the hydrogenation of arylketones using ruthenium hydride complexes as catalysts.[51] In 2001, Hartmann and Chen showed that 2-PrOH solutions of **2**, in the presence of excess DBU (DBU: 1,8-diazabicyclo[5.4.0]undec-7-ene) were not sufficient to effect the catalytic hydrogenation of acetophenone.[38,41] Rather, a source of alkali metal cations was also necessary for high activity of these systems. Kinetic experiments employing complexing crown ethers, *e.g.* [18]crown-6 ([18]crown-6: 1,4,7,10,13,16-hexaoxacyclooctadecane), showed that the relative rate of H_2 consumption during the catalytic hydrogenation of acetophenone was influenced by the identity (K > Na ~ Rb > Li) and increased with concentration of alkali metal cations at constant concentration of base. The surprising dependence of rate on the presence of alkali metal cations was attributed to a mechanism in which a cation-binding site in the Ru-amide led to an enhanced cleavage of coordinated H_2. Specifically, it was proposed that an axially coordinated group 1 cation on the nitrogen atom of the Ru-amide would withdraw electron density from the Ru center, rendering the η^2-H_2 ligand more acidic. This consequently places the alkoxide in an ideal position to deprotonate the coordinated η^2-H_2 ligand though a six-membered cyclic transition state, Scheme 1-18.

Scheme 1-18 *Mechanism for dihydrogen activation proposed by Hartmann and Chen.*

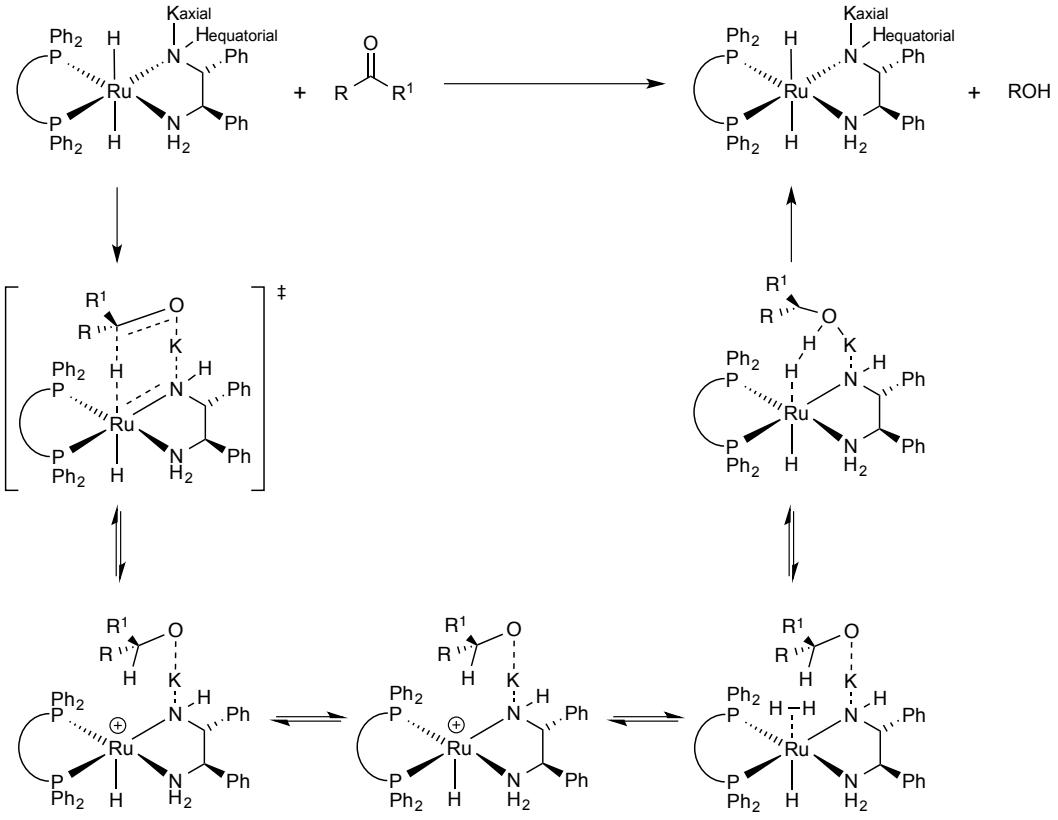

Notably, no putative intermediates were observed. Subsequent studies by Morris and Noyori were unable to confirm this pathway (*vide supra*).[39,40] For example, Morris and coworkers observed no significant rate enhancement when KO*t*-Bu was added to a ketone solution in benzene. They suggested that a possible role for the K^+ could be to precipitate the corresponding potassium salt. A similar role was suggested for Na^+ in the formation of hydrido-chloro Group 8 complexes from dichloro-complexes under an atmosphere of H_2.

Ikariya and coworkers also suggested an alcohol-assisted dihydrogen-splitting transition state to account for the rapid scrambling observed during isotope-labeling experiments.[51] Specifically, they found that during the hydrogenation of 2,2-dimethylpropiophenone a significant proportion of the

deuterium was incorporated into the solvent instead of the benzylic position of 2,2-dimethyl-phenyl-1-propanol (~7%). They calculated the H/D exchange to be greater than four times that of the catalytic hydrogenation (146 versus 33 h^{-1}, respectively). Notably, replacing $(CH_3)_2CDOH$ with $(CH_3)_2CHOD$ and D_2 resulted in an alcohol product with >90% deuterium content at the benzylic carbon. These results suggest a rapid reversible rate of hydrogen atom exchange between deuterium and the solvent prior to the reduction of the ketone. This scrambling presumably proceeds via the interconversion of Cp*Ru(amido)(η^2-D_2), **14**, and Cp*Ru(amine)D, **15**, Scheme 1-19.

Scheme 1-19 *Alcohol-assisted dihydrogen splitting transition state proposed by Ikariya and coworkers.*

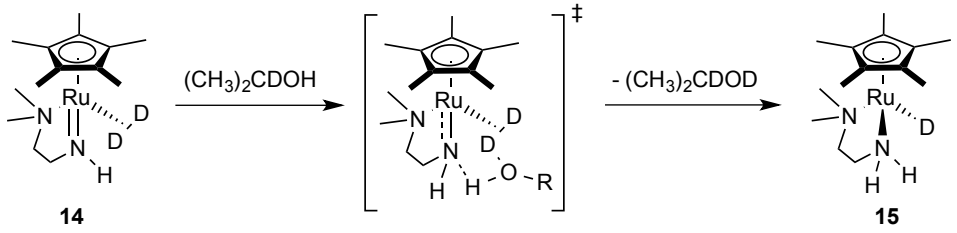

14 **15**

A similar alcohol-assisted transition state was also proposed by Morris and coworkers during a kinetic study describing the hydrogenation of acetophenone by [RuH((*R*)-BINAP)(app)], **16** (app: $HNCMe_2C_5H_4N$), under 5 atm H_2 at 22 °C in benzene.[52] Kinetic experiments using **16** showed a significant acceleration in reaction rate due to the presence of product alcohol formed during the catalytic hydrogenation. The authors also observed increased initial rates upon the addition of racemic 2-phenylethanol or 2-PrOH (somewhat less dramatic) to the reaction mixture under similar conditions. Moreover, the authors state that **16** exhibits atypical behavior in that it does not react with 1 atm H_2 at 22

°C in C_6D_6 to regenerate the active catalyst. Based on these observations the authors propose that the presence of the alcohol lowers the energy barrier for dihydrogen cleavage by hydrogen bonding to the protic N–H and cationic Ru-η^2-H_2 species, **17**, then acting as a proton acceptor, **18**, to regenerate the active catalyst, **19**, Scheme 1-20.

Scheme 1-20 *Proposed mechanism for alcohol-assisted dihydrogen cleavage using RuH_2((R)-BINAP)(app).*

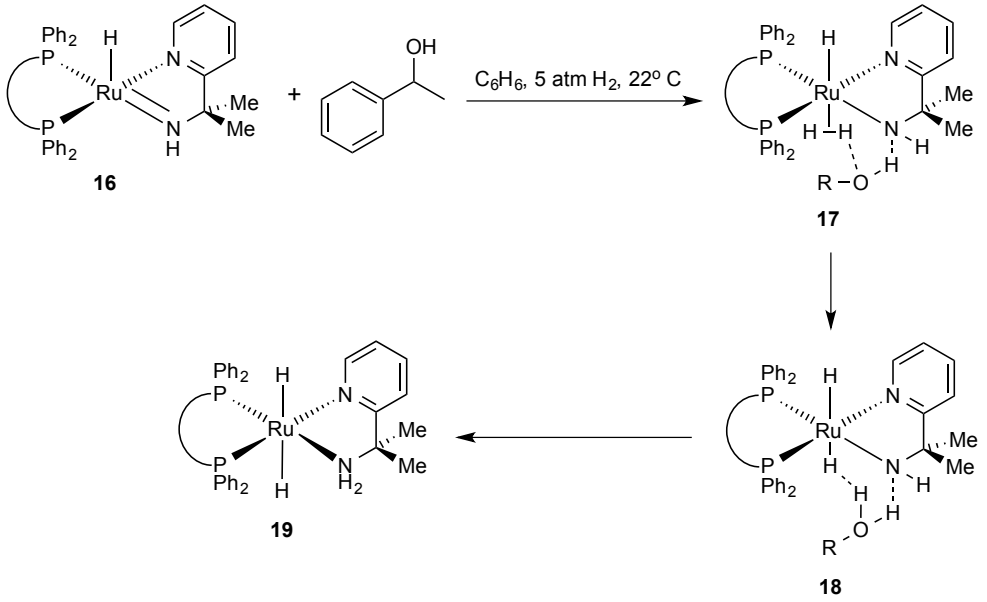

A recent computational study by Meijer and coworkers on the addition of formaldehyde to the catalyst model [$RuH(OCH_2CH_2NH_2)(\eta^2$-$C_6H_6)$] suggested that hydrogen bonding could also result in pathways that differ from the established mechanism.[53] One such pathway generates the reduced product as an alkoxide that is hydrogen bonded to alcoholic solvent molecules. The solvent molecules are then proposed to shuttle a proton from the N-H group to the alkoxide to generate the Ru-amide and product alcohol. Calculations by Morris

and coworkers have suggested an alternative pathway in which a transition state, containing an alkoxide that is hydrogen bonded to the solvent molecules collapses to form a stable Ru-alkoxide adduct.[52] Several other theoretical studies have found Ru-alkoxides to be the most stable species in their calculations.

Noyori and coworkers studied the mechanism of the asymmetric hydrogenation of ketones using BINAP/1,2-diamine Ru(II) complexes with [RuH(η^1-BH_4)((*R*)-TolBINAP)((*R*,*R*)-dpen)], **20**, a pre-catalyst, which was shown to be highly active in both the absence and presence of inorganic base.[40] Based on results of kinetic, mass spectrometric and kinetic isotope experiments, they proposed a multi-tier mechanism for the catalytic hydrogenation of ketones to account for these findings at varying concentrations of base, Scheme 1-21.

Scheme 1-21 *Mechanism for the hydrogenation of ketones described by Noyori and coworkers.*

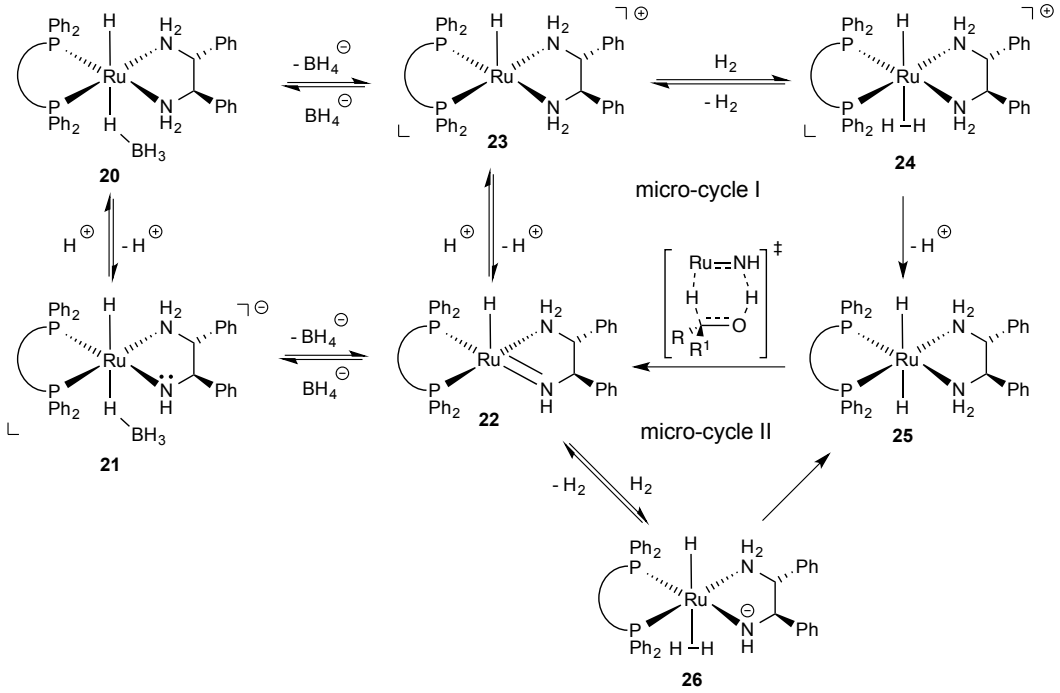

For example, at low concentrations of base, [KO*t*-Bu] = 10–15 mM, **20** was activated towards the hydrogenation via a different pathway compared to that under base-free conditions. Specifically, it was proposed that the addition of base would lead to the deprotonation of one of the protic N–H groups in the dpen moiety of **20** to form *trans*-[RuH(η^1-BH_4)(HNCH(Ph)CH(Ph)NH_2)((*R*)-BINAP)], **21**. Dissociation of the η^1-BH_4 ligand from **21** yields the 5-coordinate Ru-amide, **22**. Protonation of **22** forms the coordinatively unsaturated 16-electron cationic Ru(II) complex, **23**. In the absence of base, however, **20** was proposed to be in equilibrium with **23**. Noyori and coworkers also noted that **23** could be stabilized by ion-pairing with $[RO]^-$ or $[BH_n(OR)_{4-n}]^-$ resulting from the complete or partial reaction of the dissociated BH_4^- ligand with alcoholic solvents. Complex **23** was also suggested to be in equilibrium with the cationic dihydrogen complex, **24**.

In micro-cycle I, the authors suggested that the dihydrogen ligand of **24** is sufficiently acidic to protonate 2-PrOH to generate the Ru-dihydride, **25**.[40,54] A kinetic study revealed that the rate of alcohol production under base free conditions did not depend on H_2 pressure (*i.e.* 1–16 atm) and that the deprotonation of **24** limits the turnover of the hydrogenation cycle. Once formed, the Ru-dihydride can hydrogenate a ketone to form the product alcohol and the Ru-amide, **22**. The neutral Ru-amide could then be protonated at the amido nitrogen to regenerate **23**, which subsequently reacts with H_2 to give **24** and complete the micro-cycle I.

The main difference between micro-cycle I and II is that the η^2-H_2 ligand of **24** is deprotonated by inorganic base rather than alcohol solvent to generate the Ru-dihydride, **25**. This facile deprotonation of the η^2-H_2 ligand by KO*t*-Bu has been used to explain the 25-fold rate enhancement compared to that under base

free conditions. A similar series of steps is proposed to complete this catalytic cycle.

At higher concentrations of base, [KO*t*-Bu] = 20–130 mM, the η^1-BH_4 adduct **20** is proposed to enter the catalytic cycle via a dissociative conjugate base elimination of BH_4^- similar to that of the low base-assisted pathway. In this pathway the Ru-dihydride is generated via micro-cycle II. The overall effect is to reduce the relative contribution of micro-cycle I, and by extension **23**'s contribution to the overall rate of the hydrogenation. Specifically, under high base conditions the Ru-amide is not protonated to form the cationic complex **23**. Rather, H_2 coordinates to the Ru-amide, **22**, to form [RuH((*R*,*R*)-NHCH(Ph)CH(Ph)NH_2)(η^2-H_2)((*R*)-BINAP)], **26**, which heterolytically cleaves the η^2-H_2 ligand to generate the active catalyst. Reduction of the ketone to form the product alcohol and Ru-amide, followed by H_2 coordination, completes this micro-cycle. The authors also suggest that in addition to the lower contribution of micro-cycle I, the coordinatively saturated amide complex is less reactive to H_2 than **23** explaining the lower observed enhancement in rate *i.e.* 4–5-fold increase at higher base concentrations.

Although many model compounds for the metal ligand bifunctional mechanism have been put forward by various groups, *e.g.* Casey (*vide infra*),[55-63] Chen, Morris, Noyori, etc., the most in-depth stoichiometric study into the use of BINAP/1,2-diamine Ru(II) complexes as catalysts for the asymmetric hydrogenation of ketones both in the presence and absence of base was reported by Hamilton and Bergens.[40,43,44]

As stated previously, Noyori *et al.* suggested that the base-free hydrogenation of aryl alkyl ketones proceeds through the cationic η^2-H_2 intermediate, **24**, using 2-PrOH as solvent.[40] The authors proposed that in the

absence of base the analogous ruthenium pre-catalyst, *trans*-RuH(η^1-BH_4)((*R*)-BINAP)((*R*,*R*)-dpen)], **27**, dissociates a BH_4^- ligand to form the Ru-solvento complex, *trans*-RuH(2-PrOH-d_8)((*R*)-BINAP)((*R*,*R*)-dpen)]$^+$, **28**, ion paired with either RO^- or $[BH_n(OR)_{4-n}]^-$ resulting from the reaction between 2-PrOH and BH_4^-. They then propose that the η^2-H_2 ligand of **28** is sufficiently acidic to protonate 2-PrOH solvent in a turnover-limiting step to generate 2-$PrOH_2^+$ and **2** as the active catalyst.[40,54] Complex **2** then hydrogenates the ketone to form the product alcohol and the Ru-amide, **29**. Protonation of the Ru-amide by 2-$PrOH_2^+$ regenerates the solvent complex, **30**, which then reversibly reacts with H_2 to form **28** completing the catalytic cycle, Scheme 1-22.

Scheme 1-22 *Simplified mechanism for base-free ketone hydrogenation.*

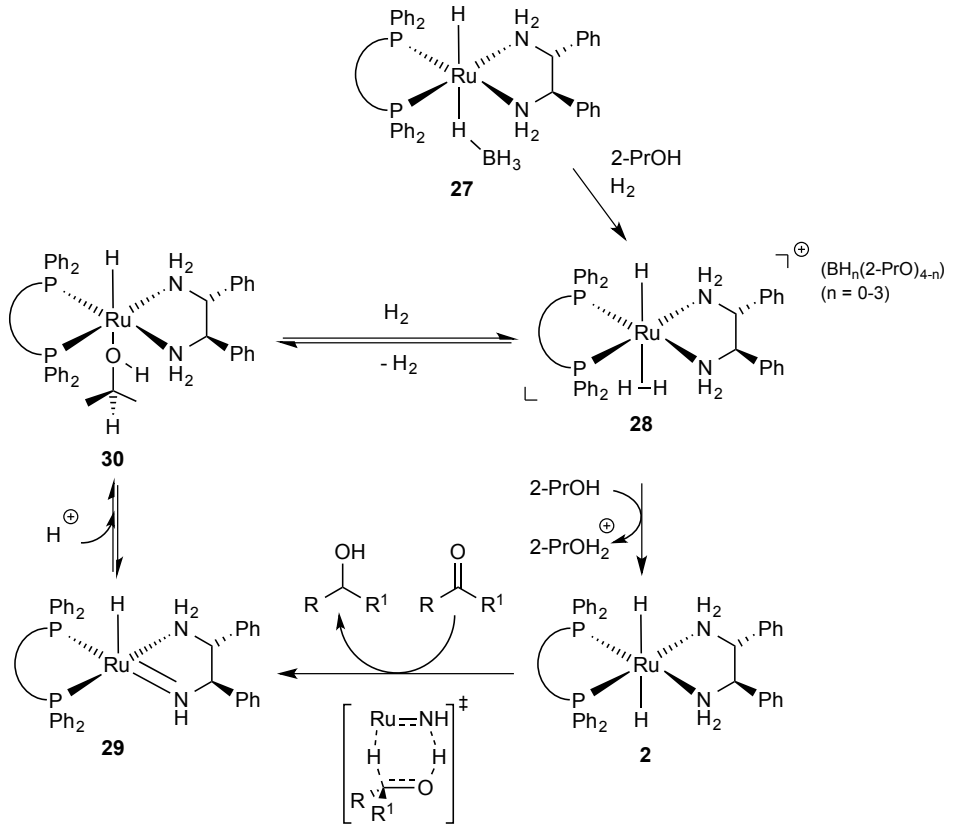

To investigate this mechanism Hamilton and Bergens independently prepared **28** by reacting a 1:1 mixture of *fac*-[RuH((*R*)-BINAP)(2-PrOH-d_8)$_3$]BF_4, **31**, with (*R*,*R*)-dpen at –60 °C under H_2 in 2-PrOH-d_8/CD_2Cl_2 (4:1 and 2:1 mixture), Eq. 1-4.[43,64,65] The η^2-H_2 ligand of **28** is very labile and has the shortest H–H bond distance reported to date. The η^2-H_2 ligand of **28** can also be easily displaced by D_2 to form *trans*-[RuH(η^2-D_2)((R)-BINAP)((R,R)-dpen)], **32**, at –60 °C. This substitution results in a sharpening and a shift of the *trans*-hydride signal to higher frequencies due to the difference in *trans*-influence of η^2-D_2 versus η^2-H_2.[66-69]

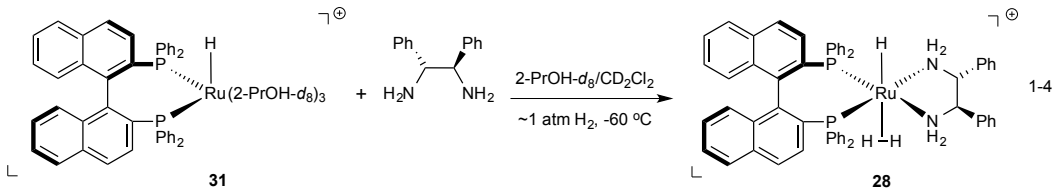

They showed that the η^2-H_2 ligand of **28** is not sufficiently acidic to protonate 2-PrOH at low temperatures.[43] However, the authors observed H-D exchange between 2-PrOH-d_8, the Ru-H and the η^2-H_2 groups upon warming to –20 °C. To investigate whether **28** could effect ketone hydrogenation, they carried out a stoichiometric reaction between **28** and acetophenone. They found no apparent reaction between a 1:1 mixture of **28** and acetophenone at –60 °C or upon warming to 0 °C. Under catalytic conditions only ~0.1% of acetophenone was hydrogenated to 1-phenylethanol (TON = 2) after 3 h using 0.05 mol% **28** under 4 atm H_2 at 30 °C in 2-PrOH, with little further improvement after 24 h. Thus, if **2** was formed it was not present in sufficient amounts to reduce acetophenone under these conditions. The authors also showed that $NaBH_4$ will

react with **28** via the displacement of the η^2-H_2 ligand upon warming to room temperature to form *trans*-RuH(η^1-BH_4)((*R*)- BINAP)((*R*,*R*)-dpen)], **27**, Eq. 1-5.

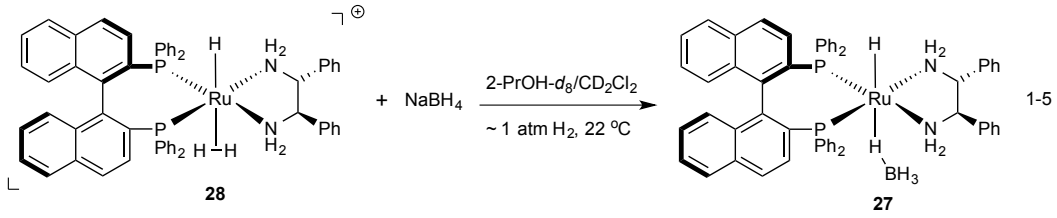

Surprisingly, **27** was found to hydrogenate acetophenone in 32% yield (TON = 640) after 3 h using 0.05 mol% Ru under 4 atm H_2 at 30 °C in 2-PrOH. Similarly, a 1:1 mixture of **28** and KO*t*-Bu was found to effect the hydrogenation of acetophenone in 78% yield (TON = 500) after 3 h using 0.16 mol% Ru.[26,27,40] Thus, **28** requires added base *e.g.* KO*t*-Bu or BH_4^- to be active towards ketone hydrogenation.[43]

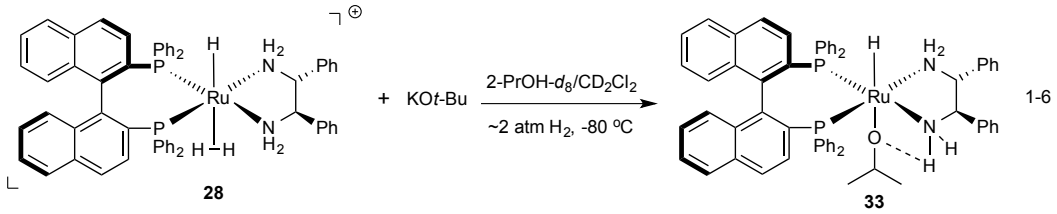

In a later study, they found that **28** reacts with 1 equiv. of KO*t*-Bu in 2-PrOH to form the alkoxide, *trans*-[RuH(2-PrO)((*R*)-BINAP)((*R*,*R*)-dpen)], **33**, instead of **2** at –80 °C, Eq. 1-6.[44] The rapid formation of **33** at –80 °C suggests that the reaction simply occurred by displacement of the labile η^2-H_2 ligand by 2-PrO^- formed by the reaction of base with 2- PrOH solvent. This observation negates the proposal by Morris and coworkers that 2-propoxide ion-pairs with

28.[39] Compound **33** was found to be remarkably stable and was readily characterized as well as isolated from THF-d_8.[44] Hamilton and Bergens attributed this stability to either a strong intra- or inter-molecular hydrogen bonding between the alkoxide oxygen, the N–H group of the amine and 2-PrOH solvent.[70] Bergman and coworkers observed similar intermolecular hydrogen bonding when phenols were added to rhodium-aryloxides.[71] Intermediate **33** was also remarkably stable towards dissolved H_2.[44] There was no evidence for the formation of **2** after prolonged exposures of **33** under ~2 atm H_2 at 22 °C for ~10 h in the absence of base, Eq. 1-7. Morris studies, on the other hand, infer that the dihydride, **3**, could be in equilibrium with the cationic Ru-solvento complex or the Ru-amide.[39] Further, recent calculations by Hasanayn and Morris suggest that alkoxides such as **33** have a higher affinity for H_2 than the Ru-amide, **29** (*vide infra*).[72]

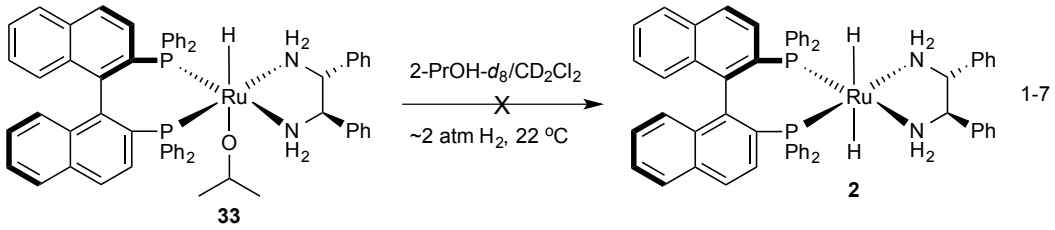

1-7

Hamilton and Bergens then opted to study the mechanism in THF-d_8 owing to the challenges with 2-PrOH-d_8. In particular, the Ru–H, Ru–η^2-H_2 and N–H groups all undergo rapid exchange with 2-PrOH-d_8 at room temperature thereby hindering the direct NMR observation of key steps in the catalytic cycle.[44] The authors reported that **28** could be prepared cleanly at –80 °C in THF-d_8. However, raising the reaction temperature revealed an equilibrium shift to the cationic Ru-solvento complex, *trans*-[RuH(THF-d_8)((*R*)-BINAP)((*R*,*R*)-dpen)], **34**,

Eq. 1-8. Notably, purging a solution of **28** in 2-PrOH with Ar at –60 °C does not give the expected solvento-complex. Rather, an unidentified Ru-species is formed (presumably by loss of H_2). This species does not regenerate **28** upon the addition of H_2.

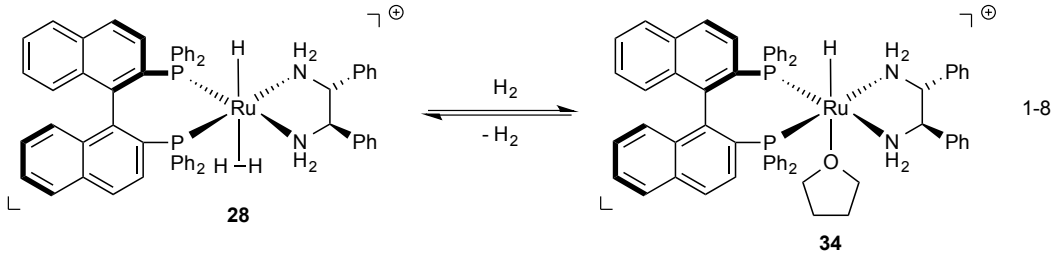

1-8

Reaction between a 1:1 mixture of **28** and KO*t*-Bu at –60 °C formed the Ru-hydroxide, *trans*-[RuH(OH)((*R*)-BINAP)((*R*,*R*)-dpen)], **35**, Eq. 1-9.[44] Later it was found that this reaction mixture was not completely dry (*vide infra*). The reactivity of **35** is analogous to **33** in that it is exceptionally stable and does not react with H_2 to form **2** even at elevated temperatures for prolonged periods.

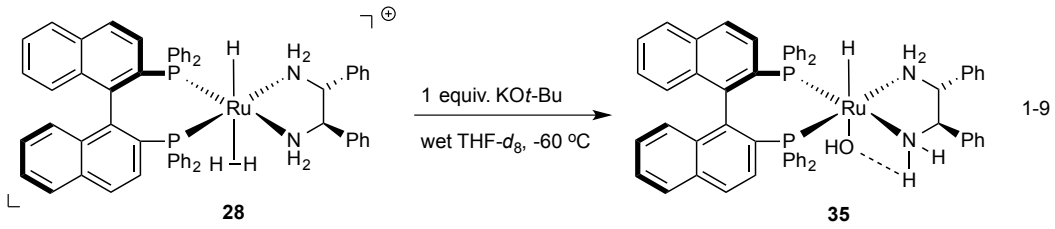

1-9

Intermediate **35** reacts with 1 equiv. excess KO*t*-Bu to form what was proposed to be a N···$H_{equatorial}$···O*t*-Bu hydrogen-bonded species, **36**. An analogous hydrogen-bonded species, **37**, is also formed with **33** under similar conditions. These species subsequently react with H_2 in <10 min to generate **2** at

–80 °C. Notably, this was the first conclusive identification of the active catalyst. The tentative assignments of the hydride and phosphorous resonances of **2** were reported by Morris and coworkers in C_6D_6.[37]

Scheme 1-23 *Synthesis of* ***2*** *from* ***35****.*

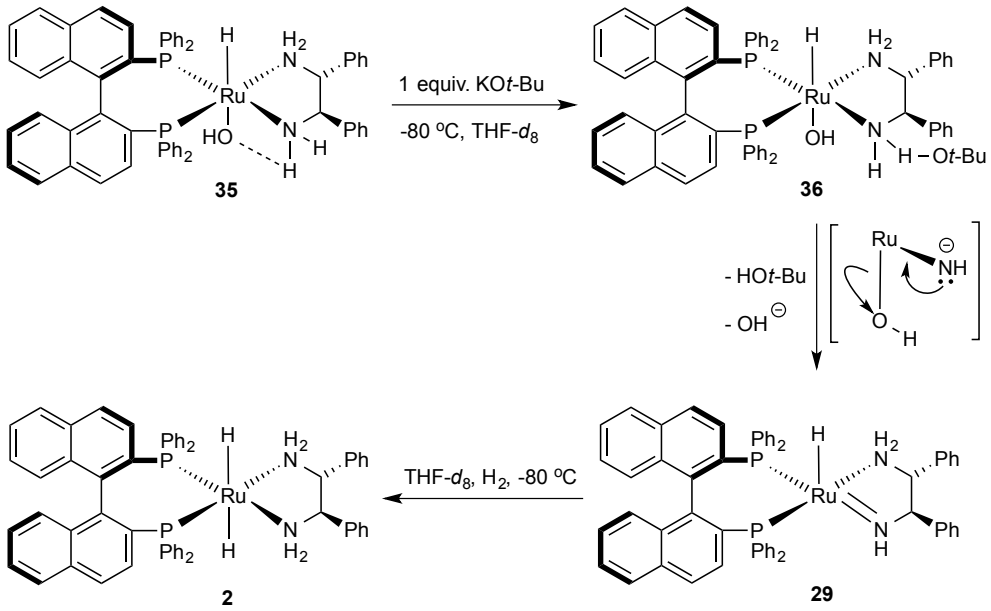

Hamilton and Bergens proposed that **2** is formed via the deprotonation of the hydrogen bonded N···$H_{equatorial}$···OR group in **33** or **36**, Scheme 1-23. An intramolecular elimination of the hydroxide or alkoxide ligand to form the Ru-amide, **29** follows. The amide then adds H_2 to form **2**.[44] Indeed, the authors found that **35** reacts with $KN[Si(CH_3)_3]_2$, a stronger more sterically hindered base, in the absence of H_2 in THF-d_8. Two diastereomers of the Ru-amide, **29**, are formed at –80 °C. Both adopt a trigonal-bipyramidal structure with a hydride *trans* to a phosphine, and with dpen occupying two equatorial positions. These diastereomers were proposed to differ by which diastereotopic nitrogen of the dpen ligand exists as the amide. Adding H_2 to a solution of **29** at –60 °C quickly

forms **2**. Moreover, the Ru-amide reacts rapidly with either 2-PrOH or H_2O to form **33** and **35**, respectively at –60 °C, Eq. 1-10.

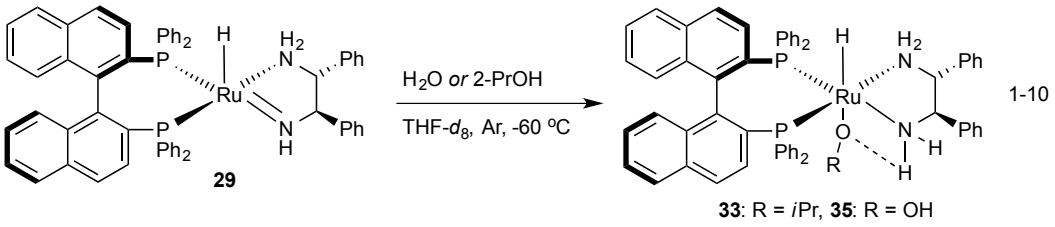

1-10

In contrast, Morris *et al.* proposed, on the basis of broad amide resonances that the analogous reaction between the model Ru-amide, **6** and 1-phenylethanol is slow, reversible, and does not go to completion under Ar at room temperature in C_6D_6.[39] The authors also state that increasing the ratio of 2-PrOH/C_6D_6 in solutions of **3** shifts the equilibrium of the reaction to produce more alkoxide. They then propose that the addition of strong bases such as KO*t*-Bu shifts this equilibrium towards the Ru-amide. This decreases the net acidity of the solvent and regenerates the dihydride under hydrogen.

The heterolytic cleavage of H_2 across the Ru-amide to generate *trans*-dihydrides such as **2** has been empirically and computationally shown to be the turnover-limiting step of the catalytic cycle (*vide supra*).[40,72] However, Hamilton and Bergens have shown that the addition of H_2 to **29** is facile at –80 °C.[44] Morris *et al.* have also stated that **4** is capable of adding H_2 at temperatures as low as –60 °C.[37] Together with the observation that **29** reacts rapidly with 2-PrOH at –60 °C, these results suggest that any free **29** formed during the catalytic hydrogenation is quickly intercepted by 2-PrOH to yield **33**.[44] Therefore, it is possible that the addition of hydrogen to **29** is turnover limiting in the presence of

excess base because the steady-state concentration of **29** is inherently low during the catalytic hydrogenation, Scheme 1-24.

Scheme 1-24 *Proposed pathway explaining the low steady-state concentration of* ***29*** *during the catalytic hydrogenation of acetophenone by* ***2*** *in 2-PrOH.*

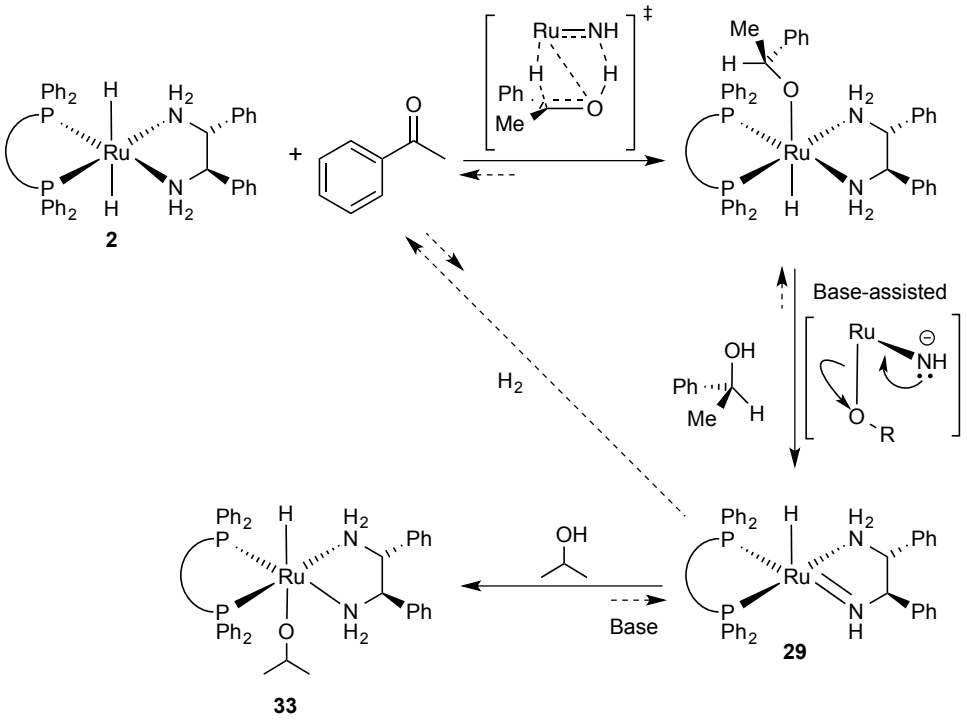

Further investigations into the possible role of base on the activity of the Noyori ketone hydrogenation catalyst led to the synthesis of two highly active intermediates resulting from the mono- or di-deprotonation of the N-H groups of the parent dihydride, **2**.[47] The mono-deprotonated dihydrides, *trans*-M[RuH_2((*R*,*R*)-HNCH(Ph)CH(Ph)NH_2)((*R*)-BINAP)], where M = K^+ and Li^+ (**38** and **39**, respectively) were prepared by reacting THF solutions of **2** with *n*-BuK or LiN[($Si(CH_3)_3)_2$] at –60 °C and –20 °C, respectively Eq. 1-11.

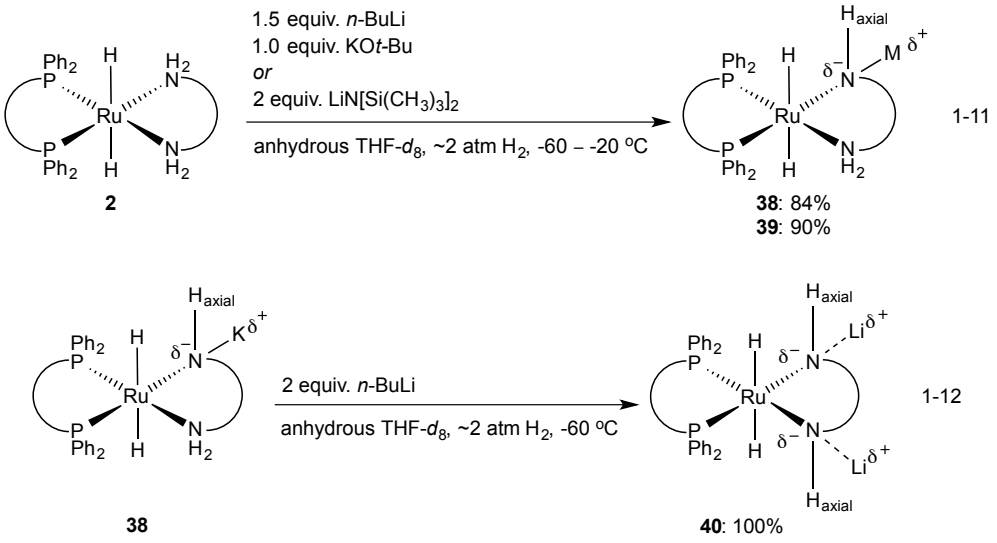

Remarkably, Bergens and coworkers found that the addition of 2 equiv. of *n*-BuLi to solutions of **38** resulted in a second deprotonation to form the *trans*-dihydride diamidate, *trans*-M_2[RuH_2((*R*,*R*)-HNCH(Ph)CH(Ph)NH)((*R*)-BINAP)], **40**, where M = Li^+, Eq. 1-12. Notably, these intermediates were not isolable but were fully characterized at various temperatures in anhydrous THF-d_8 using ^{1}H, ^{31}P{^{1}H}, ^{1}H–^{1}H gCOSY, ^{1}H–^{13}C gHSQC, ^{1}H–^{15}N gHSQC, TOSCY, and TROESY NMR experiments.

Interestingly, Bergens and coworkers observed many subtle differences between these intermediates and similar species that were proposed for ketone hydrogenations by Hartmann and Chen (*vide supra*).[38,47] First, they observed that the dihydrides were deprotonated at the equatorial positions rather than at the axial position. Second, they suggest that these species are predisposed to undergo a base-assisted elimination similar to that observed for **36** and **37** (*vide supra*). They also propose that these Ru-amidates are dramatically more active than the parent dihydride because the presence of the amidate group increases

the electron density at Ru, making the hydride ligand more nucleophilic to organic carbonyls at low temperatures in THF-d_8.

Hamilton and Bergens then investigated the addition of H_2 to acetophenone using **2** as a catalyst.[45] Contrary to expectation the addition did not form the expected Ru-amide and 1-phenylethanol (Morris *et al*. *vide supra*).[37,39] Instead, the alkoxide *trans*-[RuH(OCH(Me)(Ph))((*R*)-BINAP)((*R*,*R*)-dpen)], **41**, was formed on mixing acetophenone to a solution of **2** at –80 °C, Eq. 1-13.[45]

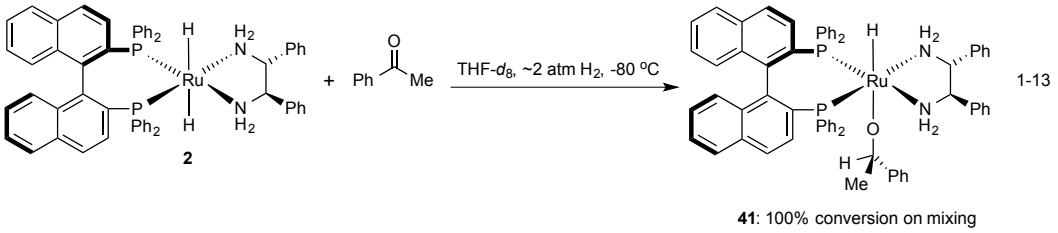

1-13

An analogous Ru-alkoxide was prepared by Baratta *et al*. via the stoichiometric reduction of benzophenone with the transfer hydrogenation catalyst, [RuH(CNN)(dppb)], **42** (HCNN: 6-(4'-methylphenyl)-2-pyridylmethylamine, dppb: $Ph_2P(CH_2)_4PPh_2$), at 20 °C in benzene.[70] The authors propose that the alkoxide **43** forms directly, rather than by the addition reaction between diphenylmethanol to the corresponding Ru-amide. They described a mechanism in which the ketone is activated towards nucleophilic attack by the hydride ligand through the formation of a hydrogen bond between the N-H group in the CNN ligand and the oxygen atom in benzophenone. Subsequent hydride transfer then forms an alkoxide ion that migrates to the Ru center to form the product alkoxide, Scheme 1-25 (top). Notably, the authors could not rule out the possibility that the alkoxide was formed via the dissociation of the NH_2

functionality to create a vacant coordination site followed by a conventional hydride transfer step, Scheme 1-25 (bottom).

Scheme 1-25 *Pathways for the formation of Ru-phenylmethoxide.*

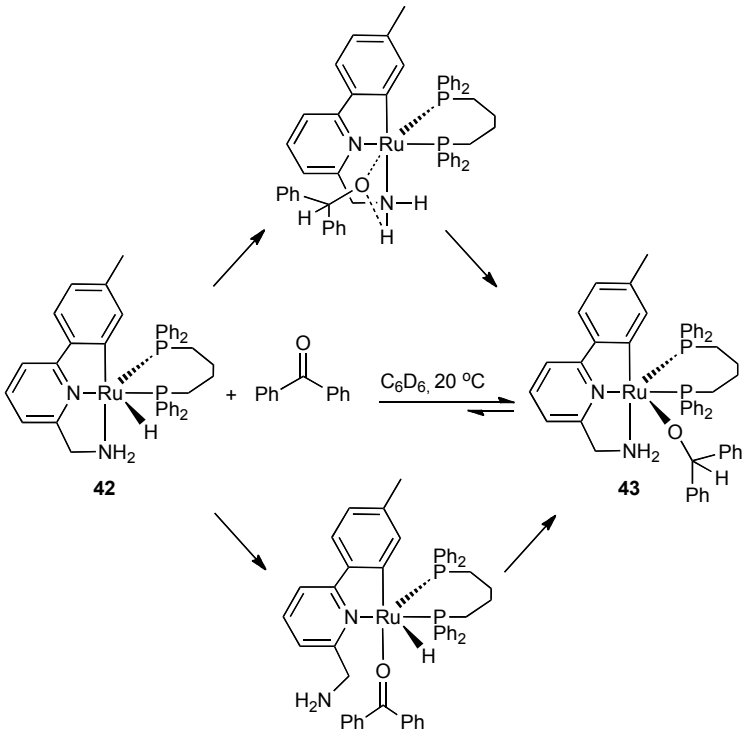

There are several possible explanations for the apparent contradictory results between the research groups of Bergens and Morris. They are the steric and electronic properties of the diamine ligands,[71,73-76] the difference between the reaction temperatures employed and the nature and identity of the reaction solvent. Firstly, the dpen ligand used in Bergens' study is less bulky than tmen used in Morris' report. Therefore the Ru center experiences more steric congestion in the latter work. Further, the methyl groups on the tmen ligand are more electron rich than the phenyl groups on dpen. As such they contribute more to pπ/dπ repulsion, in turn destabilizing the Ru-alkoxide bond. Secondly, the

room temperature reactions performed by Morris could also favor the intramolecular elimination of 1-phenylethanol from the corresponding model alkoxide.[39] Lastly, the THF solvent used by Bergens is a better hydrogen bond acceptor than benzene used by Morris, and could possibly stabilize intermediates during catalysis.

Interestingly, Morris *et al*. reported the preliminary ^{1}H and $^{31}P\{^{1}H\}$ NMR data for the corresponding diastereomeric alkoxides **13** prepared by the addition of (*S*)-1-phenylethanol, 90% *ee*, to the model dihydride, **3**.[39] Neither the ^{1}H nor $^{13}C\{^{1}H\}$ NMR data for the tmen and phenethoxide ligands of this alkoxide were reported. Approximately, 30% of the dihydride was converted into two diastereomeric alkoxides under these conditions, Scheme 1-26.

Scheme 1-26 *Morris et al.'s preparation of the model alkoxide.*

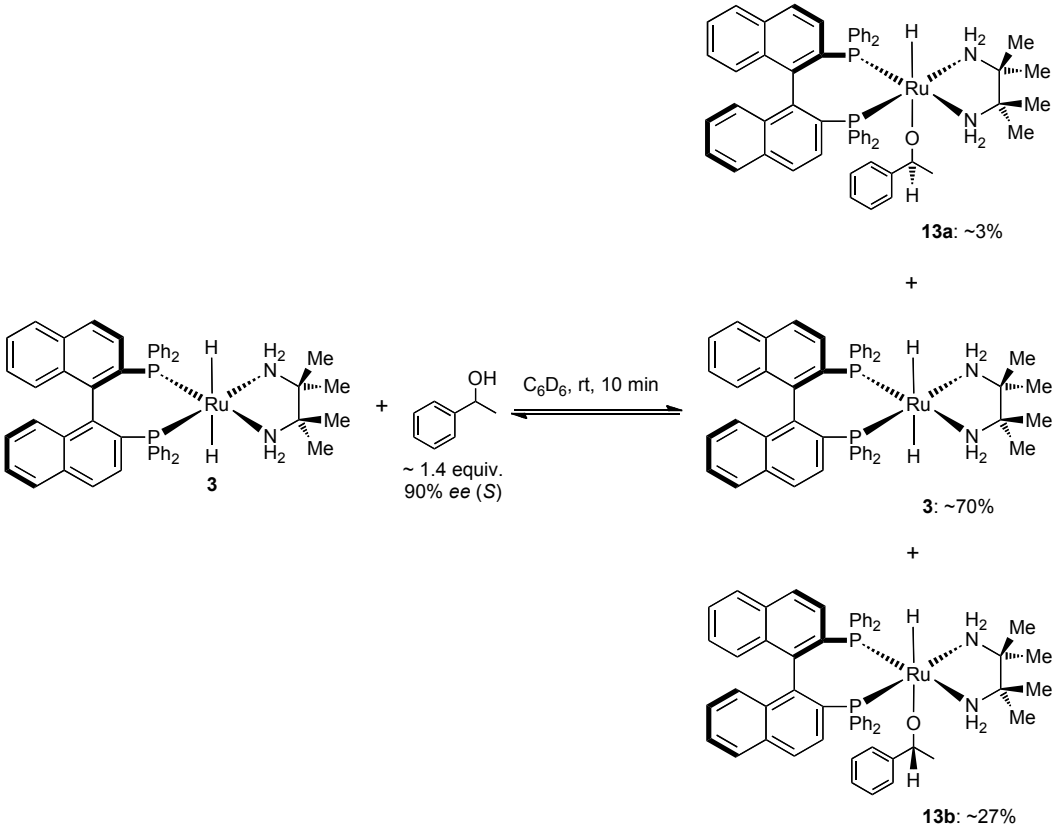

Morris and coworkers also proposed that the reaction between the model Ru-amide, **6**, and (*S*)-1-phenylethanol results in a slow 1:1 equilibrium mixture between the free alcohol/**6** and the corresponding Ru-alkoxide (**8**) via the unobserved alcohol adduct, **7**, Scheme 1-27.[39] This behavior is different from the formation of only one set of NMR signals observed by Hamilton and Bergens upon adding acetophenone to a solution of **2,** as well as the direct formation of **41** from **29** at low temperatures in THF-d_8 (*vide supra*).[45]

Scheme 1-27 *Summary of the reactivity of* ***6*** *with acetophenone.*

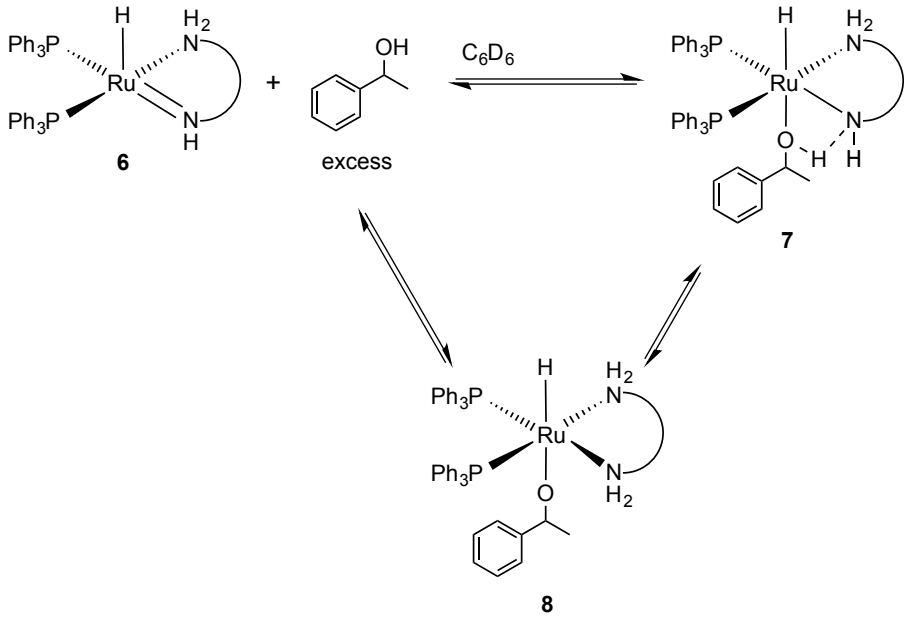

Hamilton and Bergens noted that the Ru-amide reacts quickly with alcohols to form the corresponding alkoxide at –80 °C.[44] Therefore, it is possible that 1-phenylethanol simply reacted with **29** to produce the alkoxide, **41**. A related possibility is that the addition proceeds via a pathway in which product alcohol remains hydrogen bonded to the amide nitrogen to form a Ru-amide-

alcohol adduct. This adduct then converts into the alkoxide without the direct formation of free Ru-amide and alcohol. A third possibility involves a scenario in which the carbonyl oxygen is hydrogen bonded to amine N-H, activating it towards nucleophilic attack. Alkoxide formation then occurs via a concerted process in which the hydride is transferred to the carbon of the ketone with the simultaneous formation of a ruthenium-oxygen bond without the corresponding transfer of a proton to the oxygen atom. In other words, as the transfer of a hydride to the carbonyl carbon progresses, the transfer would remove electron density from the Ru center. This loss of electron density may allow direct access to the Ru center by a hydrogen bonded alkoxide ligand to form **41.**

To discriminate between these pathways, Hamilton and Bergens used 2-PrOH and H_2 as intermolecular trapping agents.[45] Specifically, if the alkoxide **41** is formed after the bifunctional addition via the rapid reaction between 1-phenylethanol and the Ru-amide **29**, then either H_2 or 2-PrOH should trap the amide to give the dihydride or the alkoxide respectively as well. Remarkably, there was no evidence for the formation of either **2** or **33** as trapping products when frozen layers containing the dihydride (bottom layer) and a mixture of acetophenone and 2-PrOH (2 equiv. and ~150 equiv. respectively, top layer) were thawed at –80 °C in a pre-cooled NMR probe. In fact, they state that the addition was complete within 1 min, with **41** as the sole detected product, Eq. 1-14.

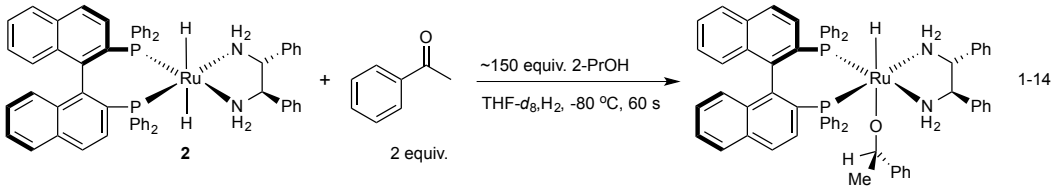

1-14

It was possible for the Ru-amide to react faster with 1-phenylethanol than with 2-PrOH.[45] However, a competition experiment between the Ru-amide, **29**, and a mixture of 1-phenylethanol and 2-PrOH (1 equiv. and 5 equiv. respectively in THF-d_8) showed that **41** and **33** were formed in a ~1:1 mixture. Thus, there exists a kinetic preference for the formation of **41** over **33**, but this preference is insufficient to account for the exclusive formation of **41** at low temperatures.

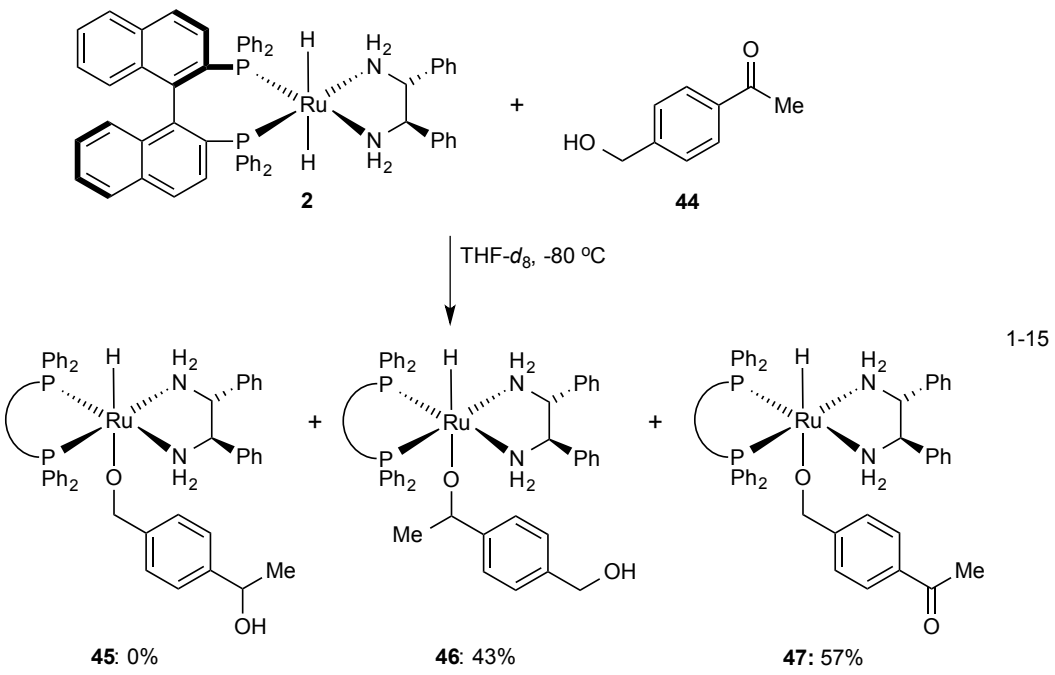

2 **44**

45: 0% **46**: 43% **47:** 57%

1-15

In a later attempt to elucidate the mechanism, Bergens and coworkers utilized a more rigorous intermolecular trapping study.[46] They studied the addition of an aryl alkyl ketone, **44**, to **2** that was predisposed to undergo product scrambling and which could be detected using NMR spectroscopy. Reduced **44** contains two alcohol groups, the primary one being more acidic and less sterically hindered. Therefore, there is a kinetic preference for the deprotonation of the primary alcohol group in the presence of **29**. Thus it was proposed that if

45 was formed, it would be strong evidence that **29** and reduced **44** are formed as the products of this addition. Remarkably, the reaction proceeded without product scrambling upon thawing at –80 °C to form **46** and **47** in 43% and 53% conversion, respectively. Despite the rapid nature of the addition, more than 50% of ketone had reacted through the primary alcohol trap which could be explained by the elimination of H_2 from **2** to form the Ru-amide, **29**, that subsequently reacts with ketone to form the alkoxide, **47**, Eq. 1-15.

Consequently, they suggest that the formation of a hydrogen bond between the carbonyl oxygen of the ketone and the amine hydrogen is essential to prevent the formation of kinetically favored primary Ru-alkoxide, **45**.[46] This hydrogen bond would then promote hydride transfer from Ru to the carbonyl carbon. The Ru center therefore becomes electron deficient which promotes Ru–OR bond formation, Eq. 1-16.

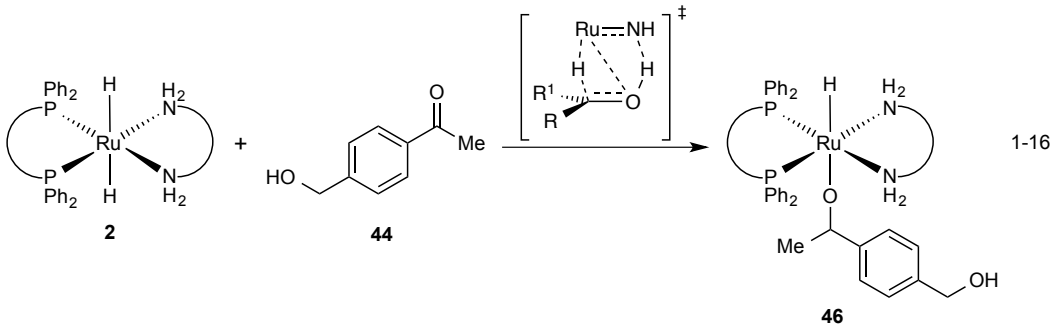

1-16

In a recent report, Hasanayn and Morris concluded that the addition of acetophenone to the catalyst model $[RuH_2(H_2P(CH_2)_2PH_2)(H_2N(CH_2)_2NH_2)]$ in a 2-PrOH mimic proceeds by a stepwise pathway. The pathway first involves the formation of a loose pre-complex, followed by a rate-limiting hydride transfer from Ru to the hydrogen-bonded carbonyl, to form a metal-alkoxide ion pair with the

alkoxide hydrogen-bonded to the N-H of a 16-electron Ru-cation ($\Delta G^{\circ\ddagger}$ for the addition = 11.5 kcal mol^{-1}, $\Delta H^{\circ\ddagger}$ = −3.5 kcal mol^{-1}, $\Delta S^{\circ\ddagger}$ −210 eu).[72] This species was then calculated to undergo a facile proton transfer from a N–H group to the alkoxide to form 1-phenylethanol and the Ru-amide (as observed by Morris using *trans*-[RuH_2((*R*)-BINAP)(tmen)]),[37,39] Scheme 1-28 (top). However, the calculated value for $\Delta S^{\circ\ddagger}$ (−210 eu) is high, negative and anomalous. It also predicts that the rate of addition decreases as temperature increases, which is also counter-intuitive.

The authors also proposed that the metal-alkoxide ion pair could undergo a simple barrier-less rotation such that the oxygen atom points directly to the coordinatively unsaturated metal center to form the Ru-alkoxide (as observed by Bergens using *trans*-[RuH_2((*R*)-BINAP((*R*,*R*)-dpen)]),[45] Scheme 1-28 (bottom). Taking Morris' and Bergens' proposals at face value, the authors essentially disagree on where their proposed transition states lie on the suggested reaction coordinate.[37,39,45]

Scheme 1-28 *Calculated pathways for metal-alkoxide ion-pair.*

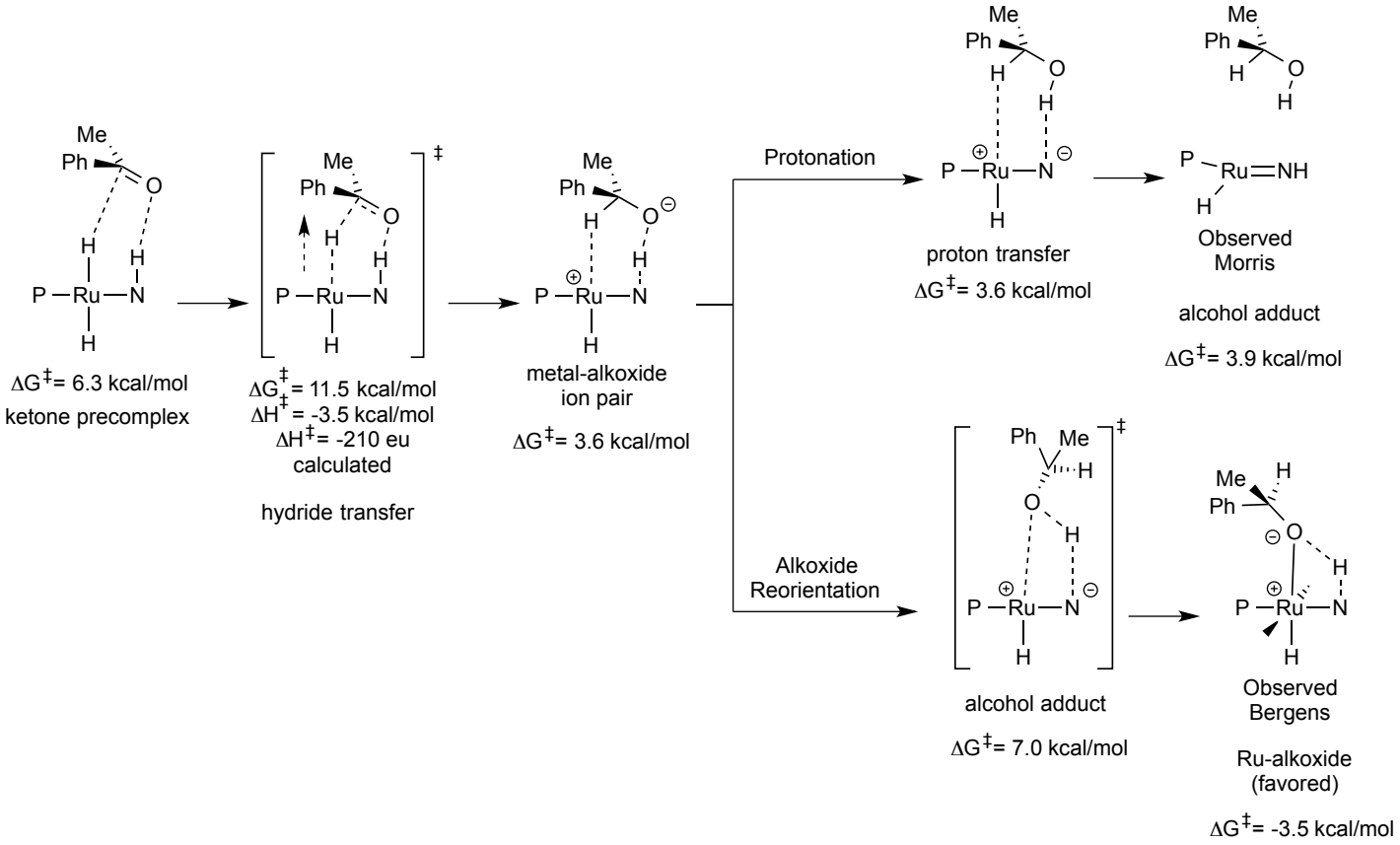

Hasanayn and Morris also computed the addition of H_2 to ruthenium alkoxides to be kinetically faster than H_2 addition to a Ru-amide.[72] Specifically, they found that the calculated $\Delta G^{\circ\ddagger}$ for the addition of H_2 to Ru–OR (16 kcal mol^{-1}) is significantly smaller than the barrier for the addition of H_2 to Ru=N (19.5 kcal mol^{-1}). These results are also anomalous in that Hamilton and Bergens have prepared the alkoxides derived from Noyori's catalyst, *trans*-[RuH_2((*R*)-BINAP)((*R*,*R*)-dpen)], and found that they are inactive towards the catalytic hydrogenation in the absence of base.[44] For example, the Ru-2-propoxide, **33**, does not react with hydrogen to generate **2** using ~2 atm H_2 at 22 °C for ~10 h. Additionally, both Morris and Bergens have shown that the addition of H_2 to the Ru-amides **4** and **29** is facile at –60 °C and –80 °C, respectively.[37,44]

Interestingly, Hasanayn and Morris equated the addition of H_2 to the model amide $RuH(H_2P(CH_2)_2PH_2)(HN(CH_2)_2NH_2)$ to a symmetry forbidden reaction.[72] In other words, they found that the molecular orbitals of the dehydrogenated complex simply have the wrong symmetry to add H_2 (HOMO = σ $(d_z^2)_{Ru}$, LUMO = π^* $(d_{xz})_{Ru} - (p_z)_N$). Therefore, the relatively strong π-bond of the Ru-amide must be broken to access an excited square-pyramidal state (HOMO = π^* $(d_{xz})_{Ru} - (p_z)_N$, LUMO = σ^* $(d_z^2)_{Ru} - (s)_H$) whose orbitals favor H_2 coordination (ΔG°_{cood} = 8.5 kcal mol^{-1}) and H_2 activation. Facile intramolecular proton transfer from the η^2-H_2 ligand to the deprotonated amine then regenerates the model catalyst.

Hamilton and Bergens reported that **41** forms 1-phenylethanol in 83% *ee* upon hydrolysis with excess 2-PrOH at –80 °C in THF-d_8.[45] This is in stark contrast to the low *ee* reported for the catalytic hydrogenation of acetophenone using **2** in THF. Interestingly, the authors found that the *ee* of 1-phenylethanol drops from 69% (*S*) (TON = 6) to 59% (*S*) (TON = 94) in THF as compared to ~80% (*S*) (TON = 1,000) in 2-PrOH using 0.1 mol% **2**, 0.25 mol% KO*t*-Bu at 30 °C and 4 atm H_2. This suggests that the *ee* was lower, reversible or both in THF. To test this hypothesis they reacted 10 equiv. of

enantiopure (*R*)-1-phenylethanol (minor enantiomer) with 10 mol% **2**, 15 mol% KO*t*-Bu at 30 °C and ~2 atm H_2 and found that the alcohol was racemized within 15 min, and continued to be racemic after 30 min under these conditions. They also showed that the racemization was somewhat faster using the Ru-amide, **29** in the absence of H_2. Therefore, they proposed that the racemization occurs via a reversible loss of H_2 from **2** to form **29**, which then rapidly adds the alcohol to form **41**. Compound **41** subsequently undergoes a rate-limiting *β*-hydride elimination (reverse of the addition reaction) to form **2** and acetophenone, Scheme 1-29. Morris and coworkers also report that the model dihydride, **3** will reversibly add H_2 to form **4,** which also reacts with excess 1-phenylethanol to generate the analogous Ru-alkoxide, **13**.[37,39]

Scheme 1-29 *Proposed mechanism for the racemization of 1-phenylethanol.*

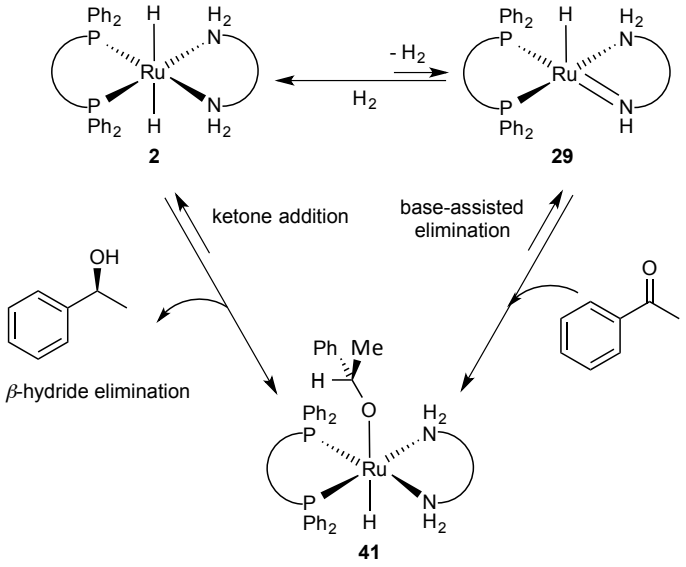

Thus, this sequence of steps suggests that the use of 2-PrOH would inhibit the racemization of the product alcohol by intercepting the Ru-amide.[45] Indeed, repeating the reaction in a 1:1 mixture of THF and 2-PrOH dramatically slowed the rate of racemization to give 84% (*R*) after 10 min (lower *ee* attributed to incomplete mixing and

localized heating), and constant *ee* thereafter for several hours. These experiments unequivocally show that 2-PrOH is essential to preserving the *ee* by forming the Ru-2-propoxide that inhibits the reaction between **29** and the product alcohol.

Other groups have investigated the mechanism for the bifunctional mechanism using model complexes. For example, Casey[55-63] and Bäckvall[77-80] independently studied the hydrogenation of polar functionalities using Shvo's catalysts, [(2,5-Ph_2-3,4-Tol_2(η^5-C_4COH))$Ru(CO)_2H$], **48**, and [(2,3,4,5-Ph_4(η^5-C_4COH))$Ru(CO)_2H$], **48b**, respectively. On the basis of deuterium labeling studies, both authors agree that the reduction of ketones (*vide infra*) proceeds via a concerted reaction *i.e.* a simultaneous transfer of a hydride on ruthenium and a protic hydrogen on oxygen to the carbon and oxygen of the ketone, respectively. Casey *et al*. found that the product of the individual kinetic isotope effect (KIE) for the reduction of benzaldehyde using **48** was roughly equal to the measured KIE when both the hydride and hydroxyl proton are replaced by deuterium (fitting the criterion for a concerted reaction), Scheme 1-30.[55]

Scheme 1-30 *KIE for the reduction of benzaldehyde using* ***48****.*

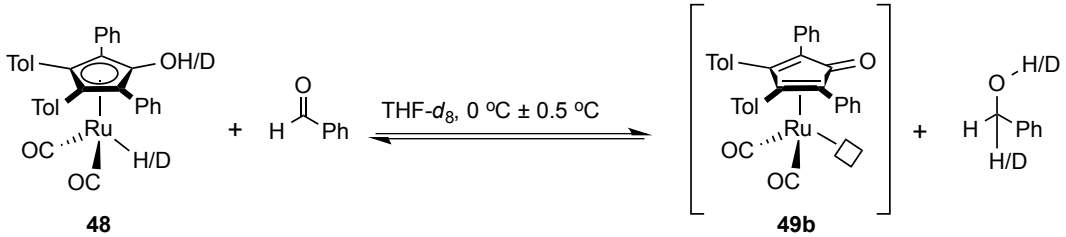

$k_{RuHOH/RuDOD}$ = 3.6 ± 0.3
$k_{RuHOH/RuDOD}$ = 2.2 ± 0.1
$k_{RuHOH/RuDOH}$ = 1.5 ± 0.2
($k_{RuHOH/RuDOH}$) ($k_{RuHOH/RuDOD}$) = 3.3

These results were corroborated by Bäckvall and coworkers during a mechanistic investigation into the oxidation of 1-(4-fluorophenyl)ethanol (the microscopic reverse

reaction of the addition) with the dehydrogenated complex, [(2,3,4,5-Ph_4(η^5-C_4CO))$Ru(CO)_2$], **49**, Scheme 1-31.[77]

Scheme 1-31 *KIE for the oxidation of 1-(4-fluorophenyl)ethanol using* ***49****.*

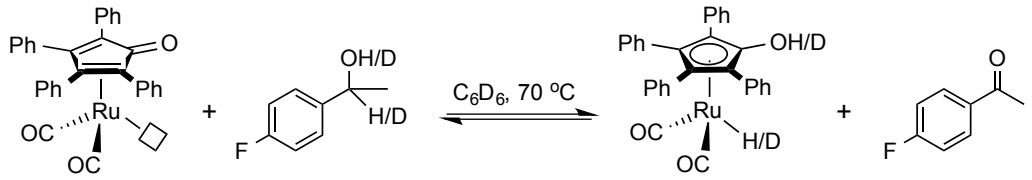

49 **48b**

$k_{RuHOH/RuDOD}$ = 4.61 ± 0.37
$k_{RuHOH/RuDOD}$ = 1.87 ± 0.17
$k_{RuHOH/RuDOH}$ = 2.57 ± 0.26
($k_{RuHOH/RuDOH}$) ($k_{RuHOH/RuDOD}$) = 4.81

Although both authors agree that Shvo's catalyst facilitates the transfer of a hydride and a proton to a ketone via a concerted process, they disagree on the mechanism of the hydrogen transfer step. Bäckvall proposed that there is initial ketone coordination with concomitant η^5 to η^3 ring slippage of the hydroxycyclopentadienyl ligand, whereas Casey suggests that the reduction occurs via the bifunctional addition mechanism, Schemes 1-32 and 1-33, respectively.

In an attempt to distinguish between the two proposed mechanisms, both research groups performed inter- and intra-molecular trapping experiments.[59,60,62,78] These investigations have focused on the use of imines rather than ketones.[55,57,60,62,78,80] This is because the reduction of imines by Shvo's complex forms kinetically stable amine complexes. In contrast, related ruthenium alcohol complexes have never been directly observed, presumably due their rapid dissociation.[60,78]

Scheme 1-32 *Bäckvall and coworkers' proposed mechanism for the inner-sphere hydrogenation of ketones.*

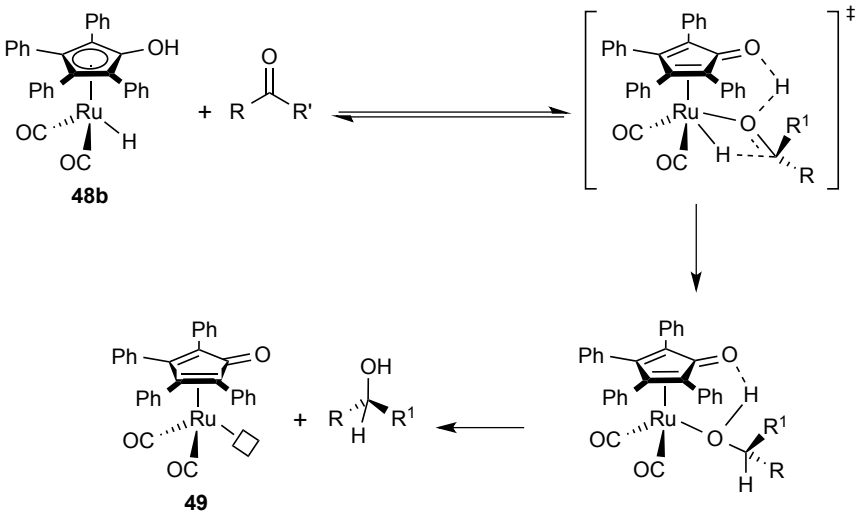

Scheme 1-33 *Casey et al.'s proposed mechanism for the outer-sphere hydrogenation of ketones.*

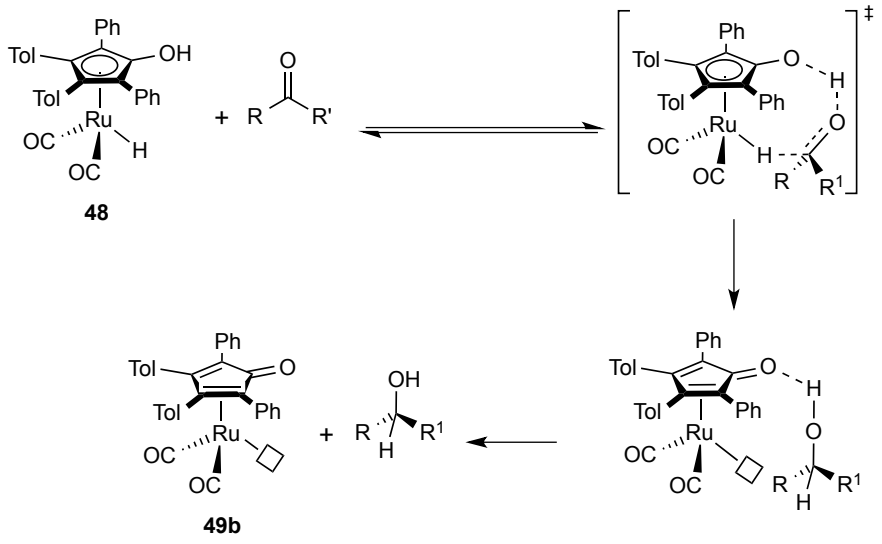

In 2005, Casey *et al*. reported the results of an intermolecular trapping study that showed that **48** would reduce the imine, **50**, in the presence of an intermolecular trap, **51** (aniline) to form the complex derived exclusively from the reduced imine.[59] This result suggests that the hydrogenation occurred via an inner-sphere mechanism. However, this

result could also be explained by a pathway in which the imine is hydrogenated to form a hydrogen-bonded species, **52**, that is confined to a solvent cage. Compound **52** could then collapse to form the ruthenium-amine expected by the inner-sphere mechanism **53**, Scheme 1-34 (top) or it can dissociate the secondary amine to give the coordinatively unsaturated Ru center, **49b** Scheme 1-34 (middle). This species can then re-add either the secondary amine to form **53** or the product of the trapping amine, **54**, *only* if **51** can efficiently penetrate the solvent cage before the secondary amine reforms the hydrogen bond to the cyclopentadienone carbonyl of **49b**, Scheme 1-34 (bottom). If this does not happen, then **53** will be the sole detected product of the reduction.

Scheme 1-34 *Proposed pathways based on Casey et al.'s intermolecular trapping study.*

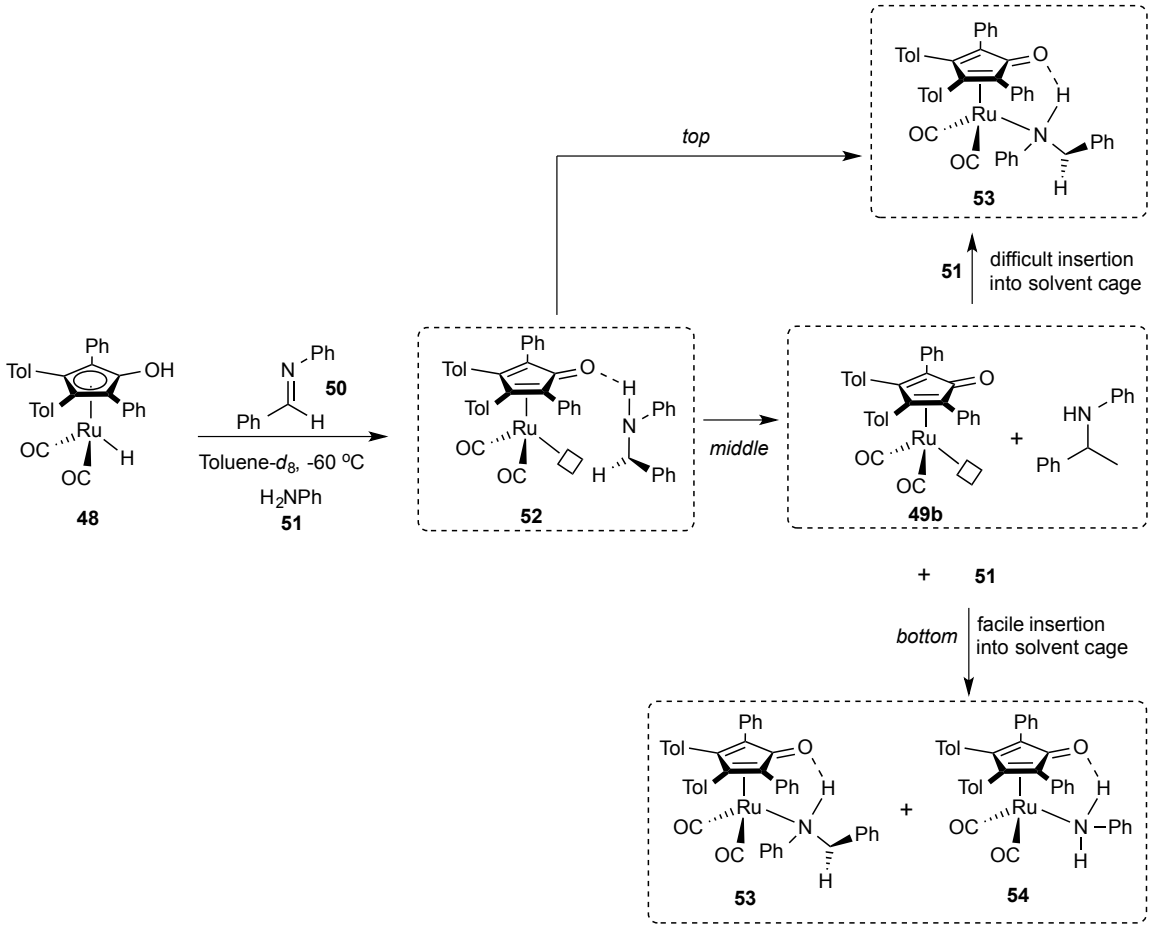

In a more rigorous intramolecular study, Casey *et al.* found that reacting a toluene-d_8 solution of **48** with the imine, H_2N-*p*-C_6H_4N=CHPh, **55**, at temperatures below –20 °C formed a 1:1 mixture of the Ru-amine complexes **56** and **57**, consistent with an outer-sphere mechanism, Eq. 1-17.[59]

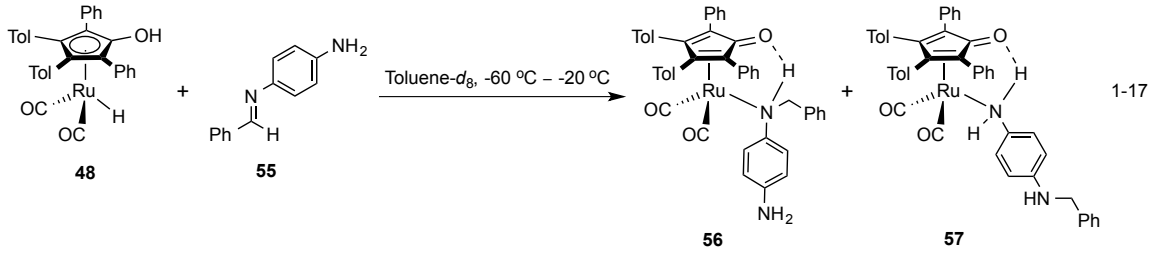

Bäckvall and coworkers, however, reported that mixing **48b** with the imine, 1,4-NH(CH_2Ph)(*c*-C_6H_{10})=NPh, **58** at –80 °C in CD_2Cl_2 formed **59** as the sole detectable product, Eq. 1-18.[78] They then suggested that Casey *et al*.'s intramolecular trapping results (*vide supra*) were due to ruthenium migration across the aromatic *π*-system.

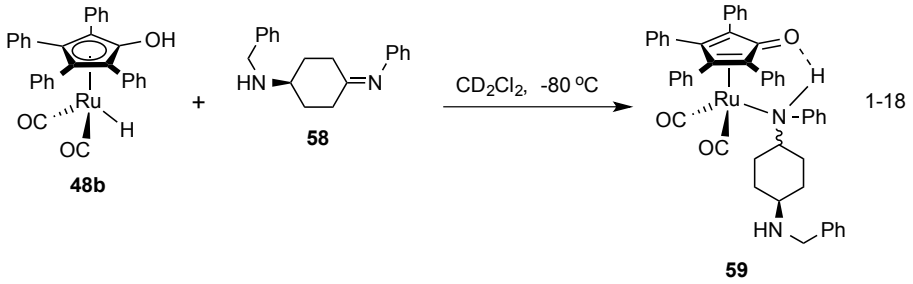

Casey remained adamant and suggested that the discrepancies between the trapping experiments were the result of the relative ability of the amines to hydrogen bond to the cyclopentadienone carbonyl. They suggested that the strength of the hydrogen bond for reduced **58** would be stronger than that of **55** because of the increased electron donation from the *p*-amino substituent (pK_a of *p*-$NH_2C_6H_4NH_3^+$ and $C_6H_5NH_3^+$ are 6.08

and 4.58, respectively).[62] However, at that time the authors did not account for the influence of the cyclohexyl substituent on **58** that would also contribute to the weakening of the hydrogen bond (pK_a of $PhCH_2NH_3^+$ and *c*-$C_6H_{11}NH_3^+$ are 9.30 and 10.64, respectively).

Casey *et al*. found that reacting a toluene solution of the pseudo-symmetric imine **60** with **48** at –45 °C formed a mixture of isomeric Ru-complexes, **61** and **62**.[62] Note that **60** does not have a thermodynamic preference for amine coordination. The ^{15}N NMR spectrum obtained at 0 °C showed four peaks that were assigned to ~3% *cis*-Ru–^{15}N, 12% *trans*-Ru–^{15}N, 21% *cis*-Ru–N and 64% *trans*-Ru–N. Specifically, about 15% of the ^{15}N-labeled amine had coordinated to ruthenium, **62**. Interestingly, the initial ratio of these complexes remained unchanged up to 24 °C and only started to change after 2 h at 50 °C. This suggests that the ratios observed at 0 °C were kinetically determined, Scheme 1-35. These results, albeit minor, provide evidence for an outer-sphere mechanism as in order to form **62**, there must be breaking of the hydrogen bond and coordination of the trapping amine.

Scheme 1-35 *Product distribution of isomeric complexes formed by reacting* ***48*** *with the pseudo-symmetric imine,* ***60****.*

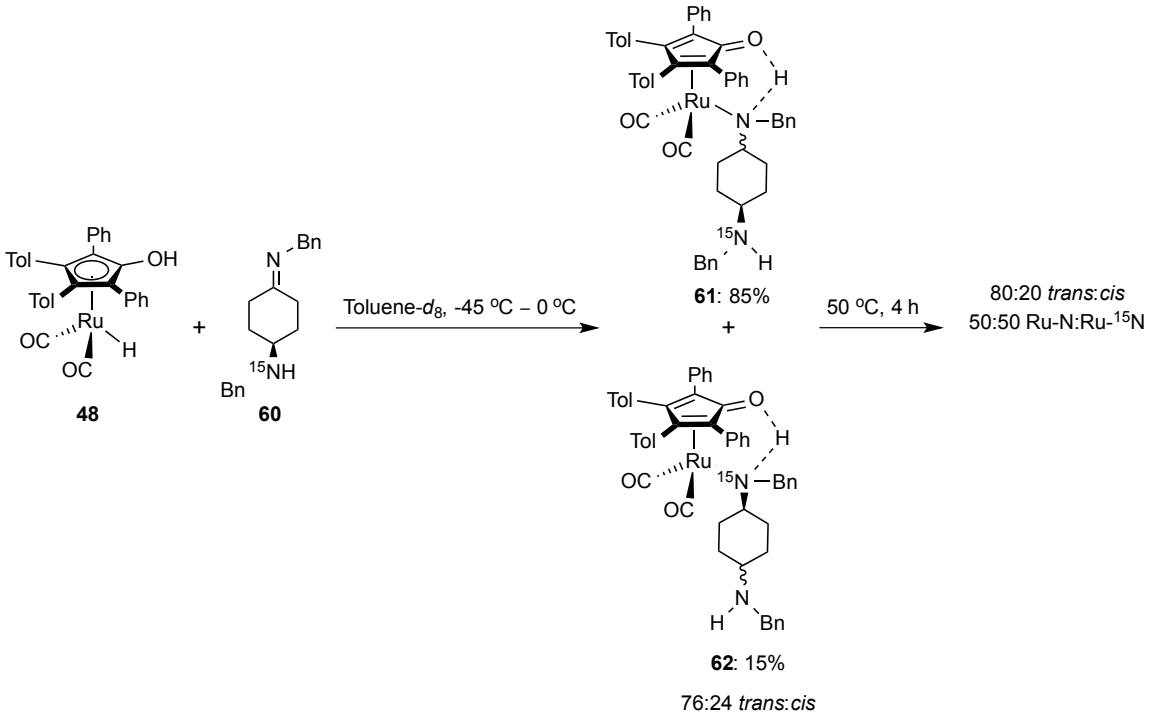

Ruthenium-catalyzed homogeneous ester hydrogenation

In recent years, less reactive carbonyl compounds such as esters have been hydrogenated with high turnovers and rates under practical conditions using **2** or bifunctional analogues that operate by metal-ligand cooperativity.[81,82] For example, Saudan and coworkers (Firmenich S. A.) have reported versatile and practical catalysts for ester hydrogenation.[83-88] In fact, the hydrogenation of methyl benzoate proceeds rapidly to give a mixture of benzyl alcohol and methanol in near quantitative yield (99% yield, TON = 1980) after 1 h in the presence of 0.05 mol% **63** and 5.0 mol% NaOMe under 50 atm H_2 at 100 °C in THF. Subsequently, the research groups of Bergens,[89] Morris[90] and Gusev[91-96] have also reported similar bifunctional systems (complexes **2**, **64** and **65**, respectively) that are also capable of reducing methyl benzoate to the corresponding mixture of alcohols in the presence of high ratios of base to catalyst (B/C) in THF solvent, Scheme, 1-36.

A handful of these systems are also active in the absence of base.[81,96-101] Remarkably, the dimeric ruthenium complex, **66**, reported by Gusev *et al.* has comparable activity to that of **2** in the absence of base under similar conditions. Catalyst **66** was also found to reduce methyl benzoate to the corresponding product alcohols in 90% yield (TON = 18,000) under modified conditions *i.e.* 0.005 mol% Ru under 50 atm H_2 at 100 °C for 17 h in THF, Eq. 1-19.[96]

Scheme 1-36 *A selective survey of ester hydrogenation systems.*

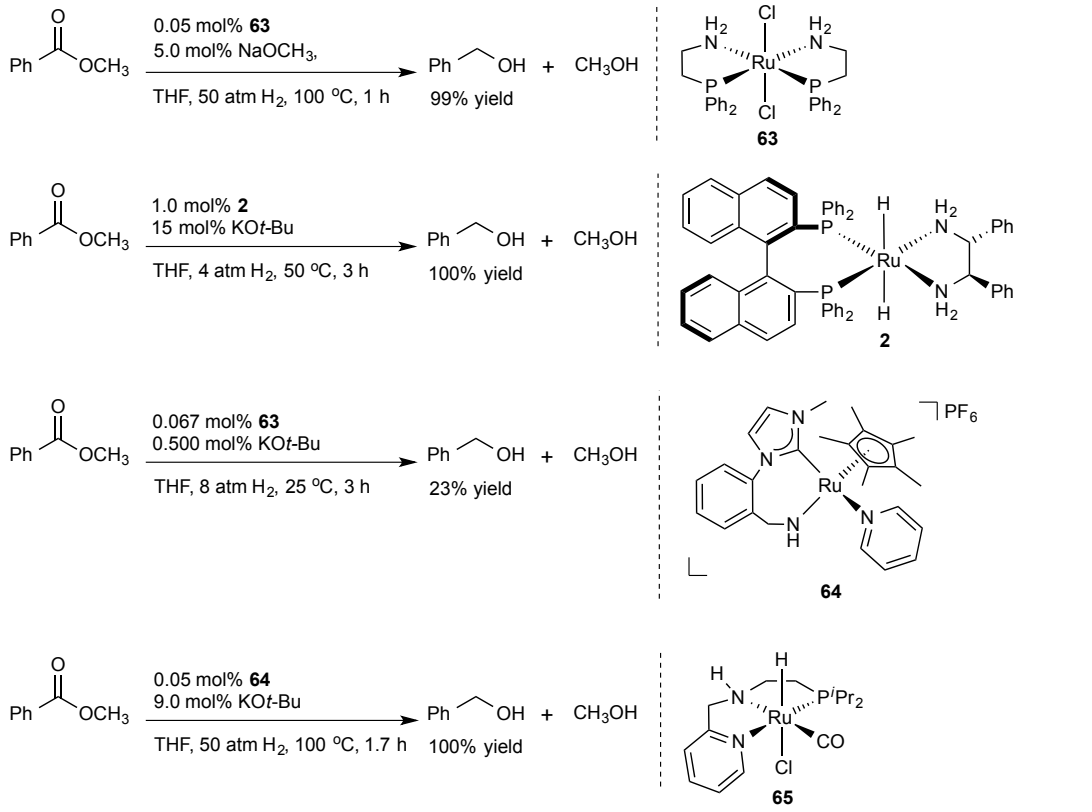

Interestingly, both Bergens and Saudan reported that their catalyst systems (**2** and **63** with base, respectively) are inactive in 2-PrOH. Takebayashi and Bergens demonstrated that the hydrogenation of esters using **2** was unexpectedly facile at low temperatures. For example, **2** stoichiometrically adds *γ*-butyrolactone to form the corresponding Ru-hemiacetaloxide, **67**, within minutes at –80 °C in THF-d_8, Eq. 1-20.

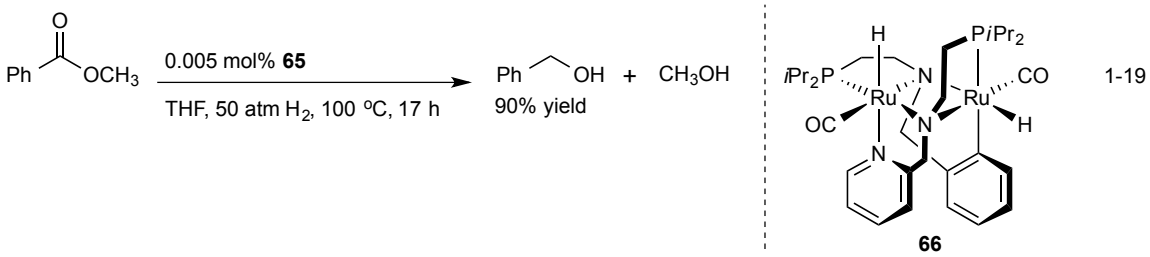

1-19

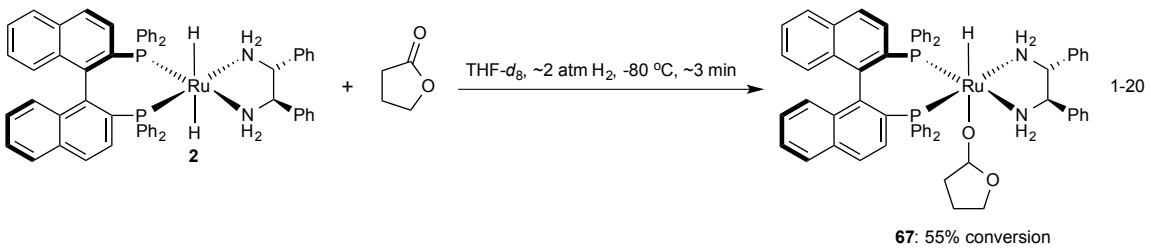

The hemiacetaloxide, **67**, is transformed into the corresponding Ru-alkoxide, **68**, slowly at –80 °C under H_2 (the reaction was then complete upon warming the mixture to –40 °C). The alkoxide ligand in **68** is the diol that results from the complete reduction of the parent lactone, Scheme 1-37.

The authors propose that the addition of lactones and esters to **2** proceeds in a similar manner to the addition of ketones (*vide supra*), as a result the alkoxides **67** and **68** would undergo a base-assisted elimination of the alkoxide ligand to generate the Ru-amide, **29**. Compound **29** can then react quickly with either H_2 (to regenerate **2**) or the product alcohol (to give the corresponding Ru-alkoxide) at low-temperatures. Under these conditions a competition would be established. Takebayashi and Bergens propose that this is the origin of the product inhibition in ester hydrogenations using **2**. They also suggest that it is the combination of high base and thermal stability of **63** under harsh reaction conditions helps to overcome product inhibition in this and related bifunctional systems.

Scheme 1-37 *Double reduction of γ-butyrolactone using* ***2*** *at low temperatures in THF-d_8.*

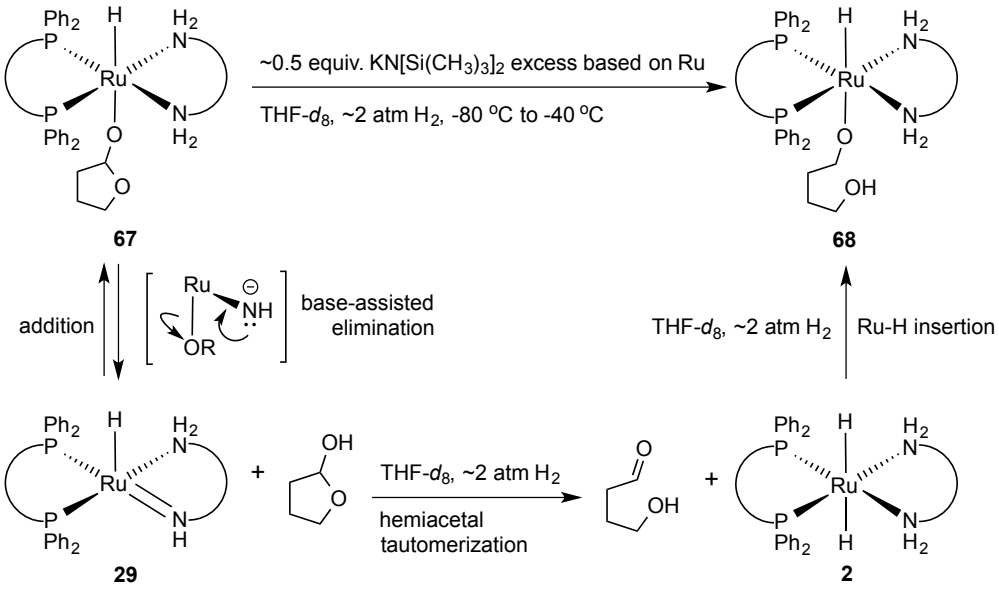

Reduction of imides

The development of sustainable and efficient strategies to reduce carboxylic acid derivatives is of particular interest to both academia and industry. In this regard, there is ongoing interest to foster new and convenient protocols to catalytically and selectively reduce imides. Figure 1-2 outlines the sequence of reductions, which might be expected for the reduction of an *N*-substituted imide.[102]

Initial mono-reduction of the imide, **69**, furnishes the cyclic hydroxy lactam, **70**, which can exist as a tautomer of the open chained aldehyde-amide, **70b**. Both of these tautomers can be reduced, the first via hydrogenolysis to the cyclic amide, **71**, and the latter to the opened chained alcohol-amide, **72**, resulting from dihydrogenation. The amides **71** and **72** can presumably undergo a similar series of reductions to give the alcohol-amine product, **73**, or the cyclic amine, **74**.

Figure 1-2 *Possible reduction pathways for an N-substituted imide*

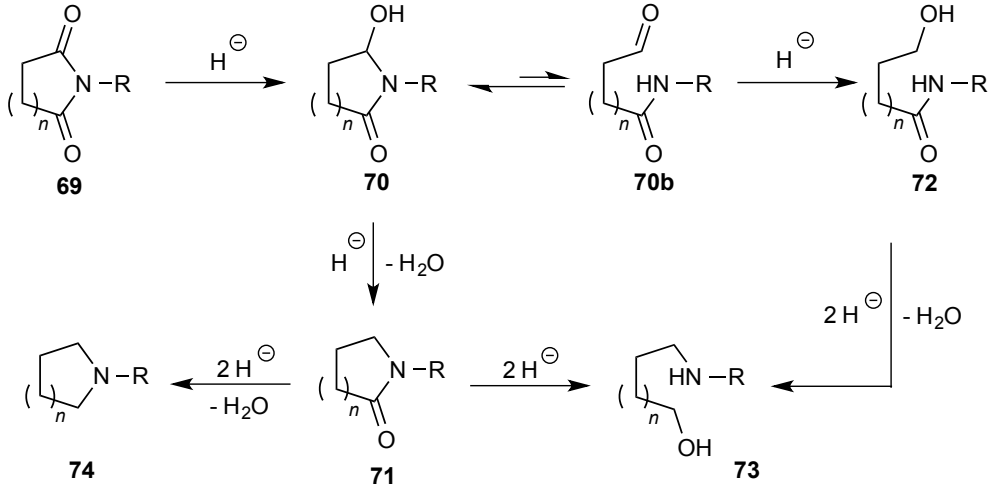

The selective transformation of *N*-substituted cyclic imides is often possible by the judicious choice of reducing agent and experimental conditions. For example, Graves and Rigdon have reported the reduction of phthalimides to isoindolinones using

stoichiometric amounts of Zn and Sn in moderate to good yields under acidic conditions.[103,104] Moreover, Beller and coworkers demonstrated that phthalimides and imidazolidine-2,4-diones could also be reduced in the presence of fluoride ions with low cost polymethylhydrosiloxane as a hydrogen source with up to 78% yield in 24 h using 5 mol% $(C_4H_9)_4NF$ at 22-65 °C in THF.[105] However, the applications of stoichiometric amounts of metal hydride reagents are more common. Strong reducing agents such as $LiAlH_4$ have been used to perform complete reductions to cyclic amines,[106,107] while cyclic hydroxy lactams have been obtained using $NaBH_4$.[108-111] Enantioselective reduction of cyclic imides to hydroxy lactams have also been reported using (*R*)-BINAL-H (up to 91% *ee*),[112] mixtures of BDMPB (BDMPB: bis(2,6-dimethylphenoxy)borane) and a 20% thiazazincolidine complex prepared *in situ* from (1*R*,2*S*)-(-)-1-phenyl-2-(1-piperidino)-1-propanethiol and diethylzinc (70–90% *ee*, limited to *N*-aryl-substituted imides)[113] and mixtures of CBS catalyst and borane[114] (68–94% *ee*).

Unlike stoichiometric reductions, the catalytic hydrogenation of imides typically produces lactams or hydroxy lactams as opposed to amines. Heterogeneous catalysts such as copper chromite[115] or Raney Ni[116] usually require forcing conditions (200–300 °C and 200–300 atm H_2) and exhibit low functional group tolerance. In contrast PtO_2 and Pd/C have been used to reduce activated amides such as *N*-acetylphthalimide to substituted hydroxy lactams under ambient conditions, 20 °C and 1 atm H_2, Eq. 1-21.[117] However, this technology is restricted to a limited substrate scope and concomitant arene reduction during the hydrogenation.

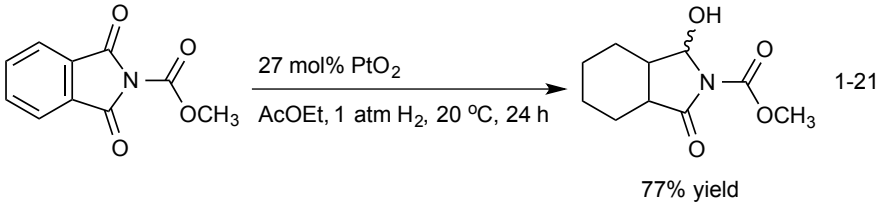

1-21

77% yield

At present, only a few organometallic complexes have been reported to perform the catalytic reduction of imides. Patton and Drago described the reduction of *N*-methylsuccinimide to 2-pyrrolidinone in the presence of water-soluble ruthenium pre-catalysts *e.g.* 1 mol% $RuCl_3 \cdot 3H_2O$, $RuCl_2(Me_2SO)_4$, or $[Ru(dmp)(H_2O)_2](PF_6)_2$ (dmp: 2,9-dimethylphenanthroline) in modest yields, <28% conversion using 1 mol% Ru under 6.8 atm H_2 at 100 °C.[118] The reaction was limited by the lack of a definitive substrate scope. Later, Bruneau, Dixneuf, and coworkers reported the Ru-catalyzed mono-hydrogenation of phthalimides and succinimides into saturated lactams using $[Ru_4H_6(p\text{-cymene})_4]Cl_2$, **75**, or $RuCl_2(p\text{-cymene})]_2$, **76**, in water.[119] Specifically, isolated yields ranging from 30-97% could be obtained using 1 mol% **75** under 60 atm H_2 at 90 °C in 13-24 h. In contrast, **76** gave conversions of up to 100% using 1-2 mol% Ru in 3-24 h under similar conditions, Scheme 1-38.

Scheme 1-38 *Hydrogenation of imides using **75** or **76**.*

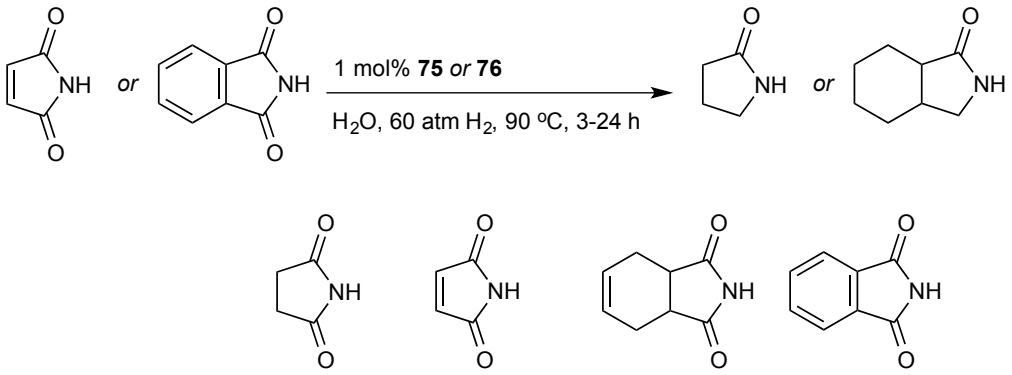

yield (%) using **75** [t = h]	87 [13]	86 [13]	97 [22]	78 [24]
yield (%) using **76** [t = h]	nd	100 [3]	100 [15]	nd

Recently, Ikariya and coworkers reported the dihydrogenation of cyclic imides using $Cp^*RuH(Ph_2P(CH_2)_2NH_2)$, **77**, prepared by reacting the corresponding chloro-complex with 1 equiv. KO*t*-Bu (in the absence of excess base) under mild reaction

conditions, Scheme 1-39. Ring opened alcohol-amides were selectively obtained in 49-99% isolated yield using 1-5 mol% catalyst under 30 atm H_2 at 80 °C for 2-18 h in 2-propanol.[120]

Scheme 1-39 *Hydrogenation of imides catalyzed by* ***77****.*

using 1 mol% **77**
R^1, R^2 = H, H
R^1, R^2 = CH_3, H
R^1, R^2 = C_6H_5, H
R^1, R^2 = 4-FC_6H_4, H

using 5 mol% **77**
R^1, R^2 = CH_3, CH_3
R^1, R^2 = CH_3, Bn

In contrast, the catalyst variants Cp*RuH($Me_2N(CH_2)_2NH_2$) and Cp*RuH($Ph_2P(CH_2)_2NMe_2$) systems exhibited no catalytic activity towards imide hydrogenation under similar conditions. This was attributed to the difference in electronic properties between tertiary phosphino- and amino- groups as well as the crucial importance of the protic NH group in the ligand for the bifunctional addition. Catalyst **77** also proved to be active towards the hydrogenation of *N*-acylcarbamates, *N*-acyloxazolidinones and *N*-acylsulfonamides to give mixtures of deacylated products, and *N*-protected amino-alcohols, respectively, in *t*-BuOH, Scheme 1-40. The rates of these reactions were found to be strongly dependent upon the electron-withdrawing nature of the substituent on the nitrogen atom, with rates increasing in the order of Cbz < Boc < CO_2CH_3 < SO_2CH_3 ≈ Ts.[121]

Scheme 1-40 *Hydrogenation of N-acylcarbamates and N-acylsulfonamides using* ***77****.*

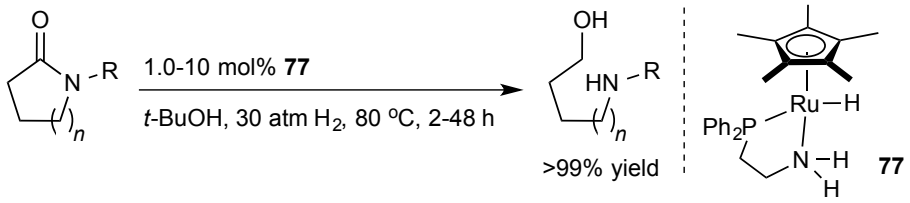

using 1.0 mol% **77** for 2 h
n = 1, R = Ms

using 5.0 mol% **77** for 24 h
n = 0, R = Boc
n = 1, R = Cbz
n = 2, R = Boc

using 10 mol% **77** for 48 h
n = 3, R = Boc
n = 3, R = Ts

Furthermore, the authors were able to carry out the first enantioselective desymmetrization of bicyclic *meso*-imides to chiral alcohol-amides using chiral Cp*RuH(P–N) based catalysts (P–N: (*S*)-2-((diphenylphosphino)methyl)pyrrolidine, **78a**, and (*S*)-2-((diphenylphosphino)methyl)piperidine], **78b**, Scheme 1-41).[120] Many prochiral bicyclic succinimides, mono- and bicyclic glutarimides were hydrogenated in 2-PrOH with up to 10 turnovers and 98% *ee* using 10 mol% Ru under 30 atm H_2 at 80 °C in 24 h.[122]

Scheme 1-41 *Enantioselective desymmetrization of bicyclic meso-imides using* ***78a*** *and* ***78b****.*

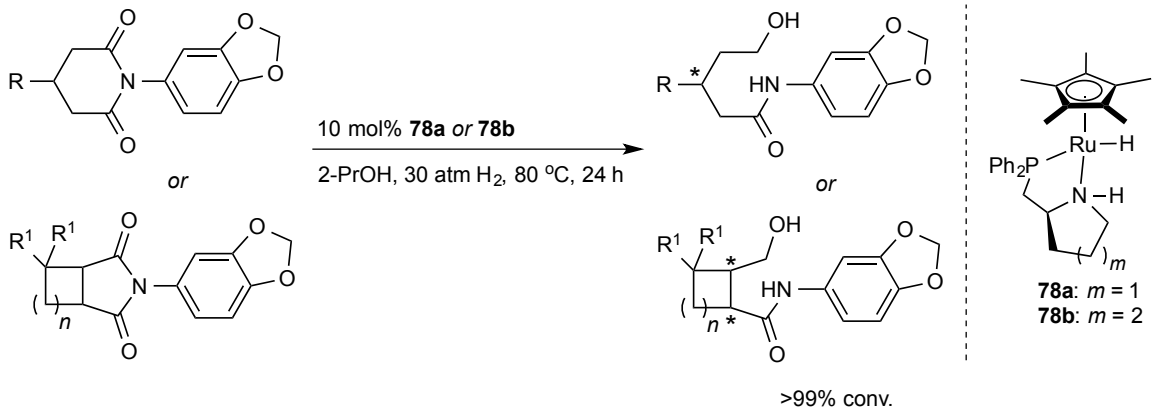

using **78a**
R = 4-FC_6H_4 98% *ee*
R = 3,4-$Cl_2C_6H_3$ 91% *ee*
R = C_6H_5 96% *ee*
R = CH_3 88% *ee*

using **78b**
n = 0, R^1 = CH_3 76% *ee*
n = 1, R^1 = H 91% *ee*
n = 2, R^1 = H 81% *ee*
n = 3, R^1 = H 92% *ee*

Bergens and coworkers demonstrated that **2** and its diethylamine analogue, **79**, could hydrogenate *N*-substituted phthalimides and succinimides with mono- and di-hydrogenation at moderate temperatures with up to 100 turnovers using 1 mol% Ru, 9 mol% KO*t*-Bu under 4 atm H_2 at in 3 h, Scheme 1-42.[123,124]

Scheme 1-42 *Achiral hydrogenation of imides using **2** or **79**.*

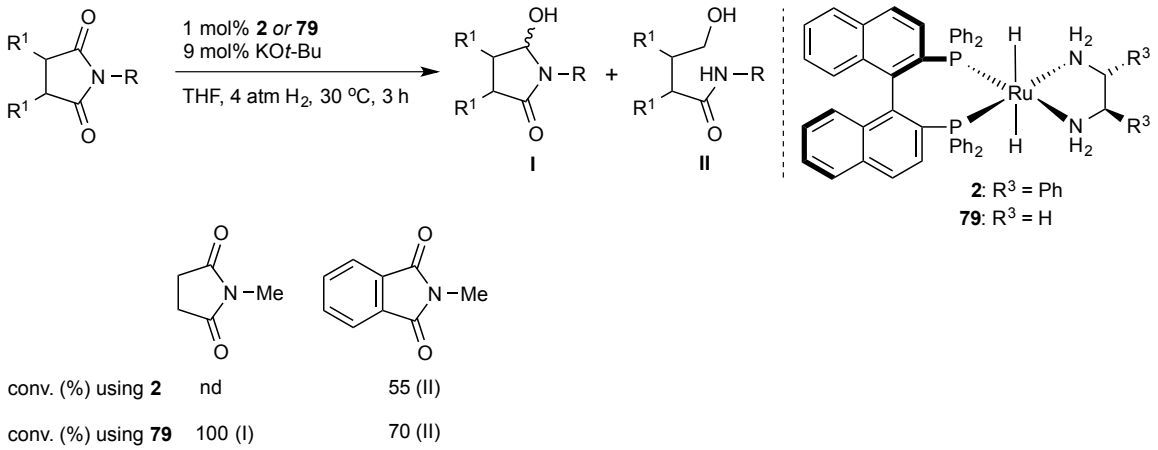

Interestingly, the combination of low reaction temperature and imide structure was found to facilitate monohydrogenation. Subsequently, a series of bicyclic meso-imides were desymmetrized via enantioselective monohydrogenation to give chiral *γ*-hydroxy lactams with up to five stereogenic centers in up to 90-99% yield, 88-97% *ee*, a C=O/C=C selectivity >99% and dr >93:7 using 0.1-1 mol% Ru, 0.9-9.9 mol% KO*t*-Bu under 50 atm H_2 at 0-22 °C in 3-57 h, Scheme 1-43.

Scheme 1-43 *Desymmetrization of bicyclic meso-imides by enantioselective monohydrogenation.*

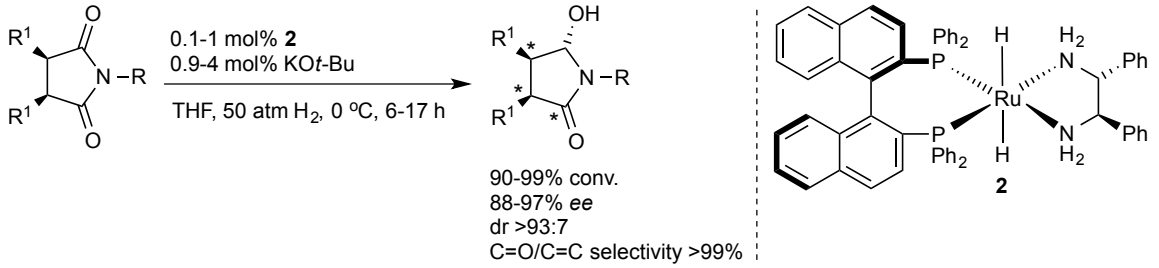

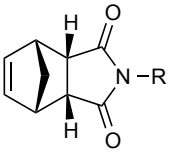

imide:**2**:KO*t*-Bu = 1000:1:9. t = 17 h

	conv. (%)	dr	*ee* (%)
R = Ph	98	99:1	96

imide:**2**:KO*t*-Bu = 500:1:9. t = 17 h

	conv. (%)	dr	*ee* (%)
R = 4-FC_6H_4	99	>99:1	97
R = 4-$NMe_2C_6H_4$	92	>99:1	97
R = 4-$OMeC_6H_4$	98	>99:1	95

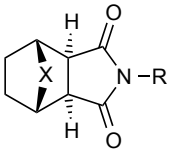

imide:**2**:KO*t*-Bu = 100:1:4. t = 6 h

	conv. (%)	dr	*ee* (%)
R = Ph, X = O	97	93:7	92

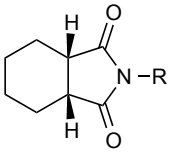

imide:**2**:KO*t*-Bu = 1000:1:99. t = 57 h

	conv. (%)	dr	*ee* (%)
R = Ph	90	97:3	88

Reduction of amides

Amide bonds are abundant in many artificial and naturally occurring chemical compounds.[125] They are prevalent in peptides, proteins, numerous chemical synthons, synthetic polymers and materials (*e.g.* polyacrylamide, nylon, Kevlar, *etc.*). Over the past few years, there have been considerable effort and incentives towards developing new synthetic strategies to access fine chemicals.[126] However, due to a lack of fundamental knowledge concerning the catalytic activation of amides, the selective transformation of this class of substrates still presents a significant challenge.[127]

The reduction of amides to amines is a particularly useful transformation, especially in the pharmaceutical industry.[128,129] Currently, stoichiometric amounts of active Al–H, B–H or Si–H are used for small to medium-scale reduction of amides.[130-132] For example, NE–100, a potent antipsychotic, can be prepared via a $LiAlH_4$ or BH_3·THF reduction of the tertiary amide, **80**, Eq. 1-22.[133] Despite their usefulness, these reagents suffer from numerous drawbacks including air and moisture sensitivity, poor atom economy, limited functional group tolerance and environmental issues regarding operational safety and disposal. Catalytic hydrogenation offers an alternative strategy to reduce amides that circumvents these fundamental issues.

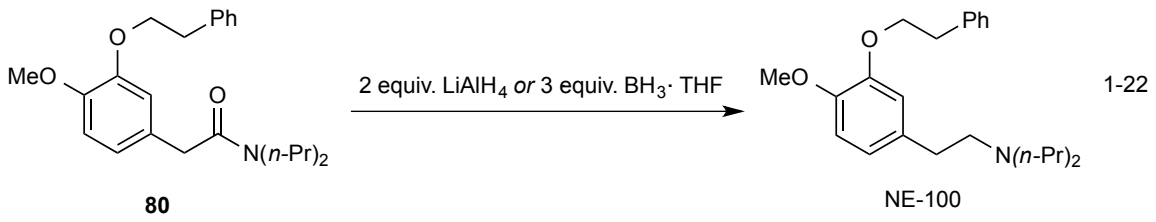

80 NE-100 1-22

Catalytic hydrogenation involves the use of hydrogen as an atom-efficient and environmentally benign reducing agent in the presence of a transition metal complex.[134] Scheme 1-44 shows the possible reductive pathways in catalytic amide hydrogenation.

Path A represents the reductive cleavage of the C=O bond, the net result of which is the elimination of water from the amide to generate amines. Path B, however, is a two-step process. The first step is C=O reduction followed by cleavage of the C–N bond to yield aldehydes and amines, the former being subsequently reduced to afford alcohols.[81]

Scheme 1-44 *Possible reductive pathways in catalytic amide hydrogenation.*

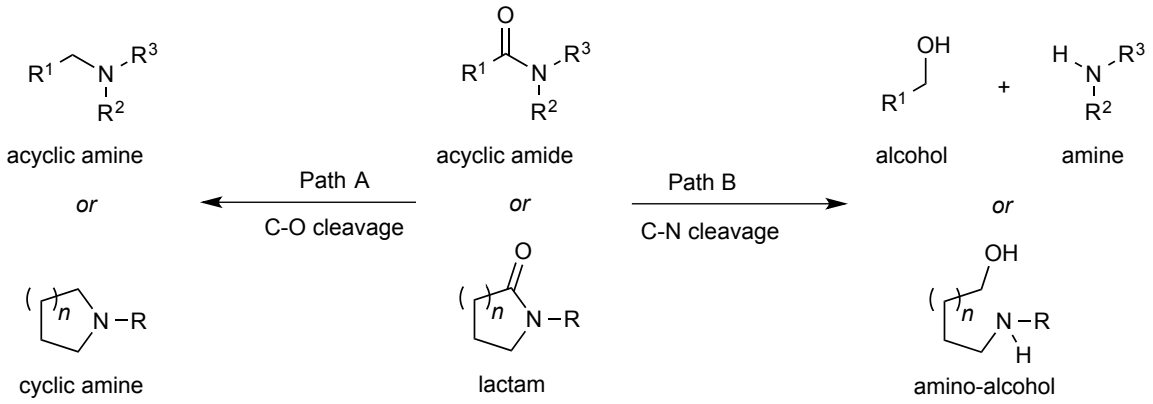

In terms of hydrogenation, amides are the least reactive class of carboxylic acid derivatives. The poor reactivity of amides has been classically explained by the strong resonance between the nitrogen lone pair and the carbonyl carbon (resonance hybrids **I** and **II,** Figure 1-3).[135,136] The overall effect is to render the carbonyl carbon less electrophilic. As a result, amides have a high thermodynamic stability and kinetic inertness. Therefore, the catalytic hydrogenation of amides typically requires forcing conditions *i.e.* high temperatures and pressures.

Figure 1-3 *Resonance delocalization in simple amides.*

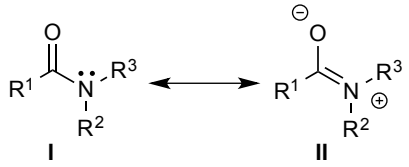

Heterogeneous amide hydrogenation

The catalytic hydrogenation of amides to produce amines was first reported by Adkins and Wojcik in 1934 in which *α*-phenylbutyramide was hydrogenated to give a mixture of 2-phenylbutylamine (73% yield, TON = 6) and di-2-phenylbutylamine (26% yield, TON = 2) under forcing conditions (12.5 mol% $CuCr_2O_4$ under 250 atm H_2 at 250 °C in 2 h, Eq. 1-23).[137,138]

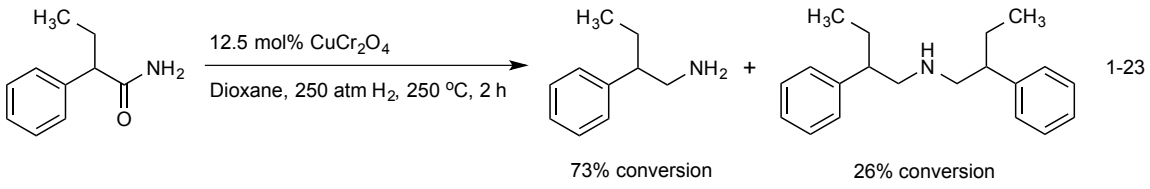

King (Procter & Gamble) subsequently improved upon this technology in 1984 by developing a catalyst system of copper chromite and zeolite.[139] He showed that the introduction of a powdered zeolite, *e.g.* Linde 4Å, resulted in greater C–O selectivity, conversions and milder reaction conditions. For example, *N*,*N*-dimethyldodecanamide was hydrogenated in near quantitative yield to give the corresponding amine with TON = 26 (92% conversion) and a C–O selectivity of 81% after 2 h using 3.0 wt. % $CuCr_2O_4$ with 18 wt. % Linde 4Å under 136 atm H_2 at 287 °C, Eq. 1-24. In contrast, in the absence of the zeolite, the amide was only hydrogenated with a selectivity of 47% and 16 turnovers under similar conditions using 3.0 wt. % $CuCr_2O_4$).

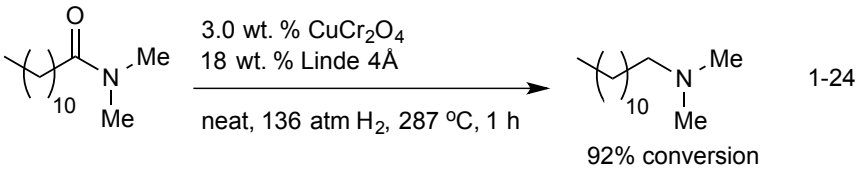

1-24

Subsequently, Forguy *et al.* disclosed a similar procedure to prepare *N*,*N*-dimethyl-*N*-alkylamines using a catalyst system comprised of a mixture of copper oxide (46%), copper chromite (46%), manganese oxide (4%) and a dialkylamine source *e.g.* dimethylamine.[140] The reductions were typically performed at 200–280 °C and 10–100 atm H_2. This methodology led to higher conversions however, the C–O selectivity was moderate (~85%) with trace dialkylated products as well as alcohols.

Moreover, Stern,[141] Bartley[142] and Gerliczy[143] showed that group 7–10 metals and metal oxides *e.g.* ReO_3, PtO_2, Raney Ni and Raney Co, could be used for the heterogeneous hydrogenation of amides. The rate and selectivity of these hydrogenations were found to be dependent upon the amide, catalyst and conditions employed. For example, Bartley and coworkers reported that acetamide could be selectively hydrogenated in cyclohexane to give ethylamine as the sole detectable product in 264 turnovers (88% conversion) using 0.3 mol% ReO_3 under 205 atm H_2 at 200 °C in 18 h, Eq. 1-25.[142] In contrast, acetanilide was hydrogenated to give a mixture of C–O and C–N cleavage products in 92 and 38 turnovers (71% and 29% conversion), respectively under the reported conditions (0.8 mol% ReO_3 under 205 atm H_2, 185 °C in 31 h).

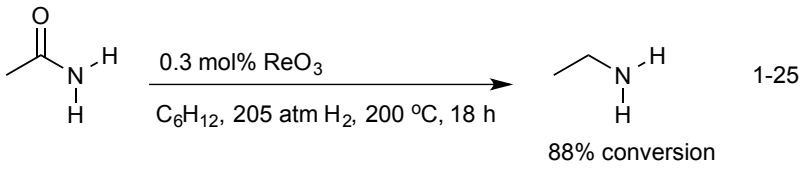

1-25

Dobson (British Petroleum) later showed that amides could also be reduced using bimetallic catalysts of group 8 and Re supported on high surface area graphite (HSAG) or silica. For example, 2.5 wt. % Pd – 5 wt. % Re on HSAG in the presence of 4Å sieves was used to hydrogenate 2.0 g propylamide under 272 atm H_2 at 200 °C but, the selectivity was poor, yielding mixtures of mono- (3%, TON = 6), di- (44%, TON = 102), and trialkylamines (18%, TON = 41).[144] Likewise, Thompson *et al.* found that 4.0 wt. % Pt – 1.0 wt. % Re catalysts supported TiO_2 in hexane were able to hydrogenate *N*-methylpyrrolidin-2-one in 92% conversion and 99% selectivity to *N*-methylpyrrolidine under 20 atm H_2 at 120 °C in 24 h, Eq. 1-26.[145] DFT calculations suggested that the Re acts as a Lewis acid to render the C=O of the amide more electrophilic; whereas the Pt acts as the hydrogenation catalyst. Unfortunately, owing to the poor solubility of amides in *n*-hexane this technology may have limited applications.

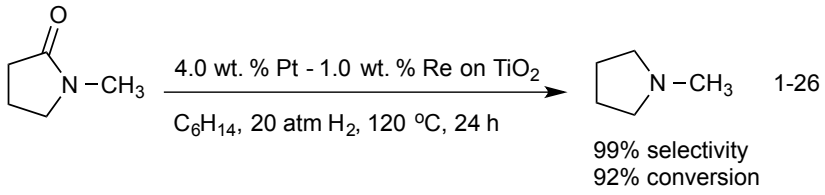

1-26

More recently, Breit and coworkers demonstrated that a wide variety of amides could be hydrogenated at lower temperatures and pressures of H_2 (160 °C and 30 atm H_2), using a graphite-supported bimetallic Pd/Re catalyst in the presence of 4Å molecular sieves.[146] Of the ~108 secondary and tertiary amides tested over 70% were hydrogenated with 100% selectivity towards C–O cleavage with ~30 of these at >99% conversion. For example, ε-caprolactam, *N*-methylpyrrolidine, *N*-acetylpiperidine and *N*-acetylpyrrolidine were all hydrogenated in DME with >99% conversion (TON = 25) and

100% selectivity to the corresponding secondary and tertiary amines using 2.0% Pd/ 10% Re/ graphite (4.0 mol%) in the presence of 4Å molecular sieves under 30 atm H_2 at 160 °C in 20 h, Eq. 1-27. The hydrogenation of primary amides was problematic. In these cases, secondary amines were obtained as the major products.

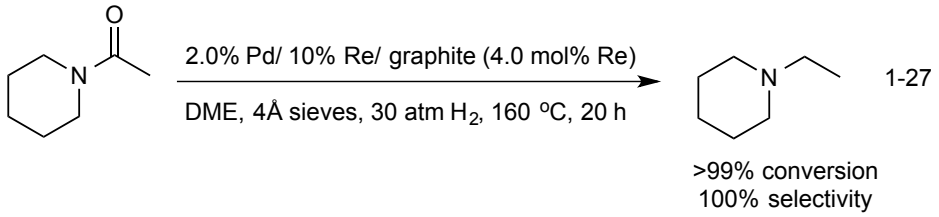

1-27

Fuchikami and coworkers reported bimetallic catalysts of Rh (Rh/Re, Rh/W and Rh/Mo) and Ru (Ru/Re and Ru/Mo) that are capable of reducing *N*-acetylpiperidine to the corresponding tertiary amine under moderately harsh reaction conditions (50-98 turnovers using 1.0 mol% bimetallic catalyst under 100 atm H_2 at 160-170 °C for 16 h in THF).[147] Notably, a variety of *N*,*N*-disubstituted amides were also hydrogenated with C–O cleavage in 62-92% conversion (TON >20) using 1.0-3.0 mol% $Rh_6(CO)_{16}/Re_2(CO)_{10}$ in DME under 100 atm H_2 at 160–180 °C in 8-16 h. The main drawback of the reaction was the concomitant reduction of aryl groups in unsaturated substrates during the hydrogenation.

In 2005, Smith (Avantium International) reported the results of a high-throughput study in which a range of bi- and tri-metallic catalysts were screened for catalytic amide hydrogenation.[148] The bi- and tri-metallic catalysts were denoted as AB, AC, BC, and ABC respectively, wherein A, is a metal chosen from Co, Fe, Ir, Pt, Rh and Ru; B is a metal chosen from Cr, Mo, Re and V; and C, is a metal chosen from Cu, In and Zn. In general, trimetallic catalysts were found to outperformed related bimetallic species. Notably, Pt/Re/In (1:1:1 molar metal ratio) supported on silica (or carbon) was found to

be the most active catalyst. It could hydrogenate 1-acetylpyrrolidine to the corresponding amine in TON = 85 after 16 h in corrosive acetic acid solvent using 1.0 mol% catalyst under 10 atm H_2 at 130 °C, Eq. 1-28.

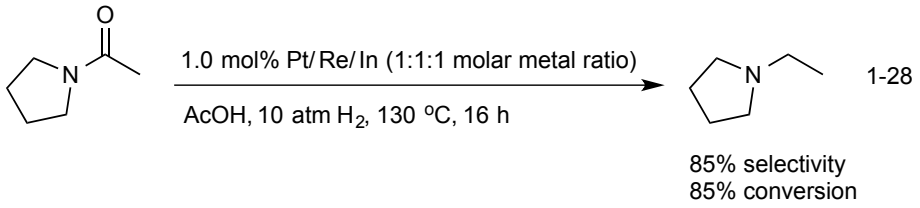

Whyman and coworkers also reported a similar series of bimetallic catalysts consisting Rh/Mo, Ru/Mo, Rh/Re and Ru/Re for the heterogeneous hydrogenation of amides. In each case, a detailed study was carried out utilizing cyclohexylamide as a test substrate.[149-151] The authors found that Ru/Re (Ru:Re = 0.25) system in DME gave the highest selectivity, 95% (TON = 24) towards the primary amine in near quantitative conversion using a catalyst loading of 4.0 mol% (based on Ru) under 100 atm H_2 at 160 °C in 16 h. The Rh/Re (Re:Rh = 0.8) gave the next highest selectivity, 90% (TON = 18) albeit under higher loadings (5.0 mol% based on Rh). In each case the optimum pressure range for the hydrogenation was between 50-100 atm H_2. The onset temperature for Rh/Re system was 10 °C less than that of the Ru/Re system (160 °C). Further, the nature of the active catalyst was found to be M'/Re (M' = Ru or Rh) and Re oxides. The high selectivity towards primary amines in these systems was explained by a mechanism, which suggests that amide dehydration to form the nitrile is preferred over a step-wise reduction to the hemiaminal, Scheme 1-45, top and bottom, respectively. The authors also suggest that the rate-limiting and subsequent rapid reduction of the resulting nitrile limits the formation of C–N cleavage products.

Scheme 1-45 *Mechanism for the hydrogenation of cyclohexylamide using Rh/Mo, Ru/Mo, Rh/Re and Ru/Re systems.*

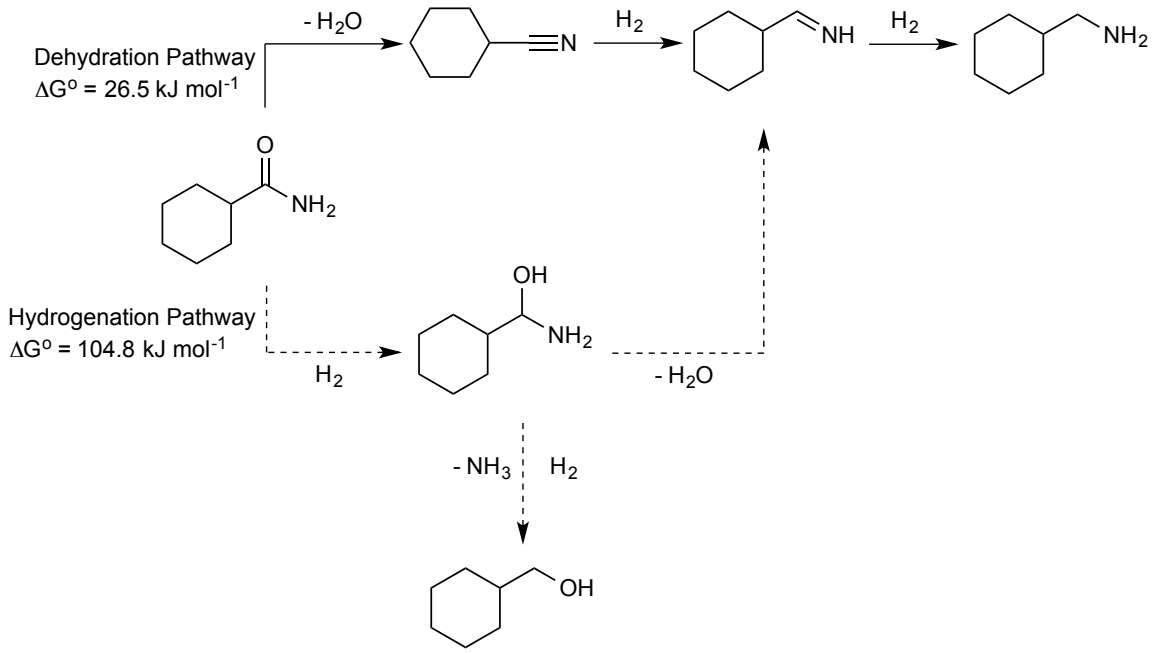

Homogeneous amide hydrogenation

The homogeneous hydrogenation of amides was first reported in a patent by Crabtree and coworkers in 2003 using 0.160 mol% $Ru(acac)_3$, **81**, (acac: acetylacetonate), 2.16 mol% Triphos^{Ph} (**82**: 1,1,1-tris(diphenylphosphinomethyl)ethane) (13.5 equiv. based on Ru) in THF under 48 atm H_2 at 164 °C.[152] The hydrogenation of propanamide proceeded with TON = 126 and low selectivity to give a complicated mixture of alcohols, amines and esters as products after 14 h. Subsequently, Cole–Hamilton and coworkers reported that the same catalyst system could quantitatively hydrogenate butanamide in THF to dibutylamine and tributylamine in ~52 and ~60 turnovers under the reported conditions (0.80 mol% Ru, 1.9 mol% **82** under 40 atm H_2 at 220 °C (internal) in 14 h).[153,154]

The absence of the desired primary amine (*n*-butylamine, **83**) was explained by a mechanism in which **83** participates in multiple side reactions, Scheme 1-46. For

example, **83** can undergo transamination with butanamide, **84**, or react with butyraldehyde, **85**, to give the amide, **86**, and/or the imine, **87**, both of which can be readily hydrogenated to give dibutylamine, **88**. Analogous to the discussion above, a similar series of side reactions can afford the tertiary amine, tributylamine, **89**. In an attempt to suppress these unwanted side reactions, the authors investigated the effect of ammonia on the selectivity for the primary amine using $[Ru_2(TriPhos^{Ph})_2Cl_3]Cl$, **90**. Notably, they found that the addition of aqueous ammonia (0.50 v/v $NH_{3(aq)}$:THF) to **90**, catalyzes the hydrogenation of butanamide to give *n*-butylamine in 97 turnovers (85% selectivity) after 14 h using 0.88 mol% Ru under 40 atm H_2 at 220 °C (internal). The addition of aqueous ammonia also led to a greater percentage of alcohol by-products due to a higher concentration of water in the reaction mixture. Additionally, the authors reported that *N*-phenylnonamide could also be quantitatively reduced with a TON = 99 (99% selectivity) using 1.0 mol% **81**, 2.0 mol% **82** in the absence of NH_3 under 40 atm H_2 at 220 °C (internal).

Scheme 1-46 *Mechanism for the formation of 2° and 3° amines from butanamide.*

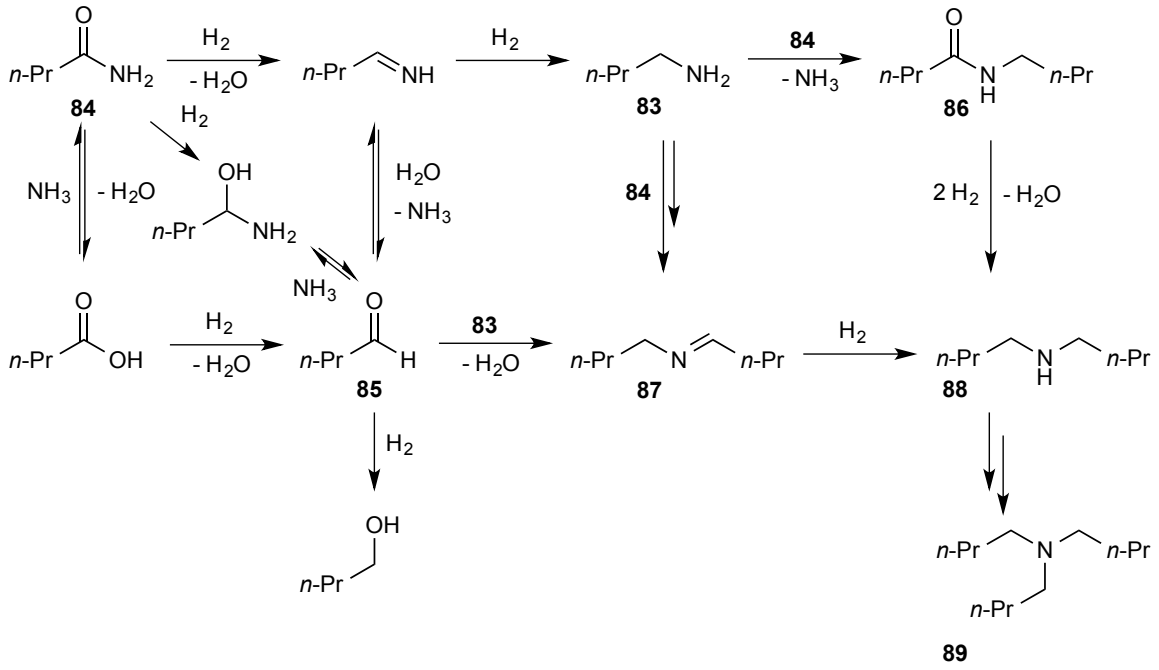

Shortly after publication the authors reported that many research groups encountered problems reproducing these results. The authors attributed this difference in reactivity to the purity of the **82**.[127,155] However, purified samples of **82** stored under an inert atmosphere also exhibited a marked decrease in activity. The authors then reported that catalytic amounts of methanesulfonic acid (MSA) could restore this activity. In particular, butanamide was quantitatively hydrogenated, but the C–O selectivity decreased to 61% (TON = 61) under the revised reaction conditions (1.0 mol% **81**, 2.0 mol% **82**, 0.50 v/v $NH_{3(aq)}$:THF under 10 atm H_2 at 200 °C with 1.5 mol% MSA in 16 h). This revised Ru/Triphos^{Ph} system was also active towards the catalytic C–O cleavage of a variety of secondary and tertiary amides using 1.0 mol% **81**, 2.0 mol% **82**, 1.0-1.5 mol% MSA under 10 atm H_2 at 200-220 °C (Figure 1-4).

To explain these results the authors propose that the two-step reduction is facilitated by a common catalytic precursor, **91** which first undergoes oxidative addition

with dihydrogen to give the *cis*–dihydride, **92**. Hydride transfer to the coordinated amide, **93** generates **94**. Reductive elimination from **94** regenerates **91** and liberates the free hemiaminal, **95**, which is highly unstable and hydrolytically cleaves to give the imine, **96** and water. The final steps of the reduction leading to the conversion of the imine to expected amine product are essentially identical to the aforementioned C=O hydrogenation discussion, Scheme 1-47.

Figure 1-4 *Hydrogenation of secondary and tertiary amides using Ru/Triphos^{Ph}/MSA.*

performed using 1.0 mol% **81**, 2.0 mol% **82**, 1.5 mol% MSA under 10 atm H_2 at 200 ^oC

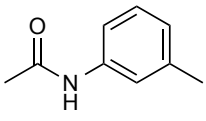

100% conversion
79% selectivity
TON = 79

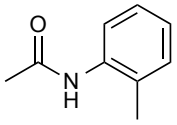

100% conversion
90% selectivity
TON = 90

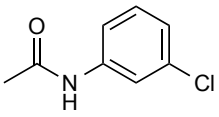

75% conversion
75% selectivity
TON = 56

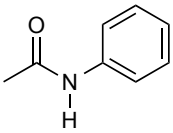

19% conversion
63% selectivity
TON = 12

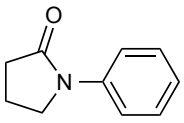

19% conversion
100% selectivity
TON = 19

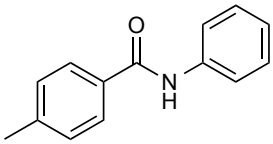

100% conversion
94% selectivity
TON = 94

performed using 1.0 mol% **81**, 2.0 mol% **82**, 1.0 mol% MSA under 10 atm H_2 at 220 ^oC

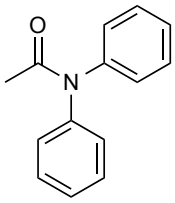

83% conversion
42% selectivity
TON = 35

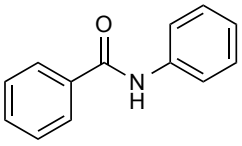

100% conversion
92% selectivity
TON = 92

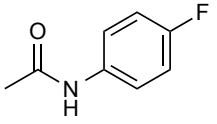

99% conversion
77% selectivity
TON = 76

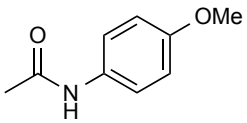

97% conversion
78% selectivity
TON = 76

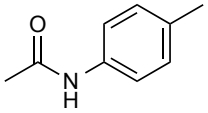

98% conversion
78% selectivity
TON = 76

Scheme 1-47 *Proposed mechanism for the hydrogenation of amides using Ru/Triphos^{Ph}.*

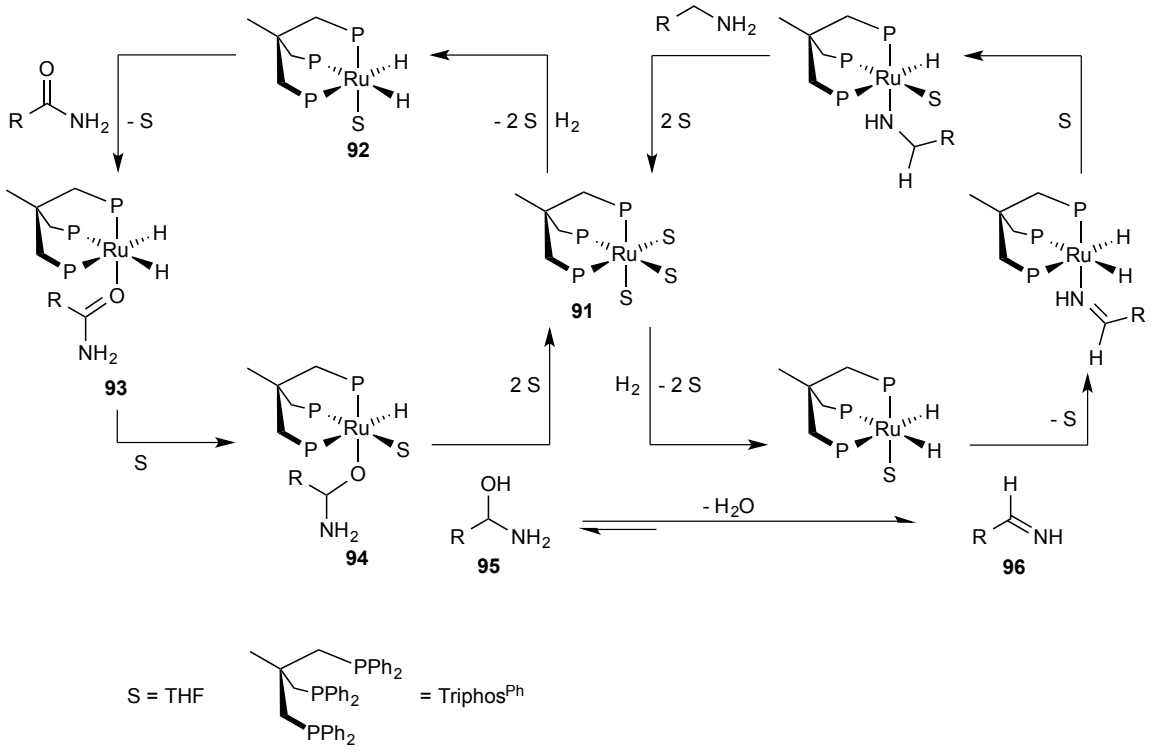

Moreover, recent computational studies by Leitner and coworkers using the same catalyst system for the hydrogenation of itaconic and levulinic acid have suggested that the complex fragment, [RuH(TriPhos^{Ph})]$^{+}$ plays a greater role in the mechanism.[156] Starting from the [RuH(TriPhos^{Ph})]$^{+}$ fragment, **97**, coordination of the amide substrate gives **98**. Hydride transfer to the coordinated carbonyl group then gives **99**. Hydrogenolysis of the metal-oxide in **99** regenerates **97** and liberates the unstable hemiaminal, **100**, that eliminates water to give the imine. A similar series of steps closes the catalytic cycle, Scheme 1-48.

Scheme 1-48 *Alternative mechanism for the hydrogenation of amides using [RuH(Triphos^{Ph})]$^{+}$.*

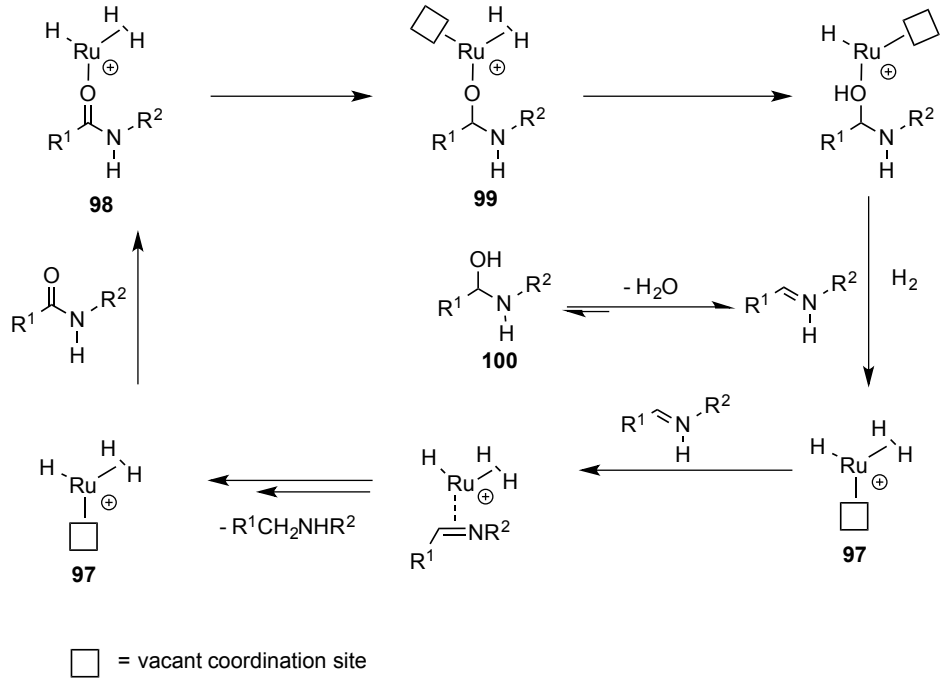

In 2009, Ikariya and coworkers demonstrated the selective hydrogenation of lactams and amides to give the corresponding mixture of C–N cleavage products.[157,158] They showed that a variety of amides could be dihydrogenated in up to 10 turnovers using the phosphine free catalyst precursor, Cp*RuCl(2-$C_5H_4NCH_2NH_2$), **101**, in the presence of 25 mol% KO*t*-Bu under 50 atm H_2 at 100 °C in 24-72 h, Scheme 1-49, top. Further, the hydrogenation was influenced by the electronic nature of the substituent on the amide nitrogen. For example, 1-phenyl-pyrrolidin-2-one was smoothly hydrogenated in 24 h using 10 mol% **101** in basic 2-PrOH to give *N*-phenyl-4-aminobutan-1-ol in 8 turnovers (73% isolated yield) under 50 atm H_2 at 100 °C, while 1-benzyl-pyrrolidin-2-one was inactive under similar conditions. Nevertheless, amides that did not bear an aryl group on nitrogen were still reduced, albeit in lower conversions. Interestingly, the same catalyst system was found to effect the selective dehydration of secondary lactams to the corresponding amines with 1-10 turnovers under the reported conditions in 2-PrOH

(10 mol% **101**, 25 mol% KO*t*-Bu under 50 atm H_2 at 100 °C in 24 h, Scheme 1-49, bottom).

Scheme 1-49 *Hydrogenation of lactams and amides using Cp*RuCl(2-$C_5H_4NCH_2NH_2$) in basic 2-PrOH.*

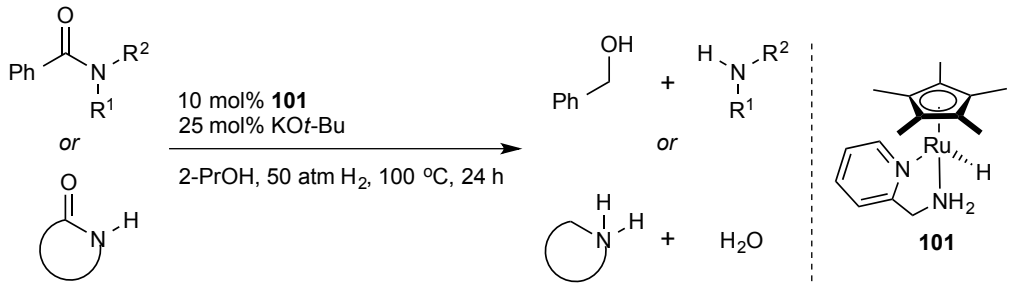

C-N cleavage	yield (%)
R^1 = H, R^2 = Ph	78
R^1 = H, R^2 = CH_3	10
R^1 = CH_3, R^2 = CH_3	80
R^1 = CH_3, R^2 = Ph	100
R^1 = -$(CH_2)_4$-	37
R^1 = -$(CH_2)_4$-	66

C-O cleavage

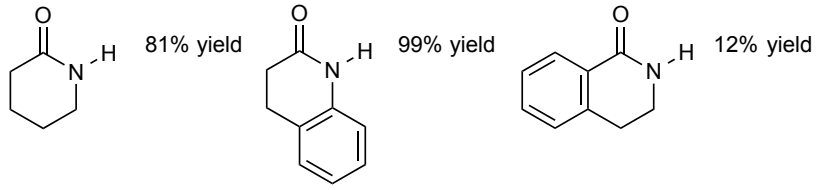

Milstein and coworkers subsequently found that the 16-electron dearomatized pincer complex RuH(NNP^{t}Bu)(CO), **102**, which catalyzes the hydrogenation of methyl benzoate after 4 h with a TON = 97 using 1.0 mol% **102** under 5.3 atm H_2 at 115 °C in dioxane could also facilitate the hydrogenation of *N*-benzyl-2-methoxyacetamide to 2-methoxyethanol and benzyl amine catalytically in 63 turnovers under neutral conditions in THF (1 mol% **102**, 10 atm H_2 at 110 °C in 48 h).[159,160] Under identical conditions the bipyridine-based analogue, **103**, proved to be more active, hydrogenating *N*-benzyl-2-

methoxyacetamide in 90 turnovers. Catalyst **103** was found to hydrogenate a variety of 2° amides, and 3° amides having ether groups, to give the products associated with C–N cleavage, Scheme 1-50.

Scheme 1-50 *Hydrogenation of amides using Milstein's bifunctional catalysts.*

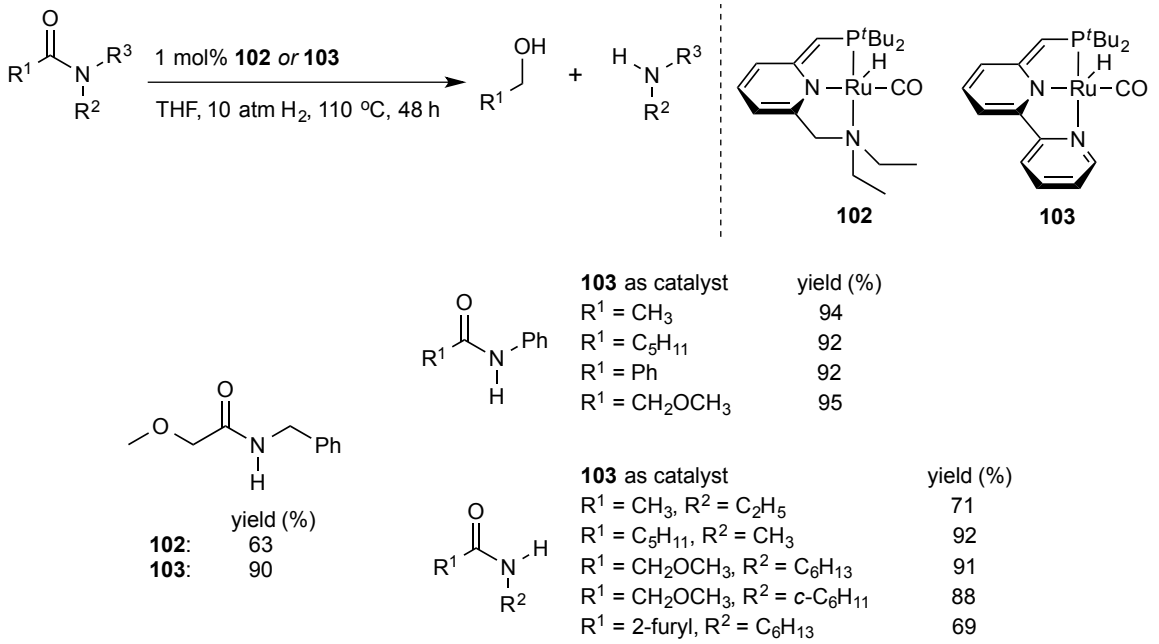

In recent developments extended bipyridine-type pincer systems have also been evaluated as catalysts for the hydrogenation of 2° amides.[161] However, these complexes were noticeably less active. For example, heating a THF solution of **103** with 100 equiv. benzanilide at 110 °C under 10 atm H_2 for 48 h resulted in 92 turnovers with C–N cleavage. In contrast, it was hydrogenated in 51 turnovers, using **104** under similar conditions, Scheme 1-51. This difference in activity was attributed to an intramolecular diastereoselective C-H activation that forms a cyclometalated product, **105**, that inhibits catalysis, Eq. 1-29.

Scheme 1-51 *Hydrogenation of benzanilide by* ***103*** *and* ***104***

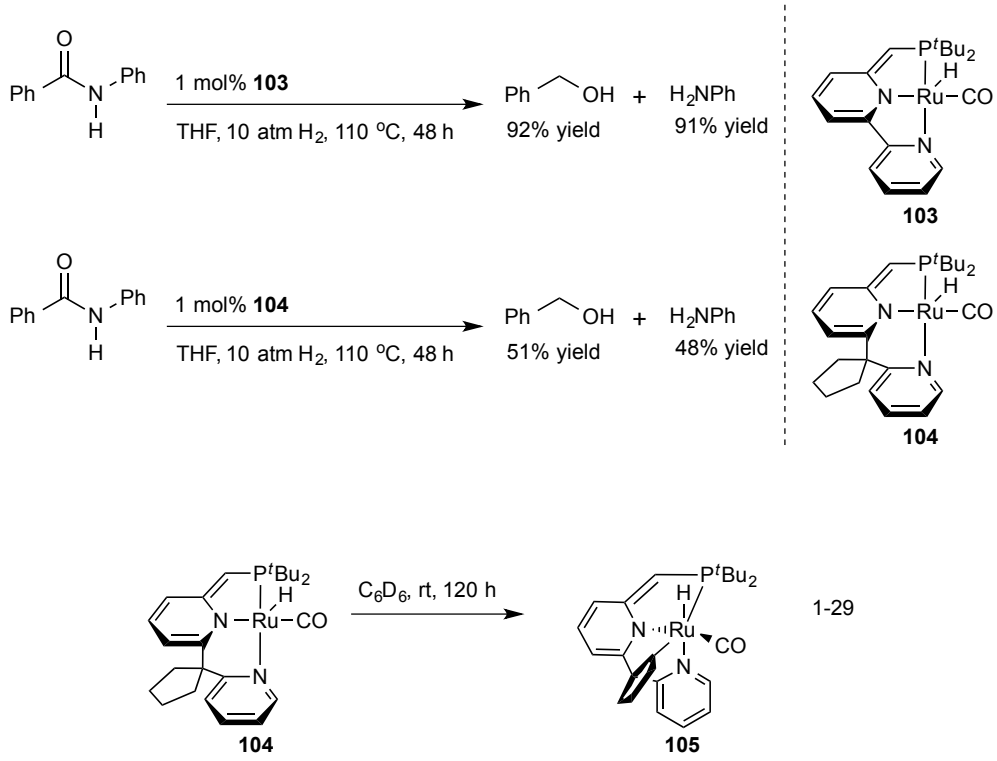

The authors proposed an inner-sphere mechanism (Scheme 1-52) that begins with dihydrogen activation by **103** (via metal-ligand cooperation) to form a coordinatively saturated *trans*-dihydride, **106**. Decoordination of the pyridyl arm provides a vacant site for amide coordination to give, **107**. Hydride transfer to the carbonyl carbon of the coordinated amide leads to the metal-alkoxide, **108**. Unlike previously described mechanisms, there is no liberation of free hemiaminal. Rather deprotonation of the benzylic arm by the adjacent NH group of the hemiaminaloxide leads to the amine product and a dearomatized complex bearing a coordinated aldehyde, **109**. The addition of dihydrogen leads to **110**, which is capable of transferring a hydride to the coordinated aldehyde to form the alkoxide, **111**. Deprotonation of the benzylic arm by the alkoxide ligand generates the alcohol and regenerates the catalyst, **103**.

Scheme 1-52 *Amide hydrogenation mechanism using Milstein's bifunctional catalyst.*

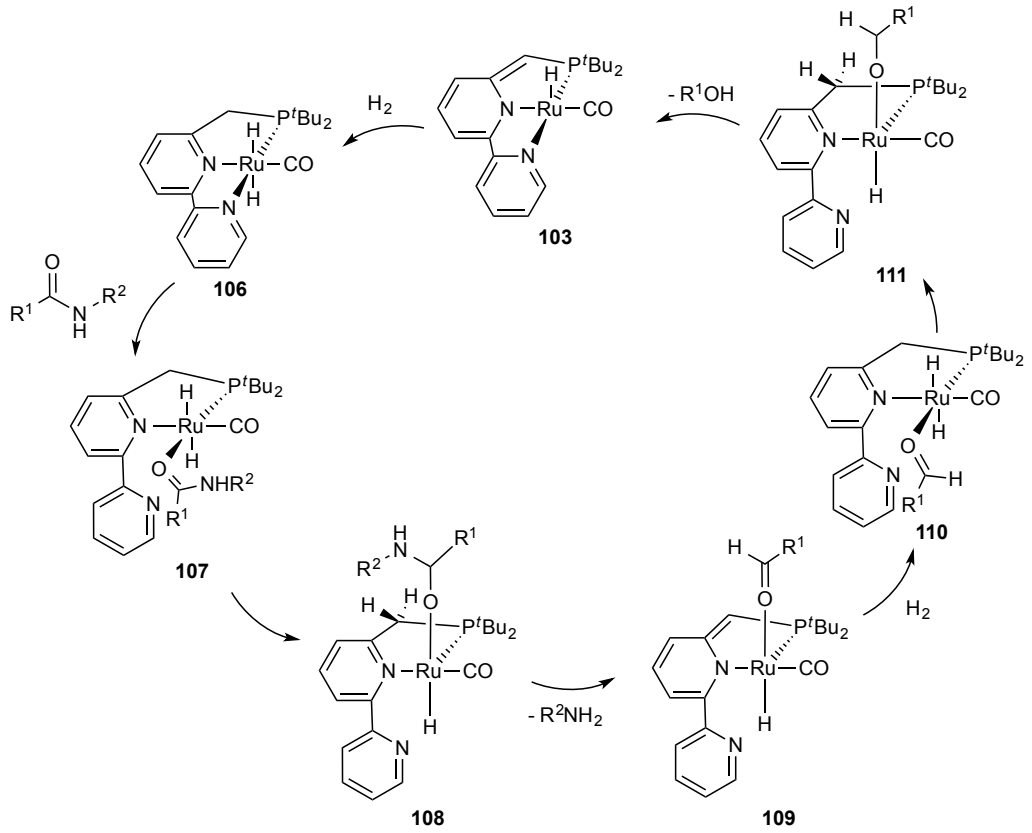

John and Bergens demonstrated that the Noyori ketone hydrogenation catalyst, **2**, can also be used to hydrogenate activated amides. Specifically, they found that heating THF solutions of **2** (2.0 mol%) with KO*t*-Bu (20 mol%) and *N*-methylsulfonylpyrrolidin-2-one under 50 atm H_2 at 100 °C gave *N*-methylsulfonyl-4-amino-1-butanol in ~27 turnover (54% conversion) after 39 h.[162,163] This result was however, inconsistent with the high activity of **2** towards ketones, imides and esters in THF.[44,45,89,123] Subsequently, they found that the combination of [Ru(η^3-C_3H_5)($Ph_2P(CH_2)_2NH_2)_2$]BF_4, **112**, or $RuCl_2(Ph_2P(CH_2)_2NH_2)_2$, **63**, in basic THF efficiently catalyzes the hydrogenation amides and lactams with moderate temperatures and pressures to give the products associated with C–N cleavage, Scheme 1-53. For example, using 0.01 mol% of **112** catalyzes the hydrogenation of *N*-phenyl-2-

pyrrolidinone to *N*-phenyl-4-aminobutan-1-ol with a TON = 7120 after 24 h at 100 °C under 50 atm H_2.

Scheme 1-53 *Hydrogenation of amides using Bergens' catalyst.*

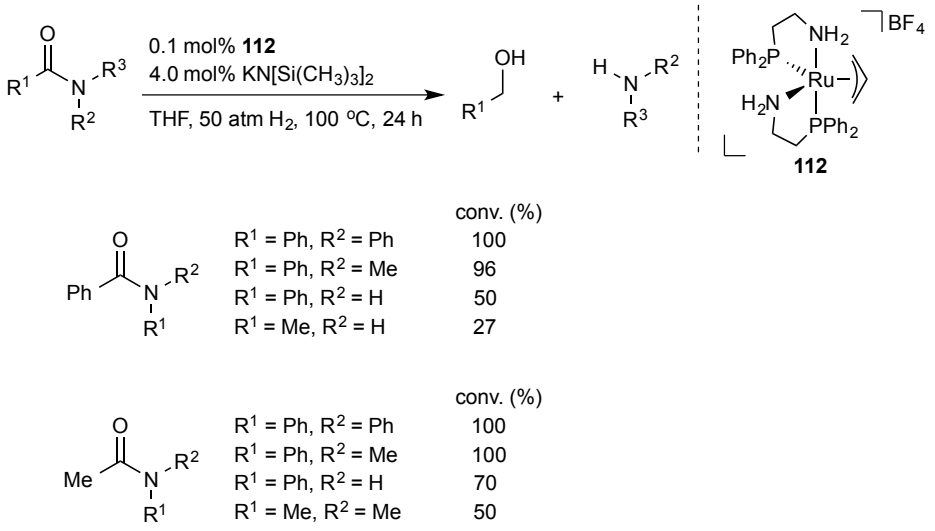

In early 2013, Saito and coworkers reported that $RuCl_2(2\text{-}C_5H_4NCH_2PPh_2)_2$, **113**, combined with the bulky base (**114**: sodium 2-methyl-2-adamantoxide) catalyzes the reduction of unactivated amides to the corresponding alcohols and amines in non polar solvent under rigorous reaction conditions (2.0 mol% **113**, 4.0-20 mol% base under 60-80 atm H_2 at 160 °C for 24-216 h in toluene, Scheme 1-54).[164] Analogous to the findings of Ikariya and coworkers, the authors observed that secondary lactams such as 2-pyrrolidin-2-one and *δ*-valerolactam will be hydrogenated with C–O cleavage under forcing conditions in basic media. Specifically, heating a toluene solution of *δ*-valerolactam with 2.0 mol% **113** and 10 mol% base under 80 atm at 160 °C for 48 h gives piperidine (major) and 5-amino-pentan-1-ol (minor) in 39 and 2 turnovers, respectively.

Scheme 1-54 *Hydrogenation of amides using Saito's catalyst.*

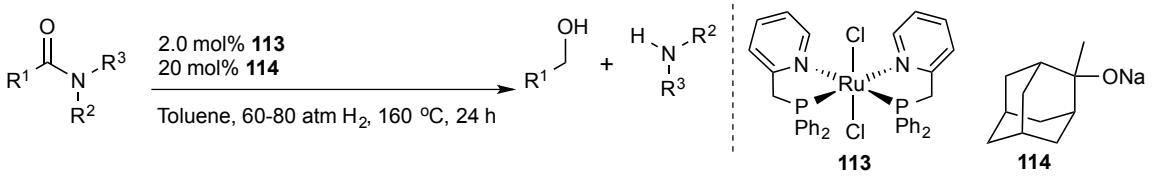

	yield (%) using 80 atm H_2
R^1 = Ph, R^2 = Me, R^3 = Me	84
R^1 = Me, R^2 = H, R^3 = Bn	95
R^1 = *t*-Bu, R^2 = H, R^3 = C_8H_{17}	9

	yield (%) using 60 atm H_2
R^1 = 4-$CF_3C_6H_4$, R^2 = H, R^3 = Bn	99
R^1 = 4-PhC_6H_4, R^2 = H, R^3 = Bn	83
R^1 = 4-MeC_6H_4, R^2 = H, R^3 = Bn	74

Preliminary $^{31}P\{^1H\}$ NMR and mass spectrometry (ESI MS) data obtained after a significant induction period (stirring **113** for 5 h under 80 atm H_2 at 160 ° C) in toluene-d_8 showed complete reduction of the aromatic moieties in **113**. These results coupled with a negative Hg test led the authors suggested that either **115** or the catalyst fragment **116** could be responsible for catalysis under these conditions.

Figure 1-5 *Tentative structures for Saito's catalyst.*

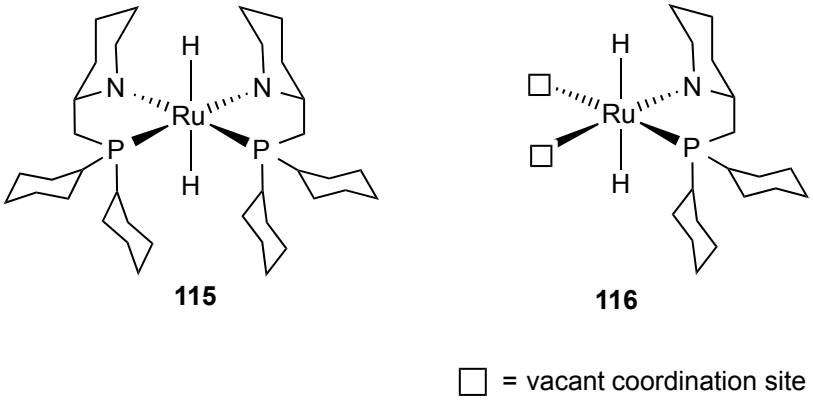

Synopsis

The development of sustainable and efficient strategies to reduce carboxylic acid derivatives has been of particular interest to both academia and industry. The products of these reductions, *i.e.* alcohols and/or amines, are useful intermediates in the synthesis of agrochemicals, pharmaceuticals, flavors, fragrances and advanced materials that are used and consumed in everyday life. Traditionally, the reduction of these classes of compounds has relied upon the use of stoichiometric amounts of metal hydride reagents (*e.g.* Al-H, B-H, Si-H *etc.*) that often have adverse industrial and environmental costs associated with their application.[130-132] Despite the significant and rapid progress in the field of aldehyde, ketone and ester hydrogenations, there has been little progress in the hydrogenation of polar functionalities bearing less electrophilic carbonyl groups such as imides and amides. This dissertation outlines recent progress towards developing conceptually "greener" bifunctional catalysts to replace stoichiometric M-H reducing agents.

Chapter 2 presents the first chemo-, diastereo- and enantiotopic group- selective monohydrogenation of cyclic *meso*-imides to produce γ-hydroxy lactams. The decision to explore this desymmetrization reaction was motivated by the remarkable activity of the dihydride, **2**, towards ketones and esters at low temperatures in THF-d_8. The results of this study were particularly significant as we show that multiple stereogenic centers can be formed from simple substrates in high *ee*, dr and C=O/C=C selectivity with one hydrogenation. We also demonstrate, among other things, the synthetic utility of γ-hydroxy lactams as versatile building blocks in organic synthesis.[123,124]

Chapter 3 continues with a mechanistic investigation into the desymmetrization of cyclic *meso*-imides that uncovers a previously unobserved, highly facile base-catalyzed bifunctional addition to imide and amide carbonyls at low temperatures in THF-d_8. This unexpected result led to the synthesis, characterization and reactivity study

of putative intermediates resulting from the deprotonation and di-deprotonation of the parent dihydride, **2**, that have been proposed to be active intermediates in the mechanism of the Noyori ketone hydrogenation.[47]

The rational design of a new catalyst system for the selective hydrogenation of amides is explored in Chapter 3. Born out of a fundamental understanding of the decomposition pathways of **2**, we have developed the most active amide hydrogenation catalyst that is capable of achieving C-N cleavage to a wide variety of amide substrates.[162,163] Further, we show that a simple modification to this catalyst system has led to a significant advancement in the potential applications of this technology to effect the "base-free" hydrogenation of amides.

Bibliography

1. Armor, J. N. *Catal. Today* **2011**, *163*, 3-9.
2. Chorkendorff, I.; Niemantsverdriet, J. W. *Concepts of Modern Catalysis and Kinetics, 2nd Edition*: *Introduction to Catalysis*; Wiley-VCH Verlag GmbH & Co. KGaA: Weinheim, 2005; pp 1-21.
3. Bartholomew, C. H.; Farrauto, R. J. *Fundamentals of Industrial Catalytic Processes, 2nd Edition*: *Catalysis: Introduction and Fundamental Catalytic Phenomena*; John Wiley & Sons, Inc.: New Jersey, 2005; pp 3-59.
4. Armor, J. *What is Catalysis or Catalyst, So What*. http://nacatsoc.org/above/what-is-catalysis/ (accessed 01/10/2013).
5. Lancaster, M. *Green Chemistry*: *An Introductory Text*; The Royal Society of Chemistry: Cambridge, 2002.
6. Transparency Market Research. *Free Market Analysis*. www.transparencymarketresearch.com/gobal-refinery-catalyst-market.html (accessed 01/10/2013).
7. Howard, P.; Morris, G.; Sunley, G. In *Catalysis in the Chemical Industry: Introduction: Catalysis in the Chemical Industry*; Chiusoli, G. P., Maitlis, P. M., Eds.; The Royal Society of Chemistry: Cambridge, 2006; pp 1-22.
8. Busacca, C. A.; Fandrick, D. R.; Song, J. J.; Senanayake, C. H. In *Applications of Transition Metal Catalysis in Drug Discovery and Development: An Industrial Perspective: Transition Metal Catalysis in the Pharmaceutical Industry*; Crawley, M. L., Trost, B. M., Eds.; John Wiley & Sons, Inc.: New Jersey, 2012; pp 1-24.
9. de Vries, J. G. In *Organometallics as Catalysts in the Fine Chemical Industry: Palladium-Catalysed Coupling Reactions*; Beller, M., Blaser, H., Eds.; Springer-Verlag: Berlin, 2012; pp 1-34.

10. Blaser, H. -U.; Pugin, B.; Spindler, F. In *Organometallics as Catalysts in the Fine Chemical Industry: Asymmetric Hydrogenation;* Beller, M., Blaser, H., Eds.; Springer-Verlag: Berlin, 2012; pp 65-102.
11. Sheldon, R. In *Green Chemistry in the Pharmaceutical Industry: Introduction to Green Chemistry, Organic Synthesis and Pharmaceuticals*; Dunn, P. J., Wells, A. S., Williams, M. T., Eds.; Wiley-VCH Verlag GmbH & Co. KGaA: Weinheim, 2010; pp 1-20.
12. Knowles, W. S. In *Asymmetric Catalysis on Industrial Scale: Challenges, Approaches and Solutions: Asymmetric Hydrogenations - The Monsanto L-Dopa Process*; Blaser, H. -U., Schmidt, E., Eds.; Wiley-VCH Verlag GmbH & Co. KGaA: Weinheim, 2004; pp 21-38.
13. Selke, R. In *Asymmetric Catalysis on Industrial Scale: Challenges, Approaches and Solutions: The Other L-Dopa Process*; Blaser, H. -U., Schmidt, E., Eds.; Wiley-VCH Verlag GmbH & Co. KGaA: Weinheim, 2004; pp 39-53.
14. Gröger, H.; Drauz, K. In *Asymmetric Catalysis on Industrial Scale: Challenges, Approaches and Solutions: Methods for the Enantioselective Biocatalytic Production of L-Amino Acids on an Industrial Scale*; Blaser, H. -U., Schmidt, E., Eds.; Wiley-VCH Verlag GmbH & Co. KGaA: Weinheim, 2004; pp 131-147.
15. Silverman, R. B. *The Organic Chemistry of Drug Design and Drug Action, 2nd Edition*; Academic Press: San Diego, 2004.
16. Murahashi, S. In *Ruthenium in Organic Synthesis: Introduction; Murahashi, S., Ed.;* Wiley-VCH: Weinheim, 2004; pp 1-3.
17. *Handbook of Homogeneous Hydrogenation*; Elsevier, C. J., de Vries, J. G., Eds.; Wiley-VCH: New York, 2006.

18. Brown, H. C.; Veeraraghavan, R. P. In *Reductions in Organic Synthesis: Sixty Years of Hydride Reductions*; Abdel-Magid, A. F., Ed.; American Chemical Society: Washington, 1996; pp 1-30.

19. Carreira, E. M.; Kvaerno, L. *Classics in Stereoselective Synthesis*; Wiley-VCH Verlag GmbH & Co. KGaA: Weinheim, 2009.

20. Ohkuma, T.; Ooka, H.; Hashiguchi, S.; Ikariya, T.; Noyori, R. *J. Am. Chem. Soc.* **1995***, 117*, 2675-2676.

21. Ohkuma, T.; Koizumi, M.; Doucet, H.; Pham, T.; Kozawa, M.; Murata, K.; Katayama, E.; Yokozawa, T.; Ikariya, T.; Noyori, R. *J. Am. Chem. Soc.* **1998***, 120*, 13529-13530.

22. Ohkuma, T.; Koizumi, M.; Ikehira, H.; Yokozawa, T.; Noyori, R. *Org. Lett.* **2000***, 2*, 659-662.

23. Ohkuma, T.; Koizumi, M.; Yoshida, M.; Noyori, R. *Org. Lett.* **2000***, 2*, 1749-1751.

24. Ohkuma, T.; Ishii, D.; Takeno, H.; Noyori, R. *J. Am. Chem. Soc.* **2000***, 122*, 6510-6511.

25. Ohkuma, T.; Sandoval, C. A.; Srinivasan, R.; Lin, Q.; Wei, Y.; Muñiz, K.; Noyori, R. *J. Am. Chem. Soc.* **2005***, 127*, 8288-8289.

26. Noyori, R.; Ohkuma, T. *Angew. Chem., Int. Ed.* **2001***, 40*, 40-73.

27. Ohkuma, T.; Koizumi, M.; Muñiz, K.; Hilt, G.; Kabuto, C.; Noyori, R. *J. Am. Chem. Soc.* **2002***, 124*, 6508-6509.

28. Morris, R. H. *Chem. Soc. Rev.* **2009***, 38*, 2282-2291.

29. Ohkuma, T. *Proc. Jpn Acad., Ser. B* **2010***, 86*, 202-219.

30. *Privileged chiral ligands and catalysts*; Zhou, Q. -L., Ed.; Wiley-VCH Verlag GmbH & Co. KGaA: Weinheim, 2011.

31. Magano, J.; Dunetz, J. R. *Org. Process Res. Dev.* **2012***, 16*, 1156-1184.

32. Bartoszewicz, A.; Ahlsten, N.; Martín-Matute, B. *Chem. Eur. J.* **2013***, 19*, 7274-7302.

33. Eisenstein, O.; Crabtree, R. H. *New J. Chem.* **2013***, 37*, 21-27.

34. Ohkuma, T.; Noyori, R. In *Handbook of Homogeneous Hydrogenation: Enantioselective Ketone and β-Keto Ester Hydrogenations (Including Mechanisms)*; de Vries, J. G., Elsevier, C. J., Eds.; Wiley-VCH Verlag GmbH & Co. KGaA: Weinheim, 2008; pp 1105-1163.

35. Shambayati, S.; Crowe, W. E.; Schreiber, S. L. *Angew. Chem., Int. Ed.* **1990***, 29*, 256-272.

36. Daley, C. J. A.; Bergens, S. H. *J. Am. Chem. Soc.* **2002***, 124*, 3680-3691.

37. Abdur-Rashid, K.; Faatz, M.; Lough, A. J.; Morris, R. H. *J. Am. Chem. Soc.* **2001***, 123*, 7473-7474.

38. Hartmann, R.; Chen, P. *Angew. Chem., Int. Ed.* **2001***, 40*, 3581-3585.

39. Abdur-Rashid, K.; Clapham, S. E.; Hadzovic, A.; Harvey, J. N.; Lough, A. J.; Morris, R. H. *J. Am. Chem. Soc.* **2002***, 124*, 15104-15118.

40. Sandoval, C. A.; Ohkuma, T.; Muñiz, K.; Noyori, R. *J. Am. Chem. Soc.* **2003***, 125*, 13490-13503.

41. Hartmann, R.; Chen, P. *Adv. Synth. Catal.* **2003***, 345*, 1353-1359.

42. Clapham, S. E.; Hadzovic, A.; Morris, R. H. *Coord. Chem. Rev.* **2004***, 248*, 2201-2237.

43. Hamilton, R. J.; Leong, C. G.; Bigam, G.; Miskolzie, M.; Bergens, S. H. *J. Am. Chem. Soc.* **2005***, 127*, 4152-4153.

44. Hamilton, R. J.; Bergens, S. H. *J. Am. Chem. Soc.* **2006***, 128*, 13700-13701.

45. Hamilton, R. J.; Bergens, S. H. *J. Am. Chem. Soc.* **2008***, 130*, 11979-11987.

46. Takebayashi, S.; Dabral, N.; Miskolzie, M.; Bergens, S. H. *J. Am. Chem. Soc.* **2011***, 133*, 9666-9669.

47. John, J. M.; Takebayashi, S.; Dabral, N.; Miskolzie, M.; Bergens, S. H. *J. Am. Chem. Soc.* **2013***, 135*, 8578-8584.

48. Robertson, A.; Matsumoto, T.; Ogo, S. *Dalton Trans.* **2011***, 40*, 10304-10310.

49. Darwish, M.; Wills, M. *Catal. Sci. Technol.* **2012***, 2*, 243-255.

50. Ikariya, T.; Blacker, A. J. *Acc. Chem. Res.* **2007***, 40*, 1300-1308.

51. Ito, M.; Hirakawa, M.; Murata, K.; Ikariya, T. *Organometallics* **2001***, 20*, 379-381.

52. Hadzovic, A.; Song, D.; MacLaughlin, C. M.; Morris, R. H. *Organometallics* **2007***, 26*, 5987-5999.

53. Handgraaf, J. -W.; Meijer, E. J. *J. Am. Chem. Soc.* **2007***, 129*, 3099-3103.

54. Abdur-Rashid, K.; Fong, T. P.; Greaves, B.; Gusev, D. G.; Hinman, J. G.; Landau, S. E.; Lough, A. J.; Morris, R. H. *J. Am. Chem. Soc.* **2000***, 122*, 9155-9171.

55. Casey, C. P.; Singer, S. W.; Powell, D. R.; Hayashi, R. K.; Kavana, M. *J. Am. Chem. Soc.* **2001***, 123*, 1090-1100.

56. Casey, C. P.; Johnson, J. B. *J. Org. Chem.* **2003***, 68*, 1998-2001.

57. Casey, C. P.; Johnson, J. B.; Singer, S. W.; Cui, Q. *J. Am. Chem. Soc.* **2005***, 127*, 3100-3109.

58. Casey, C. P.; Johnson, J. B. *Can. J. Chem.* **2005***, 83*, 1339-1346.

59. Casey, C. P.; Bikzhanova, G. A.; Cui, Q.; Guzei, I. A. *J. Am. Chem. Soc.* **2005***, 127*, 14062-14071.

60. Casey, C. P.; Johnson, J. B. *J. Am. Chem. Soc.* **2005***, 127*, 1883-1894.

61. Casey, C. P.; Bikzhanova, G. A.; Guzei, I. A. *J. Am. Chem. Soc.* **2006***, 128*, 2286-2293.

62. Casey, C. P.; Clark, T. B.; Guzei, I. A. *J. Am. Chem. Soc.* **2007***, 129*, 11821-11827.

63. Casey, C. P.; Beetner, S. E.; Johnson, J. B. *J. Am. Chem. Soc.* **2008***, 130*, 2285-2295.

64. Wiles, J. A.; Bergens, S. H.; Vanhessche, K. P. M.; Dobbs, D. A.; Rautenstrauch, V. *Angew. Chem., Int. Ed.* **2001***, 40*, 914-919.

65. Wiles, J. A.; Daley, C. J. A.; Hamilton, R. J.; Leong, C. G.; Bergens, S. H. *Organometallics* **2004***, 23*, 4564-4568.

66. Crabtree, R. H.; Habib, A. *Inorg. Chem.* **1986***, 25*, 3698-3699.

67. Earl, K. A.; Jia, G.; Maltby, P. A.; Morris, R. H. *J. Am. Chem. Soc.* **1991***, 113*, 3027-3039.

68. Bautista, M. T.; Cappellani, E. P.; Drouin, S. D.; Morris, R. H.; Schweitzer, C. T.; Sella, A.; Zubkowski, J. *J. Am. Chem. Soc.* **1991***, 113*, 4876-4887.

69. Clapham, S. E.; Guo, R.; Zimmer-De Iuliis, M.; Rasool, N.; Lough, A.; Morris, R. H. *Organometallics* **2006***, 25*, 5477-5486.

70. Baratta, W.; Chelucci, G.; Gladiali, S.; Siega, K.; Toniutti, M.; Zanette, M.; Zangrando, E.; Rigo, P. *Angew. Chem., Int. Ed.* **2005***, 44*, 6214-6219.

71. Fulton, J. R.; Holland, A. W.; Fox, D. J.; Bergman, R. G. *Acc. Chem. Res.* **2002***, 35*, 44-56.

72. Hasanayn, F.; Morris, R. H. *Inorg. Chem.* **2012***, 51*, 10808-10818.

73. Hall, H. K. *J. Am. Chem. Soc.* **1957***, 79*, 5439-5441.

74. Mayer, J. M. *Comment Inorg. Chem.* **1988***, 8*, 125-135.

75. Bergman, R. G. *Polyhedron* **1995***, 14*, 3227-3237.

76. Holland, P. L.; Andersen, R. A.; Bergman, R. G. *Comment Inorg. Chem.* **1999***, 21*, 115-129.

77. Johnson, J. B.; Bäckvall, J. -E. *J. Org. Chem.* **2003***, 68*, 7681-7684.

78. Samec, J. S. M.; Éll, A. H.; Åberg, J. B.; Privalov, T.; Eriksson, L.; Bäckvall, J. -E. *J. Am. Chem. Soc.* **2006***, 128*, 14293-14305.

79. Åberg, J. B.; Samec, J. S. M.; Bäckvall, J. -E. *Chem. Commun.* **2006**, 2771-2773.

80. Privalov, T.; Samec, J. S. M.; Bäckvall, J. *Organometallics* **2007***, 26*, 2840-2848.

81. Dub, P. A.; Ikariya, T. *ACS Catal.* **2012***, 2*, 1718-1741.

82. Saudan, L. A. In *Sustainable Catalysis: Challenges and Practices for the Pharmaceutical and Fine Chemical Industries: Hydrogenation of Esters*; Dunn, P. J., Hii, K. K., Krische, M. J., Williams, M. T., Eds.; John Wiley and Sons: New Jersey, 2013; pp 37-61.

83. Saudan, C.; Saudan, L.; Saudan, M. A. J.; Saudan, S. J. A. A. Firmenich S. A., Switzerland; Patent WO2010061350A1, 2010; p 55.

84. Saudan, L.; Dupau, P.; Riedhauser, J. -J.; Wyss, P. Firmenich S. A., Switzerland; Patent WO2006106483A1, 2006; p 40.

85. Saudan, L.; Dupau, P.; Riedhauser, J. -J.; Wyss, P. Firmenich S. A., Switzerland; Patent WO2006106484A1, 2006; p 29.

86. Saudan, L.; Saudan, C. Firmenich S. A., Switzerland; Patent WO2008065588A1, 2006; p 34.

87. Saudan, L. A. *Acc. Chem. Res.* **2007***, 40*, 1309-1319.

88. Saudan, L. A.; Saudan, C.; Becieux, C.; Wyss, P. *Angew. Chem., Int. Ed.* **2007***, 46*, 7473-7476.

89. Takebayashi, S.; Bergens, S. H. *Organometallics.* **2009***, 28*, 2349-2351.

90. W. N. O., W.; Lough, A. J.; Morris, R. H. *Chem. Commun.* **2010***, 46*, 8240-8242.

91. Acosta-Ramirez, A.; Bertoli, M.; Gusev, D. G.; Schlaf, M. *Green Chem.* **2012***, 14*, 1178-1188.

92. Bertoli, M.; Choualeb, A.; Gusev, D. G.; Lough, A. J.; Major, Q.; Moore, B. *Dalton Trans.* **2011***, 40*, 8941-8949.

93. Goussev, D.; Spasyuk, D. Canada; Patent WO2013023307A1, 2013; p 56.

94. Spasyuk, D.; Gusev, D. G. *Organometallics* **2012***, 31*, 5239-5242.

95. Spasyuk, D.; Smith, S.; Gusev, D. G. *Angew. Chem., Int. Ed.* **2013***, 52*, 2538-2542.

96. Spasyuk, D.; Smith, S.; Gusev, D. G. *Angew. Chem., Int. Ed.* **2012***, 51*, 2772-2775.

97. Ino, Y.; Kuriyama, W.; Ogata, O.; Matsumoto, T. *Top. Catal.* **2010***, 53*, 1019-1024.

98. Ino, Y.; Yoshida, A.; Kuriyama, W. Takasago International Corporation, Japan; Patent EP1970360A1, 2008; p 26.

99. Kuriyama, W.; Ino, Y.; Ogata, O.; Sayo, N.; Saito, T. *Adv. Synth. Catal.* **2010***, 352*, 92-96.

100. Zhang, J.; Balaraman, E.; Leitus, G.; Milstein, D. *Organometallics* **2011***, 30*, 5716-5724.

101. Zhang, J.; Leitus, G.; Ben-David, Y.; Milstein, D. *Angew. Chem., Int. Ed.* **2006***, 45*, 1113-1115.

102. *Comprehensive Organic Synthesis: Selectivity, Strategy & Efficiency in Modern Organic Chemistry*; Trost, B. M., Fleming, I., Schreiber, S. L., Eds.; Elsevier: Oxford, 1991.

103. Feng, S.; Panetta, C. A.; Graves, D. E. *J. Org. Chem.* **2001***, 66*, 612-616.

104. Norman, M. H.; Minick, D. J.; Rigdon, G. C. *J. Med. Chem.* **1996***, 39*, 149-157.

105. Das, S.; Addis, D.; Knöpke, L. R.; Bentrup, U.; Junge, K.; Brückner, A.; Beller, M. *Angew. Chem., Int. Ed.* **2011***, 50*, 9180-9184.

106. Gray, A. P.; Heitmeier, D. E. *J. Org. Chem.* **1969***, 34*, 3253.

107. Rice, L. M.; Reid, E. E.; Grogan, C. H. *J. Org. Chem.* **1954***, 19*, 884.

108. Horii, Z. -I.; Iwata, C.; Tamura, Y. *J. Org. Chem.* **1961***, 26*, 2273-2276.

109. Uhle, F. *J. Org. Chem.* **1961***, 26*, 2998-3001.

110. Miller, S. A.; Chamberlin, A. R. *J. Org. Chem.* **1989***, 54*, 2502-2504.

111. Hubert, J. C.; Wijnberg, J. B. P. A.; Speckamp, W. N. *Tetrahedron* **1975***, 31*, 1437-1441.

112. Matsuki, K.; Inoue, H.; Ishida, A.; Takeda, M.; Nakagawa, M.; Hino, T. *Chem. Pharm. Bull.* **1994***, 42*, 9-18.

113. Kang, J.; Lee, J. W.; Kim, J. I.; Pyun, C. *Tetrahedron Lett.* **1995***, 36*, 4265-4368.

114. Ostendorf, M.; Romagnoli, R.; Pereiro, I. C.; Roos, E. C.; Moolenaar, M. J.; Speckamp, W. N.; Hiemstra, H. *Tetrahedron: Asymmetry* **1997***, 8*, 1773-1789.

115. Paden, J. H.; Adkins, H. *J. Am. Chem. Soc.* **1936***, 58*, 2487-2499.

116. Hennige, H.; Kreher, R. P.; Konrad, M.; Jelitto, F. *Chem. Ber.* **1988***, 121*, 243-252.

117. McAlees, A. J.; McCrindle, R. *J. Chem. Soc. C* **1969**, 2425-2435.

118. Patton, D. E.; Drago, R. S. *J. Chem. Soc., Perkin Trans. 1* **1993**, 1611-1615.

119. Aoun, R.; Renaud, J. -L.; Dixneuf, P. H.; Bruneau, C. *Angew. Chem., Int. Ed.* **2005***, 44*, 2021-2023.

120. Ito, M.; Sakaguchi, A.; Kobayashi, C.; Ikariya, T. *J. Am. Chem. Soc.* **2007***, 129*, 290-291.

121. Ito, M.; Koo, L. W.; Himizu, A.; Kobayashi, C.; Sakaguchi, A.; Ikariya, T. *Angew. Chem., Int. Ed.* **2009***, 48*, 1324-1327.

122. Ito, M.; Kobayashi, C.; Himizu, A.; Ikariya, T. *J. Am. Chem. Soc.* **2010***, 132*, 11414-11415.

123. Takebayashi, S.; John, J. M.; Bergens, S. H. *J. Am. Chem. Soc.* **2010***, 132*, 12832-12834.

124. Bergens, S. H.; Takebayashi, S. University of Alberta, Canada; Patent WO2010145024A1, 2010; p 63.

125. Bailey, P. D.; Mills, T. J.; Pettecrew, R.; Price, R. A. In *Comprehensive Organic Functional Group Transformations II: Amides*; Katritzky, A. R., Taylor, R. J. K., Eds.; Elsevier: Oxford, 2005; pp 201-294.

126. Dunn, P. J. *Chem. Soc. Rev.* **2012***, 41*, 1452-1461.

127. Doods, L.; Cole-Hamilton, D. J. In *Sustainable Catalysis: Challenges and Practices for the Pharmaceutical and Fine Chemical Industries: Catalytic Reduction of Amides Avoiding $LiAlH_4$ or B_2H_6*; Dunn, P. J., Hii, K. K., Krische, M. J., Williams, M. T., Eds.; John Wiley and Sons: New Jersey, 2013; pp 1-36.

128. Constable, D. J. C.; Dunn, P. J.; Hayler, J. D.; Humphrey, G. R.; Leazer, Jr., J. L.; Linderman, R. J.; Lorenz, K.; Manley, J.; Pearlman, B. A.; Wells, A.; Zaks, A.; Zhang, T. Y. *Green Chem.* **2007***, 9*, 411-420.

129. Dugger, R. W.; Ragan, J. A.; Brown Ripin, D. H. *Org. Process Res. Dev.* **2005***, 9*, 253-258.

130. Seyden-Penne, J. *Reductions by the Alumino- and Borohydrides in Organic Synthesis, 2nd Edition*; Wiley: New York, 1997.

131. Gribble, G.W. *Chem. Soc. Rev.* **1998***, 27*, 395-404.

132. Larock, R. *Comprehensive Organic Transformations, A Guide to Functional Group Preparations, 2nd Edition;* Wiley: New York, 1999.

133. Nakazato, A.; Ohta, K.; Sekiguchi, Y.; Okuyama, S.; Chaki, S.; Kawashima, Y.; Hatayama, K. *J. Med. Chem.* **1999***, 42*, 1076-1087.

134. Sheldon, R. A.; Arends, I. W. C. E.; Hanefeld, U. *Green Chemistry and Catalysis*; Wiley-VCH Verlag GmbH & Co. KGaA: Weinheim, 2007.

135. *The Amide Linkage: Structural Significance in Chemistry, Biochemistry and Materials Science*; Greenberg, A., Breneman, C. M., Liebman, J. F., Eds.; John Wiley & Sons: New York, 2003.

136. Glover, S. A.; Rosser, A. A. *J. Org. Chem.* **2012***, 77*, 5492-5502.

137. Wojcik, B.; Adkins, H. *J. Am. Chem. Soc.* **1934***, 56*, 2419-2424.

138. Sauer, J. C.; Adkins, H. *J. Am. Chem. Soc.* **1938***, 60*, 402-406.

139. King, R. M. The Procter & Gamble Company, United States; Patent US4448998, 1984; p 3.

140. Forquy, C.; Brouard, R. Ceca, S. A., France; Patent US5075505, 1991; p 7.

141. Galinovsky, F.; Stern, E. *Ber. dtsch. Chem. Ges. A/B* **1943***, 76*, 1034-1038.

142. Broadbent, H. S.; Bartley, W. J. *J. Org. Chem.* **1963***, 28*, 2345-2347.

143. Guyer, A.; Bieler, A.; Gerliczy, G. *Helv. Chim. Acta* **1955***, 38*, 1649-1654.

144. Dobson, I. D. BP Chemicals Limited; Patent EP0286280, 1988; p 11.

145. Burch, R.; Paun, C.; Cao, X. -M.; Crawford, P.; Goodrich, P.; Hardacre, C.; Hu, P.; McLaughlin, L.; Sá, J.; Thompson, J. M. *J. Catal.* **2011***, 283*, 89-97.

146. Stein, M.; Breit, B. *Angew. Chem., Int. Ed.* **2013***, 52*, 2231-2234.

147. Hirosawa, C.; Wakasa, N.; Fuchikami, T. *Tetrahedron Lett.* **1996***, 37*, 6749-6752.

148. Smith, A. A.; Dani, P.; Higginson, P. D.; Pettman, A. J. Avantium Internation B.V., Netherlands; Patent WO2005066112A1, 2005; p 34.

149. Beamson, G.; Papworth, A. J.; Philipps, C.; Smith, A. M.; Whyman, R. *Adv. Synth. Catal.* **2010***, 352*, 869-883.

150. Beamson, G.; Papworth, A. J.; Philipps, C.; Smith, A. M.; Whyman, R. *J. Catal.* **2010***, 269*, 93-102.

151. Beamson, G.; Papworth, A. J.; Philipps, C.; Smith, A. M.; Whyman, R. *J. Catal.* **2011***, 278*, 228-238.

152. Kilner, M.; Tyers, D. V.; Crabtree, S. P.; Wood, M. A. Davy Process Technology Limited, UK; Patent WO03093208A1, 2003; p 23.

153. Magro, A. A. N.; Eastham, G. R.; Cole-Hamilton, D. *Chem. Commun.* **2007**, 3154-3156.

154. Eastham, G. R.; Cole-Hamilton, D. J.; Magro, A. A. N. Lucite International UK Limited, UK; Patent WO2008035123A2, 2008; p 36.

155. Coetzee, J.; Dodds, D. L.; Klankermayer, J.; Brosinski, S.; Leitner, W.; Slawin, A. M. Z.; Cole-Hamilton, D. J. *Chem. Eur. J.* **2013***, 19*, 11039-11050.

156. Geilen, F. M. A.; Engendahl, B.; Hölscher, M.; Klankermayer, J.; Leitner, W. *J. Am. Chem. Soc.* **2011***, 133*, 14349-14358.

157. Ikariya, T.; Ito, M.; Ootsuka, T.; Hashimoto, T. Tokyo Institute of Technology, Japan; Central Glass Company Limited; Patent WO2010073974A1, 2010; p 31.

158. Ito, M.; Ootsuka, T.; Watari, R.; Shiibashi, A.; Himizu, A.; Ikariya, T. *J. Am. Chem. Soc.* **2011***, 133*, 4240-4242.

159. Balaraman, E.; Gnanaprakasam, B.; Shimon, L. J. W.; Milstein, D. *J. Am. Chem. Soc.* **2010***, 132*, 16756-16758.

160. Milstein, D.; Gunanathan, C.; Ben-David, Y.; Balaraman, E.; Gnanaprakasam, B.; Zhang, H. Yeda Research and Development Company Limited, Israel; Patent US2012253042A1, 2012; p 54.

161. Barrios-Francisco, R.; Balaraman, E.; Diskin-Posner, Y.; Leitus, G.; Shimon, L. J. W.; Milstein, D. *Organometallics* **2013***, 32*, 2973-2982.

162. John, J. M.; Bergens, S. H. *Angew. Chem., Int. Ed.* **2011***, 50*, 10377-10380.

163. Bergens, S. H.; John, J. M. University of Alberta, Canada; Patent WO2013010275A1, 2013; p 95.

164. Miura, T.; Held, I. E.; Oishi, S.; Naruto, M.; Saito, S. *Tetrahedron Lett.* **2013***, 54*, 2674-2678.

Chapter 2

Desymmetrization of cyclic *meso*-imides via enantioselective monohydrogenation[1]

Introduction

Enantioselective desymmetrization of *meso*-compounds is one of the most efficient methods to produce multiple stereogenic centers in identical *ee*, from simple substrates in one symmetry-breaking operation.[1-3] In this context, the enantioselective desymmetrization of *meso*-anhydrides by esterification are among the most studied because of their use as intermediates in the synthesis of chiral hemi-esters, thioesters, lactones, amino acids, and ketoacids.[3] In recent years however, the catalytic desymmetrization of cyclic *meso*-anhydrides via enantioselective hydrogenation has gathered considerable attention as a powerful synthetic tool to access chiral products that are valuable to the fine chemical industry in a cost-effective and environmentally benign manner.

In the early 1980s, Ikariya and Yoshikawa reported the first example of a catalytic, asymmetric hydrogenation of prochiral or cyclic *meso*-anyhydrides using the chiral Ru catalyst, $Ru_2Cl_4(diop)_3$, **117** (diop = (–)-2,3-*O*-isopropylidene-2,3-dihydroxy-1,4-bis(diphenylphosphino)butane).[4] The chiral catalyst could discriminate between the two enantiotopic carbonyl groups of 3-substituted glutaric and 2,3-substituted succinic anhydrides to access chiral *γ*- and *δ*- lactones albeit, in moderate yields (TON of up to 64 and 84, respectively) and poor selectivity (up to 18% *ee* and 13% *ee*, respectively)

[1] A version of this chapter has been published. Takebayashi, S.; John, J. M.; Bergens, S. H. *J. Am. Chem. Soc.* **2010**, *132*, 12832-12834

under reported conditions (0.50 mol% **117**, 5.0-6.5 mol% NEt_3, 80 atm H_2, 100 °C for 5 h, Scheme 2-1). These initial results provided the impetus for future development.

Scheme 2-1 *Hydrogenation of prochiral and meso-anhydrides using* ***117****.*

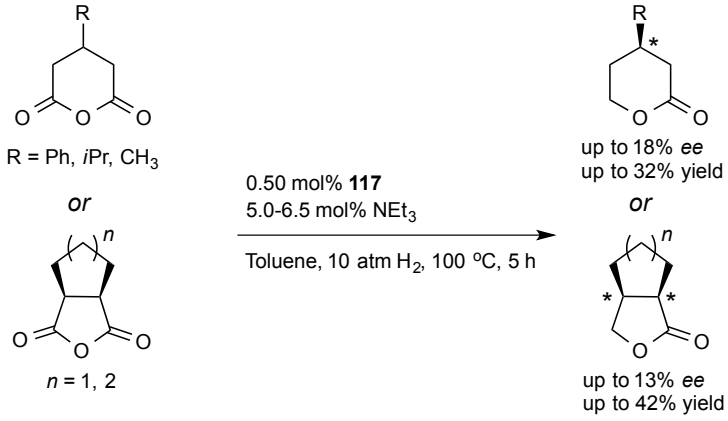

Twenty-five years later, DSM Nutritional Products reported a methodology to prepare optically active lactones from the desymmetrization of cyclic *meso*-anhydrides. A chiral catalyst (Ir-(P-P)*) generated *in situ* from a 1.0:2.1 mixture of $[Ir(COD)Cl]_2$ and (*R*)-3,5-^{t}Bu-4-MeO-MeO-BIPHEP ((*R*)-[6,6′-dimethoxy(1,1′-biphenyl)-2,2′-diyl]bis{bis[3,5-bis(1,1-dimethylethyl)-4-methoxyphenyl]phosphine), was found to effect the asymmetric hydrogenation of *cis*-1,3-dibenzyltetrahydro-2*H*-furo[3,4-d]imidazole-2,4,6-trione, **118**, to give *D*-lactone (a key intermediate for (+)-biotin synthesis) in near quantitative yields and *ee* (TON = 4800, 94.9% *ee* using 80 atm H_2, 100 °C for 19 h), Scheme 2-2.[5]

Scheme 2-2 *Asymmetric hydrogenation of* ***118*** *reported by DSM Nutritional Products.*

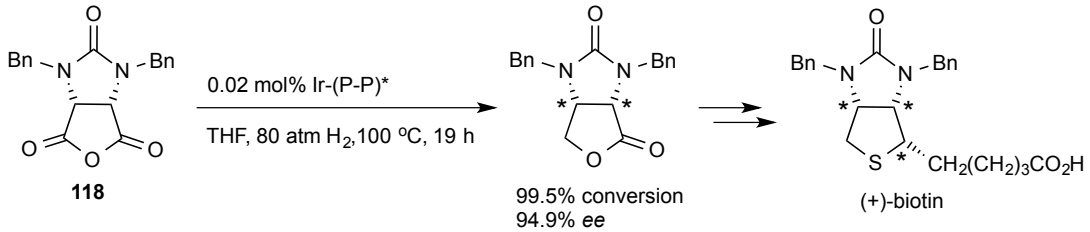

It is also important to note, that the corresponding thioanhydride analogue could also be converted directly to the thiolactone in limited selectivity and yield under more drastic reaction conditions (TON = 11 and 21% *ee* using 0.2 mol% Ir under 30 atm H_2 at 150 °C).[6] Together, these results represent a major advancement in the current methodologies used to access optically active lactones that are valuable intermediates in the synthesis of natural products or biologically active compounds.

Although, structurally related to acid anhydrides, there are only a few reported examples for the enantioselective desymmetrization of cyclic *meso*-imides by chiral M-H reagents or asymmetric hydrogenation, and only one report of imide desymmetrization by esterification.[7] Among all the known substrates the prochiral cyclic imides such as 4-substituted glutarimides, and cyclic *meso*-imides *e.g.* 3,4-disubstituted succinimides, have been shown to be the most versatile in asymmetric synthesis.

Matsuki and coworkers were the first to report a high yielding and selective strategy to desymmetrize 3,4-disubstituted succinimides using (*R*)-BINAL-H. As illustrated, in Table 2-1, variety of bicyclic *meso*-imides were converted into a mixture of *cis*- and *trans*- hydroxy lactams in 55-86% yield and 88-91% *ee* using 3.5 equiv. of the chiral auxiliary at –78 °C.[8]

Table 2-1 *Enantioselective desymmetrization of cyclic meso-imides using (R)-BINAL-H (MeOH)*

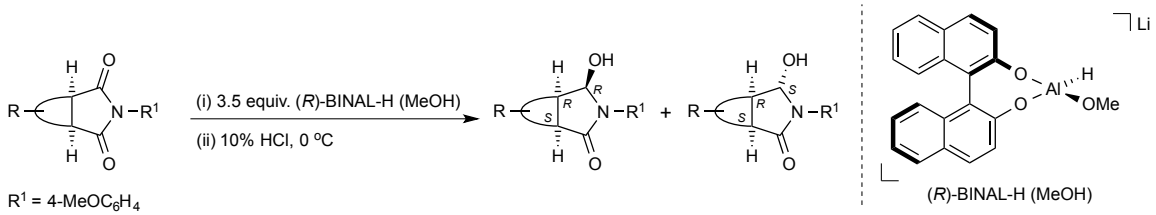

Entry	Imide	Yield (%)	*cis*:*trans*	*ee* (%)[a]
1	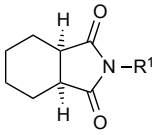	86	9:1	88
2	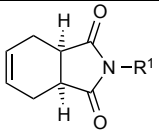	79	10:1	88
3	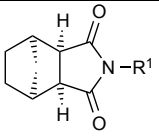	55	10:1	91

[a]Determined by HPLC analysis of the corresponding isoindolone derived from major diastereoisomer

Interestingly, the diastereomeric ratio was found to be dependent on the conditions utilized for the reaction work-up. For example, quenching the reaction mixture with 10% HCl at 0 °C for 1 h led to epimerization of the product alcohol to afford a mixture of *cis*- and *trans*- isomers (~9:1 ratio) while, quenching the reaction mixture at –78 °C resulted in the exclusive formation of the *cis*-hydroxy lactam. The high selectivity for the *cis*-hydroxy lactam was explained by a mechanism that involves preferential attack of the hydride on (*R*)-BINAL-H to the less hindered convex face of the imide that is stabilized by an n/π^* attractive orbital interaction between the oxygen non-bonding orbital and the LUMO of the imide moiety, Figure 2-1.

Figure 2-1 *Proposed transition states for the enantioselective desymmetrization of cyclic meso-imides by (R)-BINAL-H.*

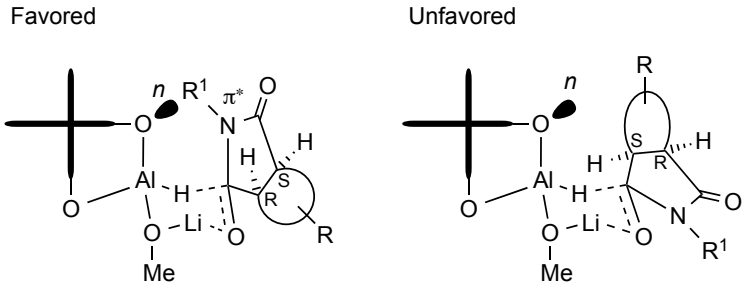

Hiemstra and coworkers also showed that mixtures of diastereotopic hydroxy lactams could be obtained from 10-50 mol% **119** (derived from (*S*)-*α*,*α*-diphenylprolinol) and 0.65-0.75 equiv. borane followed by acid treatment with 5% HCl at 0 °C.[9] However, when this diastereomeric mixture was further treated with 2.0 M H_2SO_4 in EtOH, the *trans*-ethoxy lactams were obtained as single diastereomers in moderate to good yields, Table 2-2.

Table 2-2 *Enantioselective desymmetrization of cyclic meso-imides using* ***119*** *and* $BH_3 \cdot THF$

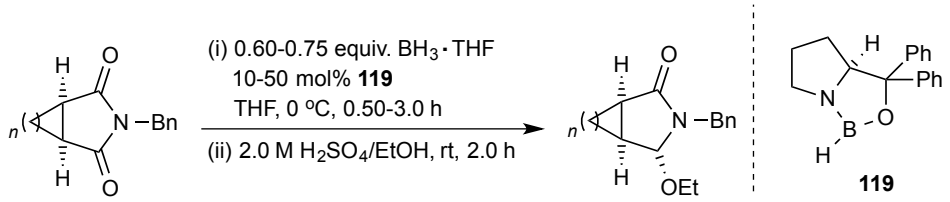

Entry	*n*	Yield (%)	*ee* (%)
1	4	87	80
2	3	85	77
3	2	68	89
4	1	94	88

The authors proposed that the kinetic product of this addition is the *cis*-hydroxy lactam resulting from the preferential attack of the hydride from the convex face of the oxazaborolidine to the least hindered *Si*-face of the imide carbonyl, Figure 2-2. This configuration minimizes the steric repulsion between the *N*-benzyl group and the auxiliary. The authors also note that a decrease in the size of the imide backbone results in an increase in the enantioselectivity through improved substrate-catalyst interaction.

Figure 2-2 *Proposed transition states for the enantioselective desymmetrization of cyclic meso-imides using* ***119*** *and* BH_3•*THF.*

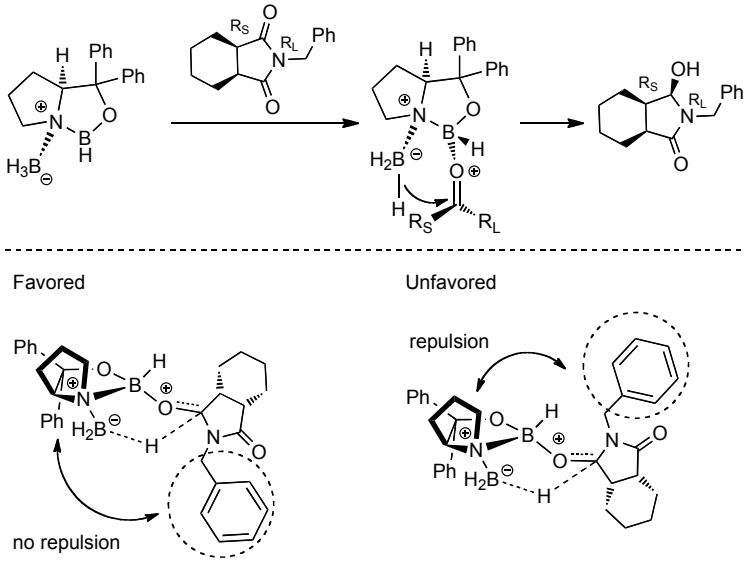

Notably, subsequent acid treatment in ethanol results in the rapid epimerization at the hydroxy carbon. This process is facilitated by an acid-catalyzed isomerization reaction in which ethanol adds across an *N*-acyliminium ion to form the thermodynamically favored *trans*-isomer that has minimal steric repulsion between the large ethoxy group and bulky imide backbone, Scheme 2-3.

Scheme 2-3 *Mechanism for the formation of the trans-ethoxy lactam.*

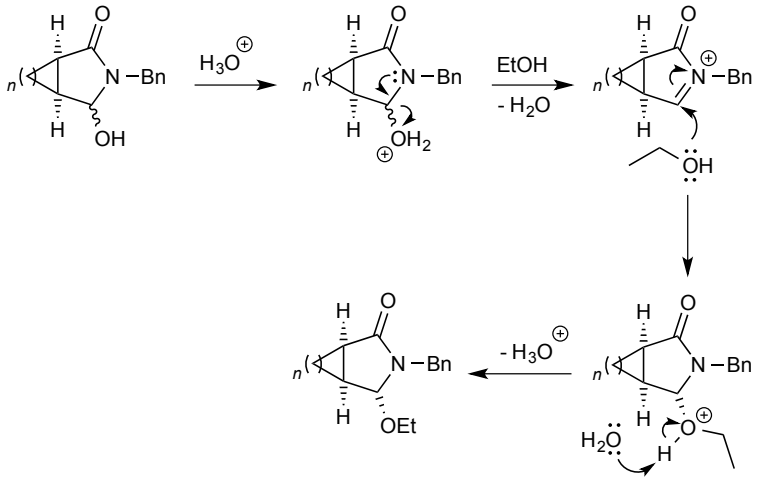

The use of achiral reducing agents such as DIBAL-H and $NaBH_4$ to access racemic *γ*-hydroxy lactams are also prevalent in industry. For example, the hydroxy lactam, **121**, a precursor to MF-310, **123**, a potential new treatment for chronic inflammation, was prepared by researchers at Merck-Frosst on a kg scale via the regioselective reduction of the succinimide, **120**, using DIBAL-H, Scheme 2-4.[10] The hydroxy lactam was obtained as a 11:1 mixture of regioisomers in 76.0% (2.24 kg) using 3.40 equiv. of DIBAL-H and a chlorobenzene/THF co-solvent at ~0 °C. Notably, the post work-up procedure consisted of first quenching the reaction mixture with acetone minimize dihydrogen production followed by treatment with 3 M tartaric acid at 45 °C to minimize the formation of emulsions and to remove any aluminum salts. The synthesis of **122** was completed by treatment of **121** with 5 equiv. $SiHEt_3$ in the presence of trifluoroacetic acid.

Scheme 2-4 *General procedure for MF-310 developed by Merck-Frosst.*

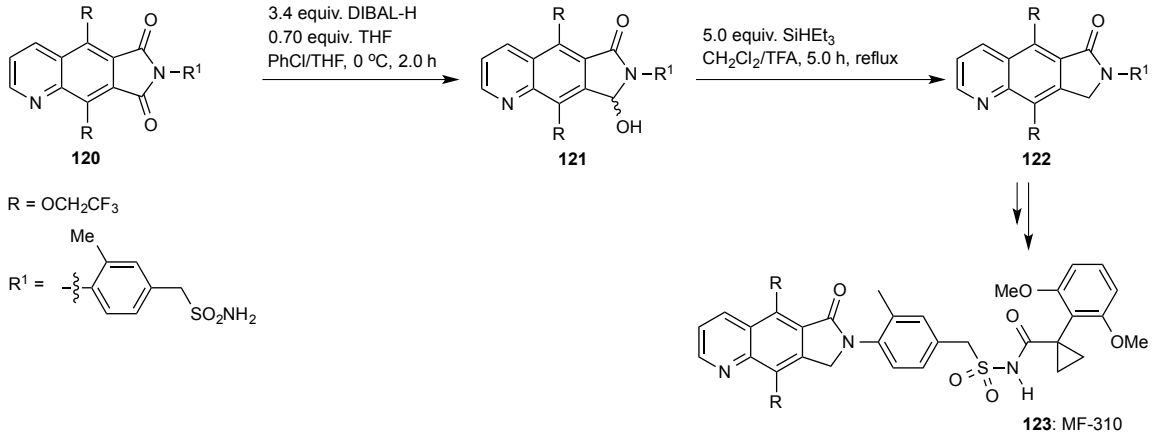

RP 29307, **126**, formed during the penultimate phase in the synthesis of eszopiclone (**127**, RP 27267), marketed by Sunovion as the sleep aid Lunesta® is also made by treatment of the succinimide, **124**, with MBH_4 (M = Na^+ or K^+), Scheme 2-5. However, strict quality control is needed to prevent the over-reduction of **125** to the ring opened derivative. This species can also be acylated in the subsequent step to give an impurity that is difficult to separate.[11]

The versatility of hydroxy lactams as precursors to commercially important as well as thought provoking compounds of academic interest *e.g.* gelsemine[12] and (+)-harmicine,[13] can be traced to their ability to be isolated as bench stable intermediates under ambient conditions, and their interesting reactivity. Hydroxy lactams are capable of forming *N*-acyliminium ions upon the addition of a Lewis or Brønsted acids.[1,2,14] These species can undergo a myriad of C–C bond forming reactions with a variety of nucleophiles such as alkenes, arenes and organometallic reagents.[15] For example, Speckmap and coworkers demonstrated that the C_5–C_{16} bond of gelsemine, a key step to assemble the bicycle[3.2.1]-octane skeleton, can be formed by an intramolecular *N*-acyliminium cyclization resulting from treating the silyl enol ether, **128**, prepared from the

mono-reduction of an earlier imide precursor, with BF_3•OEt in CH_2Cl_2 for 10 min at 10 °C (70% + 30% of C_{16}-epimer, **129**), Scheme 2-6.[16]

Scheme 2-5 *General procedure for the synthesis of eszopiclone.*

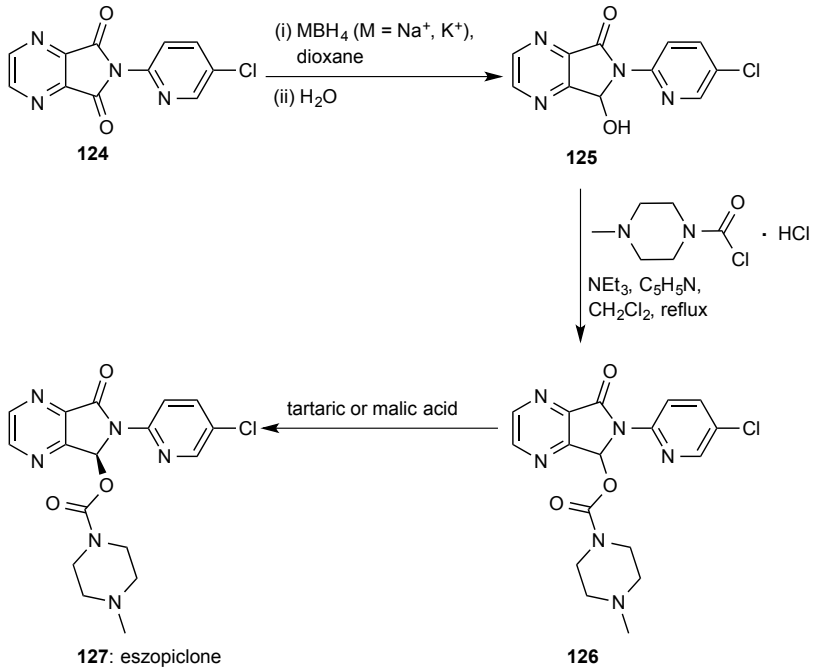

Additionally, Jacobsen and coworkers demonstrated that potentially pharmacologically active alkaloid (+)-harmicine could be prepared enantioselectively from the corresponding *N*-acyliminium ion derived from the hydroxy lactam, **130** and the chiral thiourea catalyst, **131**.[13] The authors proposed that the chiral catalyst induces enantioselectivity by forming an *N*-acyliminium chloride-thiourea complex resulting from hydrogen bonding between the thiourea and chloride ions, Scheme 2-7.

Scheme 2-6 *Synthesis of the tricyclic core of gelsemine by Speckamp and coworkers.*

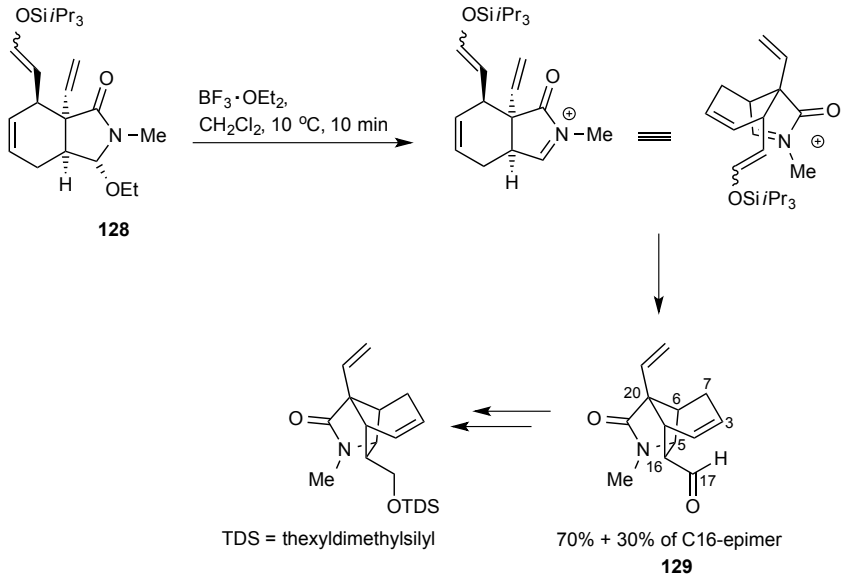

Scheme 2-7 *Synthesis of (+)-harmicine by Jacobsen and coworkers.*

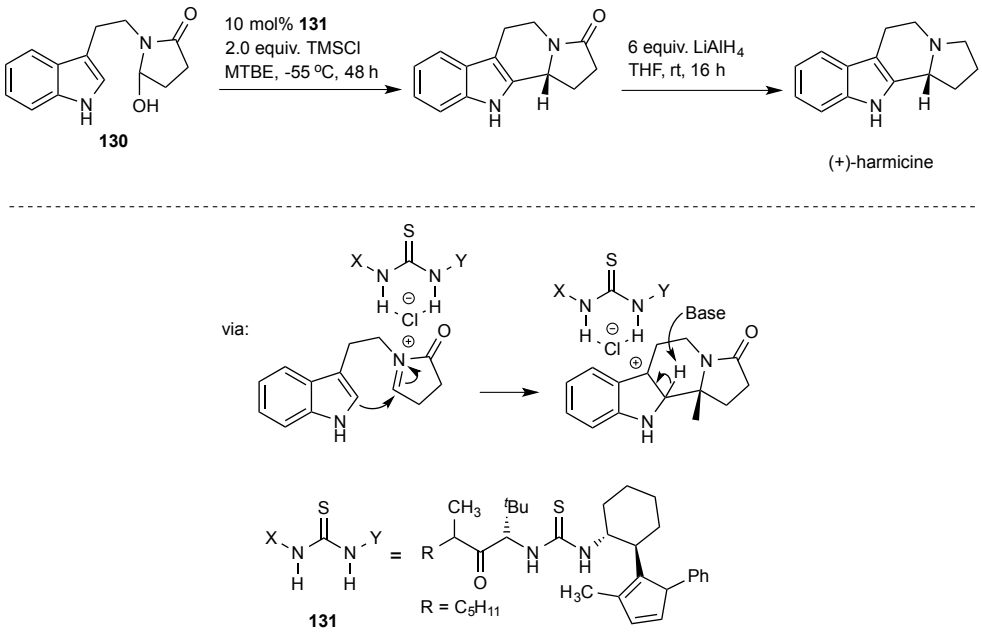

There are only a few reported examples of the enantioselective hydrogenation of prochiral imides. In 2007, Ikariya and coworkers reported the chemoselective direduction of imides into the corresponding alcohol-amides or alcohols and amides (depending on

imide structure).[17,18] For example, the authors showed that Cp*RuH($Ph_2P(CH_2)_2NH_2$), **77**, efficiently catalyzes the direduction of *N*-benzylphthalimide to give *N*-benzyl 2-hydroxymethylbenzamide in 99 turnovers under neutral conditions in 2-PrOH, Scheme 2-8.

Scheme 2-8 *Direduction of N-benzylphthalimide by* ***77****.*

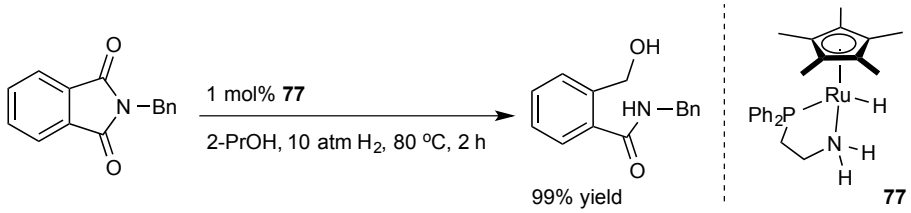

The hydrogenation was also applicable to the deprotection of primary amines from *N*-phthaloyl-protected amino acid ester derivatives in Gabriel amino acid synthesis. For example, *N*-phthaloyl-L-Phe methyl ester was quantitatively hydrogenated under neutral conditions using 10 mol% **77** to generate *N*-(*o*-hydroxymethylbenzoyl)-L-Phe methyl ester, which can undergo acid promoted cyclization to liberate phthalide and the HCl salt of L-Phe methyl ester in high yield without any loss of *ee*, Scheme 2-9.

Scheme 2-9 *Deprotection of N-phthaloyl amino acid derivative reported by Ikariya and coworkers.*

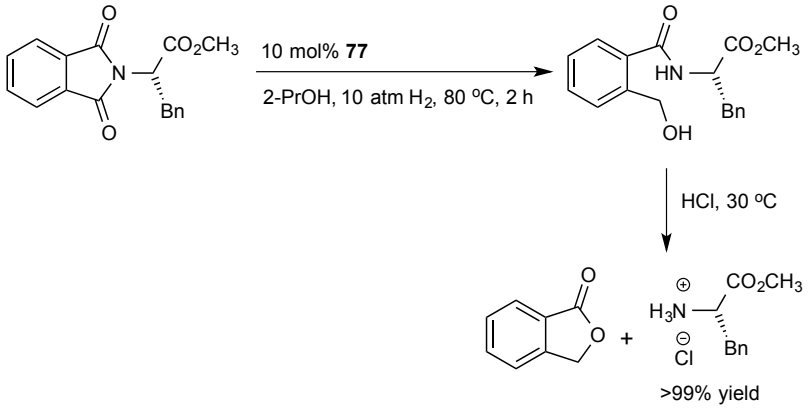

It was also demonstrated that simply replacing the 2-(diphenylphosphino)ethylamine ligand with (*S*)-2-((diphenylphosphino)methyl)pyrrolidine, **78** promoted the enantioselective hydrogenation of 4-(4-fluorophenyl)glutarimides via desymmetrization to yield the corresponding alcohol-amides in 78-99% yield (TON of 8-10) and 64-98% *ee*. The synthetic utility of the reaction was also demonstrated by preparing a useful intermediate for the synthesis of the anti-depressant (–)-paroxetine (Scheme 2-10).[17,19]

Specifically, the alcohol-amide, **133** (prepared from **132**) was first brominated using CBr_4/PPh_3, which was followed by a base induced cyclization using NaH and CAN-mediated dearylation (CAN: $(NH_4)_2Ce(NO_3)_6$) to give the chiral piperidinone, **134** which can then be transformed in multiple steps into (–)-paroxetine. In a follow up report, the authors also disclosed that similar sym-glutar- or succinimides bearing the *N*-3,4-$(OCH_2O)C_6H_3$ group could also be desymmetrized enantioselectively by hydrogenation to give functionalized chiral alcohol-amides using chiral Cp*Ru(*P*–*N*) catalysts, **78** or **78b**.

Scheme 2-10 *Preparation of (–)-paroxetine via enantioselective desymmetrization*

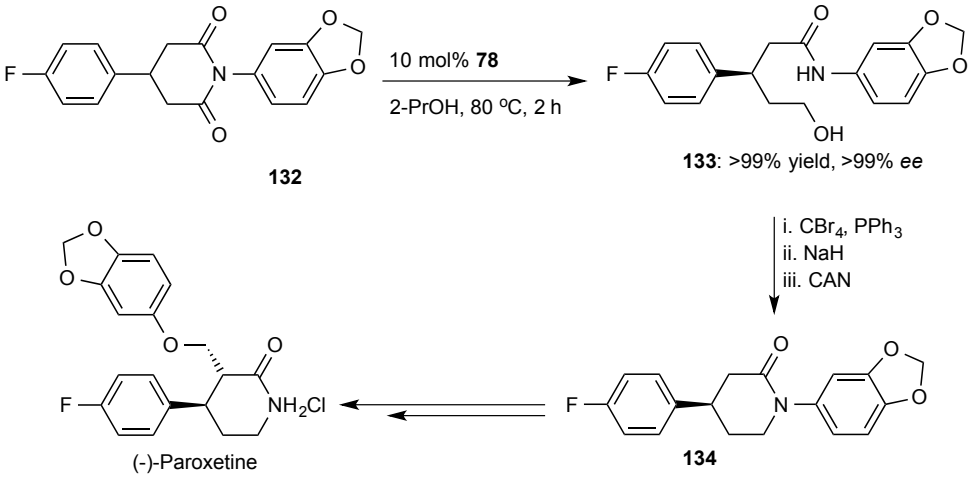

Notably, the products these hydrogenations were the ring-opened alcohol-amide resulting from the concomitant reduction of the aldehyde amide tautomer of the hydroxy lactam. The equilibrium position between the aldehyde amide tautomer and the hydroxy lactam can be subtly influenced by a number of factors including the nature of the substrate, the activity of the catalyst and reaction conditions employed. For example, Speckamp and coworkers reported the mono-reduction of several succinimides at low temperatures.[20,21] The reaction was facilitated by the portion-wise addition of 2 M HCl to a mixture of the substrate and $NaBH_4$ in ethanol at 0 °C. Under these conditions *N*-methylsuccinimide was quantitatively reduced to 1-methyl-5-ethoxy-2-pyrrolidinone, Eq. 2-1.

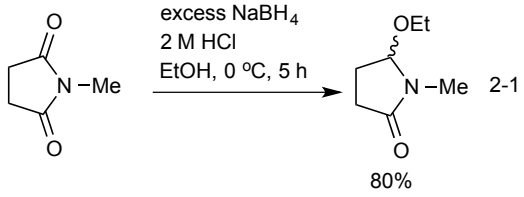

Without acid the reaction was noticeably sluggish. It was suggested that the enhancement in rate was due to either protonation and/or coordination of borane to the imide oxygen. In contrast, succinimides such as **135** can be quantitatively mono-reduced to without acid activation, Eq. 2-2.

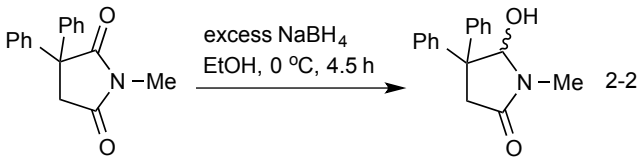

The presence of the phenyl groups on the *α*-carbon of the imide may activate the adjacent imide carbonyl towards the addition of a hydride by the favorable overlap of the forming $\sigma_{C\text{-}H}$ bond and the σ^* of the antiperiplanar C-Ph bond.[22] The *gem*-substituents may also increase the rate and/or equilibrium constant for cyclization by relieving ring strain of the abutting phenyl groups.[23] A similar effect was proposed in the lactonization of various 2-hydroxybenzenepropionic acids, Figure 2-3.[24]

Figure 2-3 *Relative lactonization rate constants for various 2-hydroxybenzenepropionic acids.*

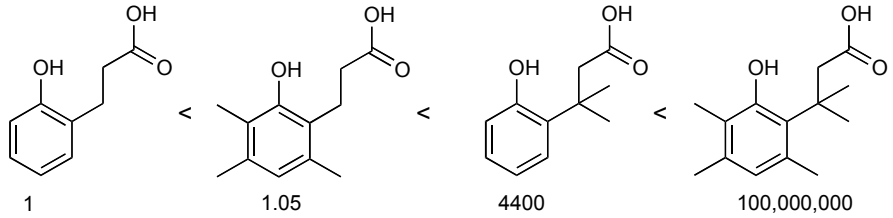

The rate and equilibrium constant for lactonization can also be increased significantly by increasing backbone rigidity. For example, Koshland and Storm showed that the rate of ring closure for an alcohol-acid with a structurally rigid norbornane backbone is ~10^4 time faster and has a K_{eq} value ~2000 time larger than that of the non-substituted alcohol-acid (Table 2-3, Entry 1 versus 3).[25,26] They also proposed that this effect was attributed to restricted rotation around the C–C bonds as well as the proximity of the OH and C=O groups.

There is neither a catalyst nor a system that is capable of effecting the homogeneous enantioselective desymmetrization of cyclic *meso*-imides by monohydrogenation in the literature. A notable example of a heterogeneous system is a PtO_2 catalyst that could effect the monohydrogenation of activated *pseudo*-bicyclic imides under mild reaction conditions, Eq. 2-3.[27] Thus the design of a simple strategy

that utilizes an appropriate catalyst, reaction conditions and imide structure to facilitate the transformation could be highly desirable to both academia and industry from a practical point of view.

Table 2-3 *Effect of backbone rigidity on alcohol-acid lactonization.*

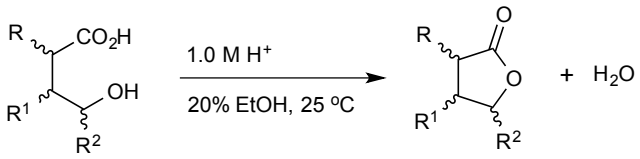

Entry	Alcohol-Acid	Rate constant of Lactonization ($M^{-1}min^{-1}$)	K_{eq}
1		0.086	6.15
2	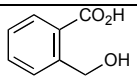	0.344	*n.d.*
3	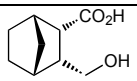	7.23	2810
4	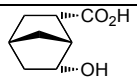	1120	12740

n.d. = no data

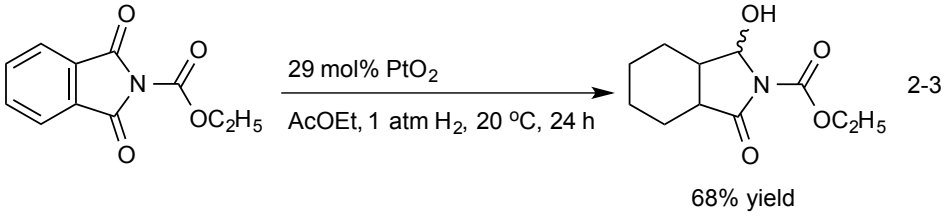

2-3

68% yield

Results and discussion

The Bergens group recently reported the low temperature preparation and mechanistic study of the Noyori ketone hydrogenation catalyst *trans*-[RuH_2((*R*)-BINAP)((*R*,*R*)-dpen)], **2**.[28-30] Compound **2** is a remarkably active carbonyl reducing agent in THF. For example, **2** rapidly adds acetophenone at –80 °C (upon mixing) to form the alkoxide, *trans*-[RuH(OCH(Me)(Ph))((*R*)-BINAP)((*R*,*R*)-dpen), **41**.[30] Complex **2** also catalyzes the hydrogenation of esters to give alcohol products under mild conditions and stoichiometrically adds *γ*-butyrolactone at –80 °C (within minutes) to form the corresponding Ru-hemiacetaloxide, **67**.[31] This unexpected high reactivity in THF led us to explore the enantioselective monohydrogenation of cyclic *meso*-imides using **2** and its variants, as catalysts under mild conditions.

Solutions of **2** and the related *trans*-[RuH_2((*R*)-BINAP)(diamine)] complexes, **79**, **136** and **137**, were prepared for this study by reacting mixtures of corresponding *trans*-[RuH(*L*)((*R*)-BINAP)(diamine)]BF_4 (*L* = η^2-H_2 or THF) species with 1–100 equiv. of KO*t*-Bu or KN[$Si(CH_3)_3$]$_2$ under H_2 (~2 atm) at –78 °C in THF.[29] The preparation of these dihydrides usually consumes ~1 equiv. of inorganic base therefore the amount of base quoted in this discussion is that which remains after the dihydrides are prepared. Figure 2-4 illustrates the catalysts and substrates investigated in this study.

Figure 2-4 *Catalysts and imide substrate scope.*

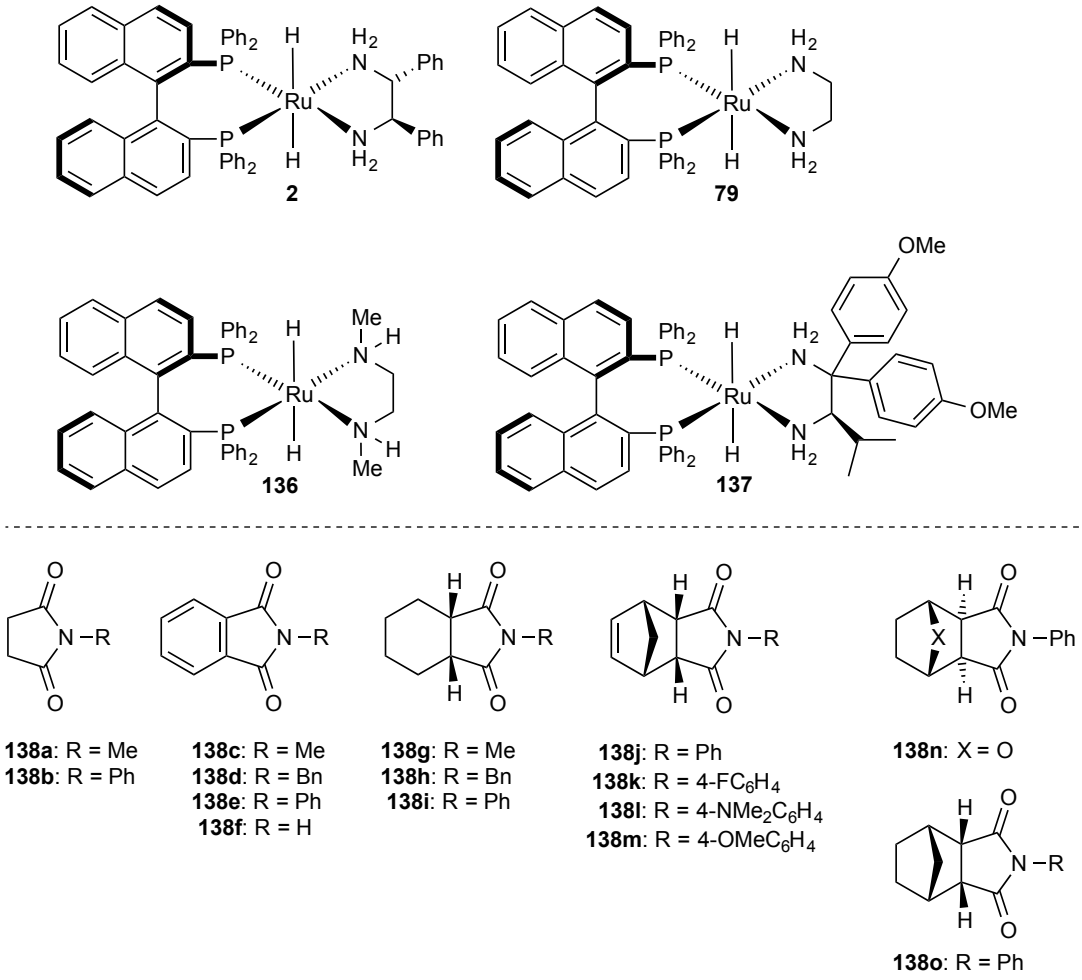

Table 2-4 summarizes the results of our achiral hydrogenations under mild reaction conditions *i.e.* 1 mol% catalyst (**2**, **79** or **136**), 9 mol% KO*t*-Bu and 4 atm H_2 at 30 °C for 3 h. Notably, **79** and **136** were inactive towards the hydrogenation of *N*-methylsuccinimide, **138a**. An analogous result was obtained using **79** and 2-PrOH instead of THF, which almost certainly can be attributed to the formation of the corresponding Ru-2-propoxide species. The imide **138a** was however, exclusively dihydrogenated to the alcohol-amide **140a** with a TOF of 33 h^{-1} using 1 mol% **79** as catalyst in THF. This result illustrates that the dihydride **79** is among the best carbonyl reduction agents in the literature. In contrast, Ikariya and coworkers could only

dihydrogenate the *N*-benzylsuccinimide (*N*-benzyl analogue of **138a**) with a TOF of 5.6 h^{-1} under relatively forcing conditions (1 mol% **77** under 30 atm H_2 at 80 °C for 18 h in 2-PrOH).[18] Later, Ikariya and coworkers reported that the dihydrogenation of *N*-benzylsuccinimide proceeds with a TON = 99 and TOF = 50 h^{-1} after 2 h using 1 mol% **77** under 10 atm H_2 at 80 °C in 2-PrOH. This result would imply that **79** is more active under milder reaction conditions.[17] To our surprise, the *N*-substituted phthalimides (**138c-e**) were exclusively mono-hydrogenated to the corresponding *γ*-hydroxy lactams in moderate to good yields, Table 2-4, entries 4-6. These results reveal two important points. The first is that substituents on the imide backbone exhibit an uncanny influence on ring-chain tautomerization, and by extension the mono/dihydrogenation selectivity for the reaction. While the nature of the *N*-substituent, has little influence upon the yield and the mono/dihydrogenation selectivity for this system. Furthermore, phthalimide, **138f** was inactive towards hydrogenation. This inactivity was ascribed to the inherent acidity of the N-H group that would consume the added base, Table 2-4, entry 7. Notably, attempts to enantioselectively hydrogenate **138c** using **2** were met with disappointment. All hydrogenations, despite the nature of the active catalyst, resulted in racemic products due to a base-catalyzed epimerization of the hydroxy lactam. Moreover, increasing the reaction temperature resulted in partial dihydrogenation, Table 2-4, entry 9. Together, these results suggest that the monohydrogenation of imides is indeed possible albeit under mild reaction conditions when the backbone of the cyclic imide favors ring closure.

Table 2-4 *Summary of achiral hydrogenations.*[a]

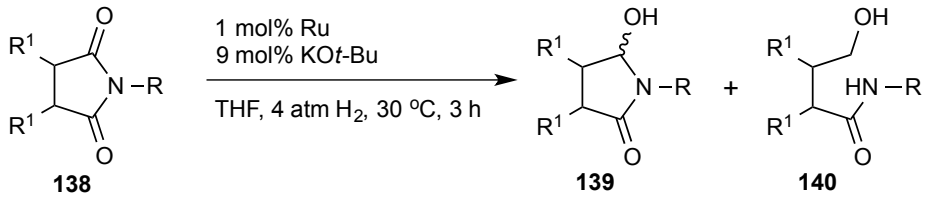

Entry	Catalyst	Imide	**138** (%)[b]	**139** (%)[b]	**140** (%)[b]
1[c]	**79**	**138a**	100	0	0
2	**136**	**138a**	100	0	0
3	**79**	**138a**	0	0	100
4	**79**	**138c**	30	70	0
5	**79**	**138d**	34	66	0
6[d]	**79**	**138e**	24	76	0
7[e]	**79**	**138f**	100	0	0
8[f]	**2**	**138c**	45	55	0
9[g]	**2**	**138c**	50	30	20

[a][Imide] = 0.33 M unless stated otherwise. [b]Determined by ^{1}H NMR. [c]Imide/**79**/KO*t*-Bu = 200:1:9, [Imide] = 0.5 M in THF/2-PrOH = 3:1. [d][Imide] = 0.11 M in THF/CH_2Cl_2 = 2:1 due to solubility of **138c**. [e][imide] = 0.17 M due to solubility of **138e**. [f]Racemic product. [g]At 60 °C

Table 2-5 outlines the results of our attempts to optimize the reaction conditions as well as to identify the best structural features to effect the enantio- and diastereo-selective hydrogenation of cyclic imides using **2** as catalyst and **138g-i** as substrates. At 30 °C and high-pressures of hydrogen (40-50 atm) all the potential candidates were reduced to give both the hydroxy lactam and alcohol-amide as products in a wide variety of product ratios, Table 2-5, entries 1-3. Interestingly, under these conditions **138i** exhibited the highest selectivity towards monohydrogenation. Lowering the reaction temperature to 0 °C further increased this selectivity without significantly affecting rate,

dr and *ee*, Table 2-5, entry 3 versus entry 4. Moreover, the catalyst loading could be decreased to 0.1 mol% without a substantial loss in conversion, dr and *ee*. Lowering the pressure of hydrogen from 50 to 10 atm however, resulted in a moderate decrease in TOF, Table 2-5, entry 4 versus entry 6. Thus, the optimum conditions required for the enantio- and diastereo-selective hydrogenation of *N*-phenyl cyclic imides was chosen to be 0 °C at 50 atm H_2.

Table 2-5 *Optimization of reaction conditions and imide structures.*[a]

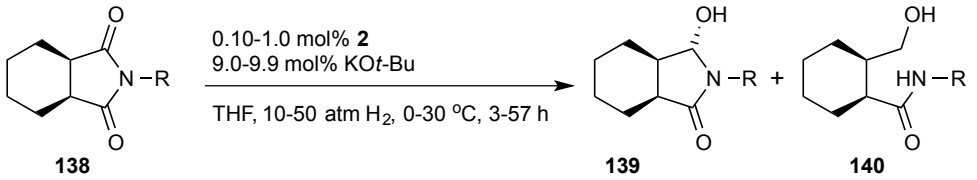

Entry	Imide	T (° C)	Time (h)	**139**[b] (%)	**140**[b] (%)	dr of **139**[b]	*ee* of **139** (%)[c]
1	**138g**[d]	30	3	8	68	nd	nd
2	**138h**[d]	30	3	26	59	nd	nd
3	**138i**	30	3	88	6	97:3	90
4	**138i**	0	4	95	0	98:2	90
5	**138i**[e]	0	57	90	trace	97:3	88
6	**138i**[f]	0	4	76	0	98:2	87

[a]Imide/**2**/KO*t*-Bu = 100:1:9, [imide] = 0.125 M, 50 atm H_2 in THF unless stated otherwise. [b] Determined by ^{1}H NMR. dr: diastereomeric ratio, nd: not determined. [c]Determined by HPLC analysis using Daicel CHIRALPAK IB column. [d]At 40 atm H_2. [e]Imide/**2**/KO*t*-Bu = 1000:1:99, [imide] = 0.25 M. [f]At 10 atm H_2.

Table 2-6 summarizes the results of our enantioselective hydrogenations using **2** and **137** as catalysts and **138b** as well as **138j-o** as substrates using the optimized conditions reported above. Remarkably, in one hydrogenation **138j** was chemo-,

diastereo- and enantio-selectively desymmetrized to yield a *γ*-hydroxy lactam bearing five stereogenic centers in 98% yield and 96% *ee* using as little as 0.1 mol% **2**, Table 2-6, entry 1. One recrystallization of **139j**, further increased its *ee* to >99%. The *para*-substituted analogues **138k-m** as well as the *exo*-*O*-bridge imide **138n** were somewhat less active towards hydrogenation, thereby requiring higher catalyst loadings of **2** and **137**, respectively (Table 2-6, entries 2-5). The norbornane imide **138o** also exhibited a lower reactivity (TON = 220, >99:1 dr, 92% *ee*) towards hydrogenation. Matshuki *et al.* also noted a similar observation during Al-H reduction of **138o**.[8] This poor reactivity is most likely attributed to the bulky nature of the norbornane ring.[32] Even under the optimized conditions reported here, *N*-phenylsuccinimide, **138b**, was exclusively dihydrogenated to the open-chain alcohol-amide further illustrating the importance of backbone rigidity to mono/dihydrogenation selectivity, Table 2-6, entry 7.

Table 2-6 *Enantioselective desymmetrization of cyclic meso-imides via monohydrogenation under optimized conditions.*[a]

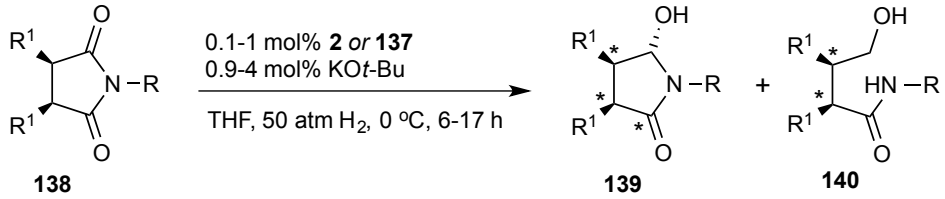

138 **139** **140**

Entry	Imide	T (° C)	Time (h)	**139**[b] (%)	**140**[b] (%)	dr of **139**[b]	*ee* of **139** (%)[c]
1[d]	**138j**	0	17	98	0	>99:1	96
2	**138k**	0	17	99	0	>99:1	97
3	**138l**	0	17	92	0	>99:1	97
4	**138m**	0	17	98	0	>99:1	95
5[e]	**138n**	0	6	97	trace	93:7	92
6[f]	**138o**	0	17	44	0	>99:1	92
7	**138b**	0	6	0	100	-	-

[a]Imide/**2**/KO*t*-Bu = 500:1:9, [imide] = 0.625 M, 50 atm H_2 in THF unless stated otherwise. [b]Determined by ^{1}H NMR. dr: diastereomeric ratio. [c]Determined by HPLC analysis using Daicel CHIRALPAK IB column. [d]Imide/**2**/KO*t*-Bu = 1000:1:9, [imide] = 1.25 M. [e]Imide/**137**/KO*t*-Bu = 100:1:4, [imide] = 0.125 M. [f]Imide/**2**/KO*t*-Bu = 100:1:4, [imide] = 0.125 M.

Figure 2-5 depicts the solid-state structures of the hydroxy lactams *trans*-**139j** and *trans*-**139k**. In addition to X-ray crystallography we utilized ^{1}H NMR spectroscopy to determine the relative stereochemistry at the hydroxy carbon of the hydroxy lactam. It was found to be exclusively *trans*. The absolute configuration of *trans*-**139j** was determined in Chapter 3.

Figure 2-5 *ORTEP drawings of hydroxy lactams trans-**139j** (left) and trans-**139k** (right) with 20% probability ellipsoids without hydrogen atoms. The absolute configuration of trans-**139j** was determined in Chapter 3.*

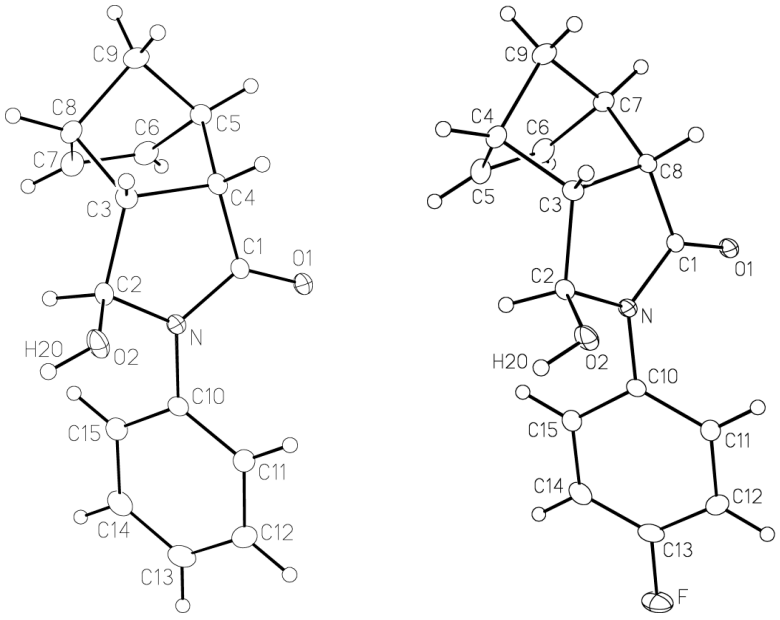

This observation does not agree with the addition of a hydride to the least hindered convex-face of the imide **138j**. Control experiments between a 5 mol% solution of KO*t*-Bu and *cis*-**139j** (the kinetic product of the hydrogenation obtained from the DIBAL-H reduction of **138j** at 0 °C under neutral conditions)[8] showed quantitative catalytic isomerization to *trans*-**139j** in THF at 0 °C. Speckamp and coworkers also observed a similar process upon the addition of excess NaOEt to a solution of *cis*-**139g**.[20] Thus, the enantiotopic group selectivity is preserved in these hydrogenations but, the *cis*-*trans* selectivity at the hydroxy carbon is not.

To demonstrate the synthetic utility of this hydrogenation we conducted two experiments. The first involved the enantio- and diastereo-selective monohydrogenation of *cis*-1,3-dibenzyl-*N*-benzyl-2-imidazolidinone-4,5-dicarboximide, **141**, to yield **142** as potential precursor to (+)-biotin.[33] However, the *trans*-isomer of **142** was obtained in near

quantitative yield (95%) with low *ee* (18%) and dr (89:11) using 2 mol% **2**, Eq. 2-4. The poor enantioselectivity of the reaction probably originated due to the reversibility of the hydrogenation at higher temperatures and/or a weaker substrate-catalyst steric interaction. We speculate that further optimization of catalyst structure as well as reaction conditions could potentially improve the diastereo- and enantio-selectivity of this reaction.

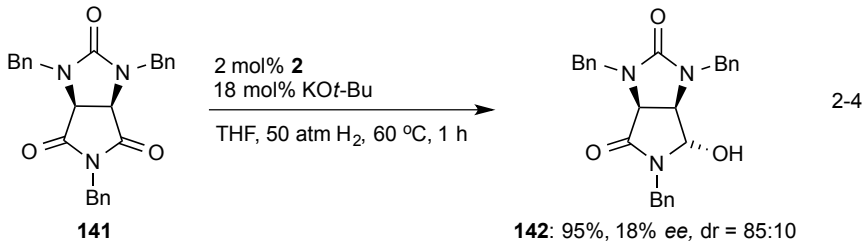

141 **142**: 95%, 18% *ee,* dr = 85:10 2-4

The latter involved using *N*-acyliminium ion chemistry to convert the hydroxy lactam *trans*-**139j** into a more desirable precursor for alkaloid synthesis. Koizumi and coworkers have reported a similar strategy to prepare chiral functionalized pyrrolines *e.g.* (+)-indolizidine from the hydroxy lactam **143** via a stereoselective *N*-acyliminium addition followed by a retro-Diels-Alder reaction, and a subsequent multi-step reduction of the unsaturated cyclic-lactam, Scheme 2-11.[34]

Scheme 2-11 *Enantioselective synthesis of (+)-indolizidine.*

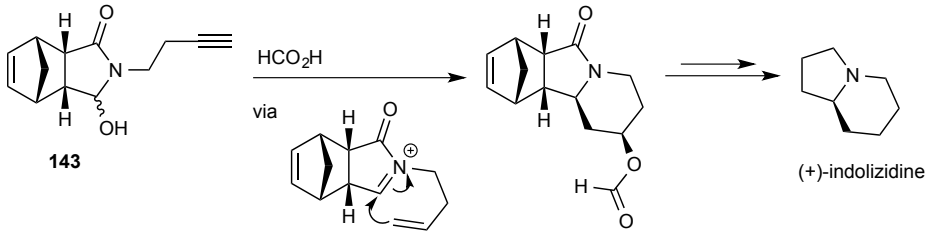

Our strategy to synthesize the polycyclic lactam **144** was first to convert *trans*-**139j** to the corresponding *N*-acyliminium ion using $BF_3{\cdot}OEt$ (either the *cis*- or *trans*-isomer of **139j** could form this *N*-acyliminium ion). [35] Addition of indene to the least-hindered convex-face of this species forms a benzylic carbocation that undergoes intramolecular cyclization with the *N*-phenyl ring followed by rearomatization to give the polycyclic lactam with two additional stereogenic centers in 90% yield and 91:9 diastereomeric ratio (dr) (Scheme 2-12). The dr can be increased to >99:1 with one recrystallization. Figure 2-6 illustrates the solid-state structure of the major diastereoisomer of **144**.

Scheme 2-12 *Synthesis of the polycyclic lactam* ***144*** *using trans-****139j*** *and indene.*

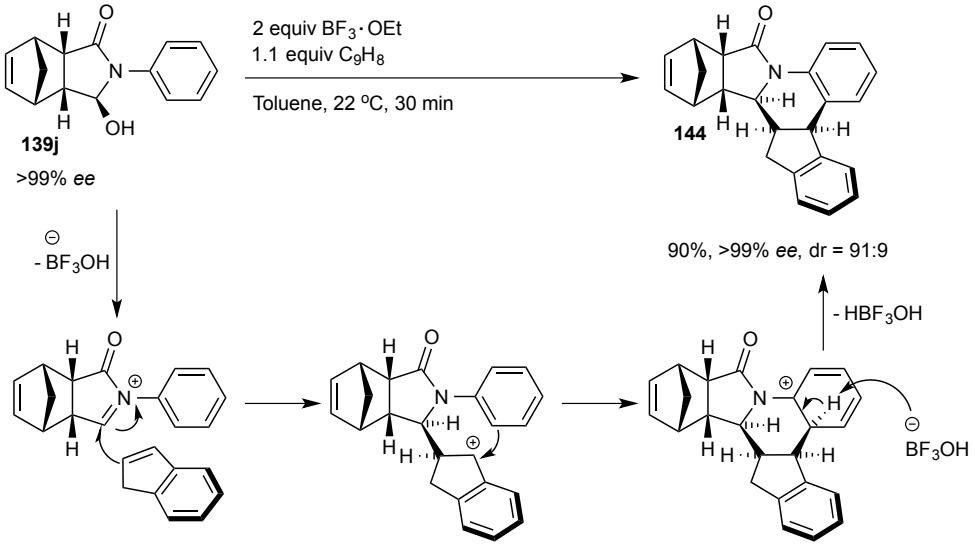

Figure 2-6 *An ORTEP drawing of the major diastereomer of* ***144*** *with 20% probability ellipsoids without hydrogen atoms. The absolute configuration was not determined.*

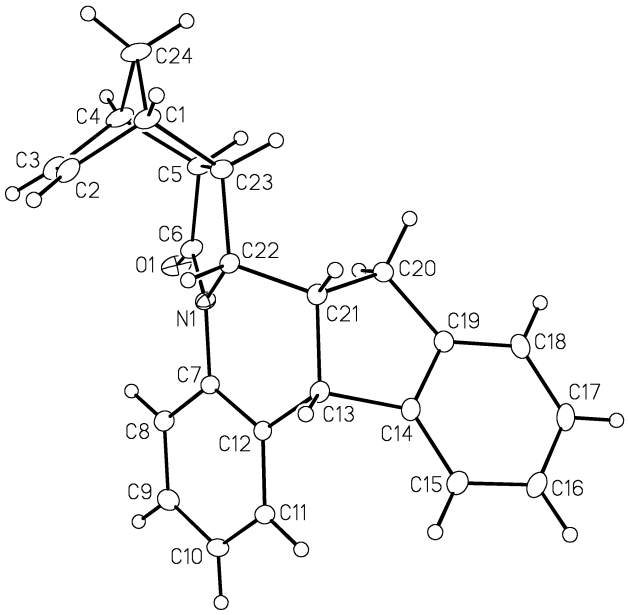

Conclusion

This chapter presents the first chemo-, diastereo- and enantio-selective desymmetrization of cyclic *meso*-imides via monohydrogenation. This desymmetrization reaction is capable of forming up to five stereogenic centers from the monohydrogenation of simple substrates. Based on our observations and reported stereochemistry obtained from M-H reduction of imides in the literature, we propose that the addition of the hydride proceeds to the less hindered convex face of the imide to form the *cis*-hydroxy lactam (the kinetic product of the hydrogenation). However, under the conditions reported herein the *cis*-hydroxy lactam is rapidly isomerized to the *trans*-hydroxy lactam (the thermodynamic product of the hydrogenation). Thus, the enantiotopic group selectivity is preserved in this hydrogenation but not the *cis*-*trans* selectivity at the hydroxy carbon. The synthetic utility of this hydrogenation and its products were also demonstrated in the preparation of potential precursors to (+)-biotin and chiral alkaloids.

Materials and methods

All pressure reactions were carried out in a glass (4 atm H_2) or steel (50 atm H_2) pressure reactor equipped with a magnetic stir bar. Deuterated solvents were obtained from Aldrich and Cambridge Isotope Laboratories. Common laboratory solvents were dried over appropriate drying agents before each experiment. For example, THF was distilled over Na/benzophenone while 2-PrOH, toluene, and DCM were dried over CaH_2.[36] Common laboratory reagents were obtained from Aldrich, Alfa Aesar, TCI America and Strem, and were used as received unless stated otherwise. *N*-methylsuccinimide and KO*t*-Bu were purchased from Aldrich. Ethylenediamine, indene and phthalimide were purchased from Anachemia, Matheson Coleman & Bell, and General Intermediates of Canada, respectively. KO*t*-Bu was purified by sublimation. Indene was purified by fractional distillation while; ethylenediamine was fractional distilled in the presence of KOH. Hydrogen gas was purchased from Praxair and was ultra high purity grade. HPLC grade hexanes (min. 99.5%) and 2-PrOH (min. 99.7%) were obtained from Caledon Laboratories Limited. ^{1}H, ^{13}C, ^{19}F and ^{31}P NMR spectra were recorded using 300 and 400 MHz Varian Inova, and 500 MHz Varian DirectDrive spectrometers. ^{1}H and ^{13}C NMR chemical shifts are reported in parts per million (δ) relative to TMS with the deuterated solvent as the internal reference. ^{31}P and ^{19}F chemical shifts are reported in parts per million (δ) relative to 85% H_3PO_4 and CCl_3F as the external references. NMR peak assignments were made using ^{1}H–^{13}C gHSQC, ^{1}H–^{13}C gHMBC and ^{1}H–^{1}H gCOSY NMR experiments. Abbreviations used for NMR spectra are s (singlet), d (doublet), dd (doublet of doublet), ddd (doublet of doublet of doublet), dt (doublet of triplet), t (triplet), tt (triplet of triplet), q (quartet), m (multiplet) and br (broad). Infrared spectra were recorded using a Nic-Plan FTIR microscope and are reported in wavenumbers (cm^{-1}). High-resolution mass spectra were recorded using an Applied BioSystems Mariner BioSpectrometry Workstation oaTOF Mass Spectrometer.

Elemental analysis data were obtained using a Carlo Erba CHNS-O EA1108 elemental analyzer. Optical rotations were measured using a Perkin Elmer 241 polarimeter. Melting points (mp) were measured using a Perkin Elmer Pyris 1 differential scanning calorimeter. HPLC analysis was performed using a Waters 600E multi-solvent delivery system equipped with a Waters 715 Ultra WISP sample processor, Waters temperature control system, Waters 990 photodiode array detector, Waters 410 differential refractometer, Waters 5200 printer plotter, and a Daicel CHIRALPAK IB (4.6 mm i.d. x 250 mm) chiral column. All *ee*'s were confirmed by comparing the HPLC chromatogram of the hydrogenation product with that of the racemic product prepared by either $NaBH_4$ *or* DIBAL-H reduction followed by acidic work-up at room temperature.[8,21]

A general procedure for the preparation of imides[37]

Under Ar, the corresponding anhydride (10 mmol), primary amine (10 mmol), and THF (15 mL) were added to a 200 mL round bottom flask equipped with a 1'' magnetic stir bar. The resulting solution was then stirred at 40 °C for 30 min. Removal of the solvent under vacuum gave the corresponding carboxylic acid-amide as a white solid. The solid was then heated to 150-200 °C, and the melt stirred for 8.0 min to 4.0 h under Ar. The extent of the reaction was monitored periodically using TLC. Once complete, the crude product was allowed to cool to room temperature where it solidified. The solid was then purified by flash chromatography using 230-400 mesh silica gel (AcOEt/*n*-hexanes) followed by recrystallization. The imides **138b-e**, **138g-k** and **138m-o** have previously been reported in the literature. Their ^{1}H NMR chemical shifts have been reported here for convenience.

138b[38] **–** Melt temperature: 170 °C for 2.00 h. Recrystallization solvents: CH_2Cl_2/EtOH. Yield: 70.0%. ^{1}H NMR (399.79 MHz, $CDCl_3$, 27.0 °C): δ 2.91 (4H, s, 2

CH_2), 7.28 (2H, m, 2 aromatic C*H*), 7.42 (1H, m, aromatic C*H*), 7.50 (2H, m, 2 aromatic C*H*)

138c[39] **–** Melt temperature: 190 °C for 1.50 h. Recrystallization solvents: acetone/H_2O. Note: 40 wt. % $MeNH_2$ in water was used as the source of amine. Yield: 78.0%. ^{1}H NMR (399.79 MHz, $CDCl_3$, 27.0 °C): δ 3.19 (3H, s, CH_3), 7.71 (2H, m, 2 aromatic C*H*), 7.85 (2H, m, 2 aromatic C*H*).

138d[39] – Melt temperature: 150 °C for 30.0 min. Recrystallization solvents: acetone/H_2O. Yield: 81.0%. ^{1}H NMR (399.79 MHz, $CDCl_3$, 27.0 °C): δ 4.86 (2H, s, CH_2), 7.30 (3H, m, 3 aromatic C*H*), 7.43 (2H, m, 2 aromatic C*H*), 7.72 (2H, m, 2 aromatic C*H*), 7.86 (2H, m, 2 aromatic C*H*)

138e[39] – Melt temperature: 200 °C for 1.00 h. Recrystallization solvents: acetone/H_2O. Yield: 81.0%. ^{1}H NMR (399.79 MHz, $CDCl_3$, 27.0 °C): δ 7.41–7.55 (5H, m, 5 aromatic C*H*), 7.80 (2H, m, 2 aromatic C*H*), 7.97 (2H, m, 2 aromatic C*H*).

138g[40] – Melt temperature: 170 °C for 10.0 min under vacuum. Sample was not recrystallized. Yield: 56.0%. ^{1}H NMR (399.79 MHz, $CDCl_3$, 27.0 °C): δ 1.41 (4H, m, 2CH_2), 1.71 (2H, m, CH_2), 1.84 (2H, m, CH_2), 2.82 (2H, m, 2 C*H*), 2.94 (3H, s, CH_3).

138h[41] – Melt temperature: 150 °C for 5.00 min. Recrystallization solvent: hot EtOH. Yield: 46.0%. ^{1}H NMR (399.79 MHz, $CDCl_3$, 27.0 °C): δ 1.38 (4H, m, 2 CH_2), 1.72 (2H, m, CH_2), 1.84 (2H, m, CH_2), 2.85 (2H, m, C*H*), 4.64 (2H, s, CH_2), 7.26–7.38 (5H, m, 5 aromatic C*H*).

138i[40] – Melt temperature: 190 °C for 4.00 h. Recrystallization solvent: hot EtOH. Yield: 90.0%. ^{1}H NMR (399.79 MHz, $CDCl_3$, 27.0 °C): δ 1.53 (4H, m, 2 CH_2), 1.93 (4H, m, 2 CH_2), 3.05 (2H, m, 2 C*H*), 7.29 (2H, m, 2 aromatic C*H*), 7.38 (1H, m, aromatic C*H*), 7.47 (2H, m, 2 aromatic C*H*).

138j[42] – Melt temperature: 160 °C for 15.0 min under vacuum. Recrystallization solvents: acetone/H_2O. Yield: 80.0%. ^{1}H NMR (399.79 MHz, $CDCl_3$, 27.0 °C): δ 1.61

(1H, m, CH_2), 1.79 (1H, dt, J = 1.6 and 8.8 Hz, CH_2), 3.43 (2H, m, 2 CH), 3.51 (2H, m, bridgehead 2 CH), 6.27 (2H, t, J = 1.8 Hz, 2 CH), 7.13 (2H, m, 2 aromatic CH), 7.36 (1H, m, aromatic CH), 7.44 (2H, m, 2 aromatic CH).

138k[43] – Melt temperature: 200 °C for 15.0 min. Recrystallization solvents: hot AcOEt/*n*-hexanes. Yield: 85.0%. ^{1}H NMR (399.79 MHz, $CDCl_3$, 27.0 °C): δ 1.61 (1H, d, J = 8.8 Hz, CH_2), 1.79 (1H, dt, J = 1.6 and 8.8 Hz, CH_2), 3.42 (2H, m, 2 CH), 3.50 (2H, m, bridgehead 2 CH), 6.25 (2H, t, J = 1.6 Hz, 2 CH), 7.10 (2H, d, J = 2.0 Hz, 2 aromatic CH), 7.12 (1H, s, 2 aromatic CH). ^{19}F NMR (376.15 MHz, $CDCl_3$, 27.0 °C): δ -112.8 (tt, J = 6.0 and 7.5 Hz).

138l – Melt temperature: 190 °C for 1.00 h. Recrystallization solvent: hot AcOEt. Yield: 80.0%. ^{1}H NMR (399.79 MHz, $CDCl_3$, 27.0 °C): δ 1.57 (1H, m, CH_2), 1.74 (1H, m, CH_2), 2.94 (6H, s, 2 CH_3), 3.37 (2H, m, 2 CH), 3.47 (2H, m, bridgehead 2 CH), 6.23 (2H, m, 2 CH), 6.69 (2H, m, 2 aromatic CH), 6.93 (2H, m, 2 aromatic CH). ^{13}C{^{1}H} NMR (100.5 MHz, $CDCl_3$, 27.0 °C): δ 40.5 (2 CH$_3$), 45.4 (bridgehead 2 CH), 45.6 (2 CH), 52.1 (CH$_2$), 112.4 (aromatic), 120.4 (aromatic), 127.2 (aromatic), 134.5 (C=C), 150.4 (aromatic), 177.4 (C=O). IR (solid): 2877, 1708, 1568, 1354, 1179 cm^{-1}. HRMS (ESI$^+$) m/z calculated for $C_{17}H_{19}N_2O_2^+$ ([M + H]$^+$): 283.1441. Found: 283.1435. Elemental analysis calculated for $C_{17}H_{18}N_2O_2$: N = 9.92, C = 72.32, H = 6.43. Found: N = 9.99, C = 72.55, H = 6.49. mp: 175.0 °C.

138m[42] – Melt temperature: 170 °C for 1.00 h. Recrystallization solvent: hot AcOEt. Yield: 60.0%. ^{1}H NMR (399.79 MHz, $CDCl_3$, 27.0 °C): δ 1.57 (1H, m, CH_2), 1.74 (1H, m, CH_2), 3.37 (2H, m, 2 CH), 3.46 (2H, m, bridgehead 2 CH), 3.78 (3H, s, CH_3), 6.23 (2H, m, 2 CH), 6.90 (2H, m, 2 aromatic CH), 7.02 (2H, m, 2 aromatic CH).

138n[44] – Melt temperature: 180 °C for 1.00 h. Recrystallization solvent: hot EtOH. Yield: 86.0%. ^{1}H NMR (399.79 MHz, $CDCl_3$, 27.0 °C): δ 1.66 (2H, m, CH_2), 1.91

(2H, m, C*H*$_2$), 3.04 (2H, s, bridgehead 2 C*H*), 5.00 (2H, m, 2 C*H*), 7.25 (2H, m, 2 aromatic C*H*), 7.36-7.50 (3H, m, 2 aromatic C*H*).

138o[45] – Melt temperature: 200 °C for 30.0 min. Recrystallization solvents: hot EtOH/H_2O. Yield: 62.0%. ^{1}H NMR (399.79 MHz, $CDCl_3$, 27.0 °C): δ 1.49 (2H, m, C*H*$_2$), 1.68 (4H, m, 2 C*H*$_2$), 2.88 (2H, m, bridgehead 2 C*H*), 3.25 (2H, m, 2 C*H*), 7.25 (2H, m, 2 aromatic C*H*), 7.39 (1H, m, aromatic C*H*), 7.48 (2H, m, 2 aromatic C*H*).

General procedure to prepare the *trans*-[RuH_2((*R*)-BINAP)(diamine)] catalyst with base[29]

A solution of [Ru((1–5–*η*)-C_8H_{11})((*R*)-BINAP)]BF_4 (0.005 *or* 0.01 mmol) in THF (0.5 mL) was mixed under H_2 (~2 atm) at 0 °C for 8 min. The resulting solution containing [RuH((*R*)-BINAP)$(THF)_3$]BF_4 was then cooled to –78 °C using a dry ice/acetone bath. A THF solution of the diamine (0.005 *or* 0.01 mmol, 0.2 mL) was then added by cannula under H_2 pressure (~2 atm) at –78°C. The contents of the NMR tube were then mixed for 10 s outside the –78 °C bath, and then returned to the bath for 20 s. This process was repeated for a total of 5 min. A THF solution of KO*t*-Bu (0.05–0.5 mmol, 0.3 mL) was then added by cannula under H_2 pressure (~2 atm) at –78 °C. The contents of the NMR tube were then mixed for 10 s outside the –78 °C bath, and then returned to the bath for 20 s. This process was repeated for a total of 5 min. During this time, the colour of the solution changed from yellow to dark red. The mixture containing *trans*-[RuH_2((*R*)-BINAP)(diamine)] and KO*t*-Bu (4.0–99 equivalents) was then used for the catalytic hydrogenation as described in the next section.

General procedure to hydrogenate imides using *trans*-[RuH_2((*R*)-BINAP)(diamine)]

A solution of the imide (1.0–10 mmol) in THF (3.0–19 mL), prepared under Ar, was added to a stainless steel autoclave equipped with a magnetic stir bar. The

atmosphere in the autoclave was then flushed with H_2 gas for ~3.0 min at 0 °C. A solution of *trans*-[RuH_2((*R*)-BINAP)(diamine)] (5.0 *or* 10 *μ*mol) and KO*t*-Bu (0.045-0.50 mmol) in THF (1.0 mL), prepared as described above, was then added by cannula under H_2 pressure. The autoclave was then pressurized to 50 atm with H_2. The reaction mixture was stirred at 0 °C under 50 atm H_2 for 6.0–57 h. The autoclave was then vented slowly at 0 °C. Precipitation of the product *γ*-hydroxy lactam was observed (entries 4-6, Table 2-5 and entries 3-6, Table 2-6). The percent conversion, diastereomeric ratio, and enantiomeric excess were determined by ^{1}H NMR spectroscopy and HPLC analysis.

Compounds **139c-e**, **140a-b** and **142** have been reported in the literature. Only the ^{1}H NMR and HPLC data for the major isomer (*trans*-isomer) will be reported here (if applicable).

139d[49] **–** ^{1}H NMR (399.79 MHz, $CDCl_3$, 27.0 °C): δ 3.43 (1H, d, *J* = 12.0 Hz, O*H*), 4.27 (1H, d, *J* = 14.8 Hz, CH_2), 4.89 (1H, d, *J* = 14.8 Hz, CH_2), 5.60 (1H, d, *J* = 11.6 Hz, C*H*), 7.2–7.6 (8H, m, 8 aromatic C*H*), 7.69 (1H, m, aromatic C*H*).

139e[49] **–** ^{1}H NMR (399.79 MHz, $CDCl_3$, 27.0 °C): δ 3.25 (1H, br, O*H*), 6.38 (1H, br, C*H*), 7.22 (1H, m, aromatic C*H*), 7.4–7.8 (8H, m, 8 aromatic C*H*).

139i – ^{1}H NMR (399.79 MHz, $CDCl_3$, 27.0 °C): δ 1.12 (2H, m, CH_2), 1.55 (2H, m, CH_2), 1.86 (1H, m, CH_2), 2.17 (1H, m, CH_2), 2.28 (1H, dt, *J* = 6.4 and 11.3 Hz, C*H*), 2.99 (1H, m, C*H*), 3.47 (1H, br d, *J* = 5.9 Hz, O*H*), 5.10 (1H, d, *J* = 4.6 Hz, C*H*OH), 7.18 (1H, m, aromatic C*H*), 7.35 (2H, m, 2 aromatic C*H*), 7.54 (2H, m, 2 aromatic C*H*). ^{13}C{^{1}H} NMR (100.5 MHz, $CDCl_3$, 27.0 °C): δ 22.8 (*C*H_2), 23.0 (*C*H_2), 23.4 (*C*H_2), 26.5 (*C*H_2), 39.5 (*C*H), 41.1 (*C*H), 88.5 (*C*HOH), 122.3 (aromatic), 125.6 (aromatic), 129.0 (aromatic), 138.2 (aromatic), 175.6 (*C*=O). IR ($CHCl_3$ cast film): 3315, 2935, 2855, 1666, 1599, 1501, 1409, 1060, 759 cm^{-1}. HRMS (ESI$^+$) m/z calculated for $C_{14}H_{17}NNaO_2^+$ ([M + Na]$^+$): 254.11515. Found: 254.11489. Elemental analysis calculated for $C_{14}H_{17}NO_2$: N =

6.06, C = 72.70, H = 7.41. Found: N = 6.01, C = 72.85, H = 7.56. $[\alpha]_D^{23}$ –34.07 (c = 1.00 g/100 mL, $CHCl_3$, 93% *ee*). mp: 133.8 °C. HPLC analysis conditions: hexanes:2-PrOH = 97:3, 30 °C, Flow rate = 0.8 mL/min, detection (UV, 210 nm). Retention times: 27.0 min (minor enantiomer), 50.8 min (major enantiomer).

***trans*-139j –** ^{1}H NMR (399.79 MHz, acetone-d_6, 27.0 °C): δ 1.47 (2H, m, CH_2), 2.76 (1H, m, C*H*), 3.21 (3H, overlapping multiplet, C*H* and 2 bridgehead C*H*), 5.04 (1H, d, *J* = 8.1 Hz, C*H*OH), 5.23 (1H, d, *J* = 8.7 Hz, O*H*), 6.08 (1H, dd, *J* = 2.8 and 5.6 Hz, C*H*), 6.19 (1H, dd, *J* = 2.8 and 5.6 Hz, C*H*), 7.12 (1H, m, aromatic C*H*), 7.28 (2H, m, 2 aromatic C*H*), 7.50 (2H, m, 2 aromatic C*H*). ^{13}C{^{1}H} NMR (100.5 MHz, ~0.7 mL of acetone-d_6 with ~0.1 mL of MeOH-d_4, 27.0 °C): δ 46.0 (bridgehead *C*H), 46.5 (bridgehead *C*H), 47.5 (*C*H), 50.4 (*C*H), 51.7 (*C*H_2), 87.5 (*C*HOH), 125.3 (aromatic), 126.7 (aromatic), 129.4 (aromatic), 134.7 (aromatic), 136.6 (*C*=C), 138.9 (C=*C*), 176.1 (*C*=O). IR ($CHCl_3$ cast film): 3187, 2968, 1666, 1594, 1502, 1428, 1330, 1228, 1076, 721 cm^{-1}. HRMS (ESI^+) m/z calculated for $C_{15}H_{15}NNaO_2^+$ ($[M + Na]^+$): 264.0995. Found: 264.09938. Elemental analysis calculated for $C_{15}H_{15}NO_2$: N = 5.81, C = 74.67, H = 6.27. Found: N = 5.86, C = 74.8, H = 6.11. $[\alpha]_D^{23}$ –168.65 (c = 1.00 g/100 mL of MeOH, >99% *ee*). mp: 120.5 °C. HPLC analysis conditions: hexanes:2-PrOH = 97:3, 30 °C, Flow rate = 0.8 mL/min, detection (UV, 210 nm). Retention Times: 41.1 min (minor enantiomer), 49.7 min (major enantiomer). Product with >99% *ee* was obtained upon single recrystallization from hot EtOH. Yield after single unoptimized recrystallization: 73.0%. Sample crystal was used for X-ray diffraction analysis.

139k – ^{1}H NMR (399.80 MHz, acetone-d_6, 27.0 °C): δ 1.44 (1H, br dt, *J* = 1.6 and 8.4 Hz, CH_2), 1.50 (1H, dt, *J* = 1.6 and 8.4 Hz, CH_2), 2.76 (1H, m, C*H*), 3.18 (1H, m, C*H*), 3.23 (2H, overlapping multiplet, C*H* and bridgehead C*H*), 5.00 (1H, d, *J* = 8.0 Hz, C*H*OH), 5.26 (1H, d, *J* = 8.8 Hz, O*H*), 6.09 (1H, dd, *J* = 3.2 and 5.6 Hz, C*H*), 6.20 (1H,

dd, *J* = 3.2 and 5.6 Hz, C*H*), 7.05 (2H, m, 2 aromatic C*H*), 7.50 (2H, m, 2 aromatic C*H*). $^{13}C\{^{1}H\}$ NMR (100.5 MHz, acetone-d_6, 27.0 °C): δ 46.0 (bridgehead *C*H), 46.5 (bridgehead *C*H), 47.4 (*C*H), 50.0 (*C*H), 51.6 (CH_2), 87.2 (*C*HOH), 115.6 (aromatic), 115.8 (aromatic), 126.4 (aromatic), 126.5 (aromatic), 134.5 (*C*=C), 136.6 (C=*C*), 159.7 (aromatic), 162.1 (aromatic), 174.8 (*C*=O). ^{19}F NMR (376.15 MHz, acetone-d_6, 27.0 °C): δ -119.3 (tt, *J* = 5.3 and 8.3 Hz). IR (CH_3OH cast film): 3219, 2975, 1667, 1514, 1436, 1254, 1074 cm^{-1}. HRMS (ESI^+) m/z calculated for $C_{15}H_{14}FNNaO_2^+$ ($[M + Na]^+$): 282.0901. Found: 282.0899. Elemental analysis calculated for $C_{15}H_{14}FNO_2$: N = 5.40, C = 69.49, H = 5.44. Found: N = 5.42, C = 69.47, H = 5.45. $[\alpha]_D^{23}$ –151.13 (c = 1.00 g/100 mL of MeOH, >99% *ee*). mp: 219.0 °C. HPLC analysis conditions: hexanes:2-PrOH = 97:3, 30 °C, Flow rate = 0.8 mL/min, detection (UV, 210 nm). Retention times: 28.1 min (minor enantiomer), 31.5 min (major enantiomer). Product with >99% *ee* was obtained upon single recrystallization from hot AcOEt. Sample crystal used for X-ray diffraction analysis.

139l – ^{1}H NMR (399.79 MHz, $CDCl_3$, 27.0 °C): δ 1.44 (1H, m, CH_2), 1.61 (1H, dt, *J* = 1.6 and 8.4 Hz, CH_2), 2.71 (1H, ddd, *J* = 1.0, 4.2, and 8.6 Hz, C*H*), 2.86 (1H, br, CHO*H*), 2.93 (6H, s, 2 CH_3), 3.23 (1H, br, C*H*), 3.28 (1H, m, C*H*), 3.35 (1H, br, C*H*), 4.84 (1H, d, *J* = 5.6 Hz, C*H*OH), 6.16 (1H, dd, *J* = 2.8 and 5.6 Hz, C*H*), 6.24 (1H, dd, *J* = 2.8 and 5.6, C*H*), 6.72 (2H, d, *J* = 8.4 Hz, 2 aromatic C*H*), 7.14 (2H, d, *J* = 8.8 Hz, 2 aromatic C*H*). $^{13}C\{^{1}H\}$ NMR (125.27 MHz, ~0.7 mL of $CDCl_3$ with ~0.1 mL of MeOH-d_4, 27.0 °C): δ 40.5 (*C*H_3), 44.9 (bridgehead *C*H), 45.3 (bridgehead *C*H), 46.3 (*C*H), 49.2 (*C*H), 51.1 (CH_2), 87.6 (*C*HOH), 112.8 (aromatic), 126.0 (aromatic), 126.5 (aromatic), 133.3 (*C*=C), 136.0 (C=*C*), 149.5 (aromatic), 176.1 (*C*=O). IR ($CHCl_3$ cast film): 3332, 3001, 1661, 1565, 1320, 1227, 1067, 801, 758 cm^{-1}. HRMS (ESI^+) m/z calculated for $C_{17}H_{21}N_2O_2^+$ ($[M + H]^+$): 285.1598. Found: 285.1592. Elemental analysis calculated for

$C_{17}H_{20}N_2O_2$: N = 9.85, C = 71.81, H = 7.09. Found: N = 9.56, C = 71.41, H = 6.80. $[\alpha]_D^{23}$ – 147.69 (c = 0.50 g/100 mL of MeOH, 97% *ee*). mp: 237.1 °C. HPLC analysis conditions: hexanes:2-PrOH = 92:8, 30 °C, Flow rate = 1.6 mL/min, detection (UV, 210 nm). Retention times: 28.1 min (minor enantiomer), 31.1 min (major enantiomer).

139m – ^{1}H NMR (399.79 MHz, $CDCl_3$, 27.0 °C): δ 1.43 (1H, d, *J* = 8.4 Hz, C*H*$_2$), 1.61 (1H, d, *J* = 8.4 Hz, C*H*$_2$), 2.71 (1H, dd, *J* = 4.2 and 8.6 Hz, C*H*), 3.05 (1H, br, CHO*H*), 3.23 (1H, br, C*H*), 3.28 (1H, m, C*H*), 3.34 (1H, br, C*H*), 3.78 (3H, s, C*H*$_3$), 4.83 (1H, s, C*H*OH), 6.14 (1H, dd, *J* = 2.8 and 5.6 Hz, C*H*), 6.23 (1H, dd, *J* = 2.8 and 5.6 Hz, C*H*), 6.86 (2H, m, 2 aromatic C*H*), 7.20 (2H, m, 2 aromatic C*H*). ^{13}C{^{1}H} NMR (125.69 MHz, $CDCl_3$, 27.0 °C): δ 45.1 (bridgehead *C*H), 45.6 (bridgehead *C*H), 46.3 (CH), 49.2 (*C*H), 51.3 (*C*H$_2$), 55.5 (*C*H$_3$), 87.3 (*C*HOH), 114.4 (aromatic), 126.6 (aromatic), 129.7 (aromatic), 133.2 (*C*=C), 136.6 (C=*C*), 158.3 (aromatic), 175.0 (*C*=O). IR ($CHCl_3$ cast film): 3194, 2976, 1644, 1514, 1249, 1069, 1035, 829, 727 cm^{-1}. HRMS (ESI$^+$) m/z calculated for $C_{16}H_{17}NNaO_3^+$ ([M + Na]$^+$): 294.1101. Found: 294.1099. Elemental analysis calculated for $C_{16}H_{15}NO_3$: N = 5.20, C = 71.36, H = 5.61. Found: N = 5.03, C = 70.88, H = 6.22. $[\alpha]_D^{23}$ –151.93 (c = 0.50 g/100 mL of MeOH, 95% *ee*). mp: 205.6 °C. HPLC analysis conditions: hexanes:2-PrOH = 97:3, 30 °C, flow rate = 0.8 mL/min, detection (UV, 210 nm). Retention times: 82.68 min (minor enantiomer), 112.85 min (major enantiomer).

139n – ^{1}H NMR (399.79 MHz, $CDCl_3$, 27.0 °C): δ 1.36 (2H, m, C*H*$_2$), 1.55 (2H, m, C*H*$_2$), 2.22 (1H, dd, *J* = 0.9 and 7.9 Hz, C*H*), 2.72 (1H, d, *J* = 7.9 Hz, C*H*), 4.48 (1H, d, *J* = 4.8 Hz, bridgehead C*H*), 4.57 (1H, d, *J* = 4.8 Hz, bridgehead C*H*), 5.02 (1H, br, O*H*), 5.21 (1H, d, *J* = 1.0 Hz, C*H*OH), 7.00 (1H, m, aromatic C*H*), 7.12 (2H, m, 2 aromatic C*H*), 7.29 (2H, m, 2 aromatic C*H*). ^{13}C{^{1}H} NMR (100.5 MHz, acetone-d_6, 27.0 °C): δ 29.0 (*C*H$_2$), 29.1 (*C*H$_2$), 50.9 (*C*H), 53.4 (*C*H), 79.8 (bridgehead *C*H), 81.6 (bridgehead

*C*H) 88.9 (*C*HOH), 124.3 (aromatic), 126.3 (aromatic), 129.3 (aromatic), 138.9 (aromatic), 174.0 (*C*=O). IR ($CHCl_3$ cast film): 3315, 2982, 2957, 1658, 1599, 1502, 1419, 1314, 1284, 1056, 747 cm^{-1}. HRMS (ESI^+) m/z calculated for $C_{14}H_{15}NNaO_3^+$ ([M + Na]$^+$): 268.09441. Found: 268.09411. Elemental analysis calculated for $C_{14}H_{15}NO_3$: N = 5.71, C = 68.56, H = 6.16. Found: N = 5.69, C = 68.54, H = 6.30. $[\alpha]_D^{23}$ –133.33 (c = 1.00 g/100 mL of MeOH, 87% *ee*). mp: 178.2 °C. HPLC analysis conditions: hexanes:2-PrOH = 95:5, 30 °C, Flow rate = 1.0 mL/min, detection (UV, 210 nm). Retention times: 38.9 min (minor enantiomer), 46.6 min (major enantiomer).

139o – ^{1}H NMR (399.79 MHz, $CDCl_3$, 27.0 °C): δ 1.30–1.60 (6H, m, 3 C*H*$_2$), 2.45 (1H, ddd, *J* = 1.1, 4.9 and 10.5 Hz, C*H*), 2.57 (1H, br t, *J* = 3.8 Hz, bridgehead C*H*), 2.71 (1H, br, bridgehead C*H*), 3.03 (1H, dd, *J* = 5.5 and 10.5 Hz, C*H*), 3.28 (1H, d, *J* = 8.3 Hz, O*H*), 5.33 (1H, d, *J* = 7.3 Hz, C*H*OH), 7.24 (1H, m, aromatic C*H*), 7.36 (2H, m, 2 aromatic C*H*), 7.48 (2H, m, 2 aromatic C*H*). $^{13}C\{^1H\}$ NMR (100.5 MHz, $CDCl_3$, 27.0 °C): δ 22.9 (*C*H$_2$), 24.8 (*C*H$_2$), 39.5 (bridgehead *C*H), 39.9 (bridgehead *C*H), 41.2 (*C*H$_2$), 48.07 (*C*H), 48.10 (*C*H) 86.0 (*C*HOH), 124.0 (aromatic), 126.4 (aromatic), 129.1 (aromatic), 137.2 (aromatic), 175.9 (*C*=O). IR ($CHCl_3$ cast film): 3347, 2960, 2881, 1673, 1597, 1500, 1409, 1066, 759 cm^{-1}. HRMS (ESI^+) m/z calculated for $C_{15}H_{17}NNaO_2^+$ ([M + Na]$^+$): 266.11515. Found: 266.11509. Elemental analysis calculated for $C_{15}H_{17}NO_2$: N = 5.76, C = 74.05, H = 7.04. Found: N = 5.61, C = 74.04, H = 7.49. $[\alpha]_D^{23}$ –113.73 (c = 1.00 g/100 mL of $CHCl_3$, 93% *ee*). mp: 153.5 °C. HPLC analysis conditions: hexanes:2-PrOH = 97:3, 30 °C, Flow rate = 0.8 mL/min, detection (UV, 210 nm). Retention times: 27.8 min (minor enantiomer), 39.1 min (major enantiomer).

140a[46] **–** ^{1}H NMR (399.79 MHz, $CDCl_3$, 27.0 °C): δ 1.81 (2H, tt, *J* = 6.2 and 6.8 Hz, C*H*$_2$), 2.30 (2H, t, *J* = 6.8 Hz, C*H*$_2$), 2.74 (3H, d, *J* = 4.8 Hz, C*H*$_3$), 3.61 (2H, br dt, *J* = 4.4 and 5.4 Hz, C*H*$_2$OH), 4.07 (1H, br, O*H*), 6.62 (1H, br, N*H*).

140b[47] **–** ^{1}H NMR (299.97 MHz, $CDCl_3$, 27.0 °C): δ 1.95 (2H, tt, *J* = 8.6 and 8.4 Hz, C*H*$_2$), 2.51 (2H, t, *J* = 9.0 Hz, C*H*$_2$), 2.96 (1H, br, O*H*), 2.72 (2H, t, *J* = 7.6 Hz, C*H*$_2$OH), 7.09 (2H, m, 2 aromatic C*H*), 7.29 (1H, m, aromatic C*H*), 7.49 (2H, m, 2 aromatic C*H*), 7.92 (1H, br, N*H*).

140c[48] **–** ^{1}H NMR (399.79 MHz, $CDCl_3$, 27.0 °C): δ 2.94 (3H, s, C*H*$_3$), 3.66 (1H, br, O*H*), 5.61 (1H, s, C*H*), 7.42 (1H, m, aromatic C*H*), 7.60 (3H, m, 3 aromatic C*H*).

142[33] **–** ^{1}H NMR (399.80 MHz, DMSO-*d*$_6$, 27.0 °C): δ 3.79, (1H, d, *J* = 9.0 Hz, C*H*) 4.09 (1H, overlapping with a CH peak, d, *J* = 16.2 Hz, C*H*$_2$) 4.13 (1H, overlapping with a CH_2 peak, d, *J* = 9.2 Hz, C*H*) 4.33 (1H, AB patterned d, *J* = 15.7, C*H*$_2$), 4.44 (1H, overlapping with a CH_2 peak, AB patterned d, *J* = 15.7, C*H*$_2$), 4.48 (1H, overlapping with a CH_2 peak, d, *J* = 15.3, C*H*$_2$), 4.67 (1H, d, *J* = 15.2, C*H*$_2$), 4.76 (1H, overlapping with a CH_2 peak, d, *J* = 8.5, C*H*OH), 4.48 (1H, overlapping with a CHOH peak, d, *J* = 16.6, C*H*$_2$), 6.43 (1H, d, *J* = 8.1, CHO*H*), 7.10–7.40 (15H, m, 15 aromatic C*H*). HPLC analysis conditions: Daicel CHIRALPAK IB column (4.6 mm i.d. × 250 mm), hexanes:2-PrOH = 95:5, 30 °C, flow rate = 0.8 mL/min, detection (UV, 210 nm). Retention times: 35.2 min (major enantiomer), 44.8 min (minor enantiomer).

Procedure for the preparation of racemic *cis*–139j:[8]

Under Ar, the imide **138j** (478 mg, 2.00 mmol), and 20.0 mL of CH_2Cl_2 were placed in a 100 mL schlenk flask equipped with a magnetic stir bar. DIBAL-H (1.50 M in Toluene, 1.40 mL, 2.10 mmol) was then added slowly to solution at –78 °C. The reaction mixture was then stirred for 2 h at –78 °C. After 2 h, 5.0 mL of acetone and 2.0 mL of H_2O was added to the reaction mixture. The cooling bath was then removed, and the mixture was stirred until it warmed to room temperature. A white precipitate was formed. The reaction mixture was then dried by addition of anhydrous $MgSO_4$, filtered using Celite® 545, and concentrated to yield a white solid. The crude product was dissolved in

AcOEt and passed through 150 mesh, neutral, activated alumina (Brockmann I). Evaporation of the solvent *in vacuo* gave the product. Formation of the *trans*-isomer was not observed. Isolated yield: 70.0%. Diastereomeric ratio: >99:1 (based on ^{1}H NMR). ^{1}H NMR (399.80 MHz, ~0.7 mL acetone-d_6 + ~0.1 mL $CDCl_3$, 27.0 °C): δ 1.45 (2H, m, CH_2), 3.11 (1H, m, bridgehead C*H*), 3.17 (3H, overlapping m, 2 C*H* and bridgehead C*H*), 5.05 (1H, d, *J* = 6.0 Hz, O*H*), 5.85 (1H, m, C*H*OH), 6.03 (1H, dd, *J* = 2.8 and 5.6 Hz, C*H*), 6.29 (1H, dd, *J* = 2.8 and 5.6 Hz, C*H*), 7.11 (1H, m, aromatic C*H*), 7.29 (4H, m, 4 aromatic C*H*). ^{13}C{^{1}H} NMR (125.69 MHz, $CDCl_3$, 27.0 °C): δ 42.6 (*C*H), 44.9 (*C*H), 46.3 (*C*H), 50.0 (*C*H), 51.8 (*C*H_2), 83.0 (*C*HOH), 124.5 (aromatic), 126.5 (aromatic), 129.1 (aromatic), 135.0 (*C*=C), 135.2 (C=*C*), 136.4 (aromatic), 173.2 (*C*=O). IR (solid): 3297, 2984, 1651, 1469, 1406, 1302, 1097 cm^{-1}. HRMS (ESI$^+$) m/z calculated for $C_{15}H_{16}NO_2^+$ ([M + H]$^+$): 242.1176. Found: 242.1177. Elemental analysis calculated for $C_{15}H_{15}NO_2$: N = 5.81, C = 74.67, H = 6.27. Found: N = 5.86, C = 74.8, H = 6.29. mp: 177.9 °C.

Isomerization of racemic *cis*–139j into *trans*–139j the presence of base

Under Argon, racemic *cis*–**139j** (51 mg, 0.21 mmol) and 3.0 mL of THF were placed in a 50 mL schlenk flask equipped with a magnetic stir bar. A white suspension was formed. A 1.0 mL solution of KO*t*-Bu in THF (1.2 mg, 0.010 mmol) was then added to the flask at 0 °C. The white suspension became clear upon the addition of base. The reaction mixture was stirred for 4 h at 0 °C. After 4 h, an aliquot of the reaction mixture was obtained and concentrated under vacuum. ^{1}H NMR analysis of the sample showed complete isomerization to *trans*-**139j**.

Synthesis of the polycyclic lactam, 144

Under Ar, *trans*-**139j** (>99% *ee*) (95 mg, 0.40 mmol), indene (50 *μ*L, 0.43 mmol), and 10 mL of toluene were placed in a 50 mL schlenk flask equipped with a magnetic stir

bar. The hydroxyl lactam, *trans*-**139j** was partially soluble in toluene. $BF_3 \cdot OEt_2$ (0.10 mL, 0.79 mmol) was then added to the flask at room temperature. The faint yellow solution that resulted was stirred for 30 min at room temperature. The reaction mixture was quenched by the addition of 5.0 mL saturated $NaHCO_3$ solution, followed by stirring for 5.0 min. The faint yellow solution became colorless upon quenching. The reaction mixture was then extracted with CH_2Cl_2 (100 mL), dried over anhydrous $MgSO_4$, gravity filtered and concentrated under vacuum. The product (a colorless oil) was analyzed by ^{1}H NMR spectroscopy and HPLC to determine the percent conversion, diastereomeric ratio, and enantiomeric excess. The HPLC chromatogram was compared to that of racemic **144** prepared from racemic **139j** that was obtained from $NaBH_4$ reduction of **138j**. Crystals of the major diastereomer were formed upon slow evaporation of an AcOEt solution. This sample was used for X-ray diffraction analysis. Percent conversion: 90.0%, diastereomeric ratio: 91:9. Enantiomeric excess: >99%.

^{1}H NMR (399.79 MHz, $CDCl_3$, 27.0 °C): δ 1.47 (1H, d, *J* = 8.4 Hz, C*H*$_2$), 1.66 (1H, dt, *J* = 1.6 and 8.4 Hz, C*H*$_2$), 2.75 (1H, m, C*H*), 2.87 (1H, dd, *J* = 10.6 and 15.4 Hz, C*H*$_2$), 3.02 (1H, dd, *J* = 8.2 and 15.4 Hz, C*H*$_2$), 3.19 (1H, br m, bridgehead C*H*), 3.21–3.30 (2H, m, 2CH), 3.41 (1H, br m, bridgehead C*H*), 3.60 (1H, t, *J* = 3.0 Hz, C*H*), 4.46 (1H, d, *J* = 8.8 Hz, C*H*), 6.17 (1H, dd, *J* = 3.2 and 5.6 Hz, C*H*), 6.35 (1H, dd, *J* = 3.2 and 5.6 Hz, C*H*), 7.04 (1H, m, aromatic C*H*), 7.14 (4H, m, 4 aromatic C*H*), 7.47 (2H, m, 2 aromatic C*H*), 8.01 (1H, dd, *J* = 1.4 and 8.2 Hz, aromatic C*H*). ^{13}C{^{1}H} NMR (100.5 MHz, $CDCl_3$, 27.0 °C): δ 32.1 (benzylic *C*H$_2$), 40.0 (*C*H), 45.5 (*C*H), 45.7 (bridgehead *C*H), 46.1 (bridgehead *C*H), 46.8 (*C*H), 51.0 (*C*H$_2$), 51.1 (*C*H), 60.8 (*C*HN), 121.3 (aromatic), 124.8 (aromatic), 124.9 (aromatic), 125.0 (aromatic), 126.4 (aromatic), 126.8 (aromatic), 127.3 (aromatic), 128.6 (aromatic), 130.1 (aromatic), 134.3 (*C*=C), 135.2 (aromatic), 136.8 (C=*C*), 141.8 (aromatic), 145.4 (aromatic), 173.3 (*C*=O). IR ($CHCl_3$ cast film): 2981, 1683, 1492, 1397, 755 cm^{-1}. HRMS (ESI$^+$) m/z calculated for $C_{24}H_{22}NO$ ([M + H]$^+$):

340.1696. Found: 340.1701. Elemental analysis calculated for $C_{24}H_{21}NO$: N = 4.13, C = 84.92, H = 6.24. Found: N = 3.92, C = 84.12, H = 6.30. $[\alpha]_D^{23}$ 124.76 (c = 1.00 g/100 mL of $CHCl_3$, >99% *ee*). mp: 211.2 °C. HPLC analysis conditions: Hexanes:2-PrOH = 97:3, 30 °C, Flow rate = 0.8 mL/min, detection (UV, 210 nm). Retention times: 19.7 min (minor enantiomer), 24.7 min (major enantiomer).

Table 2-7 *Crystallographic experimental details for trans-**139j**.*

A. Crystal Data

Formula	$C_{15}H_{15}NO_2$
Formula Weight	241.28
Crystal Dimensions (mm)	0.48 x 0.33 x 0.23
Crystal System	Orthorhombic
Space Group	$P2_12_12_1$ (No. 19)
Unit Cell Parameters[a]	
a (Å)	6.1618 (7)
b (Å)	12.7291 (14)
c (Å)	15.3398 (17)
V (Å^3)	1203.2 (2)
Z	4
ρ_{calcd} (g cm^{-3})	1.332
μ (mm^{-1})	0.089

B. Data collection and refinement conditions

Diffractometer	Bruker PLATFORM/SMART 1000 CCD[b]
Radiation (λ [Å])	graphite-monochromated Mo K*α* (0.71073)
Temperature (°C)	–80
Scan Type	scans (0.4°) (10 s exposures)
Data Collection 2*θ* limit (deg)	54.96
Total Data Collected	(-7 ≤ *h* ≤ 8, -16 ≤ *k* ≤ 16, -19 ≤ *l* ≤ 19)
Independent Reflections	2738 (R_{int} = 0.0247)

Number of Observed Reflections (*NO*)	2478 [$F_o^2 \geq 2\sigma(F_o^2)$]
Structure Solution Method	direct methods (*SHELXS–97*[c])
Refinement Method	full-matrix least-squares on F^2 (*SHELXL–97*[c])
Absorption Correction Method	multi-scan (*SADABS*)
Range of Transmission Factors	0.9799–0.9587
Data/Restraints/Parameters	2738 [$F_o^2 \geq -3\sigma(F_o^2)$] / 0 / 164
Flack Absolute Structure Parameter[d]	1.4 (11)
Goodness-of-fit (*S*)[e]	1.062 [$F_o^2 \geq -3\sigma(F_o^2)$]
Final *R* Indices[f]	
R_1 [$F_o^2 \geq 2\sigma(F_o^2)$]	0.0358
wR_2 [$F_o^2 \geq -3\sigma(F_o^2)$]	0.0866
Largest difference Peak and Hole	0.248 and –0.132 e Å^{-3}

[a]Obtained from least-squares refinement of 5008 reflections with 5.32° < 2θ < 54.84°.

[b]Programs for diffractometer operation, data collection, data reduction and absorption correction were those supplied by Bruker.

[c]Sheldrick, G. M. *Acta Crystallogr.* **2008**, *A64*, 112–122.

[d]Flack, H. D. *Acta Crystallogr.* **1983**, *A39*, 876–881; Flack, H. D.; Bernardinelli, G. *Acta Crystallogr.* **1999**, *A55*, 908–915; Flack, H. D.; Bernardinelli, G. *J. Appl. Cryst.* **2000**, *33*, 1143–1148. The Flack parameter will refine to a value near zero if the structure is in the correct configuration and will refine to a value near one for the inverted configuration. However, the low anomalous scattering power of the atoms in this structure (none heavier than oxygen) implies that the data cannot be used for absolute structure assignment, thus the Flack parameter is provided for informational purposes only. The present structural study should only be used for assignment of relative stereochemistry.

[e]$S = [\Sigma w(F_o^2 - F_c^2)^2/(n-p)]^{1/2}$ (n = number of data; p = number of parameters varied; $w = [\sigma^2(F_o^2) + (0.0427P)^2 + 0.2201P]^{-1}$ where $P = [\mathrm{Max}(F_o^2, 0) + 2F_c^2]/3$).

[f]$R1 = \Sigma||F_o| - |F_c||/\Sigma|F_o|$; $wR^2 = [\Sigma w(F_o^2 - F_c^2)^2/\Sigma w(F_o^4)]^{1/2}$.

Table 2-8 *Selected interatomic distances (Å) for trans-**139j**.*

Atom1	Atom2	Distance	Atom1	Atom2	Distance
O1	O2[a]	2.6608(14)[b]	C5	C6	1.508(2)
O1	C1	1.2321(16)	C5	C9	1.538(2)
O1	H2O[a]	1.83[b]	C6	C7	1.329(2)
O2	C2	1.4034(17)	C7	C8	1.509(2)
N	C1	1.3582(16)	C8	C9	1.543(2)
N	C2	1.4700(17)	C10	C11	1.386(2)
N	C10	1.4330(18)	C10	C15	1.388(2)
C1	C4	1.5018(19)	C11	C12	1.387(2)
C2	C3	1.533(2)	C12	C13	1.380(3)
C3	C4	1.5442(19)	C13	C14	1.378(3)
C3	C8	1.561(2)	C14	C15	1.392(2)
C4	C5	1.568(2)			

[a]At 1–*x*, 1/2+*y*, 1/2–*z*. [b]Nonbonded distance.

Table 2-9 *Selected interatomic angles (deg) for trans-**139j**.*

Atom1	Atom2	Atom3	Angle	Atom1	Atom2	Atom3	Angle
C1	N	C2	114.73(11)	C6	C5	C9	99.98(13)
C1	N	C10	122.91(11)	C5	C6	C7	107.96(14)
C2	N	C10	122.28(10)	C6	C7	C8	107.60(14)
O1	C1	N	124.33(13)	C3	C8	C7	107.05(12)
O1	C1	C4	126.42(12)	C3	C8	C9	99.64(13)
N	C1	C4	109.24(12)	C7	C8	C9	100.15(13)
O2	C2	N	109.68(12)	C5	C9	C8	93.83(12)
O2	C2	C3	111.91(12)	N	C10	C11	120.02(14)
N	C2	C3	103.62(10)	N	C10	C15	119.61(14)
C2	C3	C4	106.93(11)	C11	C10	C15	120.36(14)
C2	C3	C8	116.57(13)	C10	C11	C12	119.67(16)
C4	C3	C8	102.64(11)	C11	C12	C13	120.21(16)
C1	C4	C3	105.07(11)	C12	C13	C14	120.09(15)
C1	C4	C5	114.45(11)	C13	C14	C15	120.41(17)
C3	C4	C5	103.43(11)	C10	C15	C14	119.25(16)
C4	C5	C6	106.83(12)	O2	H2O	O1[a]	169.0[b]
C4	C5	C9	99.05(12)				

[a]At 1–x, –1/2+y, 1/2–z. [b]Angle includes nonbonded O–H…O interaction.

Table 2-10 *Crystallographic experimental details for* ***139k****.*

A. Crystal Data	
Formula	$C_{15}H_{14}FNO_2$
Formula Weight	259.27
Crystal Dimensions (mm)	0.46 x 0.27 x 0.21
Crystal System	orthorhombic
Space Group	$P2_12_12_1$ (No. 19)
Unit Cell Parameters[a]	
a (Å)	6.1944 (4)
b (Å)	12.7213 (8)
c (Å)	15.5031 (9)
V (Å^3)	1221.66 (13)
Z	4
r_{calcd} (g cm^{-3})	1.410
μ (mm^{-1})	0.104
B.	Data Collection and Refinement Conditions
Diffractometer	Bruker D8/APEX II CCD[b]
Radiation (*l* [Å])	graphite-monochromated Mo Kα (0.71073)
Temperature (°C)	–100
Scan Type	ω scans (0.3°) (20 s exposures)
Data Collection 2*q* limit (deg)	55.02
Total Data Collected	10802 (-8 ≤ *h* ≤ 8, -16 ≤ *k* ≤ 16, -20 ≤ *l* ≤ 20)
Independent Reflections	1633 (R_{int} = 0.0136)
Number of Observed Reflections (*NO*)	1587 [$F_o^2 \geq 2s(F_o^2)$]
Structure Solution Method	direct methods (*SHELXS–97*[c])
Refinement Method	full-matrix least-squares on F^2 (*SHELXL–97*[c])

Absorption Correction Method	Gaussian integration (face-indexed)
Range of Transmission Factors	0.9781–0.9539
Data/Restraints/Parameters	1633 / 0 / 173
Flack Absolute Structure Parameter[d]	1.7(10)
Goodness-of-fit (S)[e] [all data]	1.071
Final R indices[f]	
R_1 [$F_o^2 \geq 2s(F_o^2)$]	0.0295
wR_2 [all data]	0.0810
Largest Difference Peak and Hole	0.231 and –0.148 e Å^{-3}

[a]Obtained from least-squares refinement of 9934 reflections with 5.26° < 2q < 54.96°.

[b]Programs for diffractometer operation, data collection, data reduction and absorption correction were those supplied by Bruker.

[c]Sheldrick, G. M. *Acta Crystallogr.* **2008**, *A64*, 112–122.

[d]Flack, H. D. *Acta Crystallogr.* **1983**, *A39*, 876–881; Flack, H. D.; Bernardinelli, G. *Acta Crystallogr.* **1999**, *A55*, 908–915; Flack, H. D.; Bernardinelli, G. *J. Appl. Cryst.* **2000**, *33*, 1143–1148. The Flack parameter will refine to a value near zero if the structure is in the correct configuration and will refine to a value near one for the inverted configuration. However, the low anomalous scattering power of the atoms in this structure (none heavier than oxygen) implies that the data cannot be used for absolute structure assignment, thus the Flack parameter is provided for informational purposes only.

[e]$S = [\Sigma w(F_o^2 - F_c^2)^2/(n-p)]^{1/2}$ (n = number of data; p = number of parameters varied; w = $[\sigma^2(F_o^2) + (0.0490P)^2 + 0.2124P]^{-1}$ where $P = [\text{Max}(F_o^2, 0) + 2F_c^2]/3$).

[f]$R_1 = \Sigma||F_o| - |F_c||/\Sigma|F_o|$; $wR_2 = [\Sigma w(F_o^2 - F_c^2)^2/\Sigma w(F_o^4)]^{1/2}$.

Table 2-11 *Selected interatomic distances (Å) for* ***139k****.*

Atom1	Atom2	Distance	Atom1	Atom2	Distance
F	C13	1.3572(17)	C4	C5	1.507(3)
O1	O2[a]	2.7003(15)[b]	C4	C9	1.545(2)
O1	H2O[a]	1.86[b]	C5	C6	1.334(3)
O1	C1	1.2302(17)	C6	C7	1.513(2)
O2	C2	1.3995(18)	C7	C8	1.567(2)
N	C1	1.3578(16)	C7	C9	1.539(2)
N	C2	1.4703(17)	C10	C11	1.388(2)
N	C10	1.4276(18)	C10	C15	1.387(2)
C1	C8	1.5041(19)	C11	C12	1.390(2)
C2	C3	1.537(2)	C12	C13	1.373(3)
C3	C4	1.559(2)	C13	C14	1.369(3)
C3	C8	1.5484(18)	C14	C15	1.390(2)

[a]At 1–*x*, 1/2+*y*, 1/2–*z*. [b]Nonbonded distance.

Table 2-12 *Selected interatomic angles (deg) for* ***139k****.*

Atom1	Atom2	Atom3	Angle	Atom1	Atom2	Atom3	Angle
C1	N	C2	115.16(12)	C6	C7	C9	100.33(13)
C1	N	C10	122.84(12)	C8	C7	C9	98.80(12)
C2	N	C10	121.98(10)	C1	C8	C3	105.03(11)
O1	C1	N	124.53(13)	C1	C8	C7	114.52(12)
O1	C1	C8	126.35(12)	C3	C8	C7	103.18(11)
N	C1	C8	109.11(12)	C4	C9	C7	93.69(12)
O2	C2	N	108.85(12)	N	C10	C11	120.30(13)
O2	C2	C3	112.33(12)	N	C10	C15	119.73(14)
N	C2	C3	103.41(10)	C11	C10	C15	119.97(14)
C2	C3	C4	116.11(12)	C10	C11	C12	120.25(16)
C2	C3	C8	107.00(11)	C11	C12	C13	118.17(16)
C4	C3	C8	102.73(12)	F	C13	C12	118.64(17)
C3	C4	C5	107.30(12)	F	C13	C14	118.29(17)
C3	C4	C9	99.63(13)	C12	C13	C14	123.07(14)
C5	C4	C9	100.18(14)	C13	C14	C15	118.42(16)
C4	C5	C6	107.73(16)	C10	C15	C14	120.10(16)
C5	C6	C7	107.59(16)	O2	H2O	O1[a]	174.3[b]
C6	C7	C8	107.26(12)				

[a]At 1–x, –1/2+y, 1/2–z. [b]Angle includes nonbonded O–H…O interaction.

Table 2-13 *Crystallographic experimental details for* ***144****.*

A. Crystal Data	
Formula	C22H19BrN2O3
Formula weight	439.30
Crystal Dimensions (mm)	0.63 x 0.37 x 0.21
Crystal System	Orthorhombic
Space Group	*P*21212 (No. 18)
Unit Cell Parameters[a]	
a (Å)	12.7403 (5)
b (Å)	25.8323 (10)
c (Å)	12.1352 (5)
V (Å3)	3993.8 (3)
Z	8
*r*calcd (g cm^{-3})	1.461
μ (mm^{-1})	2.084
B. Data Collection and Refinement Conditions	
Diffractometer	Bruker D8/APEX II CCD[b]
Radiation (*l* [Å])	graphite-monochromated Mo Kα (0.71073)
Temperature (°C)	–100
Scan type	ω scans (0.3°) (20 s exposures)
Data Collection 2*q* limit (deg)	55.00
Total Data Collected	35335 (-16 ≤ *h* ≤ 16, -33 ≤ *k* ≤ 33, -15 ≤ *l* ≤ 15)
Independent Reflections	9140 (R_{int} = 0.0204)
Number of Observed Reflections (*NO*)	8033 [$F_o^2 \geq 2s(F_o^2)$]
Structure Solution Method	direct methods (*SHELXD*[c])
Refinement Method	full-matrix least-squares on F^2 (*SHELXL–97*[d])
Absorption Correction method	Gaussian integration (face-indexed)

Range of Transmission Factors	0.6688–0.3545
data/restraints/parameters	9140 / 0 / 505
Flack Absolute Structure parameter[e]	0.013(6)
goodness-of-fit (S)[f] [all data]	1.028
final R indices[g]	
$R1$ [$F_o^2 \geq 2s(F_o^2)$]	0.0354
wR_2 [all data]	0.0921
Largest Difference Peak and Hole	0.621 and –0.444 e Å^{-3}

[a]Obtained from least-squares refinement of 9772 reflections with 4.50° < 2q < 51.00°.

[b]Programs for diffractometer operation, data collection, data reduction and absorption correction were those supplied by Bruker.

[c]Schneider, T. R.; Sheldrick, G. M. *Acta Crystallogr.* **2002**, *D58*, 1772-1779.

[d]Sheldrick, G. M. *Acta Crystallogr.* **2008**, *A64*, 112–122.

[e]Flack, H. D. *Acta Crystallogr.* **1983**, *A39*, 876–881; Flack, H. D.; Bernardinelli, G. *Acta Crystallogr.* **1999**, *A55*, 908–915; Flack, H. D.; Bernardinelli, G. *J. Appl. Cryst.* **2000**, *33*, 1143–1148. The Flack parameter will refine to a value near zero if the structure is in the correct configuration and will refine to a value near one for the inverted configuration.

[f]$S = [\Sigma w(F_o^2 - F_c^2)^2/(n-p)]^{1/2}$ (n = number of data; p = number of parameters varied; $w = [\sigma^2(F_o^2) + (0.0479P)^2 + 1.0597P]^{-1}$ where $P = [\text{Max}(F_o^2, 0) + 2F_c^2]/3$).

[g]$R_1 = \Sigma||F_o| - |F_c||/\Sigma|F_o|$; $wR_2 = [\Sigma w(F_o^2 - F_c^2)^2/\Sigma w(F_o^4)]^{1/2}$.

Table 2-14 *Selected interatomic distances (Å) for* ***144****.*

(a) Within molecule A			*(b) within molecule B*		
Atom1	Atom2	Distance	Atom1	Atom2	Distance
Br	C1	1.898(2)	Br	C1	1.906(3)
O1	C7	1.202(3)	O1	C7	1.208(3)
O2	C7	1.370(3)	O2	C7	1.372(3)
O2	C8	1.439(3)	O2	C8	1.448(3)
O3	C9	1.219(3)	O3	C9	1.228(3)
N1	C4	1.415(3)	N1	C4	1.415(3)
N1	C7	1.350(3)	N1	C7	1.342(3)
N2	C8	1.452(3)	N2	C8	1.455(3)
N2	C9	1.373(3)	N2	C9	1.355(3)
N2	C17	1.420(3)	N2	C17	1.418(4)
C1	C2	1.366(4)	C1	C2	1.379(4)
C1	C6	1.378(4)	C1	C6	1.370(4)
C2	C3	1.386(3)	C2	C3	1.382(4)
C3	C4	1.387(3)	C3	C4	1.382(3)
C4	C5	1.396(3)	C4	C5	1.387(4)
C5	C6	1.387(3)	C5	C6	1.389(4)
C8	C15	1.525(4)	C8	C15	1.531(4)
C9	C10	1.506(4)	C9	C10	1.489(4)
C10	C11	1.571(4)	C10	C11	1.578(4)
C10	C15	1.528(4)	C10	C15	1.530(4)
C11	C12	1.506(5)	C11	C12	1.513(5)
C11	C16	1.510(6)	C11	C16	1.521(5)
C12	C13	1.323(5)	C12	C13	1.299(5)
C13	C14	1.510(4)	C13	C14	1.516(5)
C14	C15	1.566(4)	C14	C15	1.573(4)

Table 2-14 (continued) *Selected interatomic distances (Å) for* ***144****.*

(a) Within molecule A			*(b) within molecule B*		
Atom1	Atom2	Distance	Atom1	Atom2	Distance
C14	C16	1.549(6)	C14	C16	1.538(6)
C17	C18	1.382(4)	C17	C18	1.366(5)
C17	C22	1.373(4)	C17	C22	1.398(5)
C18	C19	1.404(6)	C18	C19	1.439(8)
C19	C20	1.350(6)	C19	C20	1.380(10)
C20	C21	1.343(5)	C20	C21	1.326(9)
C21	C22	1.378(5)	C21	C22	1.365(6)

Table 2-15 *Selected interatomic angles (deg) for* ***144****.*

(a) Within molecule A				*(b) within molecule B*			
C7	O2	C8	117.20(18)	C7	O2	C8	117.58(19)
C4	N1	C7	125.2(2)	C4	N1	C7	127.3(2)
C8	N2	C9	113.7(2)	C8	N2	C9	114.1(2)
C8	N2	C17	121.08(18)	C8	N2	C17	121.8(2)
C9	N2	C17	125.1(2)	C9	N2	C17	124.1(2)
Br	C1	C2	119.25(19)	Br	C1	C2	119.0(2)
Br	C1	C6	119.4(2)	Br	C1	C6	119.7(2)
C2	C1	C6	121.3(2)	C2	C1	C6	121.3(2)
C1	C2	C3	119.3(2)	C1	C2	C3	118.7(2)
C2	C3	C4	120.3(2)	C2	C3	C4	121.0(2)
N1	C4	C3	116.8(2)	N1	C4	C3	116.9(2)
N1	C4	C5	123.1(2)	N1	C4	C5	123.7(2)
C3	C4	C5	120.1(2)	C3	C4	C5	119.4(2)
C4	C5	C6	118.8(2)	C4	C5	C6	119.8(2)
C1	C6	C5	120.2(2)	C1	C6	C5	119.7(2)
O1	C7	O2	124.2(2)	O1	C7	O2	123.7(2)
O1	C7	N1	128.0(2)	O1	C7	N1	127.9(2)
O2	C7	N1	107.77(19)	O2	C7	N1	108.4(2)
O2	C8	N2	106.77(18)	O2	C8	N2	108.0(2)
O2	C8	C15	110.02(19)	O2	C8	C15	110.3(2)
N2	C8	C15	105.1(2)	N2	C8	C15	104.3(2)
O3	C9	N2	125.2(2)	O3	C9	N2	124.3(3)
O3	C9	C10	126.0(2)	O3	C9	C10	126.2(2)
N2	C9	C10	108.8(2)	N2	C9	C10	109.5(2)
C9	C10	C11	113.3(2)	C9	C10	C11	112.8(2)
C9	C10	C15	105.5(2)	C9	C10	C15	105.6(2)
C11	C10	C15	103.4(3)	C11	C10	C15	102.9(2)
C10	C11	C12	106.4(2)	C10	C11	C12	106.3(2)
C10	C11	C16	99.5(3)	C10	C11	C16	99.0(2)
C12	C11	C16	100.1(3)	C12	C11	C16	100.7(3)

Table 2-15 (continued) *Selected interatomic angles (deg) for* ***144****.*

(a) Within molecule A				*(b) within molecule B*			
C11	C12	C13	108.2(3)	C11	C12	C13	107.9(3)
C12	C13	C14	107.4(3)	C12	C13	C14	108.2(3)
C13	C14	C15	107.1(2)	C13	C14	C15	105.8(3)
C13	C14	C16	99.8(3)	C13	C14	C16	100.0(3)
C15	C14	C16	98.5(3)	C15	C14	C16	99.1(3)
C8	C15	C10	106.4(2)	C8	C15	C10	106.2(2)
C8	C15	C14	116.3(2)	C8	C15	C14	116.0(3)
C10	C15	C14	103.0(2)	C10	C15	C14	103.1(2)
C11	C16	C14	94.5(3)	C11	C16	C14	94.1(3)
N2	C17	C18	121.3(2)	N2	C17	C18	120.6(3)
N2	C17	C22	120.1(2)	N2	C17	C22	118.9(3)
C18	C17	C22	118.5(3)	C18	C17	C22	120.5(4)
C17	C18	C19	119.3(3)	C17	C18	C19	117.0(5)
C18	C19	C20	121.2(4)	C18	C19	C20	119.6(5)
C19	C20	C21	118.7(3)	C19	C20	C21	122.2(5)
C20	C21	C22	122.1(3)	C20	C21	C22	119.3(6)
C17	C22	C21	120.0(3)	C17	C22	C21	121.3(4)

Bibliography

1. Maryanoff, B. E.; Zhang, H. -C.; Cohen, J. H.; Turchi, I. J.; Maryanoff, C. A. *Chem. Rev.* **2004***, 104*, 1431-1628.

2. Royer, J.; Bonin, M.; Micouin, L. *Chem. Rev.* **2004***, 104*, 2311-2352.

3. Atodiresei, I.; Schiffers, I.; Bolm, C. *Chem. Rev.* **2007***, 107*, 5683-5712.

4. Osakada, K.; Obana, M.; Ikariya, T.; Saburi, M.; Yoshikawa, S. *Tetrahedron Lett.* **1981***, 22*, 4297-4300.

5. Bonrath, W.; Karge, R.; Netscher, T.; Roessler, F.; Spindler, F. In *Asymmetric Catalysis on Industrial Scale: Challenges, Approaches and Solutions Second Edition: Chiral Lactones by Asymmetric Hydrogenation - A Step Forward in (+)-Biotin Production;* Blaser, H. -U., Director, H. -J. F., Eds.; Wiley-VCH Verlag GmbH & Co. KGaA: Weinheim, 2010; pp 27-39.

6. Bonrath, W.; Karge, R.; Roessler, F. DSM IP Assets B. V., Netherlands; Patent WO2006108636A1, 2006; p 33

7. Ramón, D. J.; Guillena, G.; Seebach, D. *Helv. Chim. Acta* **1996***, 79*, 875-894.

8. Matsuki, K.; Inoue, H.; Ishida, A.; Takeda, M.; Nakagawa, M.; Hino, T. *Chem. Pharm. Bull.* **1994***, 42*, 9-18.

9. Ostendorf, M.; Romagnoli, R.; Pereiro, I. C.; Roos, E. C.; Moolenaar, M. J.; Speckamp, W. N.; Hiemstra, H. *Tetrahedron: Asymmetry* **1997***, 8*, 1773-1789.

10. Molinaro, C.; Gauvreau, D.; Hughes, G.; Lau, S.; Lauzon, S.; Angelaud, R.; O'Shea, P. D.; Janey, J.; Palucki, M.; Hoerrner, S. R.; Raab, C. E.; Sidler, R. R.; Belley, M.; Han, Y. *J. Org. Chem.* **2009***, 74*, 6863-6866.

11. Sharov, Y.; Zhang, L.; Du, G. -J.; Ren, J.; Cheng, M. -S. *Molecules* **2008***, 13*, 1817-1821.

12. Lin, H.; Danishefsky, S. J. *Angew. Chem., Int. Ed.* **2003***, 42*, 36-51.

13. Raheem, I. T.; Thiara, P. S.; Peterson, E. A.; Jacobsen, E. N. *J. Am. Chem. Soc.* **2007***, 129*, 13404-13405.

14. Myers, E. L.; de Vries, J. G.; Aggarwal, V. K. *Angew. Chem., Int. Ed.* **2007***, 46*, 1893-1896.

15. Yazici, A.; Pyne, S. G. *Synthesis* **2009**, 339-369.

16. Hiemstra, H.; Vijn, R. J.; Speckamp, W. N. *J. Org. Chem.* **1988***, 53*, 3882-3884.

17. Ikariya, T. In *Bifunctional Molecular Catalysis: Bifunctional Transition Metal-Based Molecular Catalysts for Asymmetric Syntheses*; Ikariya, T., Shibasaki, M., Eds.; Springer: Berlin, 2011; Vol. 37; pp 31-53.

18. Ito, M.; Sakaguchi, A.; Kobayashi, C.; Ikariya, T. *J. Am. Chem. Soc.* **2007***, 129*, 290-291.

19. Ito, M.; Kobayashi, C.; Himizu, A.; Ikariya, T. *J. Am. Chem. Soc.* **2010***, 132*, 11414-11415.

20. Wijnberg, J. B. P. A.; Schoemaker, H. E.; Speckamp, W. N. *Tetrahedron* **1978***, 34*, 179-187.

21. Hubert, J. C.; Wijnberg, J. B. P. A.; Speckamp, W. N. *Tetrahedron* **1975***, 31*, 1437-1441.

22. Vijn, R. J.; Hiemstra, H.; Kok, J. J.; Knotter, M.; Speckamp, W. N. *Tetrahedron* **1987***, 43*, 5019-5030.

23. Jung, M. E.; Piizzi, G. *Chem. Rev.* **2005***, 105*, 1735-1766.

24. Levine, M. N.; Raines, R. T. *Chem. Sci.* **2012***, 3*, 2412-2420.

25. Storm, D. R.; Koshland, D. E. *J. Am. Chem. Soc.* **1972***, 94*, 5805-5814.

26. Storm, D. R.; Koshland, D. E. *J. Am. Chem. Soc.* **1972***, 94*, 5815-5825.

27. McAlees, A. J.; McCrindle, R. *J. Chem. Soc. C* **1969**, 2425-2435.

28. Hamilton, R. J.; Leong, C. G.; Bigam, G.; Miskolzie, M.; Bergens, S. H. *J. Am. Chem. Soc.* **2005***, 127*, 4152-4153.

29. Hamilton, R. J.; Bergens, S. H. *J. Am. Chem. Soc.* **2006***, 128*, 13700-13701.

30. Hamilton, R. J.; Bergens, S. H. *J. Am. Chem. Soc.* **2008***, 130*, 11979-11987.

31. Takebayashi, S.; Bergens, S. H. *Organometallics* **2009***, 28*, 2349-2351.

32. Brown, H. C.; Kawakami, J. H. *J. Am. Chem. Soc.* **1970***, 92*, 1990-1995.

33. Chen, F. -E.; Dai, H. -F.; Kuang, Y. -Y.; Jia, H. -Q. *Tetrahedron: Asymmetry* **2003***, 14*, 3667-3672.

34. Arai, Y.; Kontani, T.; Koizumi, T. *J. Chem. Soc., Perkin Trans. 1* **1994**, 15-23.

35. Zhang, W.; Zheng, A.; Liu, Z.; Yang, L.; Liu, Z. *Tetrahedron Lett.* **2005***, 46*, 5691-5694.

36. Armarego, W. L. F.; Chai, C. L. L. *Purification of Laboratory Chemicals;* Elsevier: Oxford, 2013.

37. Sano, H.; Noguchi, T.; Tanatani, A.; Miyachi, H.; Hashimoto, Y. *Chem. Pharm. Bull.* **2004***, 52*, 1021-1022.

38. Liang, J.; Lv, J.; Fan, J. -C.; Shang, Z. -C. *Synth. Comm.* **2009***, 39*, 2822-2828.

39. Fraga-Dubreuil, J.; Comak, G.; Taylor, A. W.; Poliakoff, M. *Green Chem.* **2007***, 9*, 1067-1072.

40. Bilyard, K. G.; Garratt, P. J.; Hunter, R.; Lete, E. *J. Org. Chem.* **1982***, 47*, 4731-4736.

41. Barker, M. D.; Dixon, R. A.; Jones, S.; Marsh, B. J. *Tetrahedron* **2006***, 62*, 11663-11669.

42. Sauers, C. K.; Marikakis, C. A.; Lupton, M. A. *J. Am. Chem. Soc.* **1973***, 95*, 6792-6799.

43. Vargas, J.; Santiago, A. A.; Gavino, S. R.; Cerda, A. M.; Tlenkopatchev, M. A. *eXPRESS Polym. Lett.* **2007***, 1*, 274-282.

44. Hill, T. A.; Stewart, S. G.; Ackland, S. P.; Gilbert, J.; Sauer, B.; Sakoff, J. A.; McCluskey, A. *Bioorg. Med. Chem.* **2007***, 15*, 6126-6134.

45. Bentz, T. C.; Ryzhkov, L. R. *Spectrosc. Lett.* **2006***, 39*, 225-236.

46. Wilk, A.; Grajkowski, A.; Phillips, L. R.; Beaucage, S. L. *J. Org. Chem.* **1999***, 64*, 7515-7522.

47. Wang, X.; Guo, H.; Xie, G.; Zhang, Y. *Synth. Comm.* **2004***, 34*, 3001-3008.

48. Yuan, X. -H.; Zhang, M. -J.; Kang, C. -Q.; Guo, H. -Q.; Qiu, X. -P.; Gao, L. -X. *Synth. Comm.* **2006***, 36*, 435-444.

49. Wang, J.; Johnson, D. M. *Polym. Int.* **2009***, 58*, 1234-1245.

Chapter 3

Mechanistic insight into the desymmetrization of cyclic *meso*-imides: Identification of putative intermediates and a new pathway for carbonyl hydrogenation[1]

Introduction

Chapter 2 herein covered the first desymmetrization of cyclic *meso*-imides via enantioselective monohydrogenation.[1,2] To reiterate, we showed that the monohydrogenation of the cyclic *meso*-imide **138j** by **2** forms the hydroxy lactam *trans*-**139j** with five new stereogenic centers in 96% *ee*, Eq. 3-1. I now describe the results of a mechanistic investigation into this highly efficient desymmetrization reaction that uncovers a previously unobserved, facile base-catalyzed bifunctional addition to imide and amide carbonyls at low temperatures.

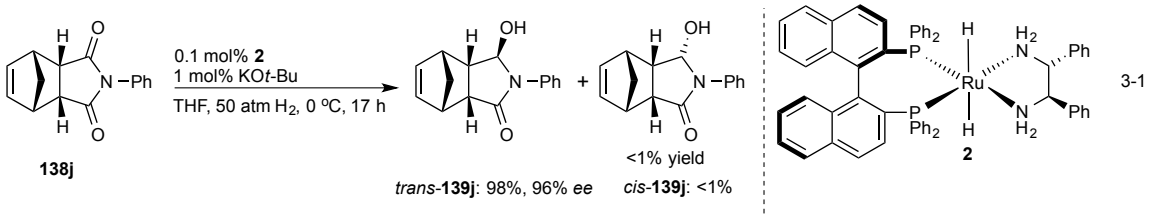

3-1

[1] A version of this chapter has been published. John, J. M.; Takebayashi, S.; Dabral N.; Miskolzie, M.; Bergens, S. H. *J. Am. Chem. Soc.* **2013**, *135*, 8578-8584.

Results and discussion

To investigate the mechanism of this hydrogenation, we prepared **2** in the rigorous absence of water and excess inorganic base by reacting mixtures of *trans*-[RuH(*L*)((*R*)-BINAP)((*R*,*R*)-dpen)]BF_4 (*L* = η^2-H_2 or THF-d_8) with 0.9 equiv. of $KN[Si(CH_3)_3]_2$ or KO*t*-Bu as base under ~2 atm H_2 at –78 °C in THF-d_8.[3] Less than 1 equivalent of base was used to ensure that no residual base was present after the formation of **2** that would otherwise catalyze the rapid *cis*-*trans* isomerization of any addition product formed.[2] These preparations also yielded mixtures of the conjugate acid *i.e.* $HN[Si(CH_3)_3]_2$ or HO*t*-Bu as well as KBF_4 that do not catalyze the isomerization of *cis*-**139j**. In some cases, trace amounts of unwanted side products were observed during the rigorous preparation of **2**, including unreacted or partially hydrogenated [Ru((1–5-*η*)-C_8H_{11})((*R*)-BINAP)]BF_4 or *trans*-[RuH(OH)((*R*)-BINAP)((*R*,*R*)-dpen)], **35**, resulting from the reaction between trace amounts H_2O and inorganic base.

We found that adding a stoichiometric amount of imide **138j** to a rigorously prepared sample of **2** formed small amounts of what appeared to be catalyst decomposition products after ~3.3 h at –60 °C (Scheme 3-1, top). Further warming resulted in more decomposition. This result was unexpected as the addition of ketones and lactones to **2** proceeds on mixing and within minutes at –80 °C.[4,5] However, the addition between **2** and **138j** *does occur* in the presence of catalytic amounts of KOH *i.e.* 0.2 equivalents relative to Ru and imide substrate, at –80 °C to give the *trans*-Ru-alkoxide, **145**, as the sole detectable product in 78% yield after 3 h (Scheme 3-1, bottom). This suggests that base promotes the activity of **2** towards carbonyl reduction.

[2] The isomerization of *cis*-**139j** into *trans*-**139j** was found to be complete upon mixing a solution of *cis*-**139j** to stoichiometric amounts of $HN[Si(CH_3)_3]_2$ and KOH (prepared by hydrolyzing $KN[Si(CH_3)_3]_2$ with H_2O) at –78 °C in THF-d_8.

Scheme 3-1 *Stoichiometric reaction between* ***2*** *and* ***138j****.*

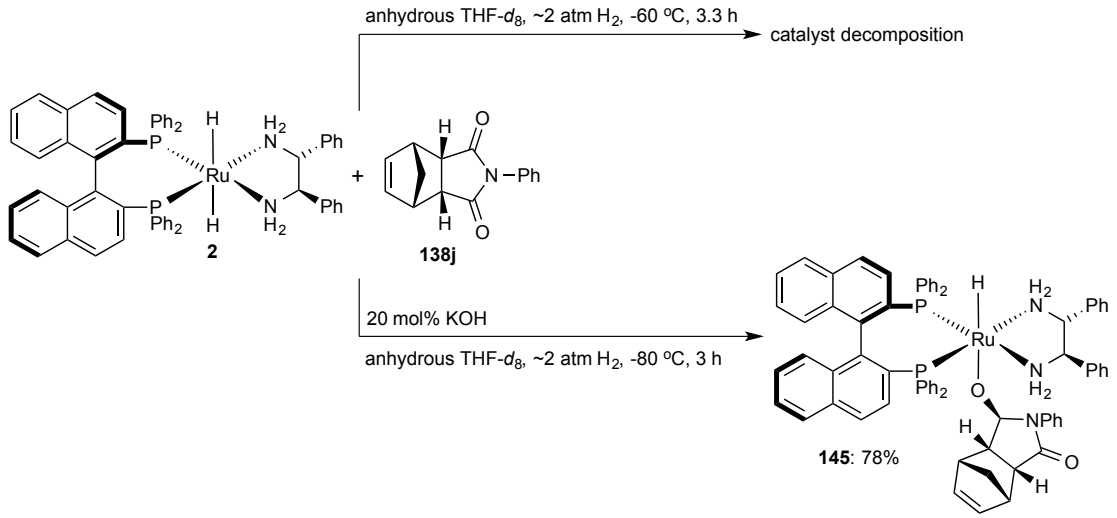

Compound **145** was characterized using a suite of NMR techniques including ^{1}H, $^{31}P\{^{1}H\}$, $^{1}H–^{13}C$ gHSQC and $^{1}H–^{1}H$ gCOSY NMR experiments, and subsequently confirmed by the addition of *trans*-**139j** to the Ru-amide, **29**, at –80 °C. The ^{1}H and ^{13}C signals from the coordinated alkoxide O–CH group in **145** were located at δ 6.13 and 96.24 ppm, respectively. These signals are shifted to higher frequency by 1.11 and 9.66 ppm, respectively, from the corresponding signals of the free hydroxy lactam. Such shifts are common with the formation of Ru–O bonds, and are most likely due to electron donation from the oxygen atom to the Ru centre.[6,7]

To rule out the possibility of substrate activation by base we reacted the imide with one equivalent of KOH, but observed no net reaction. Moreover, reacting the imide with $KN[Si(CH_3)_3]_2$ or KO*t*-Bu lead to mixtures of unidentifiable products that did not react with a stoichiometric amount of **2** at –80 °C. Similarly, no appreciable reaction was observed at –80 °C between **2** and either KOH or $KN[Si(CH_3)_3]_2$ in the presence of the conjugate acid, $HN[Si(CH_3)_3]_2$. Nevertheless, these observations do not exclude a reversible reaction between **2** and base that lies to the side of the dihydride. To explore

this possibility, we reacted a 1:1:1 mixture of **2**, HO*t*-Bu, and KBF_4 with a variant of Schlosser's base[8] (2.5 equiv. *n*-BuLi and 1 equiv. KO*t*-Bu) to form a previously unobserved intermediate, the *trans*-Ru-dihydride amidate, **38**, in 84% yield at –60 °C resulting from the deprotonation of one of the protic N–H groups in the dpen moiety, Eq. 3-2.

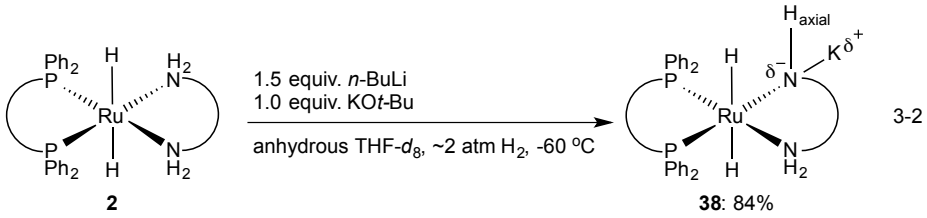

3-2

Compound **38** was not isolatable but was fully characterized at –80 °C in anhydrous THF using ^{1}H, $^{31}P\{^{1}H\}$, $^{1}H–^{1}H$ gCOSY, $^{1}H–^{13}C$ gHSQC, $^{1}H–^{15}N$ gHSQC, TOSCY, and TROESY NMR experiments. The signals for all three N−H's in **38** were identified in the ^{1}H NMR spectrum, with the $N–H_{amidate}$ at δ 0.22 ppm, the $N–H_{axial}$ at δ 2.8 ppm, and the $N–H_{equatorial}$ at δ 2.9 ppm. The single most striking observation is that the amidate ligand of **38** can be best described as singly bonded to a coordinatively saturated ruthenium center, with the lone pair on nitrogen in an equatorial disposition coordinated to a metal cation, likely potassium.

Hartman and Chen were the only other investigators to suggest that a similar species is formed during carbonyl reductions (no isolated intermediates).[9,10] On the basis of kinetic studies into the hydrogenation of ketones they suggested that **2** harbored a pre-organized cation-specific binding site that allows for the facile deprotonation of an axial N–H group to form $\mathbf{38}_{axial}$. This is rather contradictory from the equatorial disposition we observe in **38**. Somewhat analogous to the original mechanism for the bifunctional addition, they later proposed that the addition of a ketone to $\mathbf{38}_{axial}$ forms a product

alkoxide that is ionically bonded to K^+, which is also bound to the nitrogen of the complementary Ru-amide. This species could then react with H_2 to regenerate **38**$_{axial}$ and the product alcohol faster than **29** would react with H_2 to form **2** in the absence of a Lewis acid co-catalyst. However, subsequent mechanistic studies by Noyori and Morris were unable to confirm this pathway.[11,12]

Although detectable amounts of **38** were not observed in the ^1H or $^{31}P\{^1H\}$ NMR of a mixture of **2** with $KN[Si(CH_3)_3]_2$ and $HN[Si(CH_3)_3]_2$ (1:1.5:1 equiv., respectively), we reasoned that the lithium analogue, $LiN[Si(CH_3)_3]_2$ would deprotonate **2** to a greater extent, as the conjugate base, if formed, would be stabilized by the coordination of lithium to the free lone pair in the amidate. Indeed, reacting a 1:1:1 mixture of **2**, $HN[Si(CH_3)_3]_2$ and $LiBF_4$ with 2 equiv. of $LiN[Si(CH_3)_3]_2$ forms the Li-adduct (**39**) in 90% yield at –20 °C, Eq. 3-3.

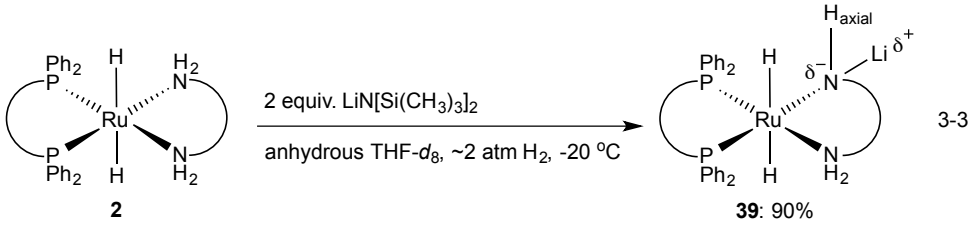

3-3

This compound was also not isolatable but was fully characterized at –20 °C using the same NMR experiments used to characterize **38**. The signals for all three N−H's were identified in the ^1H NMR spectrum of **39**, with the N−H$_{amidate}$ at δ –0.2 ppm, the N−H$_{axial}$ at δ 2.5 ppm, and the N−H$_{equatorial}$ at δ 2.6 ppm.

Figure 3-1 compares the most significant regions of the ^1H and $^{31}P\{^1H\}$ NMR spectra for the parent dihydride **2** and the mono-deprotonated dihydrides **38** and **39**. There is a pair of doublets representing the inequivalent phosphorous centers in the $^{31}P\{^1H\}$ NMR of **38** and **39**. Each species has one resonance with a chemical shift similar

to that of **2** and another shifted to lower frequency by 7.0−9.0 ppm. On the other hand, one of the hydride signals in **38** overlaps with the equivalent Ru hydride signal of **2**, while the other is shifted to lower frequency by 1.1 ppm to δ −6.1 ppm. TROESY experiments show a negative ROE correlation between the Ru hydride signal at δ −6.1 ppm and the N–$H_{amidate}$ signal at δ 0.2 ppm. This implies that the Ru−hydride is in close proximity to the N−$H_{amidate}$, and that the amidate N−H in **38** is axially oriented. Additionally, Hamilton and Bergens previously reported that KO*t*-Bu forms a hydrogen bond with the equatorial N−H of the Ru-alkoxide, *trans*-[RuH(2-PrO)((*R*)-BINAP)((*R*,*R*)-dpen)], **33**.[3] Therefore, these observations combined support the idea that the equatorial N−H's in coordinated dpen are either more accessible and/ or more acidic than the axial N−H's.

Figure 3-1 *Comparison of the δ 0.5 to –7 ppm ^{1}H (left) and δ 90 to –75 ppm $^{31}P\{^{1}H\}$ (right) NMR spectra for the trans-Ru-dihydrides **2** (bottom), **38** (middle) and **39** (top)*

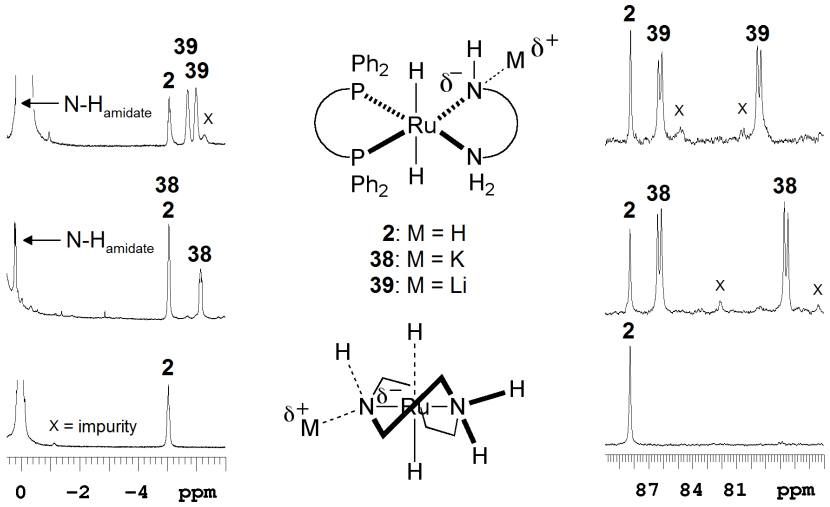

The hydride signals in **39** are slightly shifted from those of **38**. The hydride adjacent to the N−$H_{amidate}$ group in **39** exhibited a comparable chemical shift to that found in **38**. However, the Ru hydride next to the NH_2 group in **39** is at δ −5.5 ppm, ~0.5 ppm

lower than that of the neutral dihydride resonance. Unlike **38**, however, no ROE correlations could be observed between the N−$H_{amidate}$ and the adjacent hydride in **39**. Thus, the orientation of N−$H_{amidate}$ in **39** could not be unambiguously assigned. However, similarities between the ^{1}H and $^{31}P\{^{1}H\}$ NMR of **38** and **39**, coupled with the smaller size of Li^{+} compared to that of K^{+}, lead us to believe that the N−$H_{amidate}$ in **39** is axial.

Remarkably, we found that adding 2 equiv. of *n*-BuLi to a mixture of **38** at –60 °C resulted in a second deprotonation of the dpen moiety to form the *trans*-Ru-dihydride diamidate, **40**, in quantitative yield, Eq 3-4.

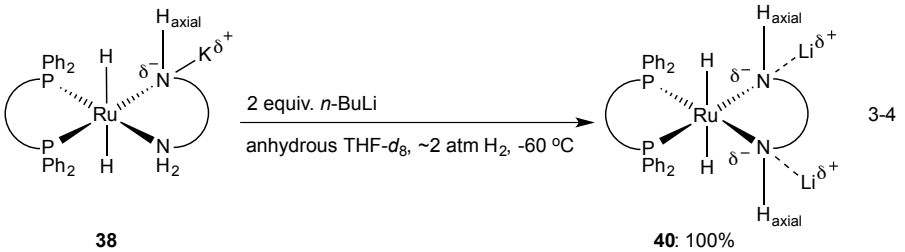

38 **40**: 100% 3-4

This compound was also not isolated but, fully characterized at −50 °C in the same manner as **38** and **39**. The C_2-dissymmetric nature of **40** resulted in equivalent hydride, N–$H_{amidate}$ and C*H*(Ph) signals, located respectively at δ −6.6, δ −0.15, and δ 2.9 ppm in the ^{1}H NMR, whereas, the $^{31}P\{^{1}H\}$ NMR of **40** consisted of a singlet at δ 76.8 ppm. TROESY NMR experiments showed significant correlations between the Ru-hydrides and amidate N−H's, and C*H*(Ph) signals. Providing evidence that the amidate N−H's in **40** are axially oriented with respect to the Ru hydride, while the coordinating cations occupy equatorial positions, Figure 3-2.

Figure 3-2 *Comparison of the δ 0.5 to –7 ppm ^{1}H (left) and δ 90 to –75 ppm $^{31}P\{^{1}H\}$ (right) NMR spectra for the trans-Ru-dihydrides* ***2*** *(bottom) and* ***40*** *(top)*

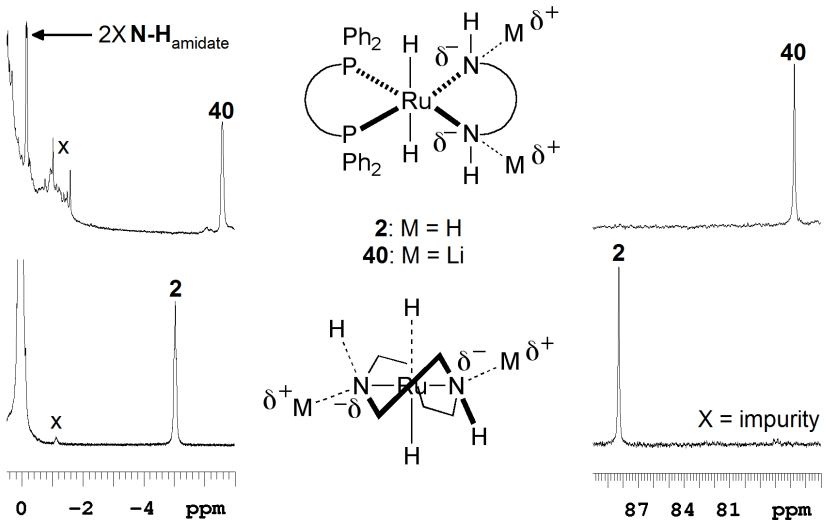

The identity of the cation in **40** could not be unambiguously assigned. We proposed that the coordinating metal is Li^{+} due to its higher stoichiometric ratio, and its stronger Lewis acidity. In an attempt to identify the cation in **40** we utilized $^{1}H–^{15}N$ HSQC NMR experiments to gather information on each nitrogen environment in these compounds. We found that the $^{15}NH_2$ and $^{15}N–H$ chemical shifts for **38** were δ 11.8 and δ 34.6 ppm at −40 °C, respectively, while those for **39** were δ 11.2 and δ 22.2 ppm at −20 °C. The ^{15}N signal for **40** was δ 22.8 ppm at −50 °C. The similarity between the $^{15}N–H$ chemical shifts in **39** and **40** led us to assign the cations in **40** as Li^{+}.

Unlike the slow decomposition reaction that was observed between **138j** and the parent dihydride **2**, the addition of **138j** to **38** was complete on mixing at −80 °C. The products of this addition were neither the Ru-alkoxide **145** nor the Ru-amide, [RuH((*R*,*R*)-HN(CH(Ph))$_2$NH$_2$)((*R*)-BINAP)], **29**, and product alcohol.[4-6,12] Unexpectedly, the products of the addition were the Ru-amide, **29** and the potassium salt of *cis*-**139j**,

146, Eq. 3-5. This is a previously unobserved active pathway for the bifunctional addition.

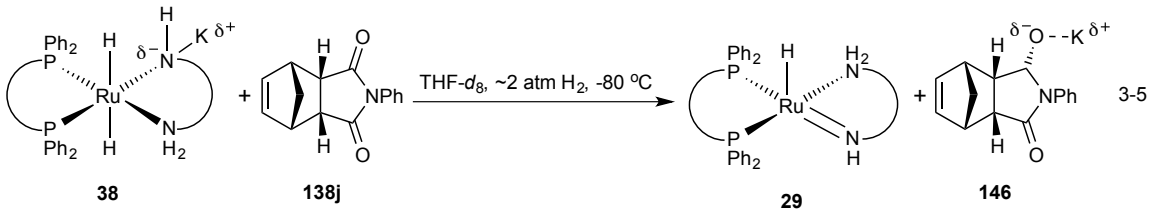

3-5

Our group previously reported that the addition of ketones and lactones to **2** generates the corresponding Ru-alkoxides, as does the KOH-catalyzed addition of **138j** to **2**, albeit, at much slower rates at −80 °C (*vide supra*). We also showed that the Ru-2-propoxide, **33**, and related compounds are inactive towards ketone hydrogenation in the absence of base under similar conditions.[3] However, these compounds do undergo a base-assisted elimination reaction where an N–H group in the dpen ligand is deprotonated to generate the Ru-amide, **29** and free 2-propoxide, Eq. 3-6.

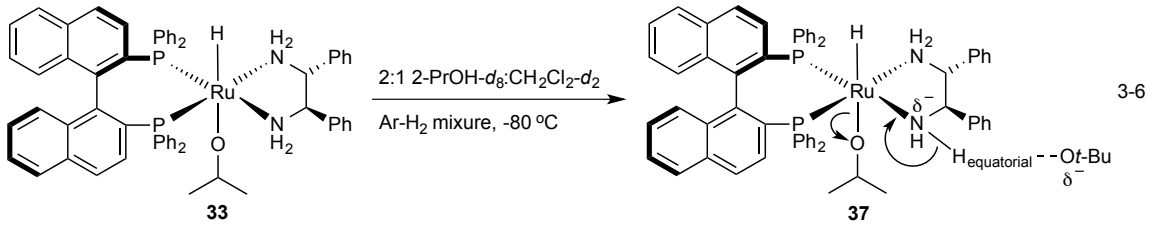

3-6

Cumulatively, the evidence from these studies suggests two important points. The first is that **38** is dramatically more active than the parent dihydride, **2**. This is attributed to the presence of the amidate group, which increases electron density at the Ru center making the hydride more nucleophilic towards imide carbonyls. Secondly, if the product of the addition between **38** and **138j** is analogous to Ru-alkoxides observed

for the additions of ketones and esters to **2**, such a species would be predisposed to undergo a "built-in base assisted elimination" to form the potassium salt of *cis*-**139j**, that is **146**, and **29**. Similarly, if the addition proceeds by rapid hydride transfer to form the corresponding alkoxide ion-pair, **147**,[13,14] this species can presumably also eliminate **146** to form **29**. Alternatively, the alkoxide in **147** can also deprotonate the N−H group to form the alcohol and the potassium analogue of the Ru-amide, **29-K**, that could then transfer a proton to give the observed product mixture, Scheme 3-2.

Scheme 3-2 *Possible pathways for the formation of* ***29*** *and* ***146*** *from* ***38****.*

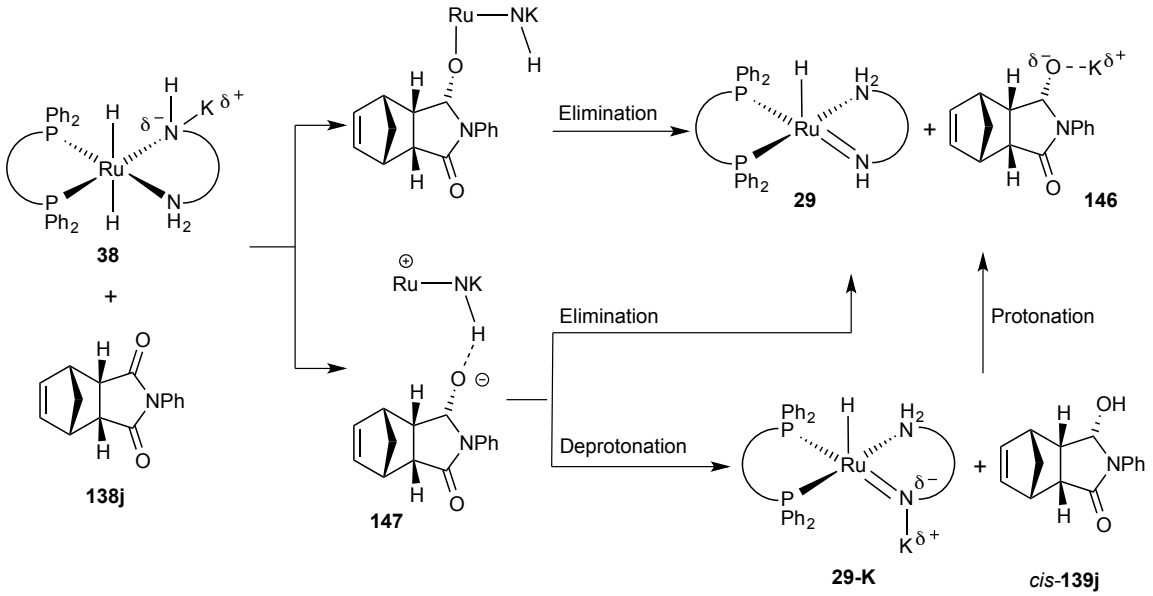

These additions could also proceed in a manner related to the bifunctional addition of ketones as described by Hartmann and Chen[9,10] via the rearrangement of **38** to $\mathbf{38}_{axial}$ or by a traditional mechanism that utilizes the unreacted NH_2 group in the deprontonated dpen moiety. In either case, a similar sequence of steps to those shown in Scheme 3-2 would give the observed products.

The addition of **138j** to **39** is noticeably slower than that of the analogous reaction involving **38**, but sill gives **29** and the lithium salt of *cis*-**139j**, that is **148**, as products in ~8% yield after 15 min at −60 °C. The presence of excess $LiN[Si(CH_3)_3]_2$ (2 equiv. relative to **2**) resulted in some substrate decomposition. However, this did not appear to affect the rate of this reaction. The difference in rate is likely due to the ability of Li^+ to form stronger nitrogen containing adducts than that of K^+. This effect essentially reduces the amount of electron density that can be donated to the Ru center by the amidate group in **39** thereby making the hydride ligand less nucleophilic towards the imide carbonyl.

Encouraged by this impressive reactivity in THF-d_8, we questioned if the mono-deprotonated analogues of **2** would stoichiometrically add amides at low temperatures. Amides are the least reactive of the carboxylic acid derivatives, and as such are one of the major remaining challenges in catalytic hydrogenation.[15] Remarkably, we found that the addition of *N*,*N*-diphenyl-2-phenoxypropionamide, **149**, to a solution of **38** reacts to form a mixture of organic potassium salts, **150**, and the neutral dihydride **2** via the addition of excess H_2 across the Ru-amide, **29**, starting at −80 °C, Eq. 3-7. Hydrolysis of these salts with excess 2-PrOH-d_8 under H_2 (~2 atm) forms the product alcohol and amine from the complete reduction of the *α*-chiral amide via C−N cleavage. It is noteworthy that no deuterium incorporation was observed at the *α*-position of the product alcohol, indicating that **38** did not simply deprotonate **149** to regenerate **2** under these conditions. Consistent with our previous observations, **39** was somewhat less reactive toward **149** than **38**, undergoing the addition starting at −60 °C.

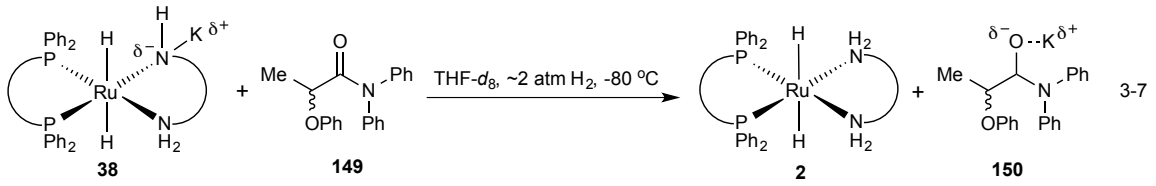

At the beginning of this discussion, I reiterated that the catalytic monohydrogenation of the cyclic *meso*-imide **138j** proceeds with 98% conversion and 96% *ee* using 0.1 mol% Ru and 1 mol% KO*t*-Bu at 0 °C and 50 atm H_2 in 17 h.[1,2] However, we found that KO*t*-Bu catalyzes the addition of **138j** to **2** at −80 °C, albeit with a slow substrate decomposition analogous to that shown between **138j** and K- or Li-N[Si(CH_3)$_3$]$_2$ (*vide supra*). We therefore believe that during the catalytic hydrogenation, a portion of the base is consumed by **138j** while some is converted into KOH by the action of residual water in the system. To confirm this scenario, we carried out a control experiment, which showed that the *ee* and absolute configuration of *trans*-**139j** formed by the stoichiometric addition of **138j** to **2** in the presence of trace water, was the same as that for the catalytic hydrogenation.

This KOH-catalyzed addition of **138j** to **2** presumably proceeds by small amounts of **38** present in solutions of **2** and KOH. This addition forms the Ru-amide, **29**, and the potassium salt of the *cis*-hydroxy lactam, **146**. Compound **146** would then react with water (conjugate acid of OH^-) to form *trans*-**139j** and regenerate KOH. To complete this pathway, we carried out a control experiment which showed that the *trans*-**139j** adds to the Ru-amide, **29**, to form the *trans*-Ru-alkoxide, **145**, on mixing at −80 °C, Scheme 3-3. The absolute configuration of the major enantiomer of *trans*-**139j** was determined using X-ray crystallography. Transforming *trans*-**139j** into the bromocarbamate, **151**, using *para*-bromophenyl isocyanate revealed that the addition occurred via the convex face of

the *S*-side enantiotopic carbonyl.[16] Thus, all the stereogenic centers on the norbornene backbone of **138j** adopt an *S*-configuration upon reduction as shown in Figure 3-3.[17]

Scheme 3-3 *Mechanism for the formation of* ***145*** *from* ***2*** *catalyzed by KOH.*

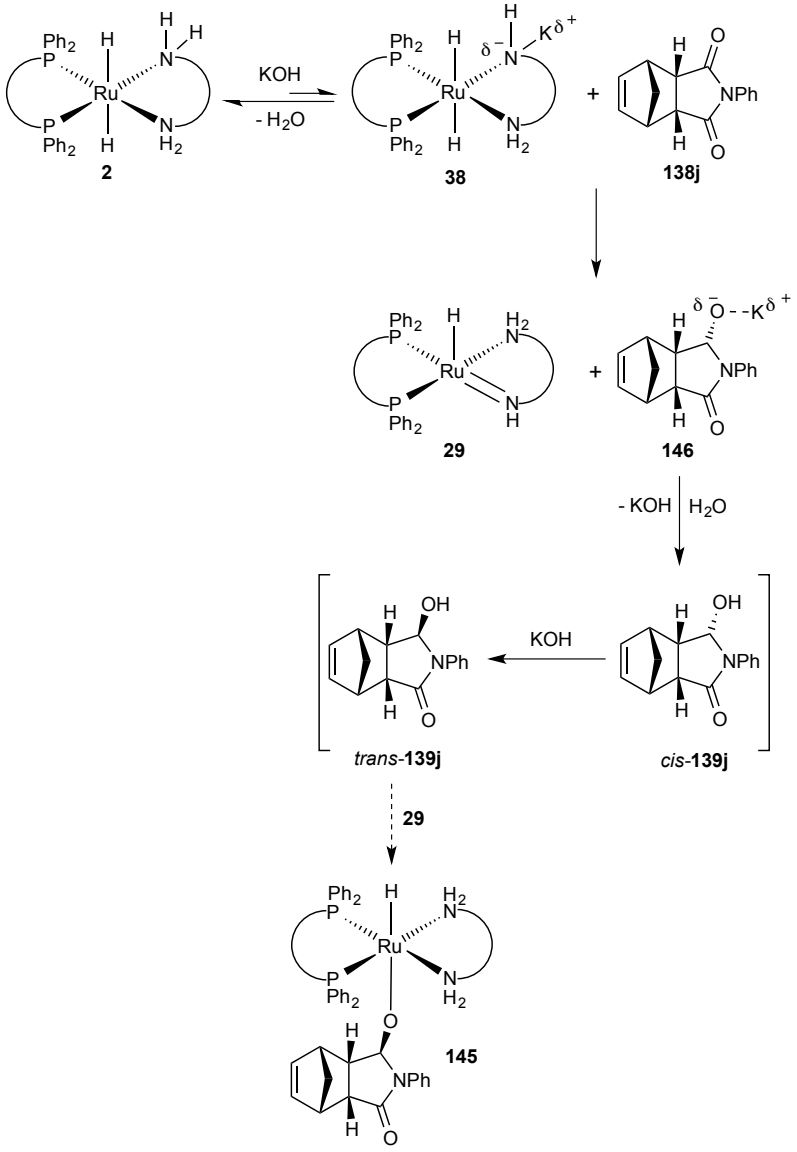

Figure 3-3 *Preparation and ORTEP drawing of* ***151*** *with 20% probability ellipsoids without hydrogen atoms.*

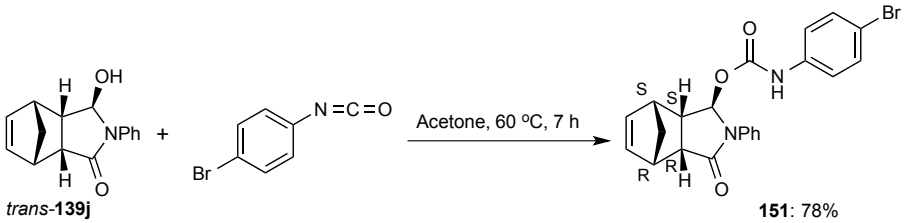

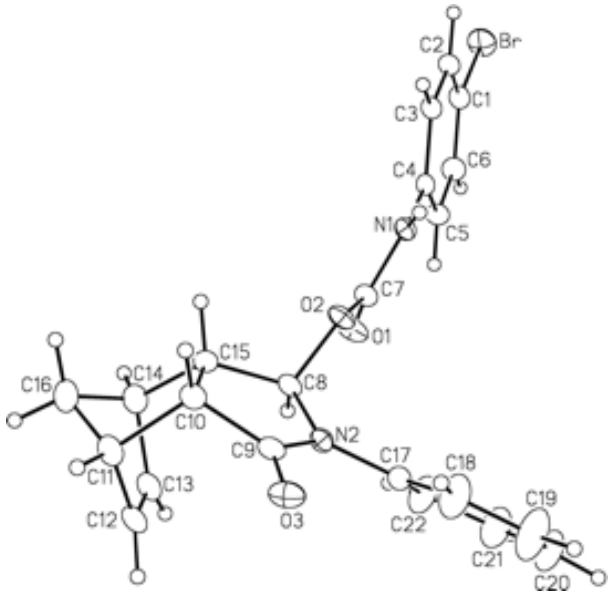

The unique structural and conformational rigidity of **2** and **138j**,[12,18,19] along with the requirement for addition to the convex face of the enantiotopic *S*-side carbonyl,[20-28] combined with published models for the enantioselection of aryl ketones to **2** make the origins of the enantioselection for the monohydrogenation of cyclic *meso*-imides readily apparent.

Several research groups including ours have provided mechanistic insight into the origins of the enantioselection for Noyori-type ketone hydrogenations either by experimental[12,29] and/or computational methods.[30-33] Together, these studies have identified three features that contribute to the enantioselective process in the bifunctional addition of aryl ketones to *trans*-RuH_2(diphosphine)(diamine) complexes. The first is that

there is a strong dipole interaction between the Ru-dihydride and ketone that results in a favored substrate approach, and an eventual hydrogen bonding interaction between the oxygen atom of the ketone carbonyl and an N–H_{axial} group of the catalyst. Secondly, the ketone is oriented in such a way to minimize the steric interactions between the conformationally rigid catalyst and substrate molecule, and lastly the formation of favourable N–$H_{equatorial}$–π attraction electrostatic interactions between the N–$H_{equatorial}$ group and the phenyl ring of the ketone.[34,35] This implies that any new reaction pathway like that described herein with the *trans*-mono-deprotonated dihydride, must proceed through bonding interactions that involve the imide carbonyl, Ru–H and the axially orientated N–$H_{amidate}$ group.

In theory, there are four possible orientations that the imide can adopt within the transition state. These are the two enantiomers of *cis*-**139j** [(*R*)- or (*S*)- *cis*-**139j**] and the two enantiomers of *trans*-**139j** [(*R*)- or (*S*)- *trans*-**139j**]. However, all reported examples of imide monoreduction using sterically less crowded M–H reagents *e.g.* BINAL-H, show that the addition to the least hindered, convex face of the carbonyl group is kinetically favored.[20-28]

Figure 3-4 illustrates the stereoelectronic consequences for the addition of **38** to convex faces of the *S*-side (**TS_A**) and *R*-side (**TS_B**) carbonyl of the imide **138j**. Inspection of molecular models shows that the N-phenyl group of the imide projects deeply into the spatial domain of the BINAP ligand, resulting in an unfavorably strong steric repulsion in **TS_B**. The *endo*-geometry of **138j**, in combination with the addition to the convex face of the *S*-side carbonyl, results in no appreciable steric crowding in **TS_A**. Additionally, the geometry of **TS_A** allows for a stabilizing N–$H_{equatorial}$–π attraction electrostatic interaction, by the lone equatorial N–H group in the deprotonated dpen moiety. Similarly, addition to the Ru–H located on the opposite side of **TS_A** in **38** is also possible, this transition state would replace the N−$H_{equatorial}$−π interaction by an N−K^+−π electrostatic interaction.[34,35]

In this scenario, the same steric forces result in the same major enantiomer. Thereby, explaining the high preference for the addition to the *S*-side of **138j**.

Figure 3-4 *Possible geometries for the addition between **38** and **138j**.*

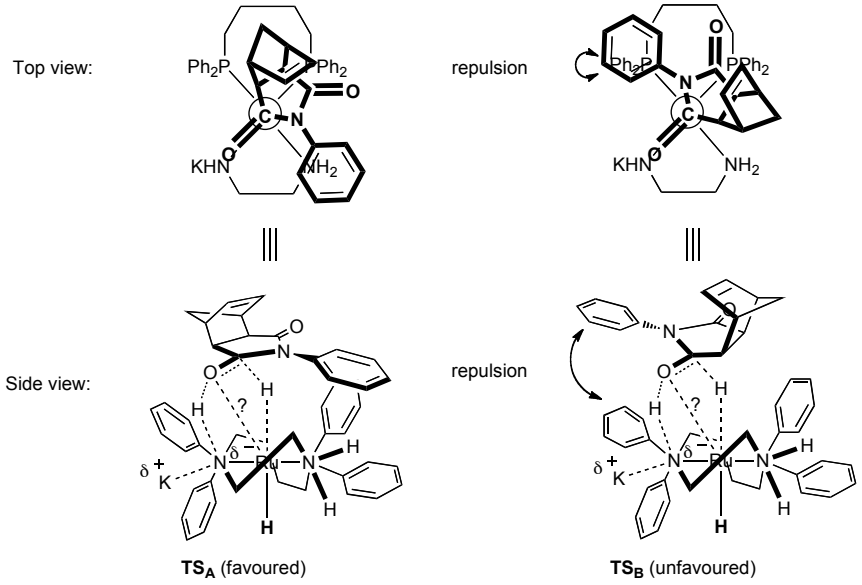

One important feature of this desymmetrization is the preservation of *ee* due to the inherent irreversibility of the addition step between **29** and the precipitated potassium salt of *cis*-hydroxy lactam, **146**, at low temperatures in THF-d_8. Although, a control experiment between **29** and the *cis*-**139j** revealed that the addition is essentially reversible forming mixtures of **2**, and the cyclic *meso*-imide **138j**, upon mixing at −80 °C, Scheme 3-4, top. The rapid base-catalyzed *cis*- to *trans*-isomerization at −80 °C prevents hydride abstraction instead forming the *trans*-Ru-alkoxide, **145**, on mixing, Scheme 3-4, bottom.

Scheme 3-4 *Reaction between* ***29*** *and cis- and trans-****139j*** *at –80 °C in THF-d_8.*

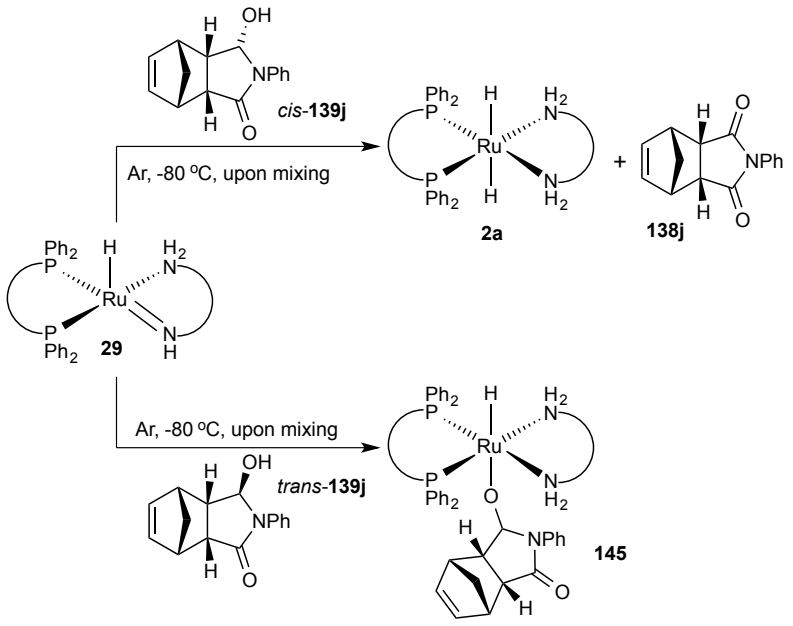

Inspection of the molecular models (Figure 3-5) show that the C–H group of *trans*-**139j**, (**TS_C**), is positioned on the inaccessible convex face of the hydroxy lactam. As a result the abstraction of hydride from *cis*-**139j**, (**TS_D**), is much easier than that in (**TS_C**). Thus, the formation of *trans*-**139j** preserves the high *ee* of the enantioselective step.

Figure 3-5 *Hydrogen abstraction from and cis- and trans-****139j****.*

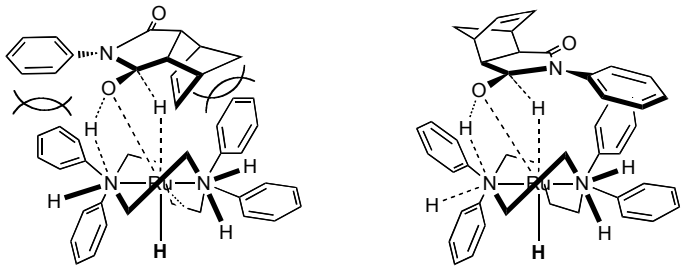

TS_C (unfavored) **TS_D** (favoured)

Conclusion

These studies revealed the first intermediates in the hydrogenation of imides and amides. It also described, a previously unobserved, facile, base catalyzed pathway for the bifunctional addition mechanism to unreactive carbonyls. Specifically, unexpected deprotonation of the parent neutral dihydride, **2**, gave rise to electron-rich intermediates that have unprecedented reducing power towards imide and amide carbonyls at low temperatures in THF-d_8. Remarkably, these deprotonated dihydrides were found to reduce imide and amide carbonyls at –80 °C and starting at –60 °C, respectively. We propose that these species are the reason for the unexplained high reactivity of Noyori-type catalysts in high base to catalyst ratios, and that these results would lead to more powerful catalysts from most bifunctional systems containing a coordinated N–H group, or with an acidic group that is in conjugation with an unsaturated nitrogen ligand (*i.e.* Milstein type complexes). Further, the origins for the high enantioselectivity observed in this desymmetrization-hydrogenation were explained using simple and well-defined models based on current literature as well as the results of these investigations. A combination of kinetic, isotope labeling, trapping and computational studies should provide greater insight into the mechanism of these additions.

Materials and methods

All reactions were carried out in silanized NMR tubes unless stated otherwise. Deuterated solvents were obtained from Cambridge Isotope Laboratories and Aldrich. Common organic solvents were distilled over appropriate drying agents. THF-d_8 was freshly distilled over Na/benzophenone and used immediately for each experiment unless stated otherwise.[36] Common laboratory chemicals were obtained from Aldrich, TCI America, Alfa Aesar and Strem and were used as received unless stated otherwise. The imide, **138j**, and the *trans*-**139j** were prepared using previously reported procedures.[1,37,38] [Ru((1–5-*η*)-C_8H_{11}))((*R*)-BINAP)]BF_4 and *N*,*N*-diphenyl-2-phenoxypropionamide, **149**, were dried under vacuum at 60 °C overnight before use. The imide, **138j**, was sublimed at 150 °C prior to use. Hydrogen gas was ultra-high purity grade purchased from Praxair. ^1H, $^{13}C\{^1H\}$, and $^{31}P\{^1H\}$ NMR spectra were taken using Varian Inova (400 MHz) and Varian DirectDrive (500 MHz) spectrometers. ^1H, and $^{13}C\{^1H\}$ NMR chemical shifts are reported in parts per million (δ) relative to TMS with the solvent as the internal reference. $^{31}P\{^1H\}$ NMR chemical shifts are reported in parts per million (δ) relative to 85% H_3PO_4 as the external reference. NMR peak assignments were made using ^1H–^{13}C gHSQC, ^1H–^{13}C gHMBC, ^1H–^1H gCOSY, TOCSY and TROESY NMR experiments. Abbreviations for NMR spectra are s (singlet), d (doublet), t (triplet), q (quartet), dd (doublet of doublet), ddd (doublet of doublet of doublet), m (multiplet), and br (broad). IR spectra were taken using Nic-Plan FTIR microscope, and are reported in wavenumbers (cm^{-1}). High-resolution mass spectra were taken using Applied BioSystems Mariner BioSpectrometry Workstation oaTOF mass spectrometer. Elemental analysis data were obtained using Carlo Erba CHNS-O EA1108 elemental analyzer. Optical rotations ($[\alpha]_D^{23}$) were measured using Perkin Elmer 241 polarimeter. Melting points (mp) were measured using Perkin Elmer Pyris 1 differential scanning

calorimeter. HPLC analysis were performed using a Waters 600E multi-solvent delivery system equipped with Waters 715 Ultra WISP sample processor, Waters temperature control system, Waters 990 photodiode array detector, Waters 410 differential refractometer, Waters 5200 printer plotter, and Daicel CHIRALPAK IB (4.6 mm i.d. × 250 mm) chiral column. All enantiomeric excesses (*ee's*) were confirmed by comparing the HPLC chromatogram of the hydrogenation product to that of the racemic product prepared by $NaBH_4$ or DIBAL-H reduction, followed by acidic work-up at room temperature.[26,28] HPLC grade hexanes (Min. 99.5%) and 2-PrOH (Min. 99.7%) were obtained from Caledon Laboratories Ltd.

Preparation of *N*,*N*-diphenyl-2-phenoxypropionamide, 149

Under N_2, 2-phenoxypropionic acid (5 g, 0.03 mol) and 30 mL of anhydrous CH_2Cl_2 were placed in a 100 mL schlenk flask equipped with a magnetic stirring bar. $SOCl_2$ (4.4 mL, 60 mmol) was then slowly added to the stirred solution at room temperature. The reaction mixture was then refluxed for 3 h. After refluxing for 3 h the mixture was allowed to cool to room temperature and the solvent removed *in vacuo*. The crude acid chloride (pale yellow solid) was then dissolved in 20 mL of fresh anhydrous CH_2Cl_2. The resulting solution was then slowly cannulated into a chilled, 0 °C, 100 mL schlenk flask containing a mixture of diphenylamine (4.2 g, 25 mmol), pyridine (4.0 mL, 50 mmol), 30 mL of anhydrous CH_2Cl_2 as well as a stirring bar. The reaction mixture was stirred and gradually allowed to warm to room temperature overnight. The reaction mixture was then transferred to a separatory funnel where the acidic mixture was neutralized using saturated $NaHCO_3$ solution (3 x 30 mL), washed with brine (20 mL) and dried using anhydrous $MgSO_4$. The $MgSO_4$ was then removed by gravity filtration before concentrating the organic layer on a rotary evaporator to yield the crude amide. The crude amide was purified by trituration in hexanes followed by recrystallization from

hot EtOH. The recrystallized solid was then dried under vacuum overnight. Isolated yield = 83%.

^{1}H NMR (399.953 MHz, DMSO-d_6, 100 °C): δ 1.40 (3H, d, J = 6.4 Hz, CH_3), 2.50 (1H, s, O*H*), 4.80 (1H, q, J = 6.4 Hz, C*H*), 6.70 (2H, d, J = 8.0 Hz, 2 aromatic C*H*), 6.90 (1H, t, J = 7.2 Hz, aromatic C*H*), 7.20–7.40 (12 H, m, 12 aromatic C*H*). ^{13}C{^{1}H} NMR (100.579 MHz, DMSO-d_6, 100 °C): δ 18.3 (*C*H$_3$), 72.2 (*C*H), 116.3 (aromatic *C*H), 121.8 (aromatic *C*H), 127.7 (aromatic *C*H), 128.0 (aromatic *C*H), 129.8 (aromatic *C*H), 128.9 (aromatic *C*H), 142.7 (aromatic *C*H), 157.6 (aromatic *C*H), 170.5 (*C*=O). HRMS (ESI^{+}) m/z calculated for $C_{21}H_{19}NnaO_2$ $(M+Na)^{+}$: 340.1308. Found: 340.1302. Difference (ppm): 1.75 ppm. Elemental analysis calculated for $C_{21}H_{19}NO_2$: C 79.47, H 6.03, N 4.41. Found: C 79.65, H 6.04, N 4.62. HPLC analysis conditions: Daicel CHIRALPAK IB (4.6 mm i.d. × 250 mm) *n*-hexanes:2-PrOH = 99:1, 30 °C. flow rate = 0.8 mL min^{-1}, detection (UV, 210 nm). Retention times: 22.0 min (first isomer), 43.9 min (second isomer).

Reaction between 2 and 138j in the rigorous absence of water and inorganic base

A solution of the dihydride (15 μmol) was prepared in THF-d_8 (0.6 mL) using 0.90 equiv. KN[Si(CH$_3$)$_3$]$_2$ (2.7 mg, 14 μmol) at –78 °C under H_2 as described previously.[3] A THF-d_8 solution of **138j** (3.6 mg, 15 μmol in 0.1 mL) was cannula under H_2 pressure to the NMR tube containing **2** at –78°C. The mixture was then introduced into the pre-cooled NMR probe at –80 °C. The first ^{1}H and ^{31}P{^{1}H} NMR spectra taken ~5 min after the substrate addition showed no detectable conversion to **145** even though substrate was present. Subsequent spectra obtained at –80 °C was consistent with this result (Figure 3-6). Warming the sample to –70 °C, then –60 °C over 4 h resulted in partial decomposition of **2**.

Figure 3-6 *The δ 10 to –10 ppm ^{1}H NMR spectrum of* ***2*** *with* ***138j*** *after 30 min at –80 °C.*

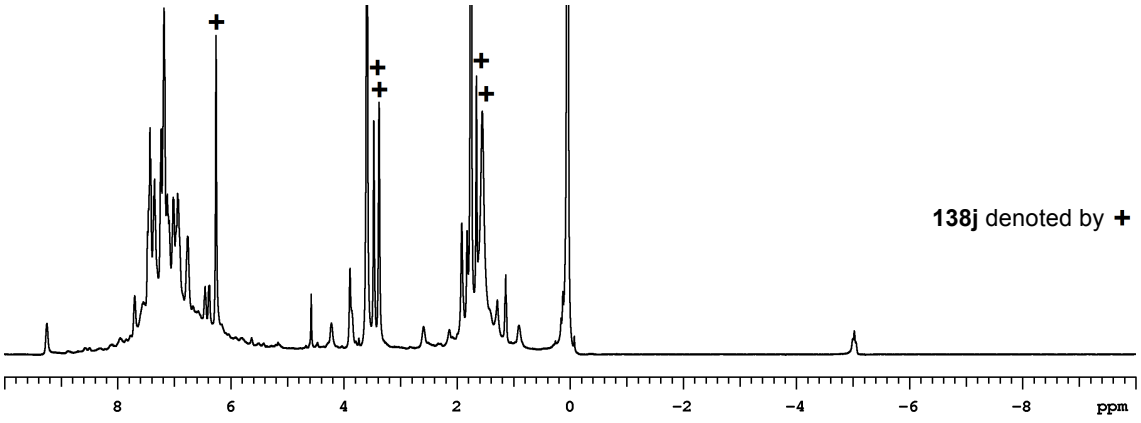

Preparation of *2* without the rigorous exclusion of water and its reaction with 138j

The dihydride**, 2** (15 *μ*mol) was prepared in THF-d_8 (0.6 mL) using 1.5 equiv. $KN(Si(CH_3)_3)_2$ (4.6 mg, 23 *μ*mol) at –78°C under H_2 as described previously, and frozen in a liquid N_2 bath.[3] A solution of **138j** in THF-d_8 (3.6 mg, 15 *μ*mol in 0.2 mL) was added to **2** at –78°C by cannula under Ar pressure. The frozen solution was partially thawed, shook and introduced into a pre-cooled NMR probe at –80 °C. The first ^{1}H NMR spectrum showed that ~46% of **138j** had reacted to form **145** as the sole detectable product. **138j** was consumed to give **145** after 1 h. Compound **145** was characterized at –80 °C using ^{1}H, ^{31}P{^{1}H}, ^{1}H–^{1}H gCOSY and ^{1}H–^{13}C gHSQC NMR experiments.

Figure 3-7 *The δ 11 to –1 ppm ^{1}H NMR spectrum of* ***145*** *at –80 °C.*

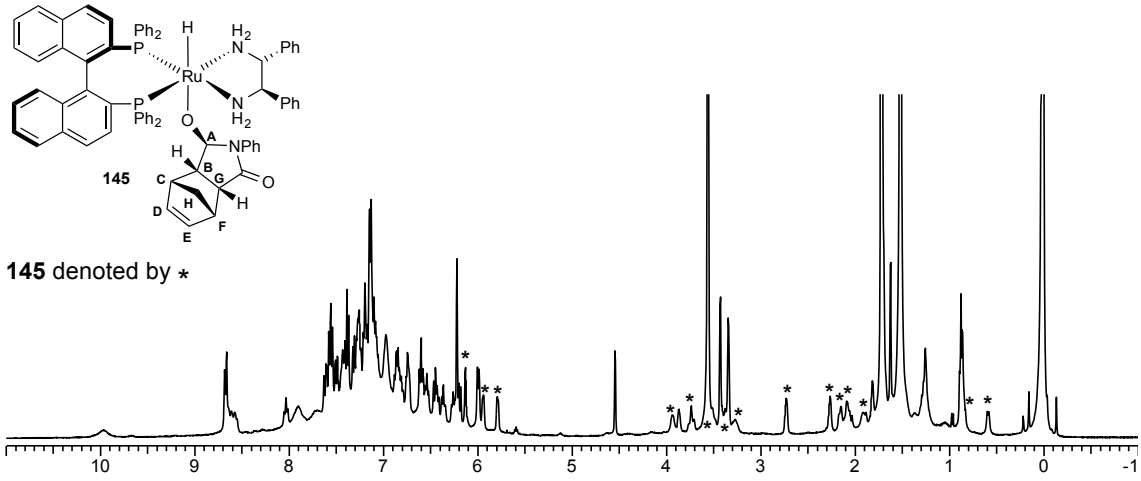

^{1}H NMR (399.95 MHz, THF-d_8, –80 °C): δ –19.0 (1H, t, $^{2}J_{P\text{-}H}$ = 27.0 Hz, Ru-H), 0.59 (1H, broad doublet, J = 8.0 Hz, C_HHH), 0.89 (1H, overlapping with a hexane peak, C_HHH), 1.90 (1H, br, C_aHNHH), 2.09 (1H, br, overlapping with a C_BH peak, C_GH), 2.15 (1H, br, overlapping with a C_GH peak, C_BH), 2.27 (1H, s, C_CH), 2.70 (1H, s, C_FH), 2.73 (1H, br, overlapping with a peak from imide, C_bHNHH), 3.38 (1H, overlapping with a peak from imide, C_aHNHH), 3.52 (1H, overlapping with a residual THF-d_8 peak, C_aHNHH), 3.74 (1H, br t, C_bHNHH), 3.94 (1H, br, C_bHNHH), 5.80 (1H, br, C_EH), 5.94 (1H, br, overlapping with a aromatic peak, C_DH), 6.13 (1H, s, C_AH), 6.00-10.0 (overlapping peaks, aromatic). $^{13}C\{^{1}H\}$ NMR (100.6 MHz, THF-d_8, –80 °C, determined using ^{1}H–^{13}C HSQC): δ 46.3 (C_CH), 47.1 (C_FH), 49.8 (C_BH), 50.6 (C_HH_2), 53.3 (C_GH), 65.4 (C_aHNH_2), 67.7 (C_bHNH_2), 96.2 (C_AH), 135.1 (C_DH), 135.3 (C_EH), 120-140 (aromatic). $^{31}P\{^{1}H\}$ NMR (161.91 MHz, THF-d_8, –80°C): δ 68.0 (2P, AB quartet, $^{2}J_{P\text{–}P}$ = 45.4 Hz).

Reaction between 2 and 138j in the presence of 20 mol% KOH

The dihydride, **2** (30 μmol) was prepared in THF-d_8 (0.4 mL) using 0.9 equiv. $KN(Si(CH_3)_3)_2$ (5.3 mg, 27 μmol) at –78 °C under H_2 as described previously.[3] A THF-d_8 of **138j** (30 μmol in 0.1 mL) was then added to **2** immersed in a dry ice/acetone bath at –78 °C by cannula under H_2 pressure. The mixture was then introduced into the pre-cooled NMR probe at –80 °C. The first ^1H and $^{31}P\{^1H\}$ NMR spectrums taken after substrate addition in the absence of catalytic amounts of KOH showed no detectable conversion to **145**. A 20% KOH solution was then prepared by reacting 0.2 equiv. $KN[Si(CH_3)_3]_2$ (1.2 mg, 6.0 μmol) with triply distilled H_2O (97 μg, 5.4 μmol) in THF-d_8 (0.3 mL). This mixture was then added at –78 °C by cannula under H_2 pressure into the tube containing the **2**–**138j** mixture immersed into a dry ice acetone bath. ^1H and $^{31}P\{^1H\}$ NMR showed ~78% conversion to **145** after 3.5 h, Figures 3-8 and 3-9. Warming the reaction mixture from –80 °C to –70 °C resulted in 88% conversion of **138j** to **145** over 20 min. 100% conversion was observed on warming the sample from –60 °C to –50 °C.

Figure 3-8 *The δ 15 to –20 ppm ^1H NMR spectrum of **145** obtained after 3.5 h at –80 °C using 20 mol% KOH.*

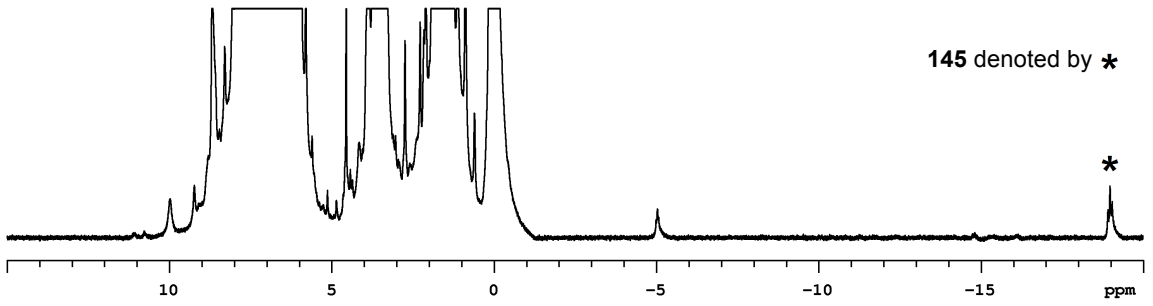

Figure 3-9 *The δ 100 to 60 ppm $^{31}P\{^{1}H\}$ NMR spectrum of* ***145*** *obtained after 3.5 h at –80 °C using 20 mol% KOH.*

2 denoted by *

145 denoted by ■

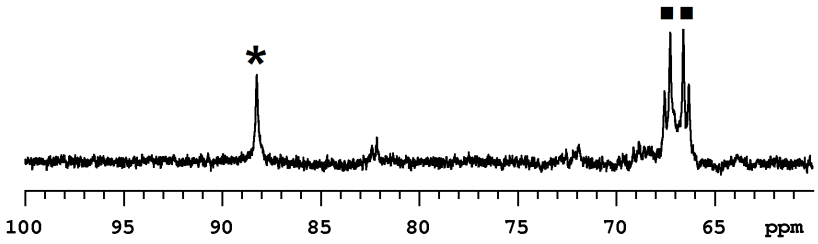

Reaction between 29 and racemic *cis*-139j in the absence of excess inorganic base

A solution of **29** (15 *μ*mol) was prepared from [RuH(*L*)((*R*)-BINAP)((*R*,*R*)-dpen)]BF_4 (*L* = η^2-H_2 or THF-d_8) in THF-d_8 (0.6 mL) using 0.9 equiv. $KN[Si(CH_3)_3]_2$ (2.8 mg, 14 *μ*mol) at –78 °C under Ar as described previously.[3] A THF-d_8 solution of racemic *cis*-**139j**[26] (3.8 mg, 15 *μ*mol in 0.2 mL) was then added by cannula under Ar pressure at –78 °C into a NMR tube containing a frozen solution of **29** at –196 °C. The frozen mixture was then partially thawed using a dry ice/acetone bath followed by inserting it into a pre-cooled NMR probe at –80 °C. The first ^{1}H and $^{31}P\{^{1}H\}$ NMR spectrums after 41 s and 90 s, respectively, showed quantitative formation of **2** and **138j** as the only detectable products on upon mixing at –80 °C (Figures 3-10 and 3-11).

Figure 3-10 *The δ 10 to –10 ppm ^{1}H NMR spectrum of* ***2*** *and* ***138j*** *formed by the addition of racemic cis-****139j*** *to* ***29*** *upon mixing at –80 °C.*

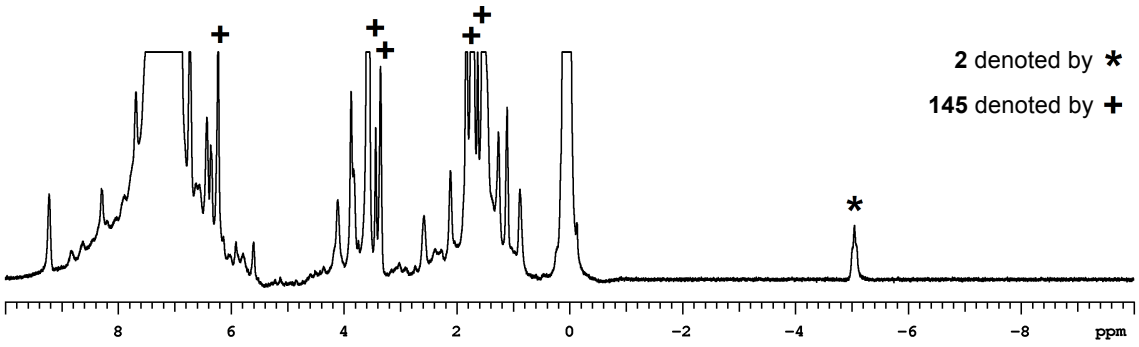

Figure 3-11 *The δ 100 to –40 $^{31}P\{^{1}H\}$ NMR spectrum of* ***2*** *formed by the addition of racemic cis-****139j*** *to* ***29*** *upon mixing at –80 °C.*

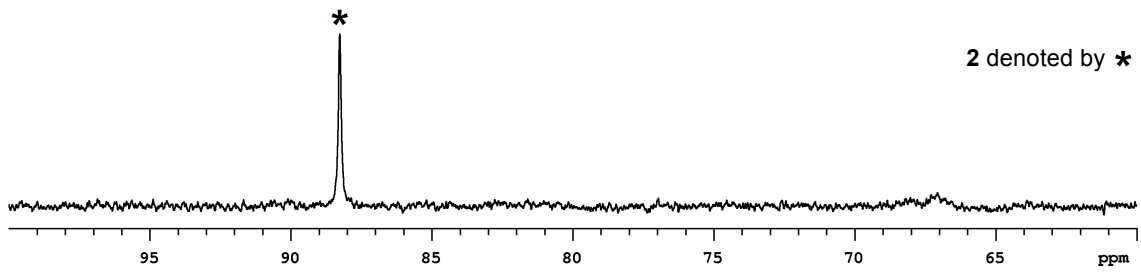

Subsequent, ^{1}H and $^{31}P\{^{1}H\}$ NMR spectra showed a slow conversion of **2** to **145**, 80%, over 6 h at –80 °C. No other species were detected during the course of the reaction. We attribute this slow rate to residual amounts of **29** acting as a weak base.

Control experiments

Reaction between **138j** and KOH

Under Ar, a solution of **138j** (3.6 mg, 15 μmol) was made in 0.3 mL of THF-d_8. A mixture of KOH and $HN[Si(CH_3)_3]_2$ made by reacting 1 equiv. of $KN[Si(CH_3)_3]_2$ (3.0 mg, 15 μmol in 0.5 mL) with triply distilled water (0.24 mL, 14μmol) was then cannulated

under H_2 pressure into a frozen solution of **138j** at –196 °C. The combined mixture was then partially thawed in an acetone/dry ice bath before placing into a pre-cooled NMR probe at –80 °C. The first ^{1}H NMR spectrum recorded showed no evidence of reaction. Warming the sample to higher temperatures also showed no appreciable reaction (Figures 3-12 and 3-13).

Figure 3-12 *Comparison of the δ 5 to –5 ^{1}H NMR spectra for $KN[Si(CH_3)_3]_2$ (bottom) and a KOH and $HN[Si(CH_3)_3]_2$ solution (top) made by the addition of triply distilled water at –80 °C in THF-d_8.*

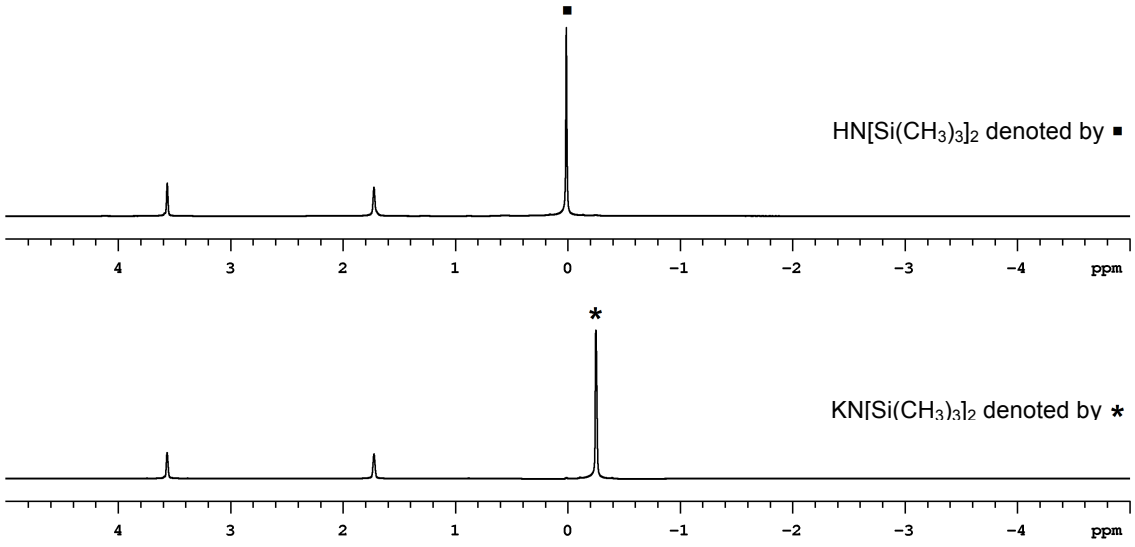

Figure 3-13 *The δ 10 to –5 ppm ^{1}H NMR spectrum of $HN[Si(CH_3)_3]_2$, KOH and **138j** at –80 °C.*

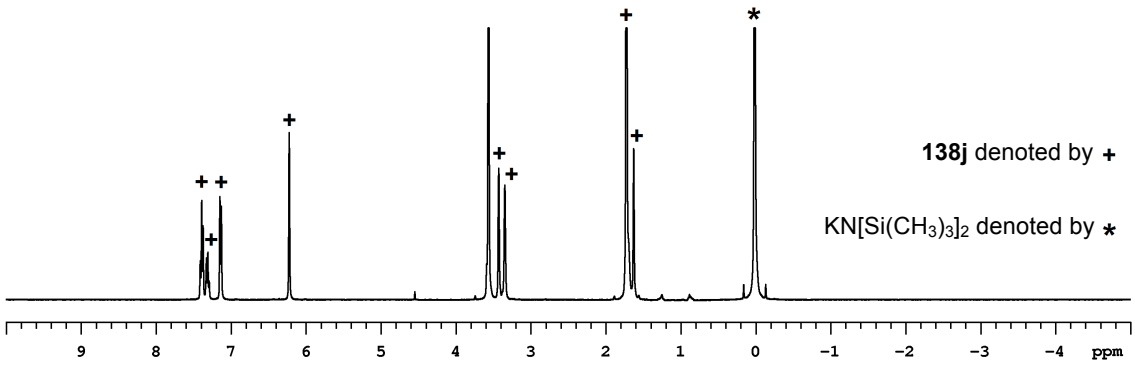

Reaction between **138j** and $KN[Si(CH_3)_3]_2$ *or* KO*t*-Bu at –80 °C

The stoichiometric reaction between **138j** and $KNSi(CH_3)_3)_2$ or at –80 °C in 0.7 mL of THF-d_8 lead to rapid, unidentifiable decomposition of the imide substrate. The products of this decomposition did not have any appreciable reaction with **2** at –80 °C. Warming this mixture also did not result in any appreciable reaction.

Synthesis of *trans*-K[RuH_2((*R*,*R*)-HNCH(Ph)CH(Ph)NH_2)((*R*)-BINAP)], 38

A solution of **2** (15 *μ*mol) was prepared in THF-d_8 (0.6 mL) using KO*t*-Bu (1.7 mg, 15 *μ*mol) at –78 °C under H_2 as described previously.[3] A mixture of KO*t*-Bu (2.5 mg, 22 *μ*mol) and *n*-BuLi (1.6 M in hexanes, 37 *μ*mol) in THF-d_8 was then added at –78 °C by cannula under H_2 pressure into a frozen solution of **2** at –196 °C. The frozen mixture was then partially thawed by inserting the tube into a dry ice/acetone bath followed by placing the sample into the pre-cooled NMR probe at –80°C. Warming the mixture to –60 °C followed by re-cooling the sample to –80 °C resulted in formation of 84% of **38**. Compound **38** was not stable beyond –40 °C. It was characterized at –80°C using a suite of NMR techniques including ^{1}H, ^{31}P{^{1}H}, ^{1}H–^{1}H gCOSY, ^{1}H–^{13}C gHSQC, TOCSY and TROESY NMR experiments.

^{1}H NMR (399.95 MHz, THF-d_8, –80 °C): δ –6.10 (1H, broad dd, *J* = 13.6 Hz, Ru-H), –5.10 (1H, broad, overlapping with parent dihydride), 0.20 (1H, d, *J* = 13.6 Hz, K^+N^-*H*), 2.80 (1H, brs, NH_{axial}H), 2.90 (1H, br, NH$H_{equatorial}$), 3.10 (1H, t, *J* = 13.6 Hz, C*H*NH_2), 3.30 (1H, br overlapping with ether peak, C*H*K^+N^-*H*), 6.00-9.40 (aromatic CH's). ^{13}C{^{1}H} NMR (100.6 MHz, THF-d_8, –80 °C, determined using ^{1}H–^{13}C HSQC): δ 74.2 (*C*H), 78.2 (*C*H), 120.0-140.0 (aromatic). ^{31}P{^{1}H} NMR (161.91 MHz, THF-d_8, –80 °C): δ 86.3 (1P, d, $^2J_{P–P}$ = 41.0 Hz), 77.6 (1P, d, $^2J_{P–P}$ = 41.8 Hz).

In some experiments mixtures of **38** and **39** were observed when layering Schlosser's base onto frozen solutions of **2**. Cooling the sample to –80 °C from –60 °C *or* physically mixing the contents (inverting the NMR tube) usually resulted in the disappearance of **39** from the reaction mixture. Additionally, the extent to which the **2** was deprotonated by either $LiN[Si(CH_3)_3]_2$ *or* Schlosser's base was found to be dependent on temperature with higher temperatures leading to more deprotonation.

Synthesis of *trans*-Li[RuH_2((*R*,*R*)-HNCH(Ph)CH(Ph)NH_2)((*R*)-BINAP)], 39

A solution of **2** (15 *μ*mol) was prepared in THF-d_8 (0.6 mL) using $LiN[Si(CH_3)_3]_2$ (2.5 mg, 15 *μ*mol) at –78 °C under H_2 as described previously.[3] A solution of $LiN[Si(CH_3)_3]_2$ (5.0 mg, 30 *μ*mol) in THF-d_8 (0.2 mL) was then added at –78°C by cannula under H_2 pressure into a frozen solution of **2** at –196 °C. The mixture was then partially thawed by inserting the tube into a dry ice/acetone bath followed by placing the sample into the pre-cooled NMR probe at –80 °C. The first ^1H and $^{31}P\{^1H\}$ NMR showed that only 34% of **39** had formed as the sole detectable product. Warming the mixture to –40 °C resulted in formation of 77% of **39**. However, warming the mixture to –10 °C resulted in the maximum formation, 90%, of **39**. Compound **39** was not stable at temperatures beyond –20 °C. It was characterized at –20 °C using a suite of NMR techniques including ^1H, $^{31}P\{^1H\}$, ^1H–^1H gCOSY, ^1H–^{13}C gHSQC and TOCSY NMR experiments.

^1H NMR (399.95 MHz, THF-d_8, –20 °C): δ –5.90 (1H, br, Ru-H), –5.60 (1H, br, Ru-H), –0.20 (1H, overlapping with excess $LiN(Si(CH_3)_3)_2$, Li^+N^-H), 2.50 (1H, br, $NH_{axial}H$), 2.60 (1H, br, $NHH_{equatorial}$), 3.10 (1H, br, $CHNH_2$), 4.20 (1H, br, CH Li^+N^-H), 6.00-8.60 (aromatic). $^{13}C\{^1H\}$ NMR (100.6 MHz, THF-d_8, –20°C, determined using ^1H–

^{13}C HSQC): δ 75.5 (*C*H), 75.1 (*C*H), 120.0-140.0 (aromatic); ^{31}P{^{1}H} NMR (161.91 MHz, THF-d_8, –20°C): δ 86.2 (1P, d, $^{2}J_{P-P}$ = 40.3 Hz), 79.3 (1P, d, $^{2}J_{P-P}$ = 40.3 Hz).

Synthesis of *trans*-Li$_2$[RuH$_2$((*R*,*R*)-HNCH(Ph)CH(Ph)NH)((*R*)-BINAP)], 40

A solution of **38** was made at –60 °C under H_2 as described above. *n*-BuLi (1.6 M in hexanes, 37 *μ*mol) was then added directly to this mixture at –78 °C using a 50 μL syringe. The NMR tube was then removed from the dry ice/acetone bath and slowly inverted to mix the contents and then quickly replaced. This process was repeated two times. The mixture was then introduced into the pre-cooled NMR probe at –60 °C. The 1st ^{1}H and ^{31}P{^{1}H} NMR showed quantitative formation of **40** as the sole detectable product. Compound **40** was characterized at –50 °C using a suite of NMR techniques including ^{1}H, ^{31}P{^{1}H}, ^{1}H–^{1}H gCOSY, ^{1}H–^{13}C gHSQC, TOCSY and TROESY NMR experiments.

^{1}H NMR (399.95 MHz, THF-d_8, –50 °C): δ –6.60 (2H, br, 2 Ru-H), –0.20 (2H, d, *J* = 10.0 Hz, 2 K^{+}N^{-}*H*), 2.9 (2H, d, *J* = 10.9 Hz, 2 C*H* K^{+}N^{-}H), 6.00-10.50 (aromatic CH's). ^{13}C{^{1}H} NMR (100.6 MHz, THF-d_8, –50 °C, determined using ^{1}H–^{13}C HSQC): δ 97.9 (2 *C*H), 130.0-150.0 (aromatic). ^{31}P{^{1}H} NMR (161.91 MHz, THF-d_8, –50 °C): δ 76.8 (2P, s).

Reaction between 38 and 138j at –80 °C

A solution of **38** was prepared at –60 °C under H_2 as described above. This solution was characterized at –80 °C by ^{1}H and ^{31}P{^{1}H} NMR before use (Figures 3-14 and 3-15). A solution of **138j** (3.6 mg, 15 *μ*mol) in THF-d_8 (0.2 mL) was then added at –78 °C by cannula under hydrogen pressure to a frozen mixture of **38** at –196 °C. The mixture was then partially thawed by inserting the tube into a dry ice/acetone bath before placing the sample into the pre-cooled NMR probe at –80 °C. The first ^{1}H and ^{31}P{^{1}H}

NMR showed quantitative conversion of **38** to **2**, **29** and **146** (neither ^{1}H or $^{31}P\{^{1}H\}$ NMR active), Figures 3-16 and 3-17.

Figure 3-14 *The δ 10 to -10 ppm ^{1}H NMR spectrum of a pre-made mixture of **2** and **38** at –80 °C.*

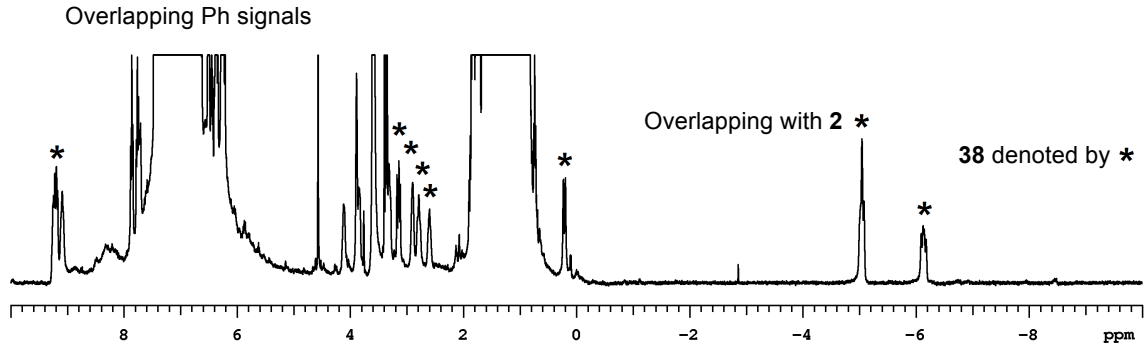

Figure 3-15 *The δ 100 to 40 ppm $^{31}P\{^{1}H\}$ NMR spectrum of a pre-made mixture of **2** and **38** at –80 °C.*

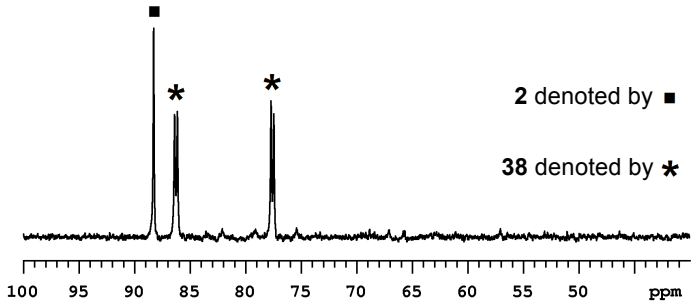

Figure 3-16 *The δ 10 to –20 ppm ^{1}H NMR spectrum of **2**, **29** and **146** formed by the reaction of **38** with **138j** at –80 °C.*

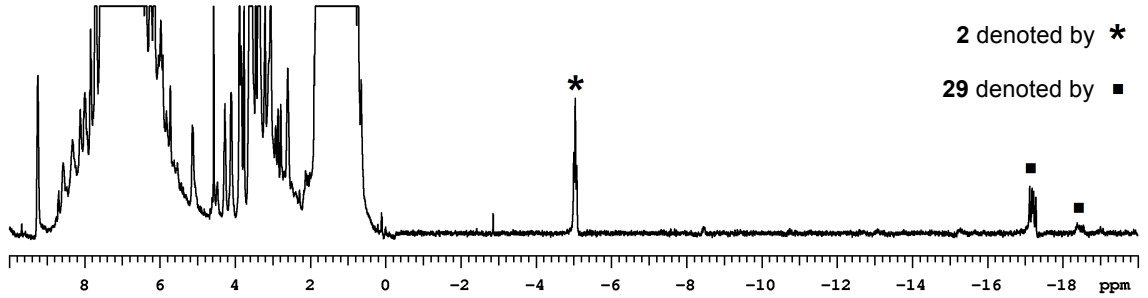

Figure 3-17 *The δ 100 to 60 ppm $^{31}P\{^{1}H\}$ NMR spectrum of **2**, **29** and **146** formed by the reaction of **38** with **138j** at –80 °C.*

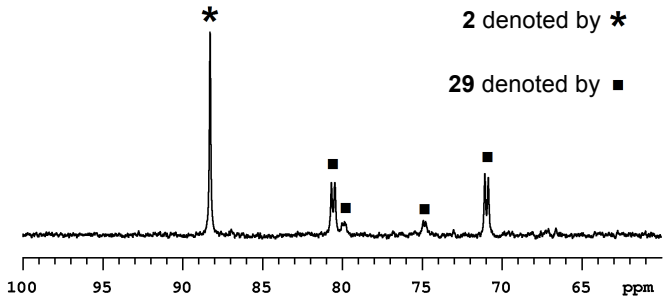

Signals associated with *trans*-**139j** were not observed in the ^{1}H NMR of the reaction mixture at –80 °C. We attribute this to the precipitation of the corresponding K^{+} or Li^{+} salt of *cis*-**139j**. Control experiments carried out between the *trans*-**139j** (>99% *ee*) and $KN[Si(CH_3)_3]_2$ at –80 °C showed a similar result. After 2 h, the remaining imide was consumed to give the **2** as the sole detectable product. We attribute this observation to the slow formation of **38** from **2** by the presence of excess Schlosser's base at –80 °C followed by its subsequent reaction with **138j** to form **29** which in turn is slowly hydrogenated to the **2** at –80 °C. The presence of *trans*-**139j** was confirmed using HPLC analysis with 97:3, *n*-hexanes:2-PrOH.

Compound **38** was more active than **39** under similar conditions. A mixture of **2** and **39** (11% and 89%, respectively) was reacted with a solution of **138j** at –80 °C. After ~1.8 h only 32% of **39** had reacted with **138j** to form **29** (based on Ru). No further conversion was observed after this time owing to decomposition of **138j** by excess $LiN[Si(CH_3)_3]_2$ present.

Reaction between 38 and 149

A solution of **38** was prepared at –60 °C under H_2 as described above. This solution was characterized by ^1H and $^{31}P\{^1H\}$ NMR before use (Figures 3-18 and 3-19). A solution of **149** (5.2 mg, 15 μmol, 1 equiv.) in 0.2 mL of THF-d_8 was transferred at –78 °C by cannula under H_2 pressure into the frozen sample of **38** at –196 °C. The frozen mixture was partially thawed by inserting the tube into a dry ice/acetone bath followed by placing the sample into the pre-cooled NMR probe at –80 °C.

The initial composition of the reaction mixture was 39% **2** and 61% **38** (based on Ru). After 15 min at –80 °C, **38** decreased by 7%. There was also an associated increase in **2**. Warming the sample to –60 °C increased **2** to 54%. At –40 °C all of the **38** initially present was consumed (Figures 3-20 and 3-21). Compound **2** (91%) was the major Ru-species, while, **29** (9%) was present in trace amounts. The Ru-amide (**29**) was hydrogenated to **2** at –40 °C. Warming the sample to –10 °C over 45 min resulted in the complete consumption of **149** (Figures 3-22 and 3-23).

Since **2** was the only detectable species present in the $^{31}P\{^1H\}$ NMR at –40°C, we attribute the hydrogenation of **149** to the slow reaction between **2** and excess Schlosser's base. The signals associated with **150** were not observed in the ^1H NMR at –80 °C due to its insolubility. However, quenching with the reaction mixture with 2-PrOH-d_8 followed by filtration through a Florisil® plug and HPLC analysis using 99:1 (*n*-hexanes:2-PrOH) showed the presence of *N,N*-diphenylamine and 2-phenoxypropanol in 33% *ee*. The di-reduced product is formed from the fast hydrogenation of the corresponding aldehyde produced upon hydrolysis by **2** at –80 °C and ~2 atm H_2. Notably, deuteration of the α-position of the alcohol was not observed, indicating that **149** is not itself deprotonate in these hydrogenations to regenerate **2**.

Figure 3-18 *The δ 10 to –10 ppm ^{1}H NMR spectrum showing the reaction between* ***38*** *and* ***149*** *at –80 °C.*

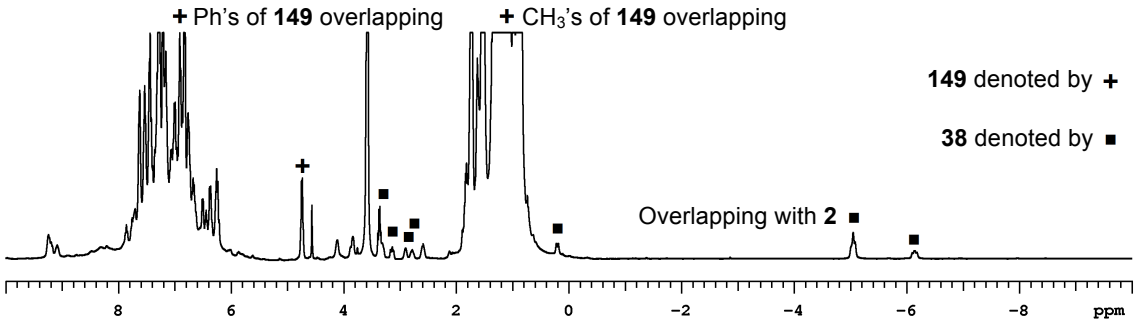

Figure 3-19 *The δ 100 to 60 ppm $^{31}P\{^{1}H\}$ NMR spectrum showing the reaction between* ***38*** *and* ***149*** *at –80 °C.*

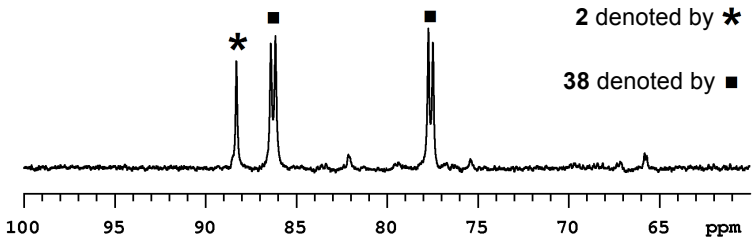

Figure 3-20 *The δ 10 to –10 ppm ^{1}H NMR spectrum showing the reaction between* ***38*** *and* ***149*** *at –40 °C.*

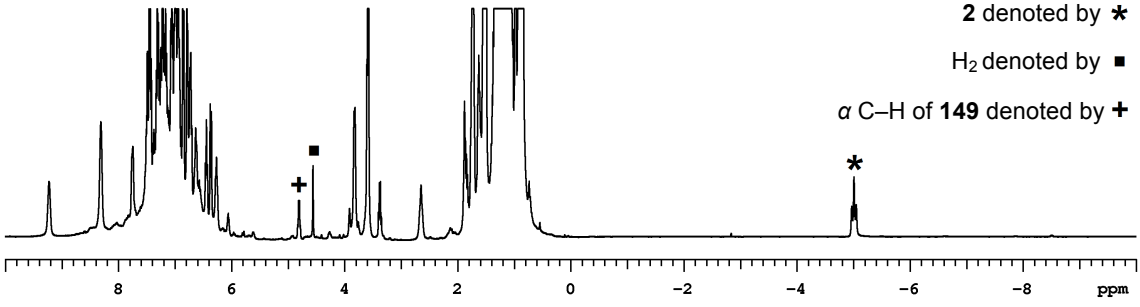

Figure 3-21 *The δ 100 to 30 ppm $^{31}P\{^{1}H\}$ NMR spectrum showing the reaction between* ***38*** *and* ***149*** *at –40 °C.*

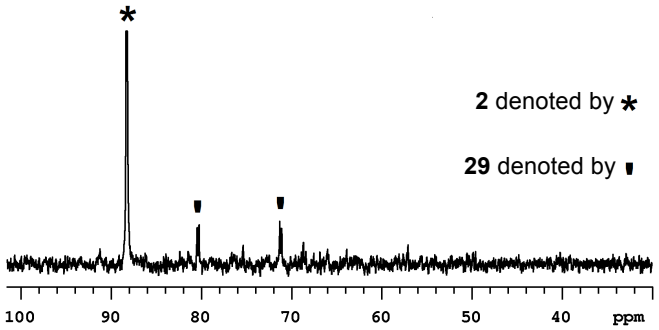

Figure 3-22 *The δ 10 to –8 ppm ^{1}H NMR spectrum showing the reaction between* ***38*** *and* ***149*** *at –10 °C.*

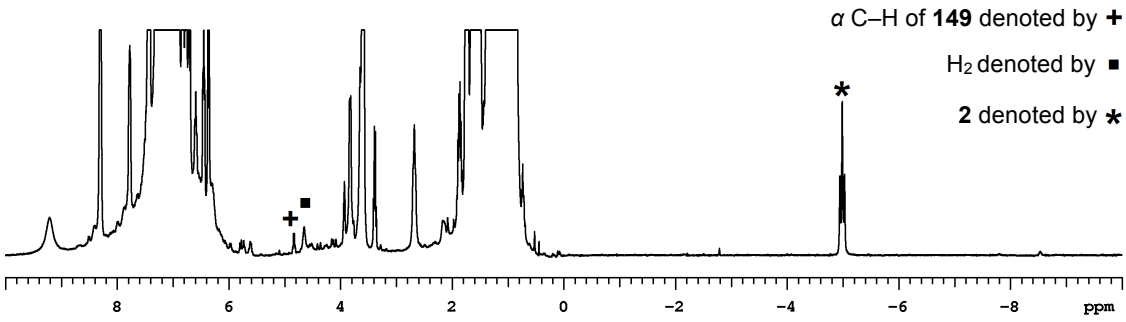

Figure 3-23 *The δ 100 to 40 ppm $^{31}P\{^{1}H\}$ NMR spectrum showing the reaction between* ***38*** *and* ***149*** *at –10 °C.*

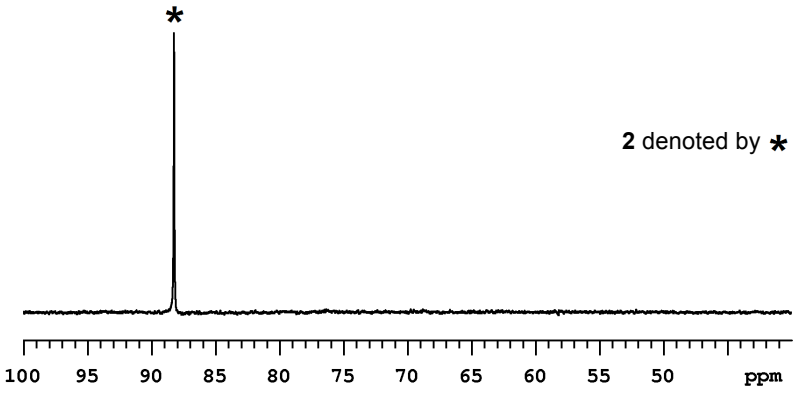

Unlike the preceding reaction, the reaction between **39** and **149** began at –60 °C. The major detectable Ru-containing species were **2** (18%), **29** (7%) and **39** (75%). At 10 °C **39** was consumed to furnish a mixture of **2** (44%) and **29** (56%). Compound **29** was then hydrogenated at room temperature to give **2** as the sole Ru-containing species. Quenching with the reaction mixture 2-PrOH followed by filtration through a florisil® plug and HPLC analysis with 99:1 (*n*-hexanes:2-PrOH) showed the presence of *N,N*-diphenylamine and 2-phenoxypropanol in 75% conversion and 21% *ee*.

Determining the absolute configuration of *trans*-139j

Under Ar, *trans*-**139j** (11 mg, 45 *μ*mol, >99% *ee*) and 4-bromophenyl isocyanate (9.3 mg, 47 *μ*mol) were placed in a NMR tube. 0.7 mL of acetone-d_6 was then added to the tube and the mixture heated at 60 °C for 7 h. 78% of *trans*-**139j** was converted into **151** during this time. 4-bromophenyl carbamic acid was also observed as insoluble crystals due to trace water in the solvent. The mixture was then concentrated under vacuum, extracted with CH_2Cl_2, and dried over $MgSO_4$. Concentration of the filtrate after gravity filtration gave **151** as a colorless oil. Crystals suitable for the X-ray diffraction analysis were grown from *n*-hexanes/AcOEt at –20 °C (Figure 3-24, Tables 3-1, 3-2 and 3-3).

^{1}H NMR (499.82 MHz, acetone-d_6, 27 °C): δ 1.52 (1H, m, CH_2), 1.57 (1H, m, CH_2), 2.96 (1H, ddd, *J* = 1.0, 4.5, and 8.5 Hz, C*H*), 3.27 (1H, m, bridgehead C*H*), 3.34 (1H, m, bridgehead C*H*), 3.36 (1H, ddd, *J* = 0.5, 5.0, and 8.5 Hz, C*H*), 6.03 (1H, s, C*H*O), 6.17 (1H, dd, *J* = 3.0 and 6.0 Hz, C*H*), 6.36 (1H, dd, *J* = 3.0 and 6.0 Hz, C*H*), 7.19 (1H, m, aromatic C*H*), 7.33 (2H, m, 2 aromatic C*H*), 7.40 (2H, m, 2 aromatic C*H*), 7.44 (2H, m, 2 aromatic C*H*), 7.48 (2H, br m, 2 aromatic C*H*). ^{13}C{^{1}H} NMR (125.69 MHz, acetone-d_6, 27°C): δ 45.3 (*C*H), 46.0 (bridgehead *C*H), 46.8 (bridgehead *C*H), 49.4 (*C*H),

51.6 (*C*H_2), 89.0 (*C*HO), 115.7 (aromatic *C*), 121.0 (appear as doublet due to the slow rotation of carbamate C-N bond, aromatic *C*H), 124.5 (aromatic *C*H), 126.9 (aromatic *C*H), 129.6 (aromatic *C*H), 132.6 (aromatic *C*H), 134.4 (*C*=C), 136.8 (C=*C*), 138.3 (aromatic *C*), 139.1 (appear as doublet due to the slow rotation of carbamate C-N bond, aromatic *C*), 153.0 (appear as doublet due to the slow rotation of carbamate C-N bond, *C*=O), 175.5 (*C*=O). IR ($CHCl_3$ cast film): 3283, 1712, 1599, 1539, 1492, 1213, 1033 cm^{-1}. HRMS (ESI^+) m/z calculated for $C_{22}H_{19}BrN_2NaO_3^+$([M + Na]$^+$): 461.0471. Found: 461.0464. Elemental analysis for $C_{22}H_{19}BrN_2O_3$: N 6.38, C 60.15, H 4.36. Found: N 6.38, C 60.38, H 4.39. $[\alpha]_D^{23}$–108.40 (c = 1.00 g/100 mL of acetone, >99% ee). mp: 167.3 °C.

Figure 3-24 *ORTEP drawing of* ***151*** *with 20% probability ellipsoids without hydrogen atoms. The absolute configuration was determined, with a Flack parameter of 0.013(6)*

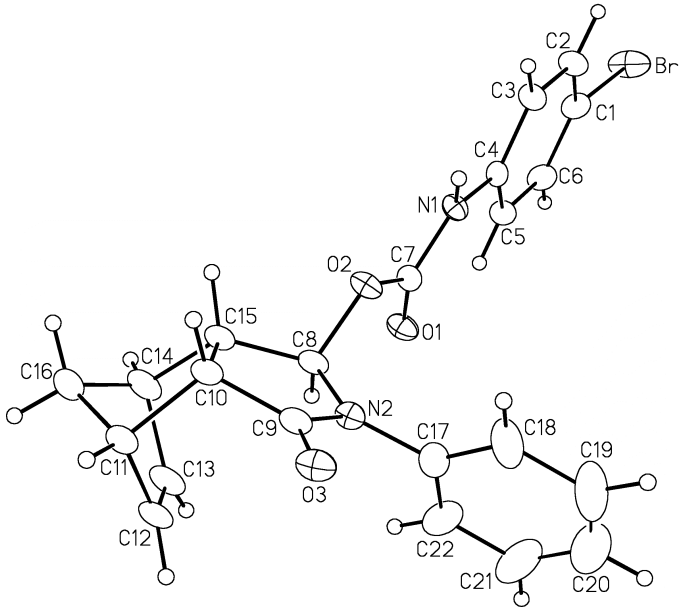

Table 3-1 *Crystallographic experimental details for* ***151****.*

A. Crystal Data

Formula	$C_{22}H_{19}BrN_2O_3$
Formula Weight	439.30
Crystal Dimensions (mm)	0.63 x 0.37 x 0.21
Crystal System	orthorhombic
Space Group	*P*21212 (No. 18)
Unit Cell Parameters[a]	
a (Å)	12.7403 (5)
b (Å)	25.8323 (10)
c (Å)	12.1352 (5)
V (Å^3)	3993.8 (3)
Z	8
ρ_{calcd} (g cm^{-3})	1.461
μ (mm^{-1})	2.084

B. Data collection and refinement conditions

Diffractometer	Bruker D8/APEX II CCD[b]
Radiation (λ [Å])	graphite-monochromated Mo Kα (0.71073)
Temperature (°C)	–100
Scan type	ω scans (0.3°) (20 s exposures)
Data collection 2θ limit (deg)	55.00
Total Data Collected	35335 (-16 ≤ *h* ≤ 16, -33 ≤ *k* ≤ 33, -15 ≤ *l* ≤ 15)
Independent Reflections	9140 (R_{int} = 0.0204)
Number of Observed Reflections (*NO*)	8033 [$F_o^2 \geq 2\sigma(F_o^2)$]
Structure Solution Method	direct methods (*SHELXD*[c])
Refinement Method	full-matrix least-squares on F^2 (*SHELXL–97*[d])
Absorption Correction Method	Gaussian integration (face-indexed)
Range of Transmission Factors	0.6688–0.3545
Data/Restraints/Parameters	9140 / 0 / 505

Flack Absolute Structure Parameter[e]	0.013(6)
goodness-of-fit (S)[f] [all data]	1.028
Final R indices[g]	
R_1 [$F_o^2 \geq 2\sigma(F_o^2)$]	0.0354
wR_2 [all data]	0.0921
Largest difference Peak and Hole	0.621 and –0.444 e Å^{-3}

[a]Obtained from least-squares refinement of 9772 reflections with 4.50° < 2θ < 51.00°.

[b]Programs for diffractometer operation, data collection, data reduction and absorption correction were those supplied by Bruker.

[c]Schneider, T. R.; Sheldrick, G. M. *Acta Crystallogr.* **2002**, *D58*, 1772-1779.

[d]Sheldrick, G. M. *Acta Crystallogr.* **2008**, *A64*, 112–122.

[e]Flack, H. D. *Acta Crystallogr.* **1983**, *A39*, 876–881; Flack, H. D.; Bernardinelli, G. *Acta Crystallogr.* **1999**, *A55*, 908–915; Flack, H. D.; Bernardinelli, G. *J. Appl. Cryst.* **2000**, *33*, 1143–1148. The Flack parameter will refine to a value near zero if the structure is in the correct configuration and will refine to a value near one for the inverted configuration.

[f]$S = [\Sigma w(F_o^2 - F_c^2)^2/(n - p)]^{1/2}$ (n = number of data; p = number of parameters varied; w = $[\sigma^2(F_o^2) + (0.0479P)^2 + 1.0597P]^{-1}$ where $P = [\text{Max}(F_o^2, 0) + 2F_c^2]/3$).

[g]$R1 = \Sigma||F_o| - |F_c||/\Sigma|F_o|$; $wR^2 = [\Sigma w(F_o^2 - F_c^2)^2/\Sigma w(F_o^4)]^{1/2}$.

Table 3-2 *Selected interatomic distance (Å) for* ***151****.*

(a) within molecule A (b) within molecule B

Atom1	Atom2	Distance	Atom1	Atom2	Distance
Br	C1	1.898(2)	Br	C1	1.906(3)
O1	C7	1.202(3)	O1	C7	1.208(3)
O2	C7	1.370(3)	O2	C7	1.372(3)
O2	C8	1.439(3)	O2	C8	1.448(3)
O3	C9	1.219(3)	O3	C9	1.228(3)
N1	C4	1.415(3)	N1	C4	1.415(3)
N1	C7	1.350(3)	N1	C7	1.342(3)
N2	C8	1.452(3)	N2	C8	1.455(3)
N2	C9	1.373(3)	N2	C9	1.355(3)
N2	C17	1.420(3)	N2	C17	1.418(4)
C1	C2	1.366(4)	C1	C2	1.379(4)
C1	C6	1.378(4)	C1	C6	1.370(4)
C2	C3	1.386(3)	C2	C3	1.382(4)
C3	C4	1.387(3)	C3	C4	1.382(3)
C4	C5	1.396(3)	C4	C5	1.387(4)
C5	C6	1.387(3)	C5	C6	1.389(4)
C8	C15	1.525(4)	C8	C15	1.531(4)
C9	C10	1.506(4)	C9	C10	1.489(4)
C10	C11	1.571(4)	C10	C11	1.578(4)
C10	C15	1.528(4)	C10	C15	1.530(4)
C11	C12	1.506(5)	C11	C12	1.513(5)
C11	C16	1.510(6)	C11	C16	1.521(5)
C12	C13	1.323(5)	C12	C13	1.299(5)
C13	C14	1.510(4)	C13	C14	1.516(5)
C14	C15	1.566(4)	C14	C15	1.573(4)

Table 3-2 (continued) *Selected interatomic distance (Å) for* ***151****.*

(a) within molecule A (b) within molecule B

Atom1	Atom2	Distance	Atom1	Atom2	Distance
C14	C16	1.549(6)	C14	C16	1.538(6)
C17	C18	1.382(4)	C17	C18	1.366(5)
C17	C22	1.373(4)	C17	C22	1.398(5)
C18	C19	1.404(6)	C18	C19	1.439(8)
C19	C20	1.350(6)	C19	C20	1.380(10)
C20	C21	1.343(5)	C20	C21	1.326(9)
C21	C22	1.378(5)	C21	C22	1.365(6)

Table 3-3 *Selected interatomic angles (deg) for* ***151****.*

(a) within molecule A				(b) within molecule B			
Atom1	Atom2	Atom3	Angle	Atom1	Atom2	Atom3	Angle
C7	O2	C8	117.20(18)	C7	O2	C8	117.58(19)
C4	N1	C7	125.2(2)	C4	N1	C7	127.3(2)
C8	N2	C9	113.7(2)	C8	N2	C9	114.1(2)
C8	N2	C17	121.08(18)	C8	N2	C17	121.8(2)
C9	N2	C17	125.1(2)	C9	N2	C17	124.1(2)
Br	C1	C2	119.25(19)	Br	C1	C2	119.0(2)
Br	C1	C6	119.4(2)	Br	C1	C6	119.7(2)
C2	C1	C6	121.3(2)	C2	C1	C6	121.3(2)
C1	C2	C3	119.3(2)	C1	C2	C3	118.7(2)
C2	C3	C4	120.3(2)	C2	C3	C4	121.0(2)
N1	C4	C3	116.8(2)	N1	C4	C3	116.9(2)
N1	C4	C5	123.1(2)	N1	C4	C5	123.7(2)
C3	C4	C5	120.1(2)	C3	C4	C5	119.4(2)
C4	C5	C6	118.8(2)	C4	C5	C6	119.8(2)
C1	C6	C5	120.2(2)	C1	C6	C5	119.7(2)
O1	C7	O2	124.2(2)	O1	C7	O2	123.7(2)
O1	C7	N1	128.0(2)	O1	C7	N1	127.9(2)
O2	C7	N1	107.77(19)	O2	C7	N1	108.4(2)
O2	C8	N2	106.77(18)	O2	C8	N2	108.0(2)
O2	C8	C15	110.02(19)	O2	C8	C15	110.3(2)
N2	C8	C15	105.1(2)	N2	C8	C15	104.3(2)
O3	C9	N2	125.2(2)	O3	C9	N2	124.3(3)
O3	C9	C10	126.0(2)	O3	C9	C10	126.2(2)
N2	C9	C10	108.8(2)	N2	C9	C10	109.5(2)
C9	C10	C11	113.3(2)	C9	C10	C11	112.8(2)
C9	C10	C15	105.5(2)	C9	C10	C15	105.6(2)
C11	C10	C15	103.4(3)	C11	C10	C15	102.9(2)
C10	C11	C12	106.4(2)	C10	C11	C12	106.3(2)
C10	C11	C16	99.5(3)	C10	C11	C16	99.0(2)

Table 3-3 (continued) *Selected interatomic angles (deg) for* ***151****.*

(a) within molecule A				(b) within molecule B			
Atom1	Atom2	Atom3	Angle	Atom1	Atom2	Atom3	Angle
C12	C11	C16	100.1(3)	C12	C11	C16	100.7(3)
C11	C12	C13	108.2(3)	C11	C12	C13	107.9(3)
C12	C13	C14	107.4(3)	C12	C13	C14	108.2(3)
C13	C14	C15	107.1(2)	C13	C14	C15	105.8(3)
C13	C14	C16	99.8(3)	C13	C14	C16	100.0(3)
C15	C14	C16	98.5(3)	C15	C14	C16	99.1(3)
C8	C15	C10	106.4(2)	C8	C15	C10	106.2(2)
C8	C15	C14	116.3(2)	C8	C15	C14	116.0(3)
C10	C15	C14	103.0(2)	C10	C15	C14	103.1(2)
C11	C16	C14	94.5(3)	C11	C16	C14	94.1(3)
N2	C17	C18	121.3(2)	N2	C17	C18	120.6(3)
N2	C17	C22	120.1(2)	N2	C17	C22	118.9(3)
C18	C17	C22	118.5(3)	C18	C17	C22	120.5(4)
C17	C18	C19	119.3(3)	C17	C18	C19	117.0(5)
C18	C19	C20	121.2(4)	C18	C19	C20	119.6(5)
C19	C20	C21	118.7(3)	C19	C20	C21	122.2(5)
C20	C21	C22	122.1(3)	C20	C21	C22	119.3(6)
C17	C22	C21	120.0(3)	C17	C22	C21	121.3(4)

Bibliography

1. Takebayashi, S.; John, J. M.; Bergens, S. H. *J. Am. Chem. Soc.* **2010***, 132*, 12832-12834.
2. Bergens, S. H.; Takebayashi, S. University of Alberta, Canada; Patent WO2010145024A1, 2010; p 63.
3. Hamilton, R. J.; Bergens, S. H. *J. Am. Chem. Soc.* **2006***, 128*, 13700-13701.
4. Takebayashi, S.; Bergens, S. H. *Organometallics* **2009***, 28*, 2349-2351.
5. Hamilton, R. J.; Bergens, S. H. *J. Am. Chem. Soc.* **2008***, 130*, 11979-11987.
6. Baratta, W.; Chelucci, G.; Gladiali, S.; Siega, K.; Toniutti, M.; Zanette, M.; Zangrando, E.; Rigo, P. *Angew. Chem., Int. Ed.* **2005***, 44*, 6214-6219.
7. Baratta, W.; Siega, K.; Rigo, P. *Chem. Eur. J.* **2007***, 13*, 7479-7486.
8. Schlosser, M. *Pure Appl. Chem.* **1988***, 60*, 1627-1634.
9. Hartmann, R.; Chen, P. *Angew. Chem., Int. Ed.* **2001***, 40*, 3581-3585.
10. Hartmann, R.; Chen, P. *Adv. Syn. Catal.* **2003***, 345*, 1353-1359.
11. Sandoval, C. A.; Ohkuma, T.; Muñiz, K.; Noyori, R. *J. Am. Chem. Soc.* **2003***, 125*, 13490-13503.
12. Abdur-Rashid, K.; Clapham, S. E.; Hadzovic, A.; Harvey, J. N.; Lough, A. J.; Morris, R. H. *J. Am. Chem. Soc.* **2002***, 124*, 15104-15118.
13. Hasanayn, F.; Morris, R. H. *Inorg. Chem.* **2012***, 51*, 10808-10818.
14. Dub, P. A.; Ikariya, T. *J. Am. Chem. Soc.* **2013***, 135*, 2604-2619.
15. Doods, D. L.; Cole-Hamilton, D. J. In *Sustainable Catalysis: Challenges and Practices for the Pharmaceutical and Fine Chemical Industries: Catalytic Reduction of Amides Avoiding $LiAlH_4$ or B_2H_6*; Dunn, P. J., Hii, K. K., Krische, M. J., Williams, M. T., Eds.; John Wiley and Sons: New Jersey, 2013; pp 1-36.

16. Nicolaou, K. C.; Li, A.; Ellery, S. P.; Edmonds, D. J. *Angew. Chem., Int. Ed.* **2009**, *48*, 6293-6295.

17. Lok, K. P.; Jakovac, I. J.; Jones, J. B. *J. Am. Chem. Soc.* **1985**, *107*, 2521-2526.

18. Di Tommaso, D.; French, S. A.; Catlow, C. R. A. *J. Mol. Struct. (Theochem.)* **2007**, *812*, 39-49.

19. Leyssens, T.; Peeters, D.; Harvey, J. N. *Organometallics* **2008**, *27*, 1514-1523.

20. Oba, M.; Koguchi, S.; Nishiyama, K. *Tetrahedron* **2004**, *60*, 8089-8092.

21. Ostendorf, M.; Romagnoli, R.; Pereiro, I. C.; Roos, E. C.; Moolenaar, M. J.; Speckamp, W. N.; Hiemstra, H. *Tetrahedron: Asymmetry* **1997**, *8*, 1773-1789.

22. Dixon, R. A.; Jones, S. *Tetrahedron: Asymmetry* **2002**, *13*, 1115-1119.

23. Shimizu, M.; Nishigaki, Y.; Wakabayashi, A. *Tetrahedron Lett.* **1999**, *40*, 8873-8876.

24. Kang, J.; Lee, J. W.; Kim, J. I.; Pyun, C. *Tetrahedron Lett.* **1995**, *36*, 4265-4368.

25. Chen, F. -E.; Dai, H. -F.; Kuang, Y. -Y.; Jia, H. -Q. *Tetrahedron: Asymmetry* **2003**, *14*, 3667-3672.

26. Matsuki, K.; Inoue, H.; Ishida, A.; Takeda, M.; Nakagawa, M.; Hino, T. *Chem. Pharm. Bull.* **1994**, *42*, 9-18.

27. Wijnberg, J. B. P. A.; Schoemaker, H. E.; Speckamp, W. N. *Tetrahedron* **1978**, *34*, 179-187.

28. Hubert, J. C.; Wijnberg, J. B. P. A.; Speckamp, W. N. *Tetrahedron* **1975**, *31*, 1437-1441.

29. Abdur-Rashid, K.; Faatz, M.; Lough, A. J.; Morris, R. H. *J. Am. Chem. Soc.* **2001**, *123*, 7473-7474.

30. French, S. A.; Di Tommaso, D.; Zanotti-Gerosa, A.; Hancock, F.; Catlow, C. R. *Chem. Commun.* **2007**, 2381-2383.

31. Di Tommaso, D.; French, S. A.; Zanotti-Gerosa, A.; Hancock, F.; Palin, E. J.; Catlow, C. R. *Inorg. Chem.* **2008**, *47*, 2674-2687.

32. Chen, Y.; Tang, Y.; Lei, M. *Dalton Trans.* **2009**, 2359-2364.

33. Chen, H. -Y.; Di Tommaso, D.; Hogarth, G.; Catlow, C. R. A. *Catal. Lett.* **2011***, 141*, 1761-1766.

34. Ooka, H.; Arai, N.; Azuma, K.; Kurono, N.; Ohkuma, T. *J. Org. Chem.* **2008***, 73*, 9084-9093.

35. Sandoval, C. A.; Shi, Q.; Liu, S.; Noyori, R. *Chem. Asian J.* **2009***, 4*, 1221-1224.

36. Armarego, W. L. F.; Chai, C. L. L. *Purification of Laboratory Chemicals*; Elsevier: Oxford, 2013.

37. Sauers, C. K.; Marikakis, C. A.; Lupton, M. A. *J. Am. Chem. Soc.* **1973***, 95*, 6792-6799.

38. Bergens, S. H.; John, J. M. University of Alberta, Canada; Patent WO2013010275A1, 2013; p 95.

Chapter 4

Reduction of amides: Accessing alcohols and amines via catalytic C–N cleavage[1]

Introduction

Amides are the least reactive of the carboxylic acid derivatives and as such are particularly challenging substrates to reduce.[1,2] On the other hand, amides are ubiquitous in nature as well as produced on a multi-ton industrial scale.[3] Thus, amides have the potential to be an easily accessible feedstock for the synthesis of useful products like alcohols and amines via their reduction.[4]

Within the past decade there has been intense effort directed towards using catalytic hydrogenation to reduce amides.[5,6] This is because of its operational simplicity and economic viability, as well as the growing awareness of the need for green chemistry.[7-9] Specifically, the recent advances in the field of heterogeneous amide hydrogenation can be found in Chapter 1. In this discussion, I will attempt to highlight and compare using specific examples, where applicable, the latest achievements in the field of homogeneous hydrogenation of amides.

The first report of a homogeneous amide hydrogenation was in a patent by Crabtree and coworkers (Davy Process Technology Limited) in 2003 using a catalyst system comprising 0.16 mol% $Ru(acac)_3$, **81**, and 2.2 mol% (13 equiv. excess based on Ru) $Triphos^{Ph}$, **82**, in which the primary (1°) amide, propanamide was hydrogenated under 48 atm H_2 and 164 °C in 21% conversion (TON = 126) with low selectivity to give a complicated mixture of alcohols, amines and esters as products in THF.[10]

[1] A version of this chapter has been published. John, J. M.; Bergens, S. H. *Angew. Chem., Int. Ed.* **2011**, *50*, 10377-10380.

Scheme 4-1 *Hydrogenation of n-butanamide and N-phenylnonamide reported by Cole-Hamilton and coworkers.*

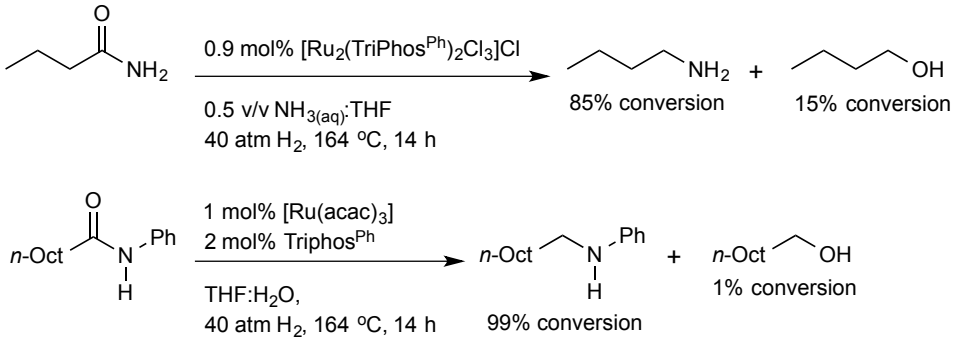

Subsequently, Cole-Hamilton and coworkers reported a Ru/Triphos^{Ph} system that hydrogenates 1° and 2° amides with a preference for the reductive cleavage for the C=O bond (Scheme 4-1).[11,12] For example the authors reported that the addition of aqueous ammonia (0.5 v/v $NH_{3(aq)}$:THF) to [Ru_2(Triphos^{Ph})$_2Cl_3$]Cl, **90**, catalyzes the hydrogenation of *n*-butanamide to give 1-butanamine in 97 turnovers, 85% selectivity after 14 h using 0.9 mol% Ru under 40 atm H_2 and 220 °C. In contrast, the hydrogenation of *N*-phenylnonamide proceeded smoothly in the absence of NH_3 to give the corresponding 2° amine in up to 99 turnovers, 99% selectivity using 1 mol% **81**, 2 mol% **82** (1 equiv. excess based on Ru) under similar conditions. In both examples, the major by-product of the hydrogenation was the corresponding 1° alcohol formed by reductive C–N cleavage or the hydrolysis of either the amide to the acid or the imine to aldehyde followed by hydrogenation, Scheme 4-2.

Scheme 4-2 *Formation of 1-butanol from n-butanamide.*

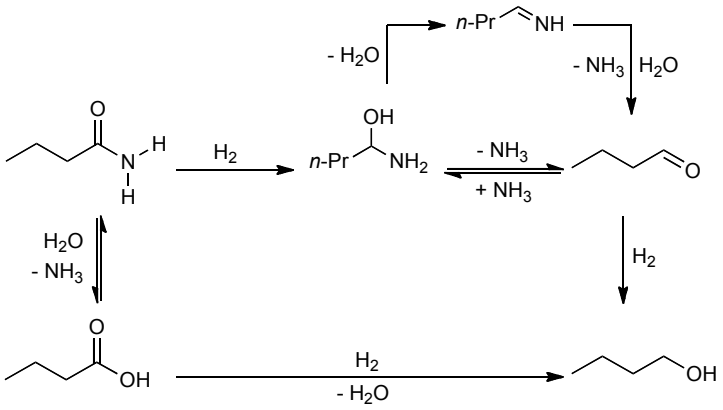

Interestingly, in a strange turn of events, the authors reported that many research groups encountered problems reproducing these results. The authors stated that the source of the irreproducibility was the purity of the Triphos^{Ph} ligand.[13] However, purified Triphos^{Ph} samples stored under an inert atmosphere also exhibited lower activity. The authors subsequently reported that the addition of a catalytic amount of methanesulfonic acid (0.5–1.5:1, MSA:Ru) could restore the activity and selectivity of the reaction. However, *n*-butanamide was hydrogenated in 61 turnovers, 61% selectivity versus 85 turnovers, 85% selectivity under the revised reaction conditions (1 mol% **81**, 2 mol% **82** (1 equiv. excess based on Ru), 0.5 v/v $NH_{3(aq)}$:THF under 10 atm H_2 at 200 °C with 1.5 mol% MSA in 16 h). This Ru/Triphos^{Ph} system was also found to catalyze the hydrogenation of *N*-phenylbenzamide (220 °C) and *N*-phenylacetamide in 92 turnovers, respectively, under somewhat similar reaction conditions. Notably, the by-product distribution was also slightly affected. Instead of typically yielding the corresponding 1° alcohol, the hydrogenation of *N*-phenylbenzamide formed unreacted *N*-benzylideneaniline and *N*,*N*-dibenzylaniline as the major by-products (TON = 4 in each case) by the sequence of steps shown in Scheme 4-3.

Scheme 4-3 *Formation of N*-benzylideneaniline and *N*,*N*-dibenzylaniline from *N*-phenylbenzamide.

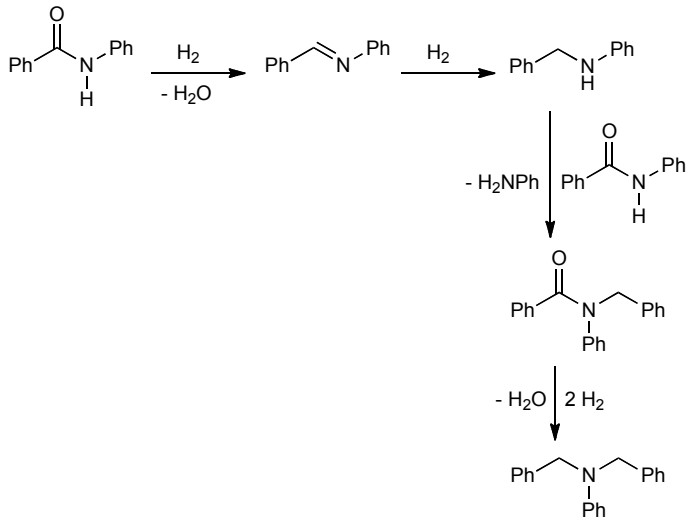

Beginning in 2009, Ikariya and co-workers laid the foundation for the reductive C–N cleavage of amides with a report that described the catalytic dihydrogenation of *N*-acylcarbamates and *N*-sulfonamides (activated amides) using Cp*RuH($Ph_2P(CH_2)_2NH_2$), **77**, made *in situ* using the corresponding chloro-complex and 1 equiv. KO*t*-Bu (based on Ru) under the reported reaction conditions (1-10 mol% **77**, 80 °C, 30 atm H_2, 2-48 h in *t*-BuOH, Eq. 4-1).[14]

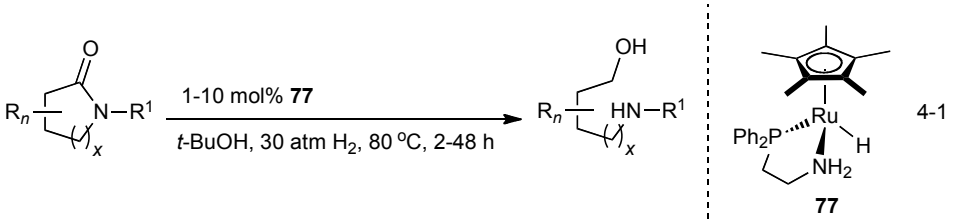

4-1

R^1 = electron withdrawing group

Rate increases in order of Cbz < Boc < CO_2CH_3 < SO_2CH_3 ≈ Ts

Subsequently, in a patent application the authors reported that a wide variety of amides and lactams could be hydrogenated in up to 10 turnovers as long as they had an

aryl group on their nitrogen using the phosphine-free Ru-precursor, Cp*RuCl(2-$C_5H_4NCH_2NH_2$), **101**, 25 mol% KO*t*-Bu at 100 °C and 50 atm H_2 for 24-72 h in 2-PrOH.[15,16] In particular, the 2° amide, *N*-phenylacetamide was hydrogenated to give a mixture of aniline and ethanol in 9 turnovers in 48 h, Scheme 4-4 (top).

Scheme 4-4 *Comparison of Ikariya's and Milstein's amide hydrogenation catalysts.*

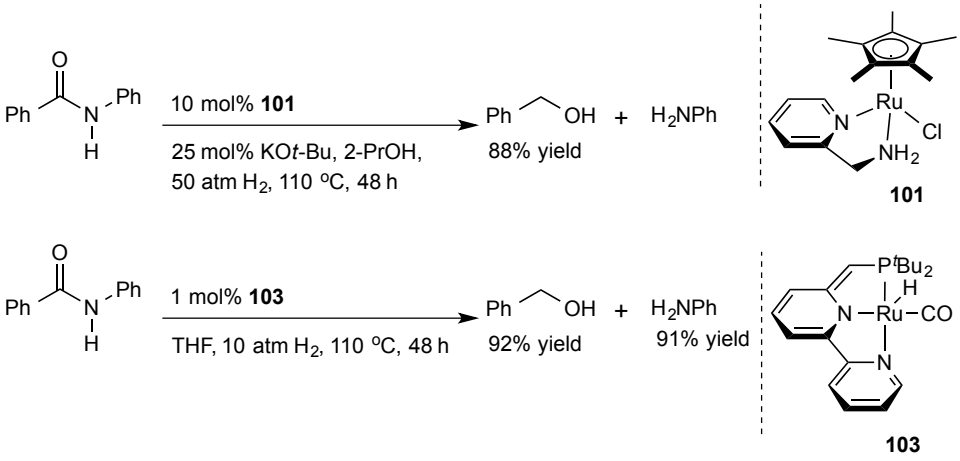

In 2010, Milstein and coworkers found that 16-electron dearomatized pincer complex RuH(NNP$^{t\text{-Bu}}$)(CO), **102**, originally reported for ester hydrogenation could also facilitate the hydrogenation of *N*-benzyl-2-methoxyacetamide to 2-methoxyethanol and benzyl amine catalytically in 63 turnovers under neutral conditions (1 mol% **101** in THF, 10 atm H_2 at 110 °C in 48 h).[17,18] However, under identical conditions the bipyridine-based analogue **103** was substantially more active, hydrogenating *N*-benzyl-2-methoxyacetamide in 90 turnovers, Scheme 4-5. Of practical significance, **103** was found to catalyze the hydrogenation of a variety of 2° amides, and 3° amides having ether groups, to give C–N cleavage. Notably, this system is one order of magnitude more active than Ikariya's system, Scheme 4-4 (bottom).

Scheme 4-5 *Hydrogenation of N-benzyl-2-methoxyacetamide by RuH(NNP$^{t\text{-}Bu}$)(CO) complexes.*

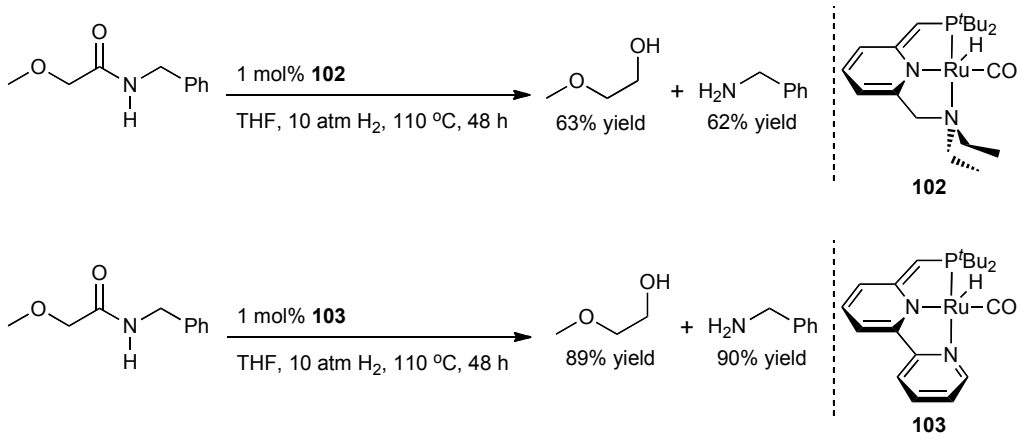

Since the discovery of **103**, modified bipyridine-type pincer systems have also been evaluated as catalysts for the hydrogenation of 2° amides.[19] These complexes exhibited lower catalytic activity in comparison to the parent system. For example, heating a THF solution of **103** with 100 equiv. *N*-phenylacetamide at 110 °C under 10 atm H_2 for 48 h resulted in 95 turnovers with C–N cleavage (Scheme 4-6, top). In contrast, *N*-phenylacetamide was hydrogenated in 57 turnovers, using **104** under similar conditions, (Scheme 4-6, middle). Compound **104** is stable at room temperature in C_6D_6 for 2 days. However, it undergoes a slow intramolecular diastereoselective C–H bond activation of the bulky spirocyclopentyl group with aromatization of the pyridine moiety to form **105** after 5 days on standing at room temperature. When **105** was employed in the hydrogenation of *N*-phenylacetamide, lower turnovers *i.e.* 25 turnovers of ethanol and aniline were obtained, (Scheme 4-6, bottom). Thus, the cyclometalation of the dearomatized complex most likely accounts for the differences in activity between **104** and the parent system, **103**. This cyclometalation also places the hydride ligand *trans* to the terminal pyridine ligand rendering the hydride less hydridic.

Scheme 4-6 *Comparison of Milstein's RuH(NNP$^{t\text{-}Bu}$)(CO) amide hydrogenation catalysts.*

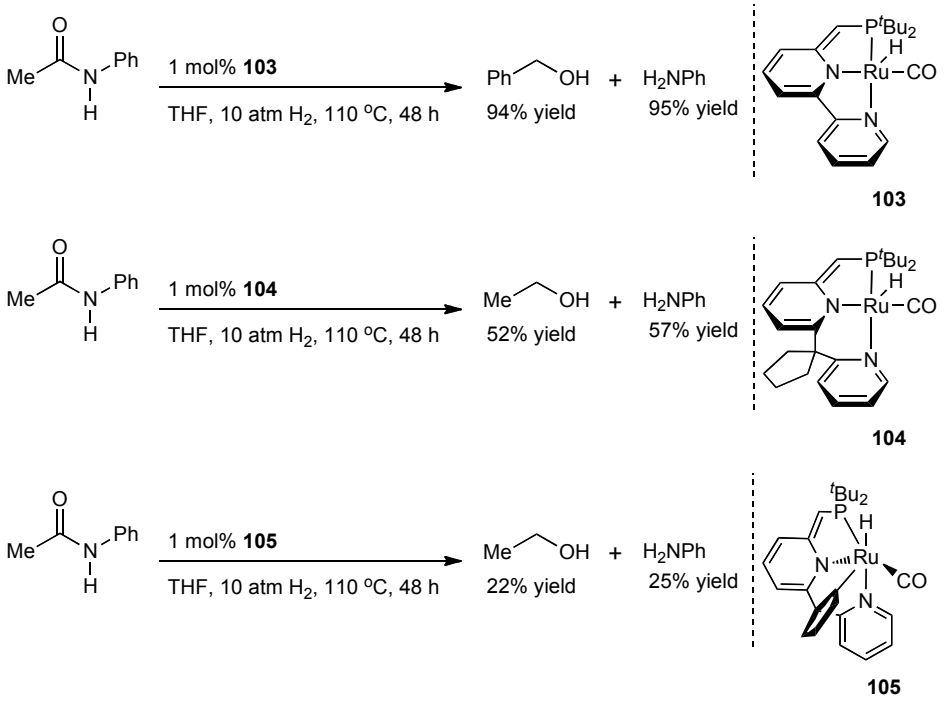

Recently, Saito and coworkers reported that the ruthenium pre-catalyst, $RuCl_2(2\text{-}C_5H_4NCH_2P(C_6H_{11})_2)_2$, **113**, in the presence of a bulky base, **114** (**114**: sodium 2-methyl-2-adamantoxide), catalyzes the hydrogenation of a series of unactivated 2° and 3° amides in toluene to give a mixture of alcohols and amines under rigorous conditions (2 mol% **113**, 4-20 mol% **114** under 60-80 atm H_2 at 160 °C for 24-216 h).[20] This system was found to hydrogenate *N*-benzylbenzamide in near quantitative yield (TON = 46) 11 turnovers lower than Milstein's dearomatized RuH(NNP$^{t\text{-}Bu}$)(CO) complex **103**, Scheme 4-7. Notably, increasing the reaction time to 48 h did not significantly improve the yield, 94 % (TON = 47). Decreasing the pressure to 60 atm H_2 had a detrimental effect on the conversion, 75% (TON = 38).

Scheme 4-7 *Comparison of Milstein's and Saito's amide hydrogenation catalysts.*

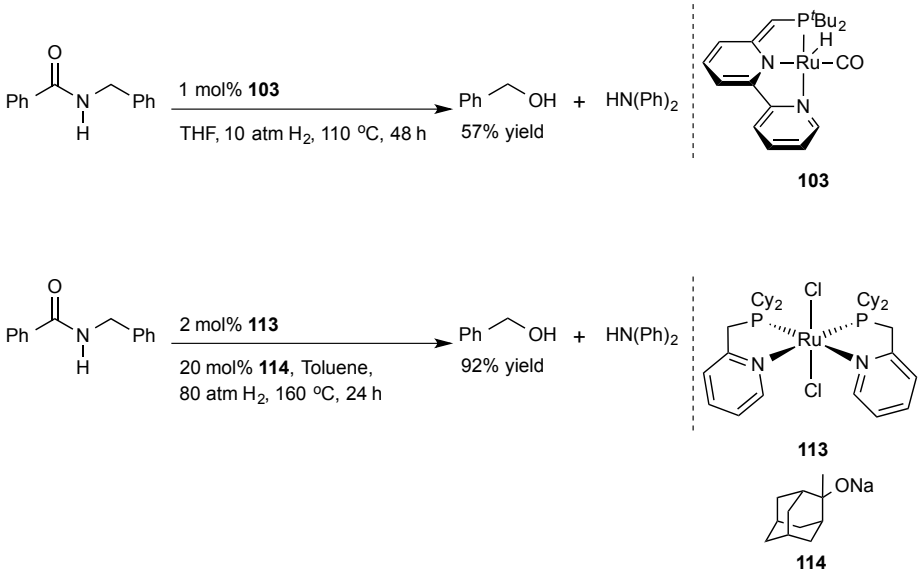

Hamilton and Bergens recently reported a high yielding, low-temperature method to prepare the Noyori ketone hydrogenation catalyst *trans*-[RuH_2((*R*)-BINAP)((*R*,*R*)-dpen)], **2**.[21] In one of the most intensive investigations into the metal-ligand bifunctional addition they discovered that the dihydride, **2**, is a remarkably active carbonyl reducing agent in THF.[22] Specifically, **2** was found to add acetophenone on mixing at –80 °C to form the product of net ketone-hydride insertion, the Ru-alkoxide, *trans*-[RuH(OCH(CH_3)(Ph))((*R*)-BINAP)((*R*,*R*)-dpen)], **41**. Since this discovery, Bergens and coworkers reported that less reactive carbonyl compounds including imides and esters could also be hydrogenated.[23,24] For example, Bergens and coworkers demonstrated that **2** efficiently catalyzes the monohydrogenation of cyclic *meso*-imides with TON up to 1000 under 50 atm H_2 at 0 °C and adds *γ*-butyrolactone within minutes at –80 °C to form the corresponding Ru-hemiacetaloxide, **67**. Further, the authors showed that **2** catalyzes the hydrogenation of esters to give alcohol products under mild conditions (1-2 mol% **2** in THF at 30-50 °C under 4 atm H_2 for 3-4 h). With this high reactivity in mind we evaluated the use of **2** towards the hydrogenation of amides.

Results and discussion

Solutions of **2** were prepared for this study by reacting mixtures of corresponding *trans*-[RuH(*L*)((*R*)-BINAP)((*R*,*R*)-dpen)]BF_4 (*L* = η^2-H_2 or THF) species with 10 equiv. of KO*t*-Bu or KN[Si$(CH_3)_3]_2$ under H_2 (~2 atm) at –78 °C in THF.[21] As ~1 equiv. of inorganic base is consumed to prepare **2** the amount of base quoted in this discussion is that, which remains after the dihydride is prepared.

Initial experiments were focused on examining the catalytic activity of **2** towards the hydrogenation of activated amides *e.g. N*-methanesulfonylpyrrolidin-2-one, **152a**, and *N*-acetylpyrrolidin-2-one, **152b**. Heating a THF solution of **2** (2 mol%) with KO*t*-Bu (20 mol%) and **152a** at 100 °C under 50 atm H_2 for 39 h gave *N*-methanesulfonyl-4-amino-1-butanol in TON = ~27, Eq. 4-2.

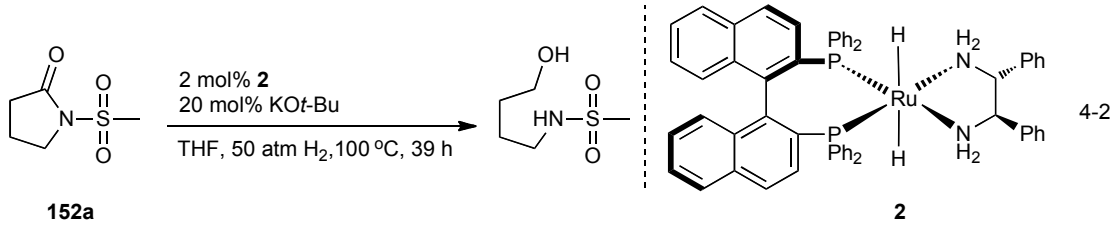

152a **2**

In contrast, the catalyst system of 1 mol% **77** reported by Ikariya and coworkers that gave a TON = >99 towards the hydrogenation of **152a** after 2 h under 30 atm H_2 at 80 °C in *t*-BuOH. The hydrogenation of **152b** catalyzed by **2** (2 mol%) with KN[Si$(CH_3)_3]_2$ (20 mol%) gave a mixture of pyrrolidin-2-one and ethanol (major) as well as *N*-acetyl-4-amino-1-butanol (minor) in ~45 turnovers under 50 atm H_2 at 80 °C in 16 h. No reaction took place with 1-phenyl-pyrrolidin-2-one, **152c** as substrate.

These modest results are in contrast to the high activity of **2** towards the reduction of ketones, imides and esters in THF (*vide supra*).[22-24] We therefore, reasoned that catalysts such as **2** are intrinsically active towards amide hydrogenation, but they

decompose at the higher temperature required for this transformation. This decomposition presumably occurs by the loss of H_2 from the dihydride followed by *β*-hydride elimination of the hydrogens *α* to the amino or amido groups. Morris and coworkers also reiterated that this process occurs in the dpen ligand in benzene solutions of **3** in the absence of H_2.[25] We hypothesized that tethering the amine and phosphine groups would maintain activity, and prevent this dissociative loss of the diamine at high temperatures.

Notably, Saudan and coworkers (Firmenich S. A.) reported that $RuCl_2(Ph_2P(CH_2)_2NH_2)_2$, **63**, is a more active than $RuCl_2(Ph_2P(CH_2)_2PPh_2)(H_2N(CH_2)_2NH_2)$, **153**, towards the hydrogenation of esters in the presence of base.[26] Specifically, they found that methyl benzoate can be hydrogenated to give the corresponding mixture of alcohols in 1980 TO (99% yield) versus 10 TO (0.5% yield) using 0.05 mol% **63** and **153**, respectively, with 5 mol% NaOMe under 50 atm H_2 at 100 °C in THF, Scheme 4-8. They also observed a marked decrease in activity under reduced H_2 pressure *i.e.* 10 atm H_2 (47% yield, TON = 940) or lower reaction temperature *i.e.* 60 °C (90% yield, TON = 1800) using 0.05 mol% **63** and 5 mol% NaOMe. Thus, this implies that the aminophosphine ligands in **63** are more resilient to decomposition under relatively forcing conditions that allows high TONs to be achieved.

Scheme 4-8 *Hydrogenation of methyl benzoate by* ***63*** *and* ***153****.*

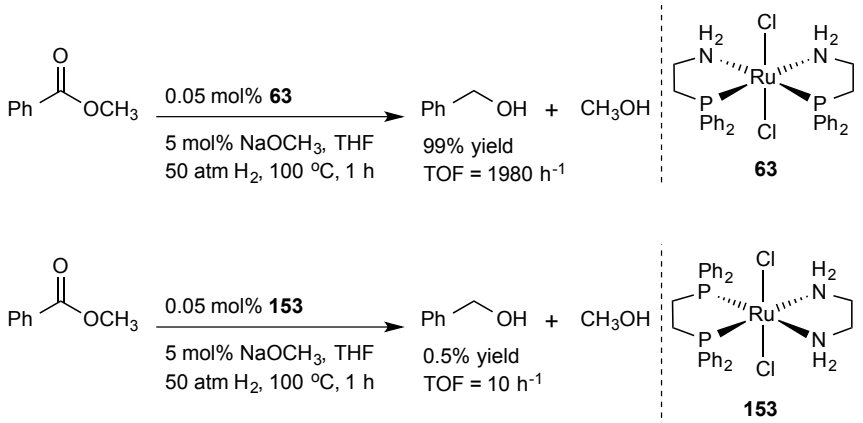

We found that adding 2 equiv. of $Ph_2P(CH_2)_2NH_2$ to a solution of *cis*-[Ru(η^3-C_3H_5)(COD)$(CH_3CN)_2$]BF_4, **154**, in THF forms isomers of the π-allyl complex (**112**) in near-quantitative conversion by displacement of the COD and MeCN ligands after 1.5 h at 60 °C, Eq. 4-3.[27]

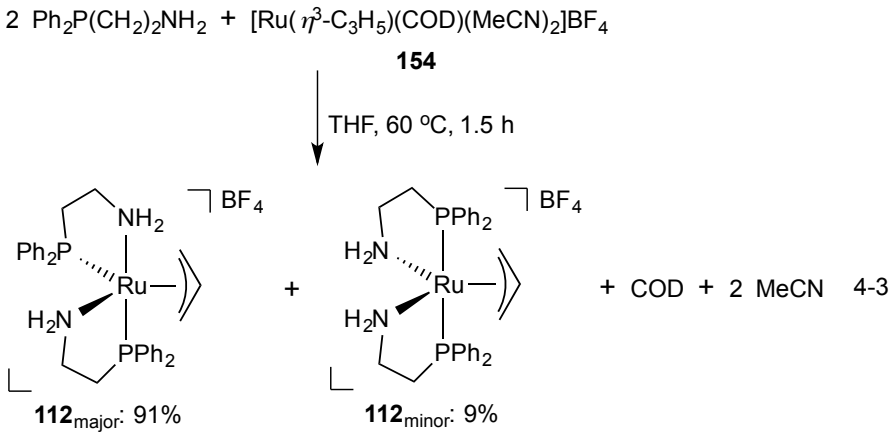

51% isolated yield of combined products

The isomers of **112** were fully characterized at –60 °C using ^{1}H, ^{31}P{^{1}H}, ^{1}H–^{1}H gCOSY, ^{1}H–^{31}P gCOSY, ^{1}H–^{31}P gHSQC, TOSCY and TROESY NMR experiments. The ^{1}H NMR signals for the allyl C–H's were δ 0.6, 1.2, 2.6, 3.1 and 3.5 ppm for **112**$_{major}$

while, the signals for **112**$_{minor}$ were located at δ 1.3, 2.4, 3.3, 3.9 and 4.0 ppm, respectively. The $^{31}P\{^{1}H\}$ NMR of **112**$_{minor}$ consisted of a singlet at δ 48.5 ppm, Figure 4-1. However, the $^{31}P\{^{1}H\}$ NMR of **112**$_{major}$ had two inequivalent phosphorous centers with a doublet similar to that of 112$_{minor}$ and the other shifted ~8 ppm to a higher frequency, Figure 4-1.

Figure 4-1 *The δ 100 to 40 ppm $^{31}P\{^{1}H\}$ NMR spectrum of **112** showing **112**$_{major}$ and **112**$_{minor}$.*

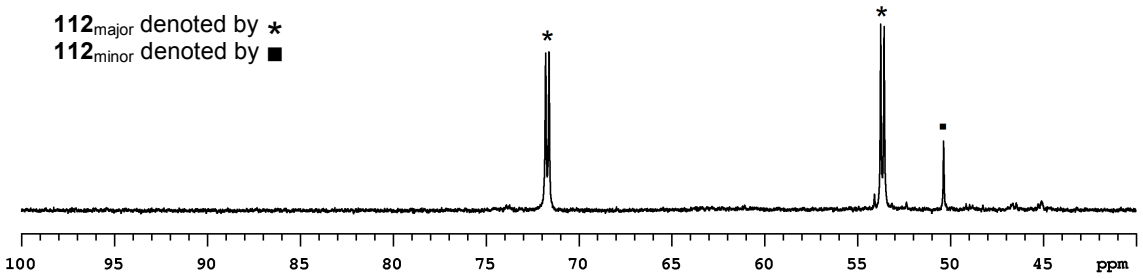

Tables 4-1 and 4-2 summarizes the results of our amide hydrogenations using **112** and KN[Si(CH$_3$)$_3$]$_2$ as the added base in THF. All hydrogenations were carried out with 0.1 mol% *in situ* generated **112**, 4–5 mol% KN[Si(CH$_3$)$_3$]$_2$ under 50 atm H_2 at 100 °C for 24 h. To our pleasant surprise, 1-phenyl-pyrrolidin-2-one, **152c**, was hydrogenated to give *N*-phenyl-4-aminobutan-1-ol in 100% conversion (TON = 1000) under these conditions, Table 4-1, entry 1. The N–Me, **152d** (entry 2) and N–H, **152e** (entry 3), analogues were much less active than N–Ph, **152c** (entry 1), whereas, the six-membered N–Ph derivative, **155**, reacted in 100% conversion (entry 4). The seven-membered unsubstituted lactam, **156** (entry 5), was more reactive than the five-membered lactam (entry 3), as expected from the greater stability of five- over seven-membered rings.

Table 4-1 *Hydrogenation of lactams using in situ prepared* ***112****.*[a]

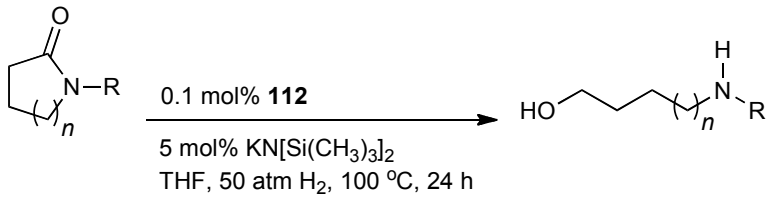

152c: R = Ph, *n* = 1 **152d**: R = Me, *n* = 1 **152e**: R = H, *n* = 1
155: R = Ph, *n* = 2 **156**: R = H, *n* = 3

Entry	Substrate	Conversion (%)[b]	TON
1	**152c**	100	1000
2	**152d**	5	50
3	**152e**	0	0
4	**155**	100	1000
5	**156**	23	230

[a]Amide/**112**/KN[Si(CH$_3$)$_3$]$_2$ = 1000/1/50. Reaction Conditions = 50 atm H_2, 100 °C, 24 h. [Amide] = 0.626 M in THF. [b]Determined by ^{1}H NMR spectroscopy.

The order of reactivity among the acyclic benzamides was –N(Ph)$_2$ ≈ –N(Ph)Me > –N(Me)$_2$, **157a-c** (entries 1–3, Table 4-2). This order is consistent with the differences in the extent of donation from the lone pair of electrons on the nitrogen atom to the carbonyl carbon of these substrates.[28] 1-Benzoyl-piperidine, **157d** (entry 4), was more active than dimethylbenzamide (entry 3), whereas secondary amides were somewhat less reactive than tertiary amides (entry 5 versus entry 1, and entry 6 versus entry 3). Similar results were obtained with the acyclic acetamides. Specifically, the order of reactivity was –N(Ph)$_2$ ≈ –N(Ph)Me > –N(Me)$_2$ (entries 7–9). The secondary acetamide, **157j** (entry 10), was less reactive than the tertiary amides **157g** and **157h** (entries 7 and 8). The lower reactivity of secondary versus tertiary amides may arise from the reaction of the secondary amide with added base.

Table 4-2 *Summary of cyclic amide hydrogenations using in situ prepared* ***112****.*[a]

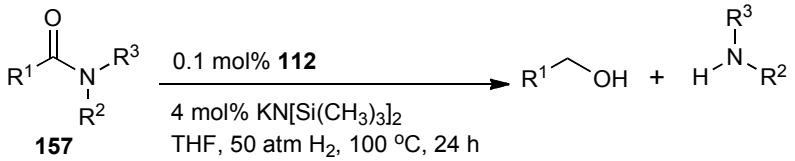

Entry	Substrate	R^1	R^2	R^3	Conversion (%)[b]	TON
1	**157a**	Ph	Ph	Ph	100[c]	1000
2	**157b**	Ph	Ph	Me	96	960
3	**157c**	Ph	Me	Me	50	500
4	**157d**	Ph	$-(CH_2)_5-$	–	82	820
5	**157e**	Ph	Ph	H	50	500
6	**157f**	Ph	Me	H	27	270
7	**157g**	Me	Ph	Ph	100	1000
8	**157h**	Me	Ph	Me	100	1000
9	**157i**	Me	Me	Me	50[d]	500
10	**157j**	Me	Ph	H	70	700

[a]Amide/**112**/$KN[Si(CH_3)_3]_2$ = 1000/1/40. Reaction Conditions = 50 atm H_2, 100 °C, 24 h. [Amide] = 0.626 M in THF. [b]Determined by ^1H NMR spectroscopy. [c]72% benzyl alcohol, 14% benzyl benzoate. [d]Anthracene used as an internal standard.

In preliminary NMR scale experiments, we found that **112** reacts with 3 equiv. of $KN[Si(CH_3)_3]_2$ under ~1 atm H_2 at 0 °C to form propylene and three ruthenium monohydrides. Moreover, the known dichloride, **63**, also forms a similar mixture of monohydride species under these conditions.[26] This mixture subsequently reacts in the presence of 10 equiv. of base under ~4 atm H_2 at 22 °C to generate a symmetrical dihydride, which was tentatively assigned to be an isomer of the *trans*-dihydride, *trans*-$RuH_2(Ph_2P(CH_2)_2NH_2)_2$ (**158**). The dihydride was not isolated, but partially characterized

using ^{1}H and $^{31}P\{^{1}H\}$ NMR spectroscopy owing to its decomposition at room temperature under ~2 atm H_2. The C_2-symmetric nature of **158** resulted in a triplet at δ –8.1 ppm in the ^{1}H NMR and a singlet located at δ 56 ppm in the $^{31}P\{^{1}H\}$ NMR, Figure 4-2 and 4-3 respectively.

Figure 4-2 *The δ -5 to -10 ppm ^{1}H NMR spectrum of **158** showing the equivalent hydride signal.*

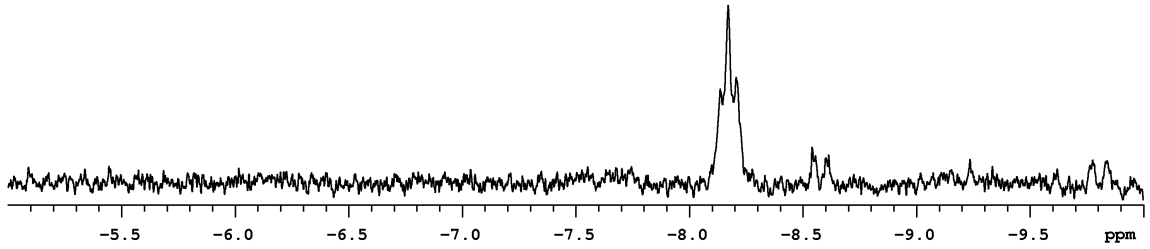

Figure 4-3 *The δ 90 to 60 ppm $^{31}P\{^{1}H\}$ NMR spectrum of **158** showing the equivalent phosphorous signal.*

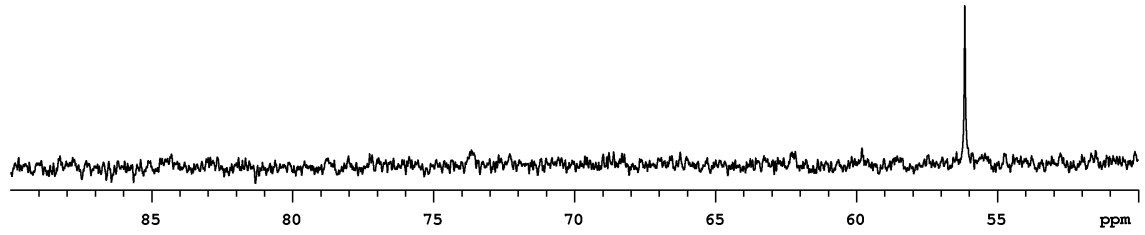

Saudan and coworkers reported that **63** forms an active ester hydrogenation catalyst with NaOMe as base in THF (*vide supra*).[26] We found that both **112** and **63** (0.01 mol%) catalyze the hydrogenation of 1-phenyl-pyrrolidin-2-one, **152c**, in 71.2% (TON = 7120) and 67.6% (TON = 6760) conversion, in the presence of 5 mol % NaOMe (Table 4-3).

The catalyst system of **112** and $KN[Si(CH_3)_3]_2$ is substantially more active than Milstein's and Ikariya's bifunctional systems.[16,17] For example, **112** catalyzes the

hydrogenation of *N*-phenylbenzamide in a TON of 500 after 24 h, compared to TON of 92 and a TON of 8 for **103** and **101** after 48 and 24 h, respectively.

Table 4-3 *Hydrogenation of 1-phenyl-pyrrolidin-2-one using* ***112*** *or* ***63*** *and NaOMe.*[a]

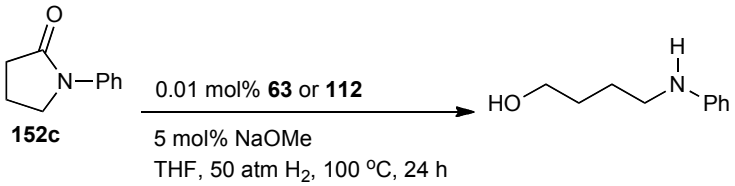

Entry	Pre-catalyst	Conversion (%)[b]	TON
1	**112**	71.2	7120
2	**63**	67.6	6740

[a]Amide/**63** or **112**/NaOMe = 10000/1/500. Reaction Conditions = 50 atm H_2, 100 °C, 24 h. [Amide] = 2.08 M in THF. [b]Determined by ^{1}H NMR spectroscopy.

To make this transformation even more efficient, it is desirable to remove the need for added base. Ruthenium hydrido tetrahydroborate complexes have long been demonstrated to efficiently catalyze the hydrogenation of various carbonyl compounds.[29-37] Thus, the use of an analogous system for the base-free hydrogenation of amides was worthy of investigation.

Our study began with investigating the activity of *trans*-[RuH(η^1-BH_4)((*R*)-BINAP)((*R*,*R*)-dpen)]BF_4, **27**, made by reacting a mixture of *trans*-[RuH(*L*)((*R*)-BINAP)((*R*,*R*)-dpen)]BF_4 (*L* = η^2-H_2 or THF) with 1 equiv. of $NaBH_4$ under ~2 atm H_2 at room temperature.[38] We found that **27** was inactive towards 1-phenyl-pyrrolidin-2-one, **152c**, under our conditions (Table 4-4, entry 1). However, reacting the *in situ* prepared cationic pre-catalyst (0.1 mol% Ru) with 5 equiv. $NaBH_4$ (0.5 mol% B) under ~2 atm H_2 at 60 °C for 20 min formed a system that reduced **152c** to *N*-phenyl-4-aminobutan-1-ol in 66% conversion (TON = 660) under 50 atm H_2 at 100 °C in 24 h (entry 2).[39] Under the

same conditions [Ru((1-3;5-6-η)-C_8H_{11})(η^6-antracene)]BF_4, **159**, was also found to promote the hydrogenation in somewhat higher conversions (entry 3, TON = 710). The combination of $RuCl_2(Ph_2P(CH_2)_2NH_2)_2$, **63**, and 5 equiv. of $NaBH_4$ was active albeit under higher loadings (0.2 mol% Ru, TON = 378, entry 4). Isolated **112** and 2 equiv. of $NaBH_4$ gave the highest TON (910) under these conditions.

Table 4-5 compares the results of our base-free and base-assisted amide hydrogenations in THF. All hydrogenations were carried out with 0.1 mol% **112** and 0.2 mol% $NaBH_4$ (Ru:B = 1:2) *or* 4 mol% $KN[Si(CH_3)_3]_2$ (Ru:Base = 1:40) under 50 atm H_2 at 100 °C for 24 h. The catalyst system of **112** with $NaBH_4$ (Ru:B = 1:2) was more active towards the hydrogenation of *N*-phenylbenzamide (TON = 710) than our previously described base-assisted hydrogenation using 4 mol% $KN[Si(CH_3)_3]_2$ (TON = 500) after 24 h. Scheme 4-9, compares this result with known homogeneous amide hydrogenation systems.[16,17] Interestingly, both systems had comparable activity towards the hydrogenation *N*-phenyl-substituted tertiary acetamides (Table 4-5, entries 2 and 3). The simple tertiary amide, *N*,*N*-dimethylacetamide was however, more resilient towards the hydrogenation TON = 240 versus TON = 500 with base (entry 4). In contrast, 1-morpholinoethanone that was smoothly hydrogenated with both systems (entry 6 versus entry 4). This difference in reactivity could be attributed to the greater ligating ability of dimethylamine under base-free conditions. *N*-phenylacetamide was also hydrogenated with higher conversions under base-free reactions (entry 5). These results imply that high conversions could be obtained through judicious matching of substrate to catalyst system.

Table 4-4 *Base-free hydrogenation of 1-phenyl-pyrrolidin-2-one using various Ru/$NaBH_4$ systems.*[a]

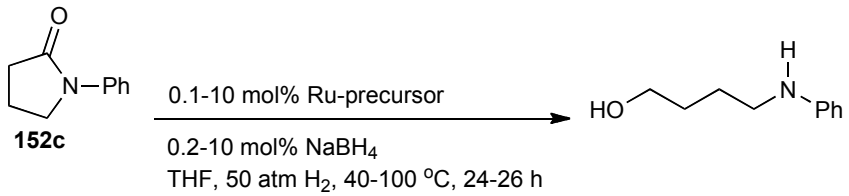

Entry	Ru/$NaBH_4$ system	Conversion (%)[b]	TON
1[c,d]	*trans*-[RuH(*L*)((*R*)-BINAP)((*R*,*R*)-dpen)]BF_4 + 1 equiv. $NaBH_4$	0	0
2[c,e]	[Ru(η^3-C_3H_5)(COD)(CH_3CN)$_2$]BF_4 + 2 equiv. $Ph_2P(CH_2)_2NH_2$ + 5 equiv. $NaBH_4$	66	660
3[c,e]	[Ru(η^6-Anthracene)(COD)]BF_4 + 2 equiv. $Ph_2P(CH_2)_2NH_2$ + 5 equiv. $NaBH_4$	71	710
4[c,f]	$RuCl_2(Ph_2P(CH_2)_2NH_2)_2$ + 5 equiv. $NaBH_4$	76	378
5[c,g]	[Ru(η^3-C_3H_5)($Ph_2PCH_2CH_2NH_2$)$_2$]BF_4 + 2 equiv. $NaBH_4$	91	913

[a]Reaction Conditions = 50 atm H_2, 100 °C, 24 h unless stated otherwise. [b]Determined by ^{1}H NMR spectroscopy. [c]Stepwise reaction. [d]Ru-precursor and $NaBH_4$ warmed to room temperature. Amide/Ru/B = 10/1/1. Adjusted Conditions = 40 °C, 26 h. [Amide] = 50 mM in THF. [e]Ru-precursor reacted with aminophosphine ligand at 60 °C for 30 min followed by heating with $NaBH_4$ at 60 °C for 20 min. Amide/Ru/B = 1000/1/5. [Amide] = 2.0 M in THF. [f]Ru-precursor reacted with $NaBH_4$ at 60 °C for 20 min. Amide/Ru/B = 500/1/5. [Amide] = 1.25 M in THF. [g]Ru-precursor reacted with $NaBH_4$ at 60 °C for 30 min. Amide/Ru/B = 1000/1/2. [Amide] = 2.0 M in THF.

Table 4-5 *Base-free versus base-assisted hydrogenation of acyclic amides.*

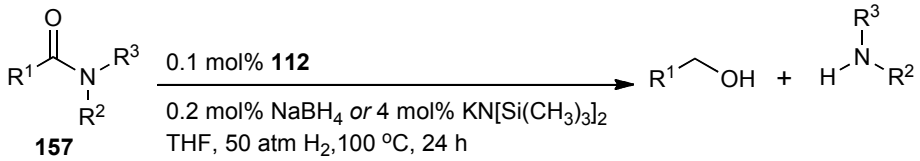

Entry	Substrate	R^1	R^2	R^3	Conversion (%)[a]		TON	
					Base-free[b]	Base-assisted[c]	Base-free	Base-assisted
1[d]	**157e**	Ph	Ph	H	71	50	710	500
2	**157g**	Me	Ph	Ph	100	100	1000	1000
3	**157h**	Me	Ph	Me	93	100	930	1000
4	**157i**	Me	Me	Me	24[e]	50[e]	240	500
5	**157j**	Me	Ph	H	80	70	800	700
6	**157k**	Me	-$(CH_2)_4$O-	–	96	100	960	1000

[a]Determined using ^{1}H NMR spectroscopy. [b]Performed using *in situ* prepared catalyst: Amide/**112**/$NaBH_4$ = 1000/1/2. Reaction Conditions = 50 atm H_2, 100 °C, 24 h. [Amide] = 2.5 M in THF. [c]Amide/**112**/$KN[Si(CH_3)_3]_2$ = 1000/1/40. Similar reaction conditions. [Amide] = 0.626 M in THF. [d]Base-free [Amide] = 2.0 M in THF. [e]Anthracene used as an internal standard.

Scheme 4-9 *Comparison of amide hydrogenation systems (in decreasing order of activity towards N-phenylbenzamide).*

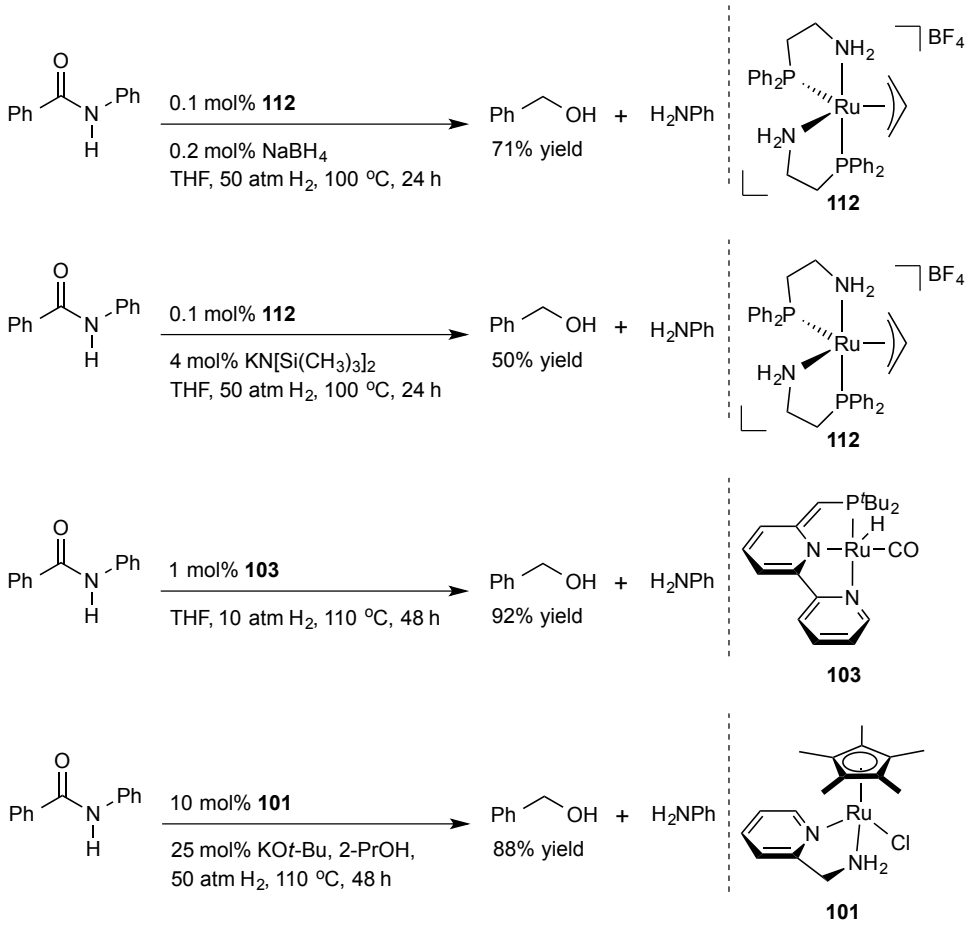

We then explored the possibility of using this catalyst system for the hydrogenation of *N*-acyloxazolidinones.[14] We found that the reduction of *N*-acetyloxazolidinone, **160a**, did not occur at low H_2 pressures regardless of the temperature *i.e.* 4-10 atm H_2, 22-100 °C. On the other hand, this substrate was hydrogenated with 68% conversion to give a mixture of products. These products were *N*-(2-acetoxyethyl)acetamide (31%, TON = 21, formed from *N*-acetylethanolamine), 2-oxazolidinone (69%), and ethanol (38%, TON = 26) using 1 mol% **112** with 2 mol% $NaBH_4$ (Ru:B = 1:2) under 50 atm H_2 at 100 °C in 24 h (Table 4-6, entry 1). Encouraged by this result, we then attempted the reductive transformation of chiral *N*-

acyloxazolidinones developed by Evans and coworkers.[40] Upon heating a THF solution of **160b** with 2 mol% **112** and 10 mol% $NaBH_4$ (Ru:B = 1:5) at 100 °C under 50 atm H_2 for 24 h, the *N*-acyloxazolidinone was hydrogenated to furnish a mixture of chiral products and an unknown product in ~37 turnovers. Subsequently, increasing the catalyst loading to 10 mol% **112** with 20 mol% $NaBH_4$ under less rigorous conditions, 50 atm H_2 and 50 °C, resulted in exclusive formation of the chiral alcohol-amine and MeOH without any loss of dr after 48 h. Using these conditions **160c** was also quantitatively and selectively reduced to a similar mixture products without any loss of dr (entry 4). This method may constitute a new approach to access chiral ligands for enantioselective transformations.

Table 4-6 *Base-free hydrogenation of N-acyloxazolidinones.*[a]

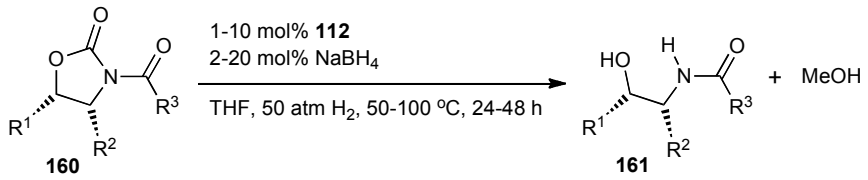

160 161

Entry	Substrate	R^1	R^2	R^3	Conversion (%)[b]	dr[b]	TON
1[c]	**160a**	H	H	Me	68[d]	-	26
2[e]	**160b**	H	*i*Pr	CH(Bn)Me	74[f]	nd	37
3[g]	**160b**	H	*i*Pr	CH(Bn)Me	100	99:1	10
4[g]	**160c**	Ph	Me	CH(Bn)Me	100	99:1	10

[a]Ru-precursor reacted with $NaBH_4$ at 60 °C for 10 min. [b]Determined using ^1H NMR spectroscopy. [c]Oxazolidinone/Ru/B = 100/1/2. Reaction Conditions: 50 atm H_2, 100 °C, 24 h. [Oxazolidinone] = 0.25 M in THF. [d]69% 2-oxazolidinone and 31% *N*-(2-acetoxyethyl)acetamide. [e]Oxazolidinone/Ru/B = 50/1/5. Reaction Conditions: 50 atm H_2, 100 °C, 24 h. [Oxazolidinone] = 63 mM in THF. [f]Mixture of chiral oxazolidinone and alcohol, ring-open alcohol-amide and trace unknown product. [g]Oxazolidinone/Ru/B = 10/1/2. Reaction Conditions: 50 atm H_2, 50 °C, 48 h. [Oxazolidinone] = 25 mM in THF.

Preliminary NMR scale experiments were unable to identify the ruthenium hydrido borohydride complex that presumably forms from the reaction between **112** and $NaBH_4$. Specifically, heating a THF-d_8 solution of **112** with 2 equiv. of $NaBH_4$ under ~2 atm H_2 at 50 °C for 8 min forms propylene and multiple Ru-monohydrides. These Ru-monohydride species did not form an isomer of *trans*-$RuH_2(Ph_2P(CH_2)_2NH_2$, which is considered to be the active catalyst in these hydrogenations.[39] Instead, they were found to decompose after prolong heating under these conditions. Interestingly, the use of 10 mol% ruthenium black resulted in the hydrogenation of the arene ring in **152c**. It is therefore unlikely that Ru nanoparticles are the active catalyst in these hydrogenations, suggesting that, the reaction is at least homogeneous.

Conclusion

In this chapter I have shown that complexes **63** and **112** are remarkably active towards the hydrogenation of simple amides without strongly activating groups. Specifically, when combined with base *e.g.* $KN[Si(CH_3)_3)_2]$ or NaOMe, the hydrogenation proceeds with the highest TON, up to 7120 after 24 h, reported to date for a homogeneous amide hydrogenation. The base-free systems of **63**, **112** or **159** (with 2 equiv. of $Ph_2P(CH_2)_2NH_2$ ligand) and $NaBH_4$ are also efficient catalysts for this reaction. In the case of *N*-phenylbenzamide, the catalyst system is substantially more active (TON = 710 after 24 h) than Milstein's and Ikariya's bifunctional catalysts. This base-free hydrogenation also catalyzes the hydrogenation of the less reactive chiral-oxazolidone core of Evan's auxillaries to yield chiral alcohol-amides that have potential applications in ligand synthesis. Further mechanistic studies will provide insight into catalyst activity, structure and stability.

Materials and methods

All pressure reactions were carried out in a glass (4 atm H_2) or steel (10-50 atm H_2) pressure reactor equipped with a magnetic stir bar. Deuterated solvents were obtained from Aldrich and Cambridge Isotope Laboratories. Common laboratory solvents were dried over appropriate drying agents before each experiment. For example, THF was distilled over Na/benzophenone while 2-PrOH, toluene, and DCM were dried over CaH_2.[41]

δ-valerolactam, *ε*-caprolactam, **156**, *N*-methylaniline, *N*-methylbenzamide, **157f**, 1-phenyl-pyrrolidin-2-one, **152c**, 2-oxazolidinone, 2-pyrrolidinone and 4*S*-(–)-isopropyl-2-oxazolidinone were obtained from Alfa Aesar. Acetyl chloride, benzoyl chloride, lithium and potassium bis(trimethylsilyl)amide, (4*S*,5*R*)-(–)-4-methyl-5-phenyl-2-oxazolidinone, *N*-phenylbenzamide, **157e**, *N*,*N*-dimethylbenzamide, **157c**, morpholine, propionyl chloride and tris(triphenylphosphine)ruthenium(II) dichloride were obtained from Aldrich. *N*,*N*-diphenylacetamide, **157g**, *N*,*N*-dimethylacetamide, **157i**, *N*-methylacetanilide, **157h**, and *N*-methylpyrrolidin-2-one, **152d**, were obtained from TCI America. Diphenylamine, 2-(diphenylphosphino)ethylamine and sodium borohydride were obtained from J.T. Baker Chemical Company, Strem and BDH Chemicals, respectively. ^{1}H, ^{13}C, ^{19}F and ^{31}P NMR spectra were recorded using 300, 400 and 600 MHz Varian Inova, and 500 MHz Varian DirectDrive spectrometers. ^{1}H and ^{13}C NMR chemical shifts are reported in parts per million (δ) relative to TMS with the deuterated solvent as the internal reference. ^{31}P and ^{19}F chemical shifts are reported in parts per million (δ) relative to 85% H_3PO_4 and CCl_3F as the external references. NMR peak assignments were made using ^{1}H–^{1}H gCOSY, ^{1}H–^{13}C gHSQC, ^{1}H–^{31}P gHSQC, TOSCY and TROESY NMR experiments. Abbreviations used for NMR spectra are s (singlet), d (doublet), dd (doublet of doublet), ddd (doublet of doublet of doublet), dt (doublet of triplet), t (triplet), tt (triplet of triplet), q (quartet), m (multiplet) and br (broad). Infrared spectra were recorded using a Nic-Plan

FTIR microscope and are reported in wavenumbers (cm^{-1}). High-resolution mass spectra were recorded using an Applied BioSystems Mariner BioSpectrometry Workstation oaTOF Mass Spectrometer. Elemental analysis data were obtained using a Carlo Erba CHNS-O EA1108 elemental analyzer.

General procedures used to synthesize amides

I. *N*-methylsulfonylpyrrolidin-2-one, **152a**, was prepared according to a procedure reported by Ikariya and coworkers.[14]

II. *N*-acetylpyrrolidin-2-one, **152b**, was prepared according to a procedure reported by MacKenzie and coworkers.[42]

III. *N*-phenylpiperidone, **155**, was prepared according to a procedure reported by Ukita and coworkers.[43]

IV. *N,N*-diphenylbenzamide, **157a**, 1-benzoylpiperidine, **157d**, 1-morpholinoethanone, **157k**, and *N*-methyl-*N*-phenylbenzamide, **157b**, were prepared according to a procedure reported by Charette and coworkers.[44]

Spectroscopic identification of amides

N-methylsulfonylpyrrolidin-2-one[14], **152a**: White powder: ^{1}H NMR (499.815 MHz, $CDCl_3$, 27 °C): δ 2.14 (2H, p, J = 7.7 Hz, CH_2), 2.57 (2H, t, J = 8.0 Hz, CH_2), 3.25 (3H, s, CH_3), 3.86 (2H, J = 7.0 Hz, CH_2).

N-acetylpyrrolidin-2-one[42], **152b**: Colorless oil: ^{1}H NMR (499.815 MHz, $CDCl_3$, 27 °C): δ 2.01 (2H, p, J = 9.0 Hz, CH_2), 2.48 (3H, s, CH_3), 2.58 (2H, t, J = 12.0 Hz, CH_2), 3.78 (2H, t, J = 11.5 Hz, CH_2).

1-phenyl-pyrrolidin-2-one[43], **152c**: White powder: ^{1}H NMR (499.815 MHz, $CDCl_3$, 27 °C): δ 2.15 (2H, p, J = 7.2 Hz, CH_2), 2.60 (2H, t, J = 8.0 Hz, CH_2), 3.86 (2H, t, J = 7.0

Hz, CH_2), 7.13 (1H, t, *J* = 7.5 Hz, aromatic CH), 7.36 (2H, t, *J* = 7.5 Hz, 2 aromatic CH), 7.60 (2H, d, *J* = 8.0 Hz, 2 aromatic CH).

N-methylpyrrolidin-2-one, **152d**: Colorless oil: ^{1}H NMR (498.122 MHz, $CDCl_3$, 27 °C): δ 2.00 (2H, p, *J* = 7.0 Hz, CH_2), 2.35 (2H, t, *J* = 8.2 Hz, CH_2), 2.82 (3H, s, CH_3), 3.36 (2H, t, *J* = 7.0 Hz, CH_2).

2-pyrrolidinone, **152e**: Viscous oil: ^{1}H NMR (499.815 MHz, $CDCl_3$, 27 °C): δ 2.05 (2H, p, *J* = 7.7 Hz, CH_2), 2.23 (2H, t, *J* = 8.0 Hz, CH_2), 3.35 (2H, t, *J* = 7.0 Hz, CH_2), 7.10 (1H, brs, NH).

N-phenylpiperidinone[43], **155**: White powder: ^{1}H NMR (498.122 MHz, $CDCl_3$, 27 °C): δ 1.93 (4H, m, 2 CH_2), 2.55 (2H, t, *J* = 6.0 Hz, CH_2), 3.63 (2H, t, *J* = 6.0 Hz, CH_2), 7.24 (3H, m, 3 aromatic CH), 7.38 (2H, m, 2 aromatic CH).

ε-caprolactam, **156**: White powder: ^{1}H NMR (498.122 MHz, $CDCl_3$, 27 °C): δ 1.62-1.76 (6H, m, 3 CH_2), 2.46 (2H, m, CH_2), 3.20 (2H, m, CH_2), 5.90 (1H, brs, NH).

N,*N*-diphenylbenzamide[44], **157a**: White powder: ^{1}H NMR (498.124 MHz, $CDCl_3$, 27 °C): δ 7.13-7.21 (8H, m, 8 aromatic CH), 7.24-7.29 (5H, m, 5 aromatic CH), 7.43 (2H, d, *J* = 7.5 Hz, 2 aromatic CH).

N-methyl-*N*-phenylbenzamide[44], **157b**: Straw colored viscous oil: ^{1}H NMR (498.122 MHz, $CDCl_3$, 27 °C): δ 3.50 (3H, s, CH_3), 7.03 (2H, d, *J* = 8.0 Hz, 2 aromatic CH), 7.15-7.19 (3H, m, 3 aromatic CH), 7.19-7.25 (3H, m, 3 aromatic CH), 7.29 (2H, d, *J* = 8.0 Hz, 2 aromatic CH).

N,*N*-dimethylbenzamide, **157c**: White powder: ^{1}H NMR (498.122 MHz, $CDCl_3$, 27 °C): δ 2.97 (3H, brs, CH_3), 3.01 (3H, brs, CH_3), 7.38- 7.40 (5H, m, 5 aromatic CH).

1-benzoylpiperidine[44], **157d**: Straw colored viscous oil, white solid upon seeding: ^{1}H NMR (499.815 MHz, $CDCl_3$, 27 °C): δ 1.40-1.70 (6H, m, 3 CH_2), 3.29 (2H, brs, CH_2), 3.70 (2H, brs, CH_2), 7.37 (5H, s, 5 aromatic CH).

Benzanilide, **157e**: Off-white powder: ^{1}H NMR (499.815 MHz, $CDCl_3$, 27 °C): δ 7.16 (1H, t, *J* = 7.2 Hz, aromatic CH), 7.38 (2H, t, *J* = 7.8 Hz, 2 aromatic CH), 7.49 (2H, t, *J* = 7.5 Hz, 2 aromatic CH), 7.55 (1H, t, *J* = 7.5 Hz, aromatic CH), 7.64 (2H, d, *J* = 8.2 Hz, 2 aromatic CH), 7.82 (1H, brs, NH), 7.86 (2H, d, *J* = 7.0 Hz, 2 aromatic CH).

N-methylbenzamide, **157f**: White powder: ^{1}H NMR (498.124 MHz, $CDCl_3$, 27 °C): δ 3.01 (3H, d, *J* = 5.0 Hz, CH_3), 6.17 (1H, brs, NH), 7.42 (2H, t, *J* = 7.5 Hz, 2 aromatic CH), 7. 48 (1H, t, *J* = 7.5 Hz, aromatic CH), 7.76 (2H, d, *J* = 8.2 Hz, 2 aromatic CH).

N,*N*-diphenylacetamide, **157g**: White powder: ^{1}H NMR (499.815 MHz, $CDCl_3$, 27 °C): δ 2.09 (3H, s, CH_3), 7.29 (4H, d, *J* = 8.0 Hz, 4 aromatic CH), 7.10-7.50 (6H, m, 6 aromatic CH).

N-methylacetanilide, **157h**: Colorless crystals: ^{1}H NMR (498.122 MHz, $CDCl_3$, 27 °C): δ 1.86 (3H, s, CH_3), 3.26 (3H, s, CH_3), 7.18 (2H, d, *J* = 7.8 Hz, 2 aromatic CH), 7.33 (1H, t, *J* = 7.5 Hz, aromatic CH), 7.42 (2H, t, *J* = 7.2 Hz, 2 aromatic CH).

N,*N*-dimethylacetamide, **157i**: Colorless liquid: ^{1}H NMR (498.122 MHz, $CDCl_3$, 27 °C): δ 2.05 (3H, s, CH_3), 2.91 (3H, s, CH_3), 2.98 (3H, s, CH_3).

Acetanilide[45], **157j**: Colorless crystals: ^{1}H NMR (499. 815 MHz, $CDCl_3$, 27 °C): δ 2.18 (3H, s, CH_3), 7.10 (1H, t, *J* = 7.5 Hz, aromatic CH), 7.15 (1H, brs, NH), 7.32 (2H, t, *J* = 8.0 Hz, 2 aromatic CH), 7.49 (2H, d, *J* = 7.5 Hz, 2 aromatic CH).

1-morpholinoethanone, **157k**: Colorless oil: ^{1}H NMR (399.794 MHz, $CDCl_3$, 27 °C): δ 3.3-3.8 (8H, m, 4 CH_2), 7.43 (5H, m, 5 aromatic CH),

General procedures used to synthesize oxazolidinones

I. *N*-acetyl-2-oxazolidinone, **160a**, was prepared according to a procedure reported by Mundy and coworkers.[46]

II. The chiral *N*-acyl-oxazolidinones, **160b**, and **160c** were prepared according to a procedure reported by Evan and coworkers.[40]

Spectroscopic identification of *N*-acyloxazolidinones

160a: White powder: ^{1}H NMR (399.84 MHz, $CDCl_3$, 27 °C): δ 2.53 (3H, s, CH_3), 4.02 (2H, t, *J* = 8.4 Hz, CH_2), 4.41 (2H, t, *J* = 7.6 Hz, CH_2)

160b: Viscous oil: ^{1}H NMR (498.118 MHz, $CDCl_3$, 27 °C): δ 0.62 (3H, d, *J* = 6.8 Hz, CH_3), 0.85 (3H, d, *J* = 7.0 Hz, CH_3), 1.18 (3H, d, *J* = 6.8 Hz, CH_3), 2.18 (1H, m, CH), 2.65 (1H, dd, *J* = 7.6 Hz, CH), 3.14 (1H, dd, *J* = 7.5 Hz, CH), 4.12-4.27 (1H, m, CH), 4.45 (1H, m, CH), 7.2 (1H, m, aromatic CH), 7.27 (4H, m, 4 aromatic CH)

160c: Viscous oil: ^{1}H NMR (498.118 MHz, $CDCl_3$, 27 °C): δ 0.75 (3H, d, *J* = 6.5 Hz, CH_3), 1.21 (3H, d, *J* = 6.5 Hz, CH_3), 2.68 (1H, dd, *J* = 8.0 Hz, CH), 3.14 (1H, dd, *J* = 7.0 Hz, CH), 4.17 (1H, m, CH), 4.78 (1H, m, CH), 5.65 (1H, d, *J* = 7.0 Hz, CH), 7.18-7.44 (10H, m, 10 aromatic CH).

General procedures used to synthesize ruthenium precursors

Synthesis of $RuCl_2(Ph_2P(CH_2)_2NH_2)_2$, **63**

63 was prepared according to the procedure reported by Morris and coworkers.[47] $^{31}P\{^{1}H\}$ NMR - (161.839 MHz, CD_2Cl_2, 27 °C): δ 55.4 (*trans*, d, $^{2}J_{P\text{-}P}$ = 32.0 Hz), 61.8 (*cis*, s), 66.8 (*trans*, d, $^{2}J_{P\text{-}P}$ = 32.0 Hz). *cis*:*trans* = 52:48 . HRMS (ESI^{*+}) m/z calculated for $C_{28}H_{32}Cl_2N_2P_2$[102Ru] (M^{*+}): 630.0456. Found: 630.0455. Elemental analysis calculated for $C_{28}H_{32}Cl_2N_2P_2Ru$: N = 4.44, C = 53.34, H = 5.12. Found: N = 4.55, C = 53.50, H = 4.94.

$[Ru(\eta^3\text{-}C_3H_5)(Ph_2P(CH_2)_2NH_2)_2]BF_4$, **112**

314 mg (750 *μ*mol) of *cis*-$[Ru(\eta^3\text{-}C_3H_5)(COD)(CH_3CN)_2]BF_4$, **154**[27] was added to a schlenk flask equipped with a stir bar under N_2 followed by 4.0 mL of freshly distilled THF. 344 mg (1.50 mmol, 2 equiv.) of $Ph_2P(CH_2)_2NH_2$ was then added to this mixture as

a 1.0 mL THF solution. The contents of the flask were then stirred and heated at 60 °C for 1.5 h. The golden brown solution was allowed to cool to room temperature before removing the solvent *in vacuo*. The crude mixture was then recrystallized from CH_2Cl_2/Et_2O to give a light yellow powder. The solid was dried under vacuum before storing under N_2. Isolated Yield = 51%. N.B. $^{31}P\{^1H\}$ NMR of the filtrate after the solvent was removed under vacuum showed that it contained **112** as the sole Ru-containing species. $^{31}P\{^1H\}$ NMR - (201.643 MHz, CD_2Cl_2, 27 °C): δ 48.5 (*minor*, s), 51.9 (*major*, d, $^2J_{P\text{-}P}$ = 29.6 Hz), 69.9 (*major*, d, $^2J_{P\text{-}P}$ = 30.2 Hz) major:minor is 91:9). HRMS (ESI^+) m/z calculated for $C_{31}H_{37}N_2P_2$[102Ru] (M^+): 601.147. Found: 601.1476. Elemental analysis calculated for $C_{31}H_{37}N_2P_2BF_4Ru$: N = 4.07, C = 54.16, H = 5.42. Found: N = 3.81, C = 54.24, H = 5.61.

Synthesis of [Ru(1-3;5-6-*η*)-C_8H_{11})(η^6-anthracene)]BF_4**, 159**

[Ru(1-3;5-6-*η*)-C_8H_{11})(η^6-anthracene)]BF_4**, 159** was prepared via a modified procedure reported by Komiya and coworkers.[48]

163 mg (389 *μ*mol) of *cis*-[Ru(η^3-C_3H_5)(COD)(CH_3CN)$_2$]BF_4, **154**[27] and 99.0 mg (559 *μ*mol) of anthracene were added to a schlenk flask equipped with a stir bar under N_2. 8.2 mL of CH_2Cl_2 was then added to the contents of this flask while stirring moderately. 77.2 μL (263 *μ*mol) of a 30% HBH_4 in Et_2O solution was then added dropwise. The color of the solution progressed from colorless to brick red then black before returning to colorless after stirring at room temperature for 1.5 h. The solution was concentrated under reduced pressure, and the crude product recrystallized from freshly distilled $CHCl_3$ and Et_2O to give a dark brown powder. The solid was dried under vacuum before storing under N_2. Isolated Yield = 62%. The ^1H NMR of **159** agreed with that previously reported.[48]

General procedures for catalyst preparation

Method 1: Procedure to prepare *trans*-$RuH_2(Ph_2P(CH_2)_2NH_2)_2$ with $KN[Si(CH_3)_3]_2$

A mixture of *cis*-[Ru(η^3-C_3H_5)(COD)(CH_3CN)$_2$]BF_4, **154**[27] (2.1 mg, 5.0 μmol) and $Ph_2P(CH_2)_2NH_2$ (2.3 mg, 10 μmol, 2 equiv.) in THF (0.5 mL) was heated in a NMR tube at 60 °C for 30 min under Ar. The contents of the NMR tube were periodically mixed outside the 60 °C bath, and then returned to the bath during the course of the 30 min. The resulting yellow solution was pre-cooled to 0 °C before transferring the NMR tube to a dry ice/acetone bath. Dihydrogen was then added to the NMR tube at –78 °C via a cannula. The contents of the NMR tube were then mixed for 10 s outside the –78 °C bath, and then returned to the bath for 20 s. This shaking process was repeated nine times. A THF solution of $KN[Si(CH_3)_3]_2$ (0.20-0.25 mmol, 40-50 equiv., 0.5 mL) was then added by cannula under H_2 pressure (~2 atm) at –78 °C. After shaking the color of the solution changed from light yellow to orange. This mixture was then used for the catalytic hydrogenation as described in the next section (Method A or B).

Method 2: Procedure to prepare *trans*-$RuH_2(Ph_2P(CH_2)_2NH_2)_2$ with NaOMe

2.5 μmol of ruthenium precursor (**112** or **63**) and 1.3 mmol of NaOMe were weighed out into two respective NMR tubes in a glove box. THF (1.0 mL) was then added by cannula under Ar pressure into each tube at room temperature. These samples were then used for the catalytic hydrogenation as described in the next section (Method A).

Method 3: Procedure to prepare *trans*-[RuH(η^1-BH_4)(*R*)-BINAP)((*R*,*R*)-dpen)] catalyst[38]

A solution of [Ru((1–5–η)-C_8H_{11})((*R*)-BINAP)]BF_4 (10 μmol) in THF (0.5 mL) was mixed under H_2 (~2 atm) at 0 °C for 8 min. The resulting solution containing [RuH((*R*)-BINAP)$(THF)_3$]BF_4 was then cooled to –78 °C using a dry ice/acetone bath. A THF

solution of (*R*,*R*)-dpen (1 *μ*mol, 0.2 mL) was then added by cannula under H_2 pressure (~2 atm) at –78 °C. The contents of the NMR tube were then mixed for 10 s outside the –78 °C bath, and then returned to the bath for 20 s. This process was repeated for a total of 5 min. This solution was then transferred by cannula under H_2 pressure (~2 atm) at –78 °C into a THF mixture of $NaBH_4$ (10 *μ*mol, 0.3 mL). The contents of the NMR tube were then mixed for 10 s outside the –78 °C bath, and then returned to the bath for 20 s. This process was repeated for a total of 60 s. The mixture containing *trans*-[RuH(η^1-BH_4)(*R*)-BINAP)((*R*,*R*)-dpen)] was then used for the catalytic hydrogenation as described in the next section (Method A).

Method 4: Procedure to prepare *trans*-RuH(η^1-BH_4)($Ph_2P(CH_2)_2NH_2)_2$

A mixture of *cis*-[Ru(η^3-C_3H_5)(COD)($CH_3CN)_2$]BF_4, **154**[27] or [Ru(1-3;5-6-*η*)-C_8H_{11})(η^6-anthracene)]BF_4**,** **159**, (20 *μ*mol) and $Ph_2P(CH_2)_2NH_2$ (40 *μ*mol, 2 equiv.) in THF (1.0 mL) was heated in a NMR tube at 60 °C for 30 min under Ar. The contents of the NMR tube were periodically mixed outside the 60 °C bath, and then returned to the bath during the course of the 30 min. This solution was then transferred by cannula under H_2 pressure (~2 atm) at room temperature onto solid $NaBH_4$ (0.10 mmol, 5 equiv.). The mixture was then heated at 60 °C for 20 min under H_2 during this time the solution color changed to brown. This mixture was then used for the catalytic hydrogenation as described in the next section (Method A).

Method 5: Procedure to prepare *trans*-RuH(η^1-BH_4)($Ph_2P(CH_2)_2NH_2)_2$

20 *μ*mol of **63** or **112** and 0.040-0.10 mmol (2-5 equiv.) of $NaBH_4$ were weighed out into two respective NMR tubes in a glove box. THF (1.0 mL) was then added by cannula under Ar pressure to the NMR tube containing the Ru-precursor at room temperature. This solution was then transferred by cannula under H_2 pressure (~2 atm)

at room temperature onto solid $NaBH_4$ (0.040-0.10 mmol, 2-5 equiv.). The mixture was then heated at 60 °C for 10-20 min under H_2 during this time the solution color changed to brown. This mixture was then used for the catalytic hydrogenation as described in the next section (Method A, B or C).

General procedures for hydrogenation

Method A: Solid amides

The amide (0.10-25 mmol, 10-10000 equiv.) was added to a stainless steel autoclave equipped with a magnetic stir bar. The autoclave was then purged with H_2 for 10 min at room temperature. 4.0-6.0 mL of THF was then added to the autoclave using a gas tight syringe. The catalyst/base mixture, prepared above, was then added by cannula under H_2 pressure followed by a 3.0-5.0 mL THF wash. The autoclave was then pressurized to 50 atm H_2. The reaction mixture was stirred at 50-100 °C for 23-25 h. The autoclave was then allowed to cool over the course of 1 h before venting at room temperature. The percent conversions were determined by ^1H NMR spectroscopy.

Method B: Liquid amide

The atmosphere of a stainless steel autoclave was purged with H_2 for 10 min at room temperature. A solution of the amide (5 mmol, 1000 equiv.) in THF (1.0 mL), prepared under Ar, was then added by a cannula under H_2 pressure followed by a 4.0 mL THF wash. The catalyst/base mixture, prepared above, was then added by cannula under H_2 pressure followed by a 2.0 mL THF wash. The autoclave was then pressurized to 50 atm H_2. The reaction mixture was stirred at 100 °C for 23 h. The autoclave was then allowed to cool over the course of 1 h before venting at room temperature. The percent conversions were determined by ^1H NMR spectroscopy.

Method C: *N*-acyloxazolidinones

The atmosphere of a stainless steel autoclave was purged with H_2 for 10 min at room temperature. A solution of the *N*-acyloxazolidinone (0.20-2.0 mmol, 10-100 equiv.) in THF (1.0 mL), prepared under Ar, was then added by a cannula under H_2 pressure followed by a 4.0 mL THF wash. The catalyst/base mixture, prepared above, was then added by cannula under H_2 pressure followed by a 2.0 mL THF wash. The autoclave was then pressurized to 50 atm H_2. The reaction mixture was stirred at 50-100 °C for 23-47 h. The autoclave was then allowed to cool over the course of 1 h before venting at room temperature. The percent conversions were determined by ^{1}H NMR spectroscopy.

Control Experiments

Ligand-free hydrogenation

4.2 mg (10 μmol) of *cis*-[Ru(η^3-C_3H_5)(COD)(CH_3CN)$_2$]BF_4, **154**,[27] and 6.0 mg (30 μmol) of KN[Si(CH_3)$_3$]$_2$ were weighed out into two respective NMR tubes. THF (1.0 mL) was then added to each of these tubes under Ar. The tube containing **154** was then heated at 60 °C for 30 min to form a yellow solution. These solutions were then used for the catalytic hydrogenation as described below.

0.10 mmol (100 equiv.) of the amide was added to a stainless steel autoclave equipped with a magnetic stir bar. The autoclave was then purged with H_2 for 10 min at room temperature. 3.0 mL of THF was then added to the autoclave using a gas tight syringe. The solution of the Ru-precursor, prepared above, was then added by cannula under H_2 pressure followed by KN[Si(CH_3)$_3$]$_2$ and a 3.0 mL THF wash. The autoclave was then pressurized to 50 atm H_2. The reaction mixture was stirred at 100 °C for 17 h. The autoclave was then allowed to cool over the course of 1 h before venting at room temperature. The percent conversions were determined by ^{1}H NMR spectroscopy. No apparent reaction was observed.

Base-free hydrogenation

A mixture of *cis*-[Ru(η^3-C_3H_5)(COD)(CH_3CN)$_2$]BF_4, **154**,[27] (2.1 mg, 5.0 μmol) and $Ph_2P(CH_2)_2NH_2$ (2.3 mg, 10 μmol, 2 equiv.) in THF (1.0 mL) was heated in a NMR tube at 60 °C for 30 min under Ar. The contents of the NMR tube were periodically mixed outside the 60 °C bath, and then returned to the bath during the course of the 30 min. The resulting yellow solution was pre-cooled to 0 °C before transferring the NMR tube to a dry ice/acetone bath. H_2 was then added to the NMR tube at –78 °C via a cannula. The contents of the NMR tube were then mixed for 10 s outside the –78 °C bath, and then returned to the bath for 20 s. This shaking process was repeated nine times. This solution was then used for the catalytic hydrogenation as described below.

0.10 mmol (100 equiv.) of the amide was added to a stainless steel autoclave equipped with a magnetic stir bar. The autoclave was then purged with H_2 for 10 min at room temperature. 3.0 mL of THF was then added to the autoclave using a gas tight syringe. The solution of **112**, prepared above, was then added by cannula under H_2 pressure followed by a 4.0 mL THF wash. The autoclave was then pressurized to 50 atm H_2. The reaction mixture was stirred at 100 °C for 17 h. The autoclave was then allowed to cool over the course of 1 h before venting at room temperature. The percent conversions were determined by ^{1}H NMR spectroscopy. No apparent reaction was observed.

Nanoparticle mediated hydrogenation

14.5 mg of ruthenium black (10.0 μmol assuming 7% of ruthenium atoms are on the surface) and 100 μmol (10.0 equiv.) of the amide were added to a stainless steel autoclave equipped with a magnetic stir bar. The autoclave was then purged with H_2 for 10 min at room temperature. 8.0 mL of THF was then added to the autoclave using a

gas tight syringe. The autoclave was then pressurized to 50 atm H_2. The reaction mixture was stirred at 100 °C for 17 h. The autoclave was then allowed to cool over the course of 1 h before venting at room temperature. The percent conversions were determined by ^{1}H NMR analysis. *N*-phenylpyrrolidin-2-one was converted into *N*-cyclohexylpyrrolidin-2-one with TON = 1 during this time.

Spectroscopic identification of products

All hydrogenation products except **161b** and **161c** are known and will not be reproduced here.

161b: ^{1}H NMR (599. 926 MHz, $CDCl_3$, 27 °C): δ 0.71 (3H, d, *J* = 7.0 Hz, CH_3), 0.78 (3H, d, *J* = 6.5 Hz, CH_3), 1.21 (3H, d, *J* = 6.0 Hz, CH_3), 1.73 (1H, m, CH), 2.53 (1H, m, CH), 2.70 (1H, m, CH), 2.95 (1H, m, CH), 3.23 (1H, bs, OH), 3.60 (3H, m, 3 CH), 5.72 (1H, bs, NH), 7.17-7.26 (5H, m, 5 aromatic CH). ^{13}C{^{1}H} NMR (175.969 MHz, $CDCl_3$, 27 °C): δ 17.9 (*C*H), 18.5 (*C*H), 19.2 (*C*H), 28.6 (*C*H), 40.4 (*C*H), 43.9 (*C*HNH), 56.9 (aromatic), 63.6 (CHOH), 126.2 (aromatic), 128.3 (aromatic), 128.8 (aromatic), 139.7 (aromatic), 176.5 (*C*=O). ^{1}H–^{15}N HSQC (498.117 MHz, $CDCl_3$, 27 °C): δ 123. HRMS (ESI^+) m/z calculated for $C_{15}H_{24}NO_2$ $(M+H)^+$: 250.18. Found: 250.1802. Difference (ppm): 0.75. **161b** is not stable for prolong periods in solution.

161c: ^{1}H NMR (599. 926 MHz, $CDCl_3$, 27 °C): δ 0.79 (3H, d, *J* = 7.2 Hz, CH_3), 1.21 (3H, d, *J* = 6.6 Hz, CH_3), 2.43 (1H, sex, *J* = 6.6 Hz, CH), 2.70 (1H, dd, *J* = 6.6 Hz, CH), 2.93 (1H, dd, *J* = 8.4 Hz, CH), 3.91 (1H, bs, OH), 4.19 (1H, m, CH), 4.75 (1H, bs, NH), 5.38 (1H, d, *J* = 7.8 Hz, CH), 7.15-7.33 (10H, m, 10 aromatic CH). ^{13}C{^{1}H} NMR (150.868 MHz, $CDCl_3$, 27 °C): δ 14.5 (*C*H), 17.7 (*C*H), 40.5 (*C*H), 43.8 (*C*H), 50.9 (*C*HNH), 76.7 (*C*HOH), 126.3 (aromatic), 126.4 (aromatic), 127.4 (aromatic), 128.0 (aromatic), 128.4 (aromatic), 128.9 (aromatic), 139.7 (aromatic), 140.7 (aromatic), 176.4

(*C*=O). $^{1}H–^{15}N$ HSQC (599.925 MHz, $CDCl_3$, 27 °C): δ 127. HRMS (ESI+) m/z calculated for $C_{19}H_{23}NO_2$ $(M+Na)^+$: 320.1621. Found: 320.1621. Difference (ppm): 0.01.

Bibliography

1. Fersner, A.; Karty, J. M.; Mo, Y. *J. Org. Chem.* **2009***, 74*, 7245-7253.

2. Glover, S. A.; Rosser, A. A. *J. Org. Chem.* **2012***, 77*, 5492-5502.

3. Bailey, P. D.; Mills, T. J.; Pettecrew, R.; Price, R. A. In *Comprehensive Organic Functional Group Transformations II: Amides*; Katritzky, A. R., Taylor, R. J. K., Eds.; Elsevier: Oxford, 2005; pp 201-294.

4. Magano, J.; Dunetz, J. R. *Org. Process Res. Dev.* **2012***, 16*, 1156-1184.

5. Dub, P. A.; Ikariya, T. *ACS Catal.* **2012***, 2*, 1718-1741.

6. Doods, D. L.; Cole-Hamilton, D. J. In *Sustainable Catalysis: Challenges and Practices for the Pharmaceutical and Fine Chemical Industries: Catalytic Reduction of Amides Avoiding $LiAlH_4$ or B_2H_6*; Dunn, P. J., Hii, K. K., Krische, M. J., Williams, M. T., Eds.; John Wiley and Sons: New Jersey, 2013; pp 1-36.

7. Dugger, R. W.; Ragan, J. A.; Brown Ripin, D. H. *Org. Process Res. Dev.* **2005***, 9*, 253-258.

8. Carey, J. S.; Laffan, D.; Thomson, C.; Williams, M. T. *Org. Biomol. Chem.* **2006***, 4*, 2337-2347.

9. Constable, D. J. C.; Dunn, P. J.; Hayler, J. D.; Humphrey, G. R.; Leazer, Jr., J. L.; Linderman, R. J.; Lorenz, K.; Manley, J.; Pearlman, B. A.; Wells, A.; Zaks, A.; Zhang, T. Y. *Green Chem.* **2007***, 9*, 411-420.

10. Kilner, M.; Tyers, D. V.; Crabtree, S. P.; Wood, M. A. Davy Process Technology Limited, UK; Patent WO03093208A1, 2003; p 23.

11. Magro, A. A. N.; Eastham, G. R.; Cole-Hamilton, D. *Chem. Commun.* **2007**, 3154-3156.

12. Eastham, G. R.; Cole-Hamilton, D. J.; Magro, A. A. N. Lucite International UK Limited, UK; Patent WO2008035123A2, 2008; p 36.

13. Coetzee, J.; Dodds, D. L.; Klankermayer, J.; Brosinski, S.; Leitner, W.; Slawin, A. M. Z.; Cole-Hamilton, D. J. *Chem. Eur. J.* **2013***, 19*, 11039-11050.

14. Ito, M.; Koo, L. W.; Himizu, A.; Kobayashi, C.; Sakaguchi, A.; Ikariya, T. *Angew. Chem., Int. Ed.* **2009***, 48*, 1324-1327.

15. Ikariya, T.; Ito, M.; Ootsuka, T.; Hashimoto, T. Tokyo Institute of Technology, Japan; Central Glass Company Limited; Patent WO2010073974A1, 2010; p 31.

16. Ito, M.; Ootsuka, T.; Watari, R.; Shiibashi, A.; Himizu, A.; Ikariya, T. *J. Am. Chem. Soc.* **2011***, 133*, 4240-4242.

17. Balaraman, E.; Gnanaprakasam, B.; Shimon, L. J. W.; Milstein, D. *J. Am. Chem. Soc.* **2010***, 132*, 16756-16758.

18. Milstein, D.; Gunanathan, C.; Ben-David, Y.; Balaraman, E.; Gnanaprakasam, B.; Zhang, H. Yeda Research and Development Company Limited, Israel; Patent US2012253042A1, 2012; p 54.

19. Barrios-Francisco, R.; Balaraman, E.; Diskin-Posner, Y.; Leitus, G.; Shimon, L. J. W.; Milstein, D. *Organometallics* **2013***, 32*, 2973-2982.

20. Miura, T.; Held, I. E.; Oishi, S.; Naruto, M.; Saito, S. *Tetrahedron Lett.* **2013***, 54*, 2674-2678.

21. Hamilton, R. J.; Bergens, S. H. *J. Am. Chem. Soc.* **2006***, 128*, 13700-13701.

22. Hamilton, R. J.; Bergens, S. H. *J. Am. Chem. Soc.* **2008***, 130*, 11979-11987.

23. Takebayashi, S.; John, J. M.; Bergens, S. H. *J. Am. Chem. Soc.* **2010***, 132*, 12832-12834.

24. Takebayashi, S.; Bergens, S. H. *Organometallics* **2009***, 28*, 2349-2351.

25. Abdur-Rashid, K.; Faatz, M.; Lough, A. J.; Morris, R. H. *J. Am. Chem. Soc.* **2001***, 123*, 7473-7474.

26. Saudan, L. A.; Saudan, C.; Becieux, C.; Wyss, P. *Angew. Chem., Int. Ed.* **2007***, 46*, 7473-7476.

27. Wiles, J. A.; Daley, C. J. A.; Hamilton, R. J.; Leong, C. G.; Bergens, S. H. *Organometallics* **2004***, 23*, 4564-4568.

28. Mucsi, Z.; Chass, G. A.; Viskolcz, B.; Csizmadia, I. G. *J. Phys. Chem. A* **2008***, 112*, 9153-9165.

29. Ohkuma, T.; Koizumi, M.; Muñiz, K.; Hilt, G.; Kabuto, C.; Noyori, R. *J. Am. Chem. Soc.* **2002***, 124*, 6508-6509.

30. Sandoval, C. A.; Ohkuma, T.; Muñiz, K.; Noyori, R. *J. Am. Chem. Soc.* **2003***, 125*, 13490-13503.

31. Guo, R.; Morris, R. H.; Song, D. *J. Am. Chem. Soc.* **2005***, 127*, 516-517.

32. Guo, R.; Chen, X.; Elpelt, C.; Song, D.; Morris, R. H. *Org. Lett.* **2005***, 7*, 1757-1759.

33. Ino, Y.; Kuriyama, W.; Ogata, O.; Matsumoto, T. *Top. Catal.* **2010***, 53*, 1019-1024.

34. Kuriyama, W.; Ino, Y.; Ogata, O.; Sayo, N.; Saito, T. *Adv. Synth. Catal.* **2010***, 352*, 92-96.

35. Kuriyama, W.; Matsumoto, T.; Ino, Y.; Ogata, O. Takasago International Corporation, Japan; Patent WO2011048727, 2011; p 62.

36. Ino, Y.; Yoshida, A.; Kuriyama, W. Takasago International Corporation, Japan; Patent EP1970360A1, 2008; p 26.

37. Zhang, J.; Balaraman, E.; Leitus, G.; Milstein, D. *Organometallics* **2011***, 30*, 5716-5724.

38. Hamilton, R. J.; Leong, C. G.; Bigam, G.; Miskolzie, M.; Bergens, S. H. *J. Am. Chem. Soc.* **2005***, 127*, 4152-4153.

39. John, J. M.; Bergens, S. H. *Angew. Chem., Int. Ed.* **2011***, 50*, 10377-10380.

40. Evans, D. A.; Ennis, M. D.; Mathre, D. J. *J. Am. Chem. Soc.* **1982***, 104*, 1737-1739.

41. Armarego, W. L. F.; Chai, C. L. L. *Purification of Laboratory Chemicals*; Elsevier: Oxford, 2013.

42. Irvine, M. W.; Patrick, G. L.; Kewney, J.; Hastings, S. F.; MacKenzie, S. J. *Bioorg. Med. Chem. Lett.* **2008***, 18*, 2032-2037.

43. Sughara, M.; Ukita, T. *Chem. Pharm. Bull.* **1997***, 45*, 719-721.

44. Barbe, G.; Charette, A. B. *J. Am. Chem. Soc.* **2008***, 130*, 18-19.

45. Stuart, D. R.; Bertrand-Laperle, M.; Burgess, K. M. N.; Fagnou, K. *J. Am. Chem. Soc.* **2008***, 130*, 16474-16475.

46. Mundy, B. P.; Kim, Y. *J. Heterocyclic Chem.* **1982***, 19*, 1221-1222.

47. Abdur-Rashid, K.; Guo, R.; Lough, A. J.; Morris, R. H.; Song, D. *Adv. Synth. Catal.* **2005***, 347*, 571-579.

48. Shibasaki, T.; Komine, N.; Hirano, M.; Komiya, S. *J. Organomet. Chem.* **2007***, 692*, 2385-2394.

Chapter 5

Conclusions and future work

Conclusions

The Noyori ketone hydrogenation catalyst, *trans*-[RuH_2((*R*)-BINAP)((*R*,*R*)-dpen)], and its variants are among the most active, influential and selective catalysts ever developed for asymmetric hydrogenation.[1-7] Previous mechanistic studies into the bifunctional addition of ketones revealed this catalyst to be a remarkable reducing agent at low temperatures in THF.[8-10] Hamilton and Bergens found that *trans*-[RuH_2((*R*)-BINAP)((*R*,*R*)-dpen)] adds acetophenone upon mixing to form *trans*-[RuH($OCH(CH_3)$(Ph)((*R*)-BINAP)((*R*,*R*)-dpen)] under ~2 atm H_2 at –80 °C in THF-d_8.[10] In contrast, Takebayashi and Bergens reported that the addition of lactones *e.g.* γ-butyrolactone and phthalide, to this catalyst occurs unexpectedly fast (*within minutes*) to form the corresponding Ru-hemiacetyloxide, and on standing forms the Ru-alkoxide of the product diol under similar conditions.[11] Despite this impressive reactivity towards organic carbonyls at low temperatures, the application of bifunctional complexes towards the reduction of less reactive carboxylic acid derivatives *e.g.* imides and amides was virtually unexplored at the onset of this research.[6,12]

In Chapter 2 of this thesis,[13,14] the high reducing power of *trans*-[RuH_2((*R*)-BINAP)((*R*,*R*)-dpen)], and its ethylenediamine analogue, *trans*-[RuH_2((*R*)-BINAP)($H_2N(CH_2)_2NH_2$)] was highlighted in the successful mono- and di-hydrogenation of phthalimides and *N*-substituted succinimides, respectively under mild conditions (0.5-1 mol% Ru, 9 mol% KO*t*-Bu under 4 atm H_2 at 30-60 °C in THF and/or 2:1 THF/CH_2Cl_2 for 3 h). This preliminary investigation indicated that the monohydrogenation is favored at low temperatures when the imide backbone favors ring-closing. Remarkably, chiral

hydroxy lactams were produced with up to five stereogenic centers in 90-99% conversion, 88-97% *ee*, dr >93:7 and a C=O/C=C selectivity >99% from monohydrogenation of bicyclic *meso*-imides (0.1-1 mol% Ru, 1-10 mol% KO*t*-Bu under 50 atm H_2 at 0-22 °C in 3-57 h). Interestingly, the stereochemistry at the hydroxy carbon was *trans* and not *cis,* the kinetic product of net hydride insertion to the less hindered convex-face of the imide carbonyl. Thus, the enantiotopic group selectivity is preserved in this hydrogenation but not the *cis*-*trans* selectivity. Moreover, the synthetic utility of these products were demonstrated by the use of *N*-acyliminium ion chemistry that increased the number of stereogenic centers from 5 to 7 in one step.

In Chapter 3,[15] the enantioselective desymmetrization of cyclic *meso*-imides was investigated using low-temperature stoichiometric experiments. This study revealed a base-catalyzed bifunctional addition to imide carbonyls. This is the first report of a base *i.e.* KOH, promoting the activity of a fully hydrogenated catalyst. Further investigation into this unexpected phenomenon led to the synthesis and characterization of novel reaction intermediates resulting from the unexpected deprotonation and di-deprotonation of the parent dihydride, *trans*-[RuH_2((*R*)-BINAP)((*R*,*R*)-dpen)]. The deprotonated dihydride, *trans*-K[RuH_2((*R*,*R*)-HNCH(Ph)CH(Ph)NH_2)((*R*)-BINAP)], was later found to have unprecedented activity towards imide (complete on mixing at –80 °C) and amide (starting at –80 °C) carbonyls at low temperatures in THF-d_8. Given the results of this mechanistic investigation, the catalytic desymmetrization-hydrogenation presumably proceeds by presence of KOH formed by the hydrolysis of KO*t*-Bu due to the presence of trace amounts of water in the substrate. Thus, the origin of the *trans*-hydroxy lactam was found to be the hydrolysis of the potassium salt of the *cis*-hydroxy lactam followed by the rapid base-catalyzed isomerization to the thermodynamically more stable *trans*-isomer. The origins of the high enantioselectivity were proposed based on this low-temperature NMR investigation, an X-ray diffraction study, and a stereochemical

analysis of diastereomeric transition states for the net hydride insertion step. The major contributing factors to the high enantioselectivity were the formation of a highly ordered transition state in the dihydride addition step and the irreversibility of this addition under basic conditions.

Encouraged by these results, the challenging hydrogenation of amides was attempted as described in Chapter 4. In contrast to the high activity of *trans*-[RuH_2((*R*)-BINAP)((*R*,*R*)-dpen)] towards ketones,[10] imides (*in presence of base*),[13-15] and esters at low temperatures in THF,[11] the catalyst exhibited moderate to low activity towards activated amides under reported reaction conditions (2-10 mol% Ru, 40 mol% inorganic base *e.g.* KO*t*-Bu or KN[$Si(CH_3)_3]_2$, under 50 atm H_2 at 100 °C in 16-39 h).[16] Based on prior mechanistic studies this difference in activity was attributed to thermal instability of *trans*-[RuH_2((*R*)-BINAP)((*R*,*R*)-dpen)] at higher temperatures.[9,10] Simply replacing the bidentate ligands with two equivalents of the strongly chelating aminophosphine, $Ph_2P(CH_2)_2NH_2$, prevented catalyst decomposition and maintained catalytic activity under moderate reaction conditions.[17] The robust system of [Ru(η^3-C_3H_5)($Ph_2P(CH_2)_2NH_2)_2$]BF_4 and base *e.g.* NaOMe or KN[$Si(CH_3)_3]_2$, was found to hydrogenate amides with the highest TON (up to 7120) to date with C–N cleavage for a homogeneous amide hydrogenation.[16,18] Preliminary mechanistic studies were used to tentatively assign the ^1H and $^{31}P\{^1H\}$ NMR resonances for the hydride and phosphorus ligands to an isomer of the active catalyst, *trans*-$RuH_2(Ph_2P(CH_2)_2NH_2)_2$. Interestingly, the analogous base-free system of [Ru(η^3-C_3H_5)($Ph_2P(CH_2)_2NH_2)_2$]BF_4 with 2 equivalents of $NaBH_4$, which presumably gives the same active catalyst via the *trans*-RuH(η^1-BH_4)($Ph_2P(CH_2)_2NH_2)_2$ complex, was also shown to be an efficient catalyst system for this reaction (24-100% conversion using 0.1 mol% Ru, 0.2 mol% B under 50 atm H_2 at 100 °C in 24 h). In particular, under similar conditions, this system was more active towards the hydrogenation of secondary amides than those reported in the current

literature.[19-23] The base-free hydrogenation was also found to catalyze the hydrogenation of the less reactive oxazolidone core of Evan's chiral auxillaries[24] to yield chiral alcohol-amides under mild conditions that have potential applications in ligand synthesis (100% conversion using 10 mol% Ru, 20 mol% B under 50 atm H_2 at 50 °C in 48 h).

Future work

The underlying theme of this work was to develop "greener strategies" for the reduction of less reactive carboxylic acid derivatives. There are, however, some areas that must be addressed before potentially developing a pilot process.[25,26] These factors include improved catalyst selectivity (functional group tolerance), an appropriate level of activity and productivity (TON >1000 and TOF >500 h^{-1} for high-value products and TON >50,000 and TOF >10,000 h^{-1} for less-expensive commodities), assessing strategies for catalyst re-use and/ or separation, and determining quality risks (factors that can affect the performance of a catalytic process). It must be noted, however, that the fulfillment of these criteria may not necessarily lead to implementation.

In Chapter 2, the selective monohydrogenation of *cis*-1,3-dibenzyl-*N*-benzyl-2-imidazolidinone-4,5-dicarboximide was attempted to serve as a potential precursor to (+)-biotin.[27] Disappointingly, we found that the enantioselectivity of the reaction was poor under the reported conditions (2 mol% *trans*-[RuH_2((*R*)-BINAP)((*R*,*R*)-dpen)], 18 mol% KO*t*-Bu under 50 atm H_2 at 60 °C for 1 h with 95% yield, 18% *ee* and dr = 85:10 in THF). Further optimization of catalyst structure and ligand electronics could potentially improve the selectivity of this reaction through enhanced catalyst-substrate interaction and reactivity that should facilitate milder reaction conditions. Notably, a method to isolate *cis*-hydroxy lactams from this and related catalyst systems has proven to be elusive.[15]

In Chapters 3, the mono-deprotonated dihydrides *e.g. trans*-K[RuH_2((*R*,*R*)-HNCH(Ph)CH(Ph)NH_2)((*R*)-BINAP)], were found to have unprecedented activity towards

imide (complete on mixing at –80 °C) and amide (starting at –80 °C) carbonyls at low temperatures in THF-d_8.[15] With such high reactivity in hand, it is only plausible that the activity of less reactive carbonyl compounds *e.g.* carbonic acid derivatives should be probed using low-temperature stoichiometric reactions. If successful it would suggest that these reactions should proceed unhindered at low temperatures with a stoichiometric amount of base. Further, a full theoretical study into the desymmetrization-hydrogenation reaction would be highly beneficial for a better understanding of the reaction mechanism.

Chapter 4 described the hydrogenation of amides with *trans*-$RuH_2(Ph_2P(CH_2)_2NH_2)_2$, this catalyst is remarkably active towards the C–N cleavage of simple aliphatic and aromatic amides.[16,18] However, to be feasible in a potential future application the current substrate scope must be increased to encompass more complex functionalized amides that have industrial relevance.[28,29] A high yielding preparation and study of the active catalyst, *trans*-$RuH_2(Ph_2P(CH_2)_2NH_2)_2$, may uncover novel deactivation and/or decomposition pathways that could facilitate the development of more active and productive catalysts through judicious variations in catalyst structure. These catalysts could also make the transformation easier at much lower reaction temperatures and pressures of H_2 that circumvents the need for specialized equipment.

The selective dehydration of amides to amines is another major area of potential research. Secondary amines have been shown to form from cyclic and bicyclic amides using bifunctional catalysts in the presence of high loadings of base under rigorous reaction conditions (2-10 mol% Ru, 20-25 mol% base under 50-80 atm H_2 at 100-160 °C for 24-216 h in THF or 2-PrOH).[6,23] These results suggest that the reductive C–O cleavage of secondary amides may be possible when cyclization favors the formation of the hydroxy lactam (product of net hydride insertion) and high temperatures favor the

loss of water to form the imine. As a result, *gem*-disubstituted amides should represent an appropriate substrate class to investigate.[30,31]

Bibliography

1. Sheldon, R. A.; Arends, I. W. C. E.; Hanefeld, U. In *Green Chemistry and Catalysis: Catalytic Reductions*; Wiley-VCH Verlag GmbH & Co. KGaA: Weinheim, 2007; pp 91-131.
2. Gladiali, S.; Taras, R. In *Modern Reduction Methods: Reduction of Carbonyl Compounds by Hydrogen Transfer*; Andersson, P. G., Munslow, I. J., Eds.; Wiley-VCH Verlag GmbH & Co. KGaA: Weinheim, 2008; pp 135-157.
3. Hedberg, C. In *Modern Reduction Methods: Carbonyl Hydrogenation*; Andersson, P. G., Munslow, I. J., Eds.; Wiley-VCH Verlag GmbH & Co. KGaA: Weinheim, 2008; pp 107-134.
4. Noyori, R.; Hashiguchi, S. In *Applied Homogeneous Catalysis with Organometallic Compounds*; Wiley-VCH Verlag GmbH: New York, 2008; pp 552-571.
5. Shang, G.; Li, W.; Zhang, X. In *Catalytic Asymmetric Synthesis: Transition Metal-Catalyzed Homogeneous Asymmetric Hydrogenation*; Ojima, I., Ed.; John Wiley & Sons, Inc: New Jersey, 2010; pp 343-436.
6. Dub, P. A.; Ikariya, T. *ACS Catal.* **2012***, 2*, 1718-1741.
7. Magano, J.; Dunetz, J. R. *Org. Process Res. Dev.* **2012***, 16*, 1156-1184.
8. Hamilton, R. J.; Leong, C. G.; Bigam, G.; Miskolzie, M.; Bergens, S. H. *J. Am. Chem. Soc.* **2005***, 127*, 4152-4153.
9. Hamilton, R. J.; Bergens, S. H. *J. Am. Chem. Soc.* **2006***, 128*, 13700-13701.
10. Hamilton, R. J.; Bergens, S. H. *J. Am. Chem. Soc.* **2008***, 130*, 11979-11987.
11. Takebayashi, S.; Bergens, S. H. *Organometallics* **2009***, 28*, 2349-2351.
12. Doods, D. L.; Cole-Hamilton, D. J. In *Sustainable Catalysis: Challenges and Practices for the Pharmaceutical and Fine Chemical Industries: Catalytic Reduction*

of Amides Avoiding $LiAlH_4$ or B_2H_6; Dunn, P. J., Hii, K. K., Krische, M. J., Williams, M. T., Eds.; John Wiley and Sons: New Jersey, 2013; pp 1-36.

13. Takebayashi, S.; John, J. M.; Bergens, S. H. *J. Am. Chem. Soc.* **2010***, 132*, 12832-12834.
14. Bergens, S. H.; Takebayashi, S. University of Alberta, Canada; Patent WO2010145024A1, 2010; p 63.
15. John, J. M.; Takebayashi, S.; Dabral, N.; Miskolzie, M.; Bergens, S. H. *J. Am. Chem. Soc.* **2013***, 135*, 8578-8584.
16. John, J. M.; Bergens, S. H. *Angew. Chem., Int. Ed.* **2011***, 50*, 10377-10380.
17. Saudan, L. A.; Saudan, C.; Becieux, C.; Wyss, P. *Angew. Chem., Int. Ed.* **2007***, 46*, 7473-7476.
18. Bergens, S. H.; John, J. M. University of Alberta, Canada; Patent WO2013010275A1, 2013; p 95.
19. Balaraman, E.; Gnanaprakasam, B.; Shimon, L. J. W.; Milstein, D. *J. Am. Chem. Soc.* **2010***, 132*, 16756-16758.
20. Milstein, D.; Gunanathan, C.; Ben-David, Y.; Balaraman, E.; Gnanaprakasam, B.; Zhang, H. Yeda Research and Development Company Limited, Israel; Patent US2012253042A1, 2012; p 54.
21. Ito, M.; Ootsuka, T.; Watari, R.; Shiibashi, A.; Himizu, A.; Ikariya, T. *J. Am. Chem. Soc.* **2011***, 133*, 4240-4242.
22. Ikariya, T.; Ito, M.; Ootsuka, T.; Hashimoto, T. Tokyo Institute of Technology, Japan; Central Glass Company, Limited; Patent WO2010073974A1, 2010; p 34.
23. Miura, T.; Held, I. E.; Oishi, S.; Naruto, M.; Saito, S. *Tetrahedron Lett.* **2013***, 54*, 2674-2678.
24. Evans, D. A.; Ennis, M. D.; Mathre, D. J. *J. Am. Chem. Soc.* **1982***, 104*, 1737-1739.
25. Blaser, H. -U. *Chem. Commun.* **2003**, 293-296.

26. Naud, F.; Spindler, F.; Rueggeberg, C. J.; Schmidt, A. T.; Blaser, H. -U. *Org. Process Res. Dev.* **2007***, 11*, 519-523.

27. Chen, F. -E.; Dai, H. -F.; Kuang, Y. -Y.; Jia, H. -Q. *Tetrahedron: Asymmetry* **2003***, 14*, 3667-3672.

28. Kotian, P. L.; Lin, T. -H.; El-Kattan, Y.; Chand, P. *Org. Process Res. Dev*. **2005**, *9*, 193-197.

29. Alimardanov, A.; Nikitenko, A.; Connolly, T. J.; Feigelson, G.; Chan, A. W.; Ding, Z.; Ghosh, M.; Shi, X.; Ren, J.; Hansen, E.; Farr, R.; MacEwan, M.; Tadayon, S.; Springer, D. M.; Kreft, A. F.; Ho, D. M.; Potoski, J. R. *Org. Process Res. Dev*. **2009**, *13*, 1161-1168.

30. Jung, M. E.; Piizzi, G. *Chem. Rev.* **2005***, 105*, 1735-1766.

31. Levine, M. N.; Raines, R. T. *Chem. Sci.* **2012***, 3*, 2412-2420.